DL/R34
CONF-750234--

DARESBURY STUDY WEEKEND SERIES No. 8

THREE PARTICLE PHASE SHIFT ANALYSIS AND MESON RESONANCE PRODUCTION:

proceedings of the Daresbury Study Weekend, 1-2 February, 1975

Edited by J. B. Dainton and A. J. G. Hey

Science Research Council
DARESBURY LABORATORY
Daresbury, Warrington, WA4 4AD

DISCLAIMER

Printed by McCorquodale Printers Ltd., Newton-le-Willows, Merseyside.

DARESBURY STUDY WEEKEND SERIES No. 8

THREE PARTICLE PHASE SHIFT ANALYSIS AND MESON RESONANCE PRODUCTION

proceedings of the Daresbury Study Weekend
1-2 February, 1975

Edited by

J. B. Dainton
Daresbury Laboratory

and

A. J. G. Hey
University of Southampton

Science Research Council
DARESBURY LABORATORY
1975

THIS PAGE

WAS INTENTIONALLY

LEFT BLANK

FOREWORD

In recent years much effort has been devoted to the complex problems of spin-parity analysis of three particle systems. A lot has already been learnt from the application of such techniques to reactions involving the production of three mesons. Large scale spectrometer experiments with their immense statistics are now turning their attention to these systems. It therefore seemed timely to devote a study weekend to explanation and discussion of the three particle partial wave analysis "black box".

The purpose of this Daresbury Study Weekend was intended to be somewhat different from its predecessors. We invited those with practical experience of the analysis techniques to explain themselves to others who, in the near future, would be confronted with thousands, if not millions, of events. We invited theoreticians to explain and discuss the validity and limitations of such analyses and what may be learnt from the results. Our hope is that these proceedings reflect to some degree the interest and excitement of the resulting meeting and that they will be of use to those who are or will be involved with the study of multibody reactions.

Neither the meeting nor the publication of these proceedings would have been possible without the generous support of the Daresbury Laboratory. In particular we thank Mrs. Shirley Lowndes and Miss Linda Houghton for holding our hands throughout the whole affair, Miss Ann Haskayne for much excellent typing, Mr. Ian Sharp for help with proof-reading and Mr. Geoff Berry for his excellent art-work. We are grateful to the speakers both for their talks and for their co-operation in the preparation of these proceedings, and to Professor A. Donnachie for his support, encouragement and guidance. Roger Cashmore was of great assistance during the planning of this meeting.

John Dainton

Tony Hey

THIS PAGE

WAS INTENTIONALLY

LEFT BLANK

C O N T E N T S

INTRODUCTORY REMARKS :

QUARKS, MESONS AND THREE PARTICLE PHASE SHIFT ANALYSIS

A.J.G. Hey,
University of Southampton.

THIS PAGE

WAS INTENTIONALLY

LEFT BLANK

INTRODUCTORY REMARKS: QUARKS, MESONS, AND THREE-PARTICLE PHASE SHIFT ANALYSIS

by

A.J.G. Hey
Department of Physics, University of Southampton

A21

The interest in three particle phase shift analysis must surely derive from the hope that it can answer many important questions for quark schemes of hadrons. The following brief remarks are intended as a guide to those uninitiated into quark model predictions for meson spectroscopy and associated outstanding unanswered questions.

The basic spectroscopic quark model[1] prescribes that the allowed meson SU(6) multiplets (J^P and SU(3)) are those of a quark-antiquark system - just a spin 1/2 fermion-antifermion system plus SU(3). (for the moment we ignore charm and SU(4)[2]). We therefore have the relations

$$\underset{\sim}{J} = \underset{\sim}{L} + \underset{\sim}{S} \qquad P = (-1)^{L+1} \qquad C = (-1)^{L+S}$$

where $\underset{\sim}{L}$ is the total quark orbital angular momentum, $\underset{\sim}{S}$ the quark spin (1 or 0) and $\underset{\sim}{J}$ the physical spin of the resonance. An harmonic oscillator interaction is often used as some sort of guide to the expected meson spectrum. This is shown in fig.1 where we note that at the n = 2 level there are two L-values allowed. (The n = 2, L = 0 state is often referred to as a radial excitation of the ground state.) Compared with the baryon spectrum[3] progress has been slow. The dismal state of confusion of the L = 1 meson multiplet is illustrated in figs.2(a) and 2(b).

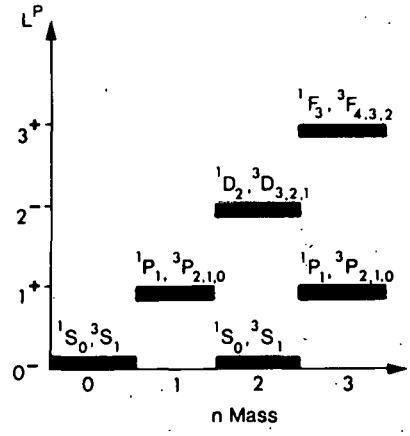

Fig.1 Harmonic oscillator spectrum for the mesons Notation $^{2S+1}L_J$

J^{PC}	I = 1	I = 1/2	I = 0	I = 0
2^{++}	A_2	K^{**}	f	f'
1^{++}	A_1	Q_A	D	E
0^{++}	δ	κ	ε	S^*
1^{+-}	B	Q_B		

J^{PC}	I = 1	I = 1/2	I = 0	I = 0
2^{++}	A	K^{**}	f	f'
1^{++}				
0^{++}				
1^{+-}	B			

Fig.2. Status of L = 1 meson multiplet (a) Optimistic (b) Pessimistic.

What are the reasons for this conspicuous lack of progress?

One reason is perhaps obvious. The $q\bar{q}$ resonances of unnatural spin parity cannot decay to two pseudoscalar mesons, and one must turn to three meson systems - hence this meeting. The most important reason for the slow progress is, however, the lack of stable meson targets. Most information on two and three meson systems derives from the following types of production reactions.

1. VIRTUAL PION TARGETS

Using a pion or a photon beam incident on nucleons one may extract from the very small momentum transfer data the pion pole contribution

2. REGGEON TARGETS

In these types of analyses one makes assumptions concerning the reaction mechanism producing the multimeson system.

Unfortunately, most data derives from diffractive reactions involving Pomeron exchange and it is here that one is involved in interpretation problems and discussion of the Deck model[4]. It is possible that non-diffractive reactions despite their small cross sections may have fewer "background" problems.

In the next few years, three particle phase shift analysis of much high quality data from these two types of processes should provide some of the long-sought answers in spectroscopy. These answers are important beyond SU(3) spectroscopy. For the charm interpretation of the ψ or J, and the ψ', the decays of the ψ' into the ^1P and ^3P $(q\bar{q})$ states are very important for the charmonium scheme[2], and it is clear that we need to understand the SU(3) ^1P and ^3P states. It is interesting that sequential decays of the ψ and ψ' involving photons will be very important for finding new charmonium states if they exist, and it is possible that such methods may also be useful in conventional spectroscopy. For example, simple quark model calculations[5] indicate that $g \to A_2\ \pi$ and $g \to A_1\ \pi$ could be substantial decay modes.

When we have disentangled the resonance spectrum one can then go on to test quark schemes for the decays of resonances. For the baryons, there now exists much detailed information on $N\pi$, $\Delta\pi$, $N\gamma$, and $N\rho$ decay modes. Isobar model analyses of $\pi\pi N$ systems have been vital for testing SU(6) models in a meaningful way. Furthermore, $SU(6)_w$ analyses can help determine the radial excitation structure of the baryon spectrum: there are indications that this may be different from that predicted by a simple harmonic oscillator model for baryons[6].

In conclusion I list below some of the urgent problems in meson spectroscopy that we can hope to answer by a better understanding of three phase shift analysis applied to meson systems:-

1. The A_1 "crisis" and the whole SU(6) × O(3) structure.
2. The helicity structure of decays and $SU(6)_w$ models.
3. The radial excitation structure. How should the $\rho'(1600)$ best be classified? This is important for charm schemes of the ψ and ψ'.
4. Mixing systematics. So far, (ω,ϕ) and (f,f'), S = 1 resonances are magically mixed and the (η,η') system, S = 0, unmixed. Is this simple correspondence with quark spin a general feature?
5. Zweig's "Twig" Rule. This forbids disconnected quark diagrams as in $\phi \to 3\pi$ (fig.3(a)). An excited state of the ϕ would enable one to test a subtle variant of this rule[7], namely $\phi^* \to \phi\pi\pi$ (fig.3(b)). A possible candidate for such a test is the expected ϕ partner of the $\omega(1675)$ in the 3^{--} nonet[8].

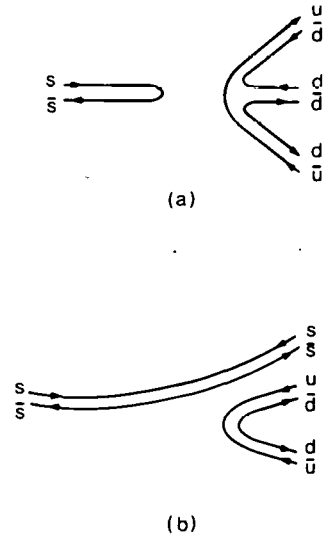

Fig.3 Quark diagrams (a) for $\phi \to 3\pi$ (b) for $\phi^* \to \phi\pi\pi$.

The moral of these remarks is that although charm and SU(4) have more glamour, (not a new quantum number), understanding SU(3) and SU(6) meson spectroscopy is just as vital for real progress.

I thank John Dainton for comments.

REFERENCES

1. Two recent reviews of quark models are H.J.Lipkin, Phys. Reports C8, (1973) and J.L. Rosner, Phys. Reports (to be published).

2. See M.K. Gaillard, B.W. Lee and J.L. Rosner, FERMILAB-Pub-74/86-THY and FERMILAB-Pub-75/14-THY which describes the charm hypothesis in detail.

3. J.L. Rosner, report to XVII Int. Conf. on High Energy Physics, London 1974 (Ed. J.R. Smith).

4. See Berger's talk, these proceedings.

5. H. Burkhardt and A.J.G. Hey, preprint in preparation.

6. R.J. Cashmore, A.J.G. Hey and P.J. Litchfield, Southampton University Preprint, THEP 74/5-6.

7. H. Harari, SLAC-PUB-1514

8. See Wagner's talk, these proceedings.

THIS PAGE

WAS INTENTIONALLY

LEFT BLANK

SESSION 1

Chairman: A.J.G. Hey

THE FORMALISM OF THREE PARTICLE PARTIAL WAVE ANALYSIS

Invited Talk

THREE MESON PARTIAL WAVE ANALYSIS - BASIC THEORY

G.T. Jones
University of Birmingham

Contribution

SOURCES OF INCOHERENCE IN 3-BODY PARTIAL WAVE ANALYSIS

R.J. Cashmore
Nuclear Physics Laboratory, University of Oxford

THIS PAGE

WAS INTENTIONALLY

LEFT BLANK

THREE MESON PARTIAL WAVE ANALYSIS - BASIC THEORY

by

G.T. Jones
University of Birmingham

A21

1. INTRODUCTION

In recent years, studies of baryonic three particle states produced in s-channel reactions such as

have yielded many new resonances. The reason for this success is that improved partial wave techniques have been applied to high-statistics experimental data. The resonances that have been found are, on the whole, very well described by the symmetry schemes SU(6) ⊗ O(3) and $SU(6)_w$.

The spectroscopy of three meson systems has not progressed so much because mesons are only produced in exchange processes such as

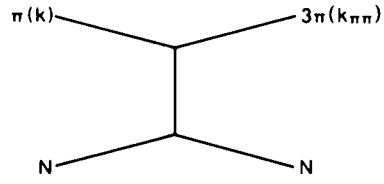

This makes life harder for a variety of reasons: usually one does not know how to parametrize the exchanged system; the production of the three-meson system is complicated by t-dependent form factors, to mention but two.

Nevertheless, in the last three or four years, our understanding of three-meson systems produced in t-channel reactions has increased greatly, due mainly to the efforts of Ascoli and co-workers at the University of Illinois[1-4]. They developed a partial wave analysis in which the 'decay' distribution of the three meson system (a function of two Dalitz plot variables and three Euler angles) is fitted for density matrix elements and certain decay parameters. By fitting in the five dimensional space, one does not throw away (as one does, for example, in a Dalitz plot analysis) information on the interference between amplitudes for producing three meson states of different spin-parity.

More recently, a similar analysis was developed at Lawrence Berkeley Laboratory[5]. The main difference between this and the Illinois analysis is that it determines amplitudes, not density matrix elements. It is encouraging to know that these analyses agree very well, at least for diffractively produced three meson systems.

Perhaps the most tantalising question arising from these analyses is: "where is the A_1?" A resonating A_2 has been seen again and again, but no resonating A_1. This, and other questions, are discussed by other speakers at this meeting.

The aim of this talk is to introduce the formalism and thereby provide a framework upon which to build.

2. TWO MESON PARTIAL WAVE ANALYSIS

Experimental results on the production of many body systems (data summary tapes) consist of four-momenta from which continuous distributions may be obtained; for example, in the reaction $\pi N \to (2\pi)N$, angular distributions of the pions can be plotted. From these distributions partial wave analyses yield information on the angular momentum states involved. This is what the theoreticians want because their models, being Lorentz invariant, give answers in terms of angular momentum states.

One cannot do a partial wave analysis without the appropriate link between the continuous description of particle states and the equivalent discrete description. To illustrate this point let us consider the reaction a + b → 1 + 2 + 4. Where a, 1, and 2 are mesons while b and 4 are nucleons. (Comparisons

of 2 meson and 3 meson partial wave analyses will be made later.)

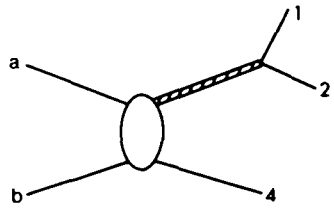

The amplitude can be written

$$f_{\lambda_b\lambda_4} = \langle \underset{\sim}{p}_1\ \underset{\sim}{p}_2;\ \underset{\sim}{p}_4\ \lambda_4\ |U|\ \underset{\sim}{p}_a;\ \underset{\sim}{p}_b\ \lambda_b\rangle = \langle \underset{\sim}{p}_{12}\ M_{12}\ \phi\ \theta;\ \underset{\sim}{p}_4\ \lambda_4\ |U|\ \underset{\sim}{p}_a;\ \underset{\sim}{p}_b\ \lambda_b\rangle \quad (1)$$

Here the momenta $\underset{\sim}{p}$ and helicities λ are taken in the overall centre-of-mass system, and U is a 'transition operator' which conserves angular momentum and parity.

Now the 2-particle system described by $|\underset{\sim}{p}_{12}\ M_{12}\ \phi\ \theta\rangle$ is equally well described by $|\underset{\sim}{p}_{12}\ M_{12}\ J_{12}\ \Lambda_{12}\rangle$ where J_{12} is the spin of the (12)-system and Λ_{12} is its helicity in the overall centre-of-mass system. If we choose the axis of quantization to be along the (12)-direction of motion then $\Lambda_{12} = m$, the third component of angular momentum. Also for a decay like $K^*(890) \to K\pi$, the relative orbital angular momentum ℓ of the K and π is just J_{12}. So $J_{12} \equiv \ell$, $\Lambda_{12} \equiv m$.

The link between the continuous and discrete descriptions of the two particle states is given by

$$\langle \underset{\sim}{p}_{12}\ M_{12}\ \phi\ \theta\ |\underset{\sim}{p}_{12}\ M_{12}\ \ell\ m\rangle = Y_\ell^m(\phi,\theta) = \sqrt{\frac{2\ell+1}{4\pi}}\, D^{(\ell)*}_{mo}(\phi,\theta,0) \quad (2)$$

(The Y_ℓ^m's are the eigenfunctions of a quantum mechanical dumbell.) Expanding the expression for $f_{\lambda_b\lambda_4}$ in terms of angular momentum states we obtain

$$f_{\lambda_b\lambda_4} = \sum_{\ell m} \langle \underset{\sim}{p}_{12}\ M_{12}\ \phi\ \theta;\ \underset{\sim}{p}_4\ \lambda_4\ |\ \underset{\sim}{p}_{12}\ M_{12}\ \ell m;\ \underset{\sim}{p}_4\ \lambda_4\rangle \langle \underset{\sim}{p}_{12}\ M_{12}\ \ell m;\ \underset{\sim}{p}_4\ \lambda_4\ |U|\ \underset{\sim}{p}_a;\ \underset{\sim}{p}_b\ \lambda_b\rangle \quad (3)$$

It is usual to fix $\underset{\sim}{p}_{12} = 0$, i.e., to work in the (12)-centre-of-mass. For a small enough mass interval M_{12} is considered fixed. Also, if we are considering pure $K^*(890)$, for example, then ℓ is fixed at $J_{12} = 1$. The expression for $f_{\lambda_b\lambda_4}$ can be written

$$f_{\lambda_b\lambda_4} = \sum_m Y_\ell^m(\phi,\theta)\ f_{\lambda_4 m,\lambda_b} \quad (4)$$

and the cross section is proportional to

$$W \equiv \sum_{\lambda_b\lambda_4} |f_{\lambda_b\lambda_4}|^2 \equiv \sum_{mm'} Y_\ell^m(\phi,\theta) \sum_{\lambda_4\lambda_b} f_{\lambda_4 m,\lambda_b} f^*_{\lambda_4 m',\lambda_b} Y_\ell^{m'*}(\phi,\theta) \quad (5a)$$

$$\equiv \sum_{mm'} Y_\ell^m(\phi,\theta)\ \rho_{mm'}(s,t,M_{12})\ Y_\ell^{m'*}(\phi,0) \quad (5b)$$

Let us look at a specific example, $K^*(890) \to K\pi$. If we incorporate the fact that parity is conserved in the production process the expression for W becomes

$$W = \frac{3}{4\pi}\left\{\frac{1}{2}(1-\rho_{00}) + \frac{1}{2}(3\rho_{00}-1)\cos^2\theta - \rho_{1-1}\sin^2\theta\cos^2\phi - \sqrt{2}\,\mathrm{Re}\,\rho_{10}\sin^2\theta\cos\phi\right\} \quad (6)$$

The density matrix elements are determined by taking moments or by a maximum likelihood method[6].

It is worth noticing that Im ρ_{10} does not appear in eqn.(6) and thus cannot be determined.

3. THREE MESON PARTIAL WAVE ANALYSIS

With three mesons in the final state the angular momentum algebra becomes somewhat harder but the ideas are more or less the same. Consider the reaction

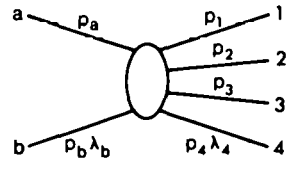

where 1, 2, and 3 are spinless mesons while b and 4 are baryons. In the helicity representation the amplitude for this reaction can be written

$$f_{\lambda_b\lambda_4} \equiv \langle \underset{\sim}{p}_1\ \underset{\sim}{p}_2\ \underset{\sim}{p}_3;\ \underset{\sim}{p}_4\ \lambda_4|U|\ \underset{\sim}{p}_a;\ \underset{\sim}{p}_b\ \lambda_b\rangle \quad (7)$$

where the momenta $\underset{\sim}{p}$ and helicities λ are taken in the overall centre-of-mass system (helicity is not a Lorentz invariant) and where U is a 'transition'

operator which conserves angular momentum and parity. Equivalently, we can write

$$f_{\lambda_b\lambda_4} = \langle \underset{\sim}{p}_{123}\ M_{123}\ \Phi_{13}\ \Theta_{13}\ M_{13}\ \psi_{13}\ \chi_{13};\ \underset{\sim}{p}_4\ \lambda_4 \mid U \mid \underset{\sim}{p}_a;\ \underset{\sim}{p}_b\ \lambda_b \rangle \quad (8)$$

Here: $\underset{\sim}{p}_{123} = \underset{\sim}{p}_1 + \underset{\sim}{p}_2 + \underset{\sim}{p}_3$ = momentum of (123) system in overall centre-of-mass; M_{123} = invariant mass of particles 1, 2, and 3; Φ_{13} and Θ_{13} are the azimuthal and polar angles of the (13) system in the (123) rest frame (either the helicity system or the Gottfried-Jackson system can be used); M_{13} = invariant mass of particles 1 and 3; ψ_{13} and χ_{13} are the azimuthal and polar angles of particle 3 in the (13) rest frame. In this description we are picturing the three particle state

$$|\underset{\sim}{p}\ M\ \Phi\ \Theta\ M\ \psi\ \chi\ldots\rangle$$

as two 'dumbell' systems, with particles 1 and 3 going round each other as well as (13) and 2 going round each other. When we go to the equivalent discrete representation, the continuous variables Φ_{13}, θ_{13}, ψ_{13}, and χ_{13} are replaced by the discrete variables J, Λ, j_{13}, and λ_{13} where

- J = spin of the (123) system;
- Λ = helicity of the (123) system in the overall centre-of-mass;
- j_{13} = spin of the (13) system;
- λ_{13} = helicity of the (13) system in the (123) rest system.

The link between the two states

$$|\underset{\sim}{p}_{123}\ M_{123}\ \Phi_{13}\ \Theta_{13}\ M_{13}\ \psi_{13}\ \chi_{13}\rangle$$

and

$$|\underset{\sim}{p}_{123}\ M_{123}\ J\ \Lambda\ M_{13}\ \psi_{13}\ \chi_{13}\rangle$$

is

$$\langle \underset{\sim}{p}_{123}\ M_{123}\ \Phi_{13}\ \Theta_{13}\ M_{13}\ \psi_{13}\ \chi_{13} | \underset{\sim}{p}_{123}\ M_{123}\ J\ \Lambda\ M_{13}\ j_{13}\ \lambda_{13}\rangle = \sqrt{\frac{2J+1}{4\pi}}\sqrt{\frac{2j+1}{4\pi}} \cdot D^{(J)*}_{\Lambda\lambda_{13}}(\Phi_{13},\Theta_{13},0)\ D^{(j)*}_{\lambda_{13}0}(\psi_{13},\chi_{13},0) \quad (9)$$

Expanding in terms of three particle states of definite angular momentum and then changing variables a few times to get things into a convenient form, one can show that the cross section is proportional to

$$W = \sum \mathscr{M}^{J^P\Lambda n\ell jn}(\phi,\theta,\gamma,s_1,s_2)\ \rho^{J^P\Lambda n\ell jn}_{J'^{P'}\Lambda'n\ell'j'n}(s,t,M_{123},s_n) \left[\mathscr{M}^{J'^{P'}\Lambda'n\ell'j'n}(\phi,\theta,\gamma,s_1,s_2)\right]^* \quad (10)$$

The sum is over all possible values of $J^P\Lambda n\ell jn$ and $J'^{P'}\Lambda'n\ell'j'n$. Full details of the various steps involved are given in ref.(4). Before going on to say what all the symbols mean one should note that this formula has the same form as eqn.(5b):

$$W \equiv \sum_{qq'} \mathscr{M}_q\ \rho_{qq'}\ \mathscr{M}^*_{q'} \quad \text{with } q \equiv \{J^P\Lambda n\ell jn\} \quad (11)$$

In the case of the K^* decay we only asked questions about one angular momentum quantum number, namely m,

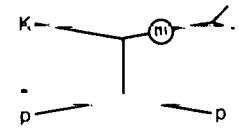

In the reaction a + b → 1 + 2 + 3 + 4 we ask questions about more angular momentum quantum numbers, namely $J^P\Lambda n\ell jn$. To see what they mean consider the picture.

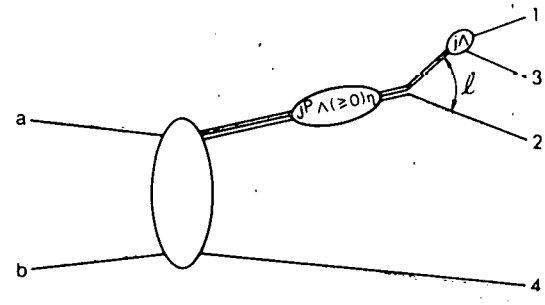

This corresponds to n = 2 i.e., particles 1 and 3 are coupled. (The subscripts on j, λ, and ℓ are no longer necessary.)

If one sums over all allowable values of $J^P\Lambda n\ell j$ <u>any one</u> of the three couplings (n = 1, 2, or 3) gives a <u>complete exact description</u> of the reaction.

Next let us consider the kinematical variables. (There are three more than in the case of di-meson production because there is one more particle!)

The angles ϕ, θ, and γ give the orientation of the 3-meson plane in the (123)-rest system (see ref.(4) for details).

The quantities s_n are the squares of the invariant masses of the two mesons involved in coupling n.

The quantities s, t, and M_{123} are, respectively, the square of the centre-of-mass energy, the square of the 4-momentum transfer between incident and recoiling nucleons, and the invariant mass of the (123)-system. Notice:

(1) The density matrix depends on s_n (i.e., it varies over the Dalitz plot).

(2) The absence of λ in eqn.(10); it has been replaced by ℓ (and there is a Clebsch-Gordan coefficient in $\mathscr{M}$ to take care of things).

(3) An N x N density matrix has N^2 real numbers in it, and so it is clear that assumptions have to be made before one can start fitting data.

(4) A new quantity η has been introduced; it is the eigenvalue (± 1) of the reflection operator in the production plane

$$\mathcal{Y} = \exp(-i\pi J_y)\mathbb{P} \qquad (12)$$

where $\mathbb{P}$ = parity operator.

What is η?

If one defines

$$|J^P \Lambda_\eta\rangle = c_\Lambda \{|J^P \Lambda \ldots\rangle + \eta\, \varepsilon(-1)^{\Lambda} |J^P -\Lambda \ldots\rangle\}$$

where $\varepsilon = P(-1)^{J+1}$, $c_\Lambda = \sqrt{\frac{1}{2}}$ for $\Lambda \neq 0$ and $c_\Lambda = \frac{1}{2}$ for $\Lambda = 0$, one can replace, for example, the basic 1^+ states $|1^+1\rangle$, $|1^+0\rangle$, and $|1^+ -1\rangle$ by

$$|1^+ 1+\rangle = \sqrt{\tfrac{1}{2}} \{|1^+1\rangle - |1^+ -1\rangle\}$$

$$|1^+ 0+\rangle = |1^+0\rangle$$

$$|1^+ 1-\rangle = \sqrt{\tfrac{1}{2}} \{|1^+1\rangle + |1^+ -1\rangle\}$$

Notice that in the $|J^P \Lambda\eta\rangle$ states we have $\Lambda \geq 0$. There are two advantages of the $\{|J^P \Lambda\eta\rangle\}$ representation:

(i) the density matrix is diagonal in η (provided that we do not measure polarization and that the y-axis is taken as the production plane normal);

(ii) $\eta = +1$ corresponds to natural parity exchange and $\eta = -1$ corresponds to unnatural parity exchange.

(5) Rank of the density matrix is 2.

In full, the density matrix ρ of eqn.(10) is given by

$$\rho^{\ell\ell' jj' n(n)}_{J^P \Lambda\eta, J'^{P'} \Lambda'\eta}(s,t,M_{123},s_n) = \sum h^{J^P \ell j n\eta}_{\Lambda\lambda_b\lambda_4} \left(h^{J'^{P'} \ell' j' n\eta}_{\Lambda\lambda_b\lambda_4}\right)^* \qquad (13)$$

where h is the amplitude for producing a three meson state $|J^P \Lambda \ell j n\eta\rangle$ and a recoil with helicity λ_4; the helicity of the target is λ_b.

Now parity conservation in the production process imposes the conditions

$$h^{J^P \ell j n\eta}_{\Lambda\lambda_b\lambda_4} = \eta(-1)^{1+\lambda_b+\lambda_4} h^{J^P \ell j n\eta}_{\Lambda\ -\lambda_b\ -\lambda_4} \qquad (14)$$

on the amplitudes h.

From eqns.(13) and (14) the density matrix can be written

$$\rho^{\ell\ell' jj' n(n)}_{J^P \Lambda\eta, J'^{P'} \Lambda'\eta} = 2 \left\{ h^{J^P \ell j n\eta}_{\Lambda\,+\,+} \left(h^{J'^{P'} \ell' j' n\eta}_{\Lambda\,+\,+}\right)^* + h^{J^P \ell j n\eta}_{\Lambda\,+\,-} \left(h^{J'^{P'} \ell' j' n\eta}_{\Lambda\,+\,-}\right)^* \right\} \qquad (15)$$

Now it is a mathematical fact that the matrix $\mathscr{A}$ formed from a vector a according to the prescription

$$\mathscr{A} \equiv \begin{pmatrix} a_1 \\ a_2 \\ \vdots \\ a_N \end{pmatrix} (a_1^* \; a_2^* \; \ldots \; a_N^*) \qquad (16)$$

can only have one non-zero eigenvalue. Equation (15) shows that the density matrix ρ is of the form

$$\rho = \begin{pmatrix} a_1 \\ a_2 \\ \vdots \\ a_N \end{pmatrix} (a_1^* \; a_2^* \; \ldots \; a_N^*) + \begin{pmatrix} b_1 \\ b_2 \\ \vdots \\ b_N \end{pmatrix} (b_1^* \; b_2^* \; \ldots \; b_N^*) \qquad (17)$$

So, ρ can have at most two non-zero eigenvalues for a given η, corresponding to spin-flip and non-spin-flip at the nucleon vertex. This is strictly true at fixed s, t, and M_{123}.

4. ASSUMPTIONS

In order to reduce the number of unknown parameters to a reasonable amount several assumptions have to be made.

(a) Assume $\boxed{J \leq J_{max}}$ where J_{max} can be estimated from a moments analysis.

(b) For simplicity let us consider the specific reaction

$$K^+p \to K^+\pi^+\pi^-p \qquad (18)$$
$$\quad 1\ 2\ 3$$

To emphasise the fact that the amplitude $f_{\lambda_b\lambda_4}$ can be written in terms the n = 1 or n = 2 couplings we shall write it

$$f_{\lambda_b\lambda_4} \sim \frac{1}{2}\left(\sum_{j_1}^{\infty} + \sum_{j_2}^{\infty}\right) \qquad (19)$$

This is EXACT.

Assume

$$\boxed{f_{\lambda_b\lambda_4} \sim \sum_{j_1}^{2} + \sum_{j_2}^{2}} \qquad (20)$$

That the 1/2 is missing in eqn.(20) reflects the assumption that the high partial waves in one particular coupling are covered by the low partial waves in the other.

This assumption is motivated by the observations that the $(K^-\pi^+)$ and $(\pi^-\pi^+)$ effective mass distributions show $K^*(890)$, $K^*(1420)$, ρ and f signals and also that phase shift analyses find that s, p, and d waves are enough to describe the $(K^-\pi^+)$ and $(\pi^-\pi^+)$ systems at low masses.

Overlap between some or all of the n = 1 couplings and the n = 2 couplings corresponds to, and is counted as, interference between 'decay modes' (strictly speaking, we have not talked about any decays yet).

(c) Assume

$$\boxed{h^{J^P\ell jn\eta}_{\Lambda\lambda_b\lambda_4}(s,t,M_{123},M_n) = \bar{h}^{J^P\ell jn\eta}_{\Lambda\lambda_b\lambda_4}(s,t,M_{123}) \cdot BW^{(jn)}(M_n)\, q^j(M_n)\, p^\ell(M_{123},M_n)} \qquad (21)$$

Here one is adopting Watson's[7] idea of a final state interaction to factorize the M_n dependence out of the density matrix (or amplitude). The quantities q^j and p^ℓ are the usual angular momentum barrier factors while BW parametrizes the mass dependence of the di-meson system either by a Breit-Wigner or by phase shifts. (This assumption violates unitarity).

(d) These three assumptions are still not enough to reduce the number of parameters to a realistic level. Consider the reaction

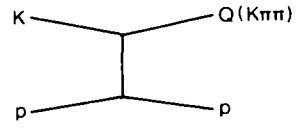

How many parameters would be needed if we were to try the hypotheses of Table 1? The answer is 49; the N x N density matrix has 49 real parameters in it. The list in Table 1 does not include any $K\pi$, $K\varepsilon$, $K^*(1420)\pi$, or Kf 'decay modes'. With the number of parameters going up as N^2 the situation is hopeless

Table 1

J^P	ℓ	Λ	η	Decay Mode	j	n
0^-	P	0	+	$K^*\pi$	1	2
0^-	P	0	+	$K\rho$	1	1
1^+	S	0	+	$K^*\pi$	1	2
1^+	S	0	+	$K\rho$	1	1
1^+	S	1	+	$K^*\pi$	1	2
2^-	P	0	+	$K^*\pi$	1	2
2^-	P	0	+	$K\rho$	1	1

Assume

$$\boxed{h^{J^P\ell jn\eta}_{\Lambda\lambda_b\lambda_4}(s,t,M_{123}) = T^{J^P\eta}_{\Lambda\lambda_b\lambda_4}(s,t,M_{123})\; C^{J^P\ell jn}(s,t,M_{123})} \qquad (22)$$

Here we are factorizing the amplitude h into (i) a production amplitude T which is independent of ℓ, j, and n, and (ii) a decay parameter C which is independent of Λ, λ_b, λ_4, and η.

It is now possible to define new 'reduced density matrix elements' given by

$$\rho^{(s,t,M_{123})}_{J^P\Lambda\eta,J'^{P'}\Lambda'\eta} = \sum_{\lambda_b\lambda_4} T^{J^P\eta}_{\Lambda\lambda_b\lambda_4}\left(T^{J'^{P'}\eta}_{\Lambda'\lambda_b\lambda_4}\right)^* \qquad (23)$$

Now that we only have one density matrix row per $J^P\Lambda\eta$ combination, the number of parameters is greatly reduced. For the example considered above, the number drops from 49 to 16. In addition, there are three complex decay constants C to be determined. This makes a total of 22 parameters. (By means of a suitable normalization convention it is possible to put one $C^{J^P\ell jn}$ equal to unity for every $J^P\Lambda\eta$ state considered.)

Note 1. For pure resonance production, assumption 4 is automatically satisfied.

5. METHOD OF ANALYSIS

5.1 Features

The quantities C and ρ (actually their averages over finite ranges of t and M_{123}, and perhaps s) are determined by a maximum likelihood method.

Here we mention briefly some of the features of the Illinois analysis.

(i) The program rigorously takes account of any biases or non-uniform acceptances (so long as they are understood). The reason for this is that at fixed s, t, and M_{123} a knowledge of ϕ, θ, γ, s_1, and s_2 completely describes an event (up to a rotation). In other words one can calculate the 4-momenta of the particles from s, t, M_{123}, ϕ, θ, γ, s_1 and s_2. Thus it is possible, for example, to ask of an individual event in the reaction $K^+p \to K^+\pi^+\pi^-p$, "Does the $p\pi^+$ effective mass correspond to the Δ^{++}?", and hence to remove that event. The same is done to the Monte Carlo events used to generate integrals.

(ii) The density matrix is constrained to be positive definite. This is done by transforming from density matrix element space to eigenvalue and eigenvector space where the constraints take on a particularly simple form - that the eigenvalues must be positive.

(iii) By fitting in terms of all five 'decay' variables one uses up all the information contained in the event. In analyses such as moments analyses or Dalitz plot analyses one integrates away information (furthermore it is impossible to correct for biases properly in such analyses).

(iv) It is possible to measure some imaginary parts of density matrix elements. This is made possible by the presence of the imaginary parts of the di-meson parametrizations. The idea is the following. The distribution being measured is of the form

$$W \sim \mathrm{Re}\,(\rho_{ij}\,\mathscr{M}_i^*\,\mathscr{M}_j)$$

$$= (\mathrm{Re}\,\rho_{ij})(\mathrm{Re}\,\mathscr{M}_i^*\,\mathscr{M}_j) - (\mathrm{Im}\,\rho_{ij})(\mathrm{Im}\,\mathscr{M}_i^*\,\mathscr{M}_j)$$

The only complex number in $\mathscr{M}$ is in the parametrization of the Breit-Wigner. To measure $(\mathrm{Im}\,\rho_{ij})$ one must have $(\mathrm{Im}\,\mathscr{M}_i^*\,\mathscr{M}_j) \neq 0$. For more details see refs.(4) and (8).

5.2 What does one measure?

One actually determines products $C\,\rho\,C^*$ (remember one C for each J^P can be fixed to an arbitrary complex number which is taken to be unity). From these one can calculate (see ref.(4)):

(i) the number of events in a given $J^P\Lambda\eta$ state;

(ii) for a given $J^P\Lambda\eta$ state, the number of events in given decay modes and the extent to which they interfere;

(iii) a 'coherence factor' which measures the extent to which amplitudes for producing states of different spin-parity interfere;

(iv) The relative phases of amplitudes for producing states of different spin-parity (this can be done only if the coherence factor is consistent with one).

In conclusion, it is perhaps worth stating the obvious - that what comes out of partial wave programs depends on what is put in. The basic assumptions discussed in this talk are being questioned and some of the findings are discussed in these proceedings.

REFERENCES

1. G.Ascoli et al, Phys. Rev. Letts. 25, (1970) 962.

2. G.Ascoli et al, Phys. Rev. D7, (1973) 669.

3. P.V.Brockway, Ph.D. Thesis, University of Illinois, Urbana, (1970).

4. J.D.Hansen, G.T.Jones, G.Otter and G.Rudolph, Nucl. Phys. B81, (1974) 403.

5. R.J.Cashmore in Phenomenology of Particles at High Energies, Ed. R.L.Crawford and R.Jennings, (N.Y., London, Academic Pr., 1973).

6. N.Schmidtz, CERN Report, CERN 65-24, (1965).

7. K.M.Watson, Phys. Rev. 88, (1952) 1163.

8. M.G.Bowler, CERN Report, CERN-Phys. 73-40, (1973).

SOURCES OF INCOHERENCE IN 3-BODY PARTIAL WAVE ANALYSIS

by

A21

R.J. Cashmore,
Nuclear Physics Laboratory, University of Oxford,
Keble Road, Oxford OX1 3RH

In this presentation I will try to define all the sources of incoherence that can occur in the analysis of 3-particle states in production experiments. This is not meant to be a complete and rigorous treatment but rather a guide. This means that the examples will necessarily be simple and often stupid. Nonetheless they will contain extreme examples of situations that do occur. I have separated each origin as much as possible. In practice the true situation will correspond to a combination of all of these sources.

The method followed is to present a model reaction and then see how it is dealt with by both the density matrix approach (Illinois method) and the amplitude analysis approach (SLAC/LBL method). I will always regard the amplitudes as true production amplitudes for simplicity of discussion (see V. Chaloupka's talk for the mathematical generalization of this)

The basic relationship between the density matrix approach and the amplitude analysis approach is embodied in the relation

$$\rho^{nn'} = f^{n}_{++} \; f^{n'*}_{++} + f^{n}_{+-} \; f^{n'*}_{+-} \qquad (1)$$

where n represents any group of quantum numbers we consider e.g. $J^{P}LM(\pi K^{*})$ and ++(+-) are the nucleon helicities before and after the reaction.

By incoherence we mean

(a) $$|\rho^{nn'}|^2 = \xi |\rho^{nn}|^2 \; |\rho^{n'n'}|^2 \qquad (2)$$

where $$\xi < 1 \qquad (3)$$

(b) Some states n are only produced with non-flip and others n' are only produced with flip of the nucleon indices. They will then be incoherent in the decay distributions. This is the simplest way to envisage incoherence in the amplitude analysis, but not the only way. Application of eqn.(1) will then result in $\xi < 1$.

The following examples use M^{n} to represent the decay amplitude for the state n into the final 3 bodies. It is important to remember that this in no way depends on the nucleon helicity labels.

We now proceed to the examples.

Example 1: Incoherence due to presence of both nucleon flip and non-flip indices.

Model: Suppose we have state n produced with nucleon non-flip and state n' produced with flip. They cannot interfere. Then the final distribution is given by

$$d^5\sigma = |f^{n}_{++} \; M^{n}|^2 + |f^{n'}_{+-} \; M^{n'}|^2 \qquad (4)$$

$$= |f^{n}_{++}|^2 \; |M^{n}|^2 + |f^{n'}_{+-}|^2 \; |M^{n'}|^2 \qquad (5)$$

Density Matrix Approach: Here we attempt to fit the distribution with a formula

$$\rho^{nn} \; |M^{n}|^2 + \rho^{nn'} \; M^{n} \; M^{n'*} + \rho^{n'n'} \; |M^{n'}|^2 \qquad (6)$$

The fit of (6) to (5) will clearly give $\rho^{nn'} = 0$

i.e. $$|\rho^{nn'}|^2 \neq \rho^{nn} \; \rho^{n'n'} \qquad (7)$$

and we have incoherence. ($\xi = 0$).
The density matrix deals with this approach satisfactorily.

Amplitude Analysis: First assume we use only spin non-flip waves (spin coherence) and we thus attempt to fit (5) with a formula of the type

$$|f^{n} \; M^{n} + f^{n'} \; M^{n'}|^2$$

$$\sim f^{n} f^{n*} \; |M^{n}|^2 + f^{n} f^{n'*} \; M^{n} M^{n'*} + |f^{n'}|^2 \; |M^{n'}|^2 \qquad (8)$$

We clearly force an interference term and thus we will be unable to obtain a sensible fit. Thus amplitude analysis with spin coherence will be disastrous.

However, if we allow both flip and non-flip amplitudes

$$|\sum_n f^n_{++} M^n|^2 + |\sum_{n'} f^{n'}_{+-} M^{n'}|^2 \qquad (9)$$

we can clearly obtain a good fit to (5). Thus amplitude analyses must have at least two independent sets of terms.

Example 2: Decay Coherence

This essentially enters because one tries to reduce the size of the general density matrix by introducing some assumptions. These assumptions are motivated by resonance domination. If we have a resonance which decays into $\pi\varepsilon$ and $\pi\rho$ then these branching fractions will be identical for all magnetic substates that the resonance is produced in (rotational invariance)

Then

$$\left.\begin{aligned} f^{m\varepsilon} &= c^{\varepsilon}\ f^{m} \\ f^{m\rho} &= c^{\rho}\ f^{m} \end{aligned}\right\} \qquad (10)$$

where f^m is the amplitude for production of resonance R in magnetic substate $m(J_z)$ and c^ε, c^ρ are independent of m. The generalization of (10) to non-resonant amplitudes is my definition of decay coherence. This then implies that

$$\rho^{(m\varepsilon)(m'\rho)} = c^{\varepsilon}\ c^{\rho *}\ \rho^{mm'} \qquad (11)$$

Model: Suppose we have

(i) a resonance produced in the m = 1 state which only decays into $\pi\rho$ (with no nucleon flip);

(ii) a 'Deck mechanism' which only populates the m = 0 state of $\pi\varepsilon$ (with no nucleon flip).

Then the true distribution will be given by

$$d^5\sigma = |f^{1\rho}|^2\ |M^{1\rho}|^2 + |f^{0\varepsilon}|^2\ |M^{0\varepsilon}|^2 + f^{1\rho}\ f^{0\varepsilon *}\ M^{1\rho}\ M^{0\varepsilon *} \qquad (12)$$

Density Matrix Approach: We attempt to describe (12) with the form

$$\begin{aligned} &\rho^{11}[|c^\rho|^2\ |M^{1\rho}|^2 + c^\rho c^{\varepsilon *}\ M^{1\rho} M^{1\varepsilon *} + |c^\varepsilon|^2\ |M^{1\varepsilon}|^2] \\ &+ \rho^{00}[|c^\rho|^2\ |M^{0\rho}|^2 + c^\rho c^{\varepsilon *}\ M^{0\rho} M^{0\varepsilon *} + |c^\varepsilon|^2\ |M^{0\varepsilon}|^2] \\ &+ \rho^{10}[|c^\rho|^2\ M^{1\rho}\ M^{0\rho *} + c^\rho c^{\varepsilon}\ M^{1\rho} M^{0\varepsilon *} \\ &\qquad + |c^\varepsilon|^2\ M^{1\varepsilon}\ M^{0\varepsilon *}] \end{aligned} \qquad (13)$$

We clearly use a formula (13) which forces interferences that are not present in the data and hence we will obtain an unreliable fit (which is very poor). Thus this form of density matrix approach gives a wrong answer.

Of course we will preserve generality if relation (11) is not imposed (with an increase in the number of fit parameters).

Amplitude Analysis: In this case we will fit with the form

$$d^5\sigma \propto |f^{1\rho}\ M^{1\rho} + f^{0\rho}\ M^{0\rho} + f^{1\varepsilon}\ M^{1\varepsilon} + f^{0\varepsilon}\ M^{0\varepsilon}|^2 \qquad (14)$$

and simply find $f^{0\rho} = \rho^{1\varepsilon} = 0$.

Thus in this case the amplitude analysis will give immediately the correct result.

Of course assumptions (10) can be made in an amplitude analysis and the problems described previously will occur.

Example 3: A combination of examples 1 and 3 to represent an assumption commonly made in the Illinois approach.

We often consider partial waves which can lead to different final state orbital angular momenta e.g. 1^+ which can give both S and D wave $\pi\rho$ systems.

Model: Suppose we have

(i) Deck model which gives only S-wave $\pi\rho$ systems in the 1^+0^+ wave (i.e. $M(J_z) = 0$) with nucleon non-flip;

(ii) A resonance ($J^P = 1^+$) produced in the M = 0 state with nucleon spin-flip and which only decays through the D-wave $\pi\rho$ system.

The true distributions are then

$$d^5\sigma = |f^{0S}_{++}|^2\ |M^{0S}|^2 + |f^{0D}_{+-}|^2\ |M^{0D}|^2 \qquad (15)$$

Density Matrix Approach: Here we make the assumption of (11) (with S and D instead of ε, ρ) and attempt to fit (14) with the following form

$$\rho^{00}[|c^S|^2\ |M^{0S}|^2 + c^S\ c^{D*}\ M^{0S}\ M^{0D*} + |c^D|^2\ |M^{0D}|^2] \tag{16}$$

We clearly force an interference term which will result in unreliable fits. Note in this case we do not get the warning signal of $\xi < 1$ since we are only considering the on-diagonal matrix element. The signature of this type of problem will be poor fits.

The most general form

$$\rho^{0S\ 0S}\ |M^{0S}|^2 + \rho^{0S\ 0D}\ M^{0S}\ M^{0D*} + \rho^{0D\ 0D}\ |M^{0D}|^2 \tag{17}$$

would give a good fit with $\rho^{0S\ 0D} = 0$.

Amplitude Analysis: Here we will fit with the form

$$|f^{0S}_{++}\ M^{0S} + f^{0D}_{++}\ M^{0D}|^2 + |f^{0S}_{+-}\ M^{0S} + f^{0D}_{+-}\ M^{0D}|^2 \tag{18}$$

and immediately find that the S-wave comes from one term and the D-wave from the other. Note however it is essential that one has the presence of both terms in the sum

Incoherence due to binning in M and t

Before going onto examples of this I want to remind you of the distributions with which we fit.

Density Matrix Approach

$$\rho^{n_1n_1}\ |M^{n_1}|^2 + \rho^{n_1n_2}\ M^{n_1}\ M^{n_2*} + \rho^{n_2n_2}\ |M^{n_2}|^2 \tag{19}$$

Amplitude Analysis

$$|f^{n_1}_{++}|^2\ |M^{n_1}|^2 + f^{n_1}_{++}\ f^{n_2*}_{++}\ M^{n_1}\ M^{n_2*} + |f^{n_2}_{++}|^2\ |M^{n_2}|^2$$
$$+ \{|f^{n_1}_{+-}|^2\ |M^{n_1}|^2 + f^{n_1}_{+-}\ f^{n_2*}_{+-}\ M^{n_1}\ M^{n_2*} \tag{20}$$
$$+ |f^{n_2}_{+-}|^2\ |M^{n_2}|^2\}$$

Example 4: Different t distributions for production of n_1 and n_2.

Model: Suppose we have the following situation

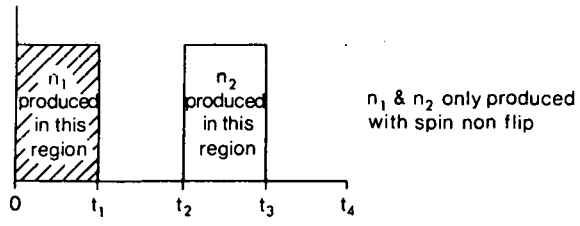

and we fit in a t bin which runs from 0 to t_4. The true distribution in the bin is

$$d^5\sigma = |f^{n_1}|^2\ |M^{n_1}|^2 + |f^{n_2}|^2\ |M^{n_2}|^2 \tag{21}$$

since n_1 and n_2 can never interfere.

Density Matrix Approach: We clearly obtain the result

$$\rho^{n_1n_2} = 0 \tag{22}$$

Thus we find that the density matrix approach gives us the correct result.

(Remember $\rho^{n_1n_2} = \int \sum_{\substack{++\\+-}} f^{n_1}\ f^{n_2*}\ dt$)

Amplitude Analysis:

In this case we will force an interference term and thus get an unreliable result. At first sight you might think we can escape by putting n_1 into spin non-flip and n_2 into spin flip. This would be true if we only had two waves. However we only need to introduce a third state n_3 to show that in general we cannot escape the problem in this way.

Of course we are not in general presented with such pathological cases and one way of escaping this type of problem is to deliberately expose the t dependence (e.g. put in e^{bt} or te^{bt} in the amplitude for a particular partial wave).

It should here be pointed out that there is a warning in the density matrix approach of this type of check - the rank of the density matrix will increase.

Example 5: Different phase variations in the production amplitudes of n_1 and n_2.

Model: Suppose we have the following situation

(i) n_1 production amplitude always real;

(ii) n_2 production amplitude real for $0 < t < t_1$ and imaginary for $t_1 < t < t_2$ where $t_1 = \frac{t_2}{2}$

(and the amplitudes are the same size and constant). Moreover suppose that in (19) and (20) $M^{n_1}\ M^{n_2*}$ is only real. Then only in $0 < t < t_1$ will we find any interference effects. The true distribution in the bin is

$$d^5\sigma = |f^{n_1}_{++}|^2\ |M^{n_1}|^2 + \frac{1}{2}\,\mathrm{Re}(f^{n_1}_{++}\ f^{n_2*}_{++})\ M^{n_1n_2*}$$
$$+ |f^{n_2}_{++}|^2\ |M^{n_2}|^2 \tag{23}$$

Density Matrix Approach: This is fine we just get an off-diagonal element $\rho^{n_1 n_2 *}$ which implies $\xi = \frac{1}{2}$

Amplitude Analysis: Here we run into problems because we specify the size of the interference term as $f^{n_2} f^{n_2 *}$, i.e. it would be twice as big. Thus we get an unreliable result.

Once again you might think we can escape by putting $\frac{1}{2} f^{n_2}$ in the first term of (20) and $\frac{1}{2} f^{n_2}$ in the second term. This would work. However introducing a third wave n_3 would lead to problems from which we could not escape.

Examples 4 and 5 have been pathological in origin. However we do meet these types of problems in practice:

(i) different t distributions are common for different waves;

(ii) different phase variations with t are quite common, e.g. pure imaginary diffractive production (1^+) and Regge phases (e.g. for the A_2).

Examples 6 and 7

These are repeats of 4 and 5 with t replaced by M, i.e. all the same sorts of incoherence can arise from variations within mass bins as well as t bins.

The incoherences of examples 4, 5, 6 and 7 are due solely to binning. If we could go to infinitesimal bins we would not have these problems. The problems are reduced however by explicitly demonstrating the various mass and t dependence of the amplitudes and their phases.

All of these effects will result in an increase in the rank of the density matrix. They can be coped with in an amplitude analysis only by increasing the number of incoherent terms (see V.Chaloupka - these proceedings).

Example 8: Resolution Effects

I just remark here that incoherence can also be due to finite experimental resolution - a fact discussed by Chaloupka in these proceedings.

Example 9: Bad parameterization of the model

If one uses wrong decay amplitudes, e.g. Breit-Wigner phases, this can again result in apparent incoherences.

Summary: In summary we see that there are many potential sources of incoherence. They are usually identified by poor fits and/or increase in the rank of the density matrix. However once identified the sources can in general be explicitly demonstrated in the fitting amplitudes and many of the problems removed.

Finally it should be stated that generally life is not as bad as these examples could imply.

I must thank G. Thompson for reading these notes and for discussions on the Illinois program. Any remaining incoherence is due solely to me!

SESSION 2

Chairman: J.B. Dainton

3π ANALYSES USING THE ILLINOIS METHOD

Invited Talk

RESULTS OF 3π ANALYSES BY THE ILLINOIS GROUP

U.E. Kruse
Max-Planck-Institut f. Physik u. Astrophysik, Munich

Contribution

A SPIN PARITY ANALYSIS OF THE $\pi^-\pi^+\pi^+$ SYSTEM PRODUCED COHERENTLY IN 4 GeV/c π^+d INTERACTIONS

B.J. Stacey
University of Birmingham

THIS PAGE

WAS INTENTIONALLY

LEFT BLANK

RESULTS OF 3π ANALYSES BY THE ILLINOIS GROUP

by

A21

U.E. Kruse
Max-Planck-Institut für Physik und Astrophysik†
Munich

INTRODUCTION

This summary presents some of the results from the partial wave analyses carried out on the 3π system by the Illinois group. Many people have worked on the analyses described: G. Ascoli, D. Brockway, B. Crawley, R. Cutler, L. Eisenstein, R. Hauft, J.D. Hansen, M. Ioffredo, L.M. Jones, R. Klanner, T. Roberts, P. Schultz, B. Weinstein and H.W. Wyld. Also many experimental groups have generously contributed data which made these analyses possible; we have therefore been able to examine data from bubble chambers for beam momenta between 5 and 25 GeV and from spectrometers for beam momenta of 23, 25, and 40 GeV/c. This summary is divided into six sections. The first section is a description of the resolution of the 3π mass spectrum into partial waves, and the next three sections describe the A_2, A_1, and A_3 properties. In the fifth section, some results from a study of a Reggeized Deck model are presented, and in the sixth section results from an examination of a Regge amplitude for A_2 production are given.

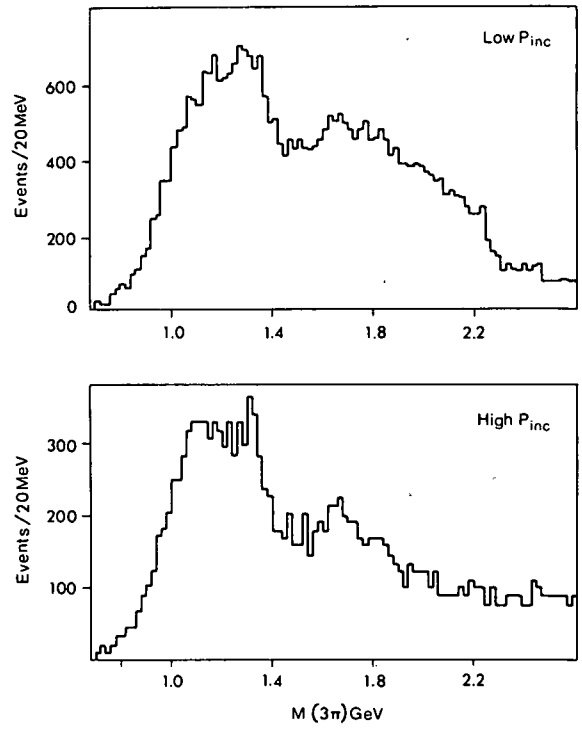

Fig.1 $\pi^+\pi^-\pi^-$ *mass spectra for* π^-p *bubble chamber collaboration, low* P_{inc} *refers to data from 5 to 7.5 GeV/c, high* P_{inc} *to data from 11 to 25 GeV/c. Data from ref.(1).*

1. RESOLUTION OF THE 3π SPECTRUM INTO PARTIAL WAVES

Figure 1 shows the 3π mass spectra produced in the reactions $\pi^-p \to \pi^-\pi^-\pi^+p$ as seen in a series of bubble chamber experiments. In the figure, the low incident momentum data include experiments at 5, 7 and 7.5 GeV/c, the high incident momentum data come from experiments between 11 and 25 GeV/c. The Illinois partial wave method, which I shall call FIT, has allowed us to resolve these mass distributions into the various partial waves. In fig.2, the contributions of the large states with $J^P = 0^-$, 1^+, 2^-, 2^+, and 3^+ are shown for the data with high incident momenta[(1)]. The peaks in $1^+(A_1)$, $2^+(A_2)$, and $2^-(A_3)$ are now seen and in the next sections some of the important features of these enhancements are given. The A_2 results will be presented first since they exhibit the features expected of a resonance, followed by the results for the A_1 and A_3.

Our analyses were carried out in terms of the density matrix elements and decay amplitudes. From these density matrix elements amplitudes and phase differences between amplitudes can be determined using

$$\rho^{JP1,JP1} = |R_1 e^{i\alpha_1}|^2 = R_1^2$$

$$\rho^{JP2,JP2} = |R_2 e^{i\alpha_2}|^2 = R_2^2$$

$$\rho^{JP1,JP2} = \varepsilon R_1 e^{i\alpha_1} (R_2 e^{i\alpha_2})^* = \varepsilon R_1 R_2 e^{i(\alpha_1 - \alpha_2)}.$$

†On leave from University of Illinois, Urbana.

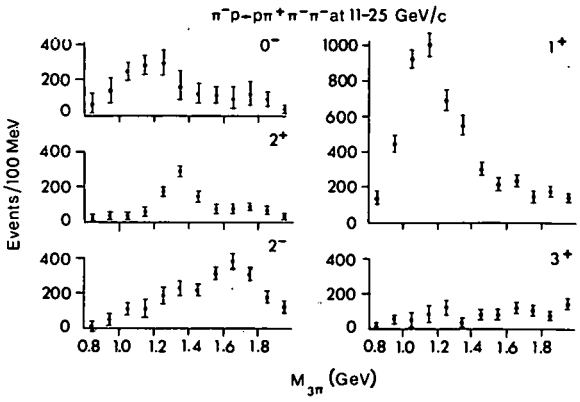

Fig. 2 Contributions of $J^P = 0^-$, 1^+, 2^-, 3^+, 3^+ states versus M(3π) for 11-25 GeV/c data with $t' < 0.7$ GeV^2. Data from ref. (1).

In these expressions R_1 and α_1 are the magnitude and phase of the amplitude for the state 1 with spin-parity JP1 and similarly R_2 and α_2 for another state 2 with spin-parity JP2. The factor ε measures the coherence between the two states.

We have used these prescriptions to obtain the values for the intensities R^2 and relative phases $(\alpha_1 - \alpha_2)$ which will be shown in some of the following figures. For a simple Breit-Wigner resonance without background, we expect to see a strong shift in the phase α_1 of the resonant state as we go through the peak of the enhancement. In any real case, the variation of the phase α_2 of the non-resonant reference state can distort the behaviour of $\alpha_1 - \alpha_2$ even for a simple Breit-Wigner resonance. We therefore have tried to plot those relative phases which are reasonably determined in order to find the common contribution of the phase α_1 of the partial wave JP1 being examined.

2. A_2

In fig.3 are shown the intensity of the $2^+D(\rho\pi)$ state and the relative phases of this state with respect to $1^+P(\varepsilon\pi)$ and $1^+S(\rho\pi)$ as observed in π^-p interactions at 40 GeV/c[2]. The curves shown give a relativistic D wave Breit-Wigner fit to the data. The A_2 thus gives a beautiful example of a simple Breit-Wigner resonance.

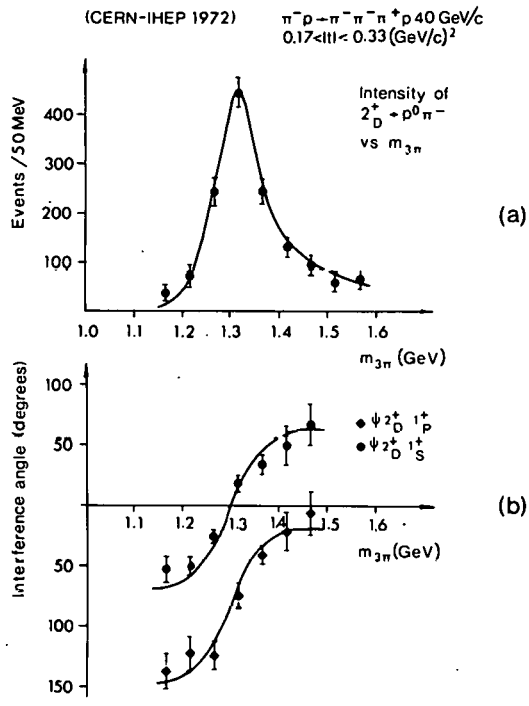

Fig. 3 (a) Intensity of 2^+D wave at 40 GeV/c versus M(3π). (b) Phase of 2^+D wave relative to 1^+ waves versus M(3π). Data from ref. (2).

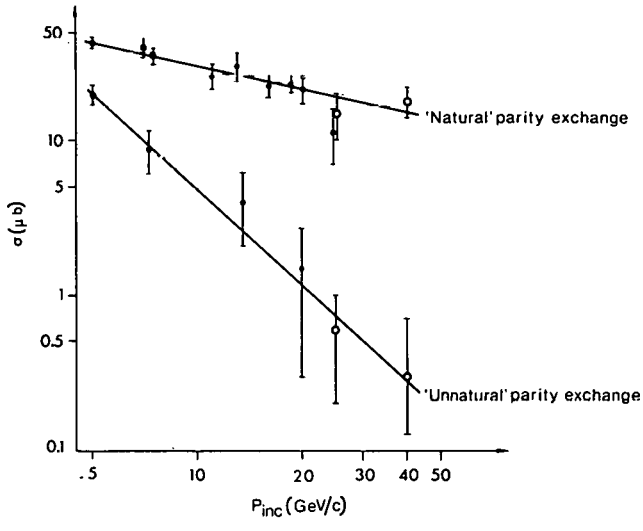

Fig. 4 Dependence on incident momentum of natural and unnatural parity contributions to the A_2 cross section in the 3π mass interval 1.2 to 1.4 GeV. Data from refs. (1) and (2). Solid lines are fits $\sigma \sim P_{inc}^{-n}$ with n = 0.51 and 2.

By performing the partial wave analysis on data from different incident beam momenta, we can obtain the dependence on incident momentum for the production cross section of the A_2^- with $\rho^0\pi^-$ decay. In fig.4, the natural parity exchange contribution from $d\sigma/dt(\rho_{11} + \rho_{1-1})$ and the unnatural parity exchange contribution from $d\sigma/dt\ \rho_{00}$ and $d\sigma/dt(\rho_{11} - \rho_{1-1})$ are shown as a function of incident momentum. The lines represent fits of form $p_{inc}^{-0.15}$ and p_{inc}^{-2}. We will return to a discussion of the behaviour of the natural parity exchange component in sect.6.

3. A_1

The A_1 or 1^+ enhancement near 1.2 GeV is more complicated than the A_2. The situation is summarized in fig.5 using the data from ref.(2). The intensities of the various states show that only $1^+S(\rho\pi)$ shows a significant enhancement in this region; 1^+P is relatively smooth and 1^+D is negligible. The states 0^-S, 1^+P, and 2^-P should provide reasonable references for phase variations of the 1^+S state. There is no evidence for a systematic phase variation of 1^+S that we might expect for a simple resonance. The analyses of other π^-p experiments agree well with these conclusions.

4. A_3

The A_3 near 1.65 GeV shows a strong enhancement only in the $2^-S(f\pi)$ state. In fig.6 the overall 2^- wave and the contributions from $2^-S(f\pi)$ and $2^-P(\rho\pi)$ are shown for the high incident momenta π^- (11-25 GeV/c) of ref.(1). The A_3 has also been studied for π^- at 40 GeV/c[2] and π^+ between 8 and 24 GeV/c[3,4]. There appears to be general agreement that only $2^-S(f\pi)$ shows a significant enhancement, however the experiments show different results for the phase differences. The comparisons are given in fig.7 for π^-p bubble chamber results from 11-25 GeV/c[1], for π^-p spectrometer results at 40 GeV/c[2], for π^+p bubble chamber results at 13 GeV/c[3], and for π^+p bubble chamber results at 8, 16, and 24 GeV/c[4]. The π^+ data analyses[3,4] were carried out by other groups using the FIT program. In fig.7 we see that there is general agreement on the 2^-S - 2^-P phase difference; no significant variation is found by

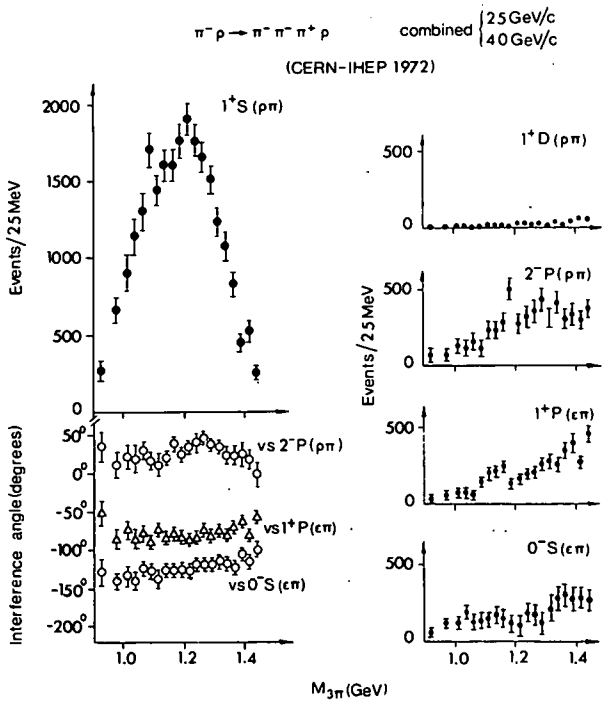

Fig.5 Intensities of different partial waves and phase differences of the 1^+S wave relative to 0^-S, 1^+P, and 2^-P in the A_1 region. Data from ref.(2)

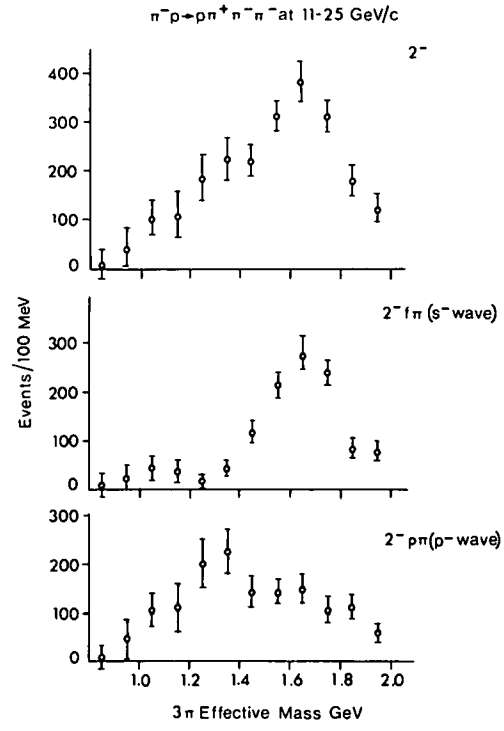

Fig.6 Intensities of the 2^- partial waves versus $M(3\pi)$. Data from ref.(1).

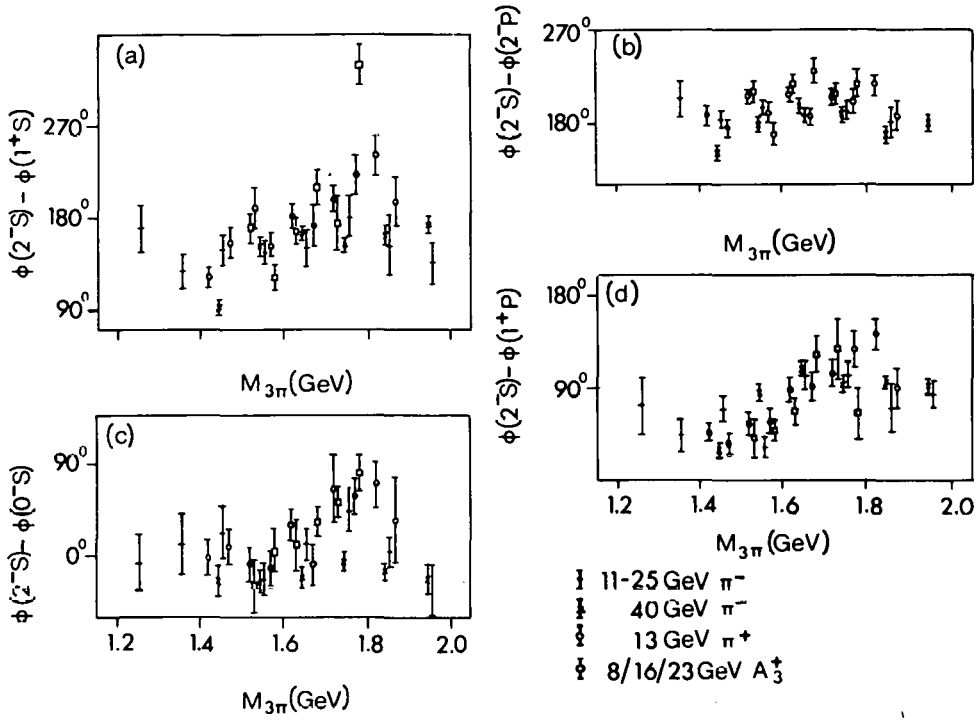

Fig.7 Phase of $2^-S(f\pi)$ wave relative to $1^+S(\rho\pi)$, $2^-P(\rho\pi)$, $0^-S(\varepsilon\pi)$, and $1^+P(\varepsilon\pi)$ in the A_3 region. Data from refs. (1-4).

any group. The π^-p data show no significant variation for the other phase differences, however the π^+p data do indicate phase increases of 2^-S relative to some of the other phases. Differences in background, e.g. Δ^{++} production, may be the source of the apparent discrepancy. It would be desirable to clarify this question with high statistics experiments at high incident momenta where the backgrounds from Δ^{++} should be less significant.

5. REGGEIZED DECK MODEL

A Reggeized Deck model has been explored in the hope of clarifying our understanding of the 3π system outside of the resonant A_2 wave. This work appears in two parts. In the first part[5] a partial wave analysis is made of our amplitude in the Deck model and the results of the amplitude analysis are compared with the results of the usual FIT program applied to Monte Carlo events generated according to the Deck amplitude squared. In the second part[6] Monte Carlo events generated according to the Deck amplitude squared are compared with experimental events in the A_1 and A_3 regions. In both parts, the Deck amplitude is calculated using on-shell $\pi\pi$ scattering and on-shell πp scattering together with a Reggeized π exchange as indicated in fig.8.

From the partial wave analysis of the Deck amplitude in the first part, we can obtain a direct prediction of the magnitude and absolute phase of the various partial wave components. In fig.9, the behaviour of the $1^+S(\rho\pi)$ part of the Deck amplitude is shown as a function of W, the mass of the 3π system, and $\sqrt{s_1}$ the mass of the $\pi^+\pi^-$ system. We note that the phase varies only slowly throughout the A_1, A_2 mass region and that the phase of the 1^+S state at the mass of the A_2 is roughly 155^0. We will refer to this value again in sect.6. The behaviour of the other important amplitudes are given in ref.(5). The results from the amplitude analysis were then compared to the results of the partial wave fitting program FIT applied to a set of Monte Carlo events generated

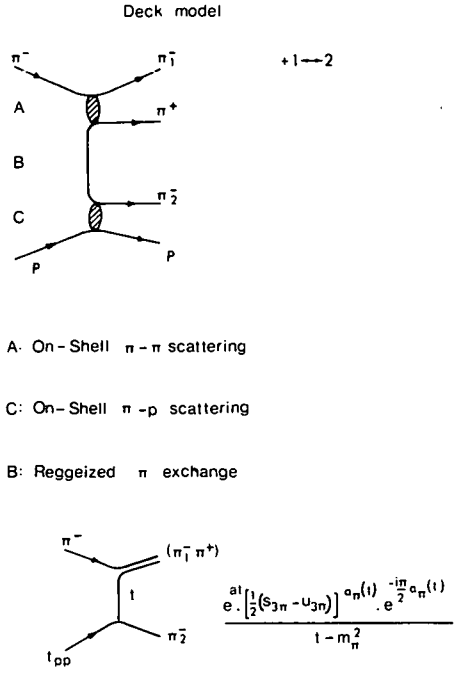

Fig.8 Diagram for Reggeized Deck model for the reaction $\pi^- p \to p\pi^+\pi^-\pi^-$.

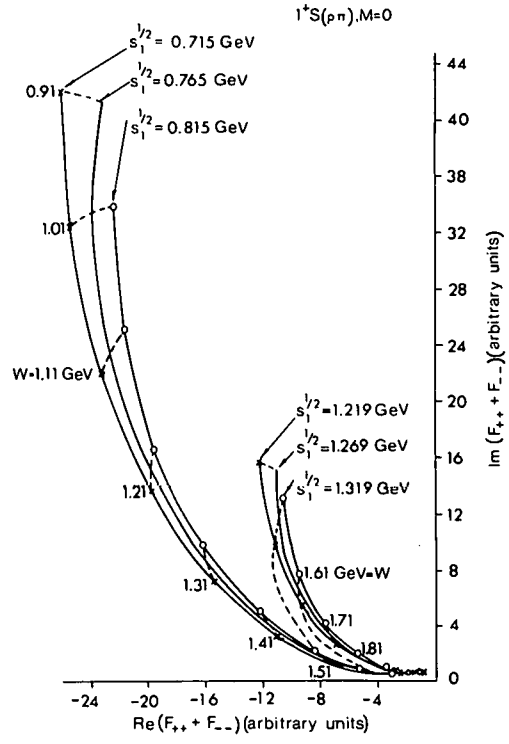

Fig.9 Argand diagram for the 1^+S partial wave as a function of 3π mass W and $\pi^+\pi^-$ mass $\sqrt{s}$ for P_{inc} = 16 GeV/c and t' = -0.05 GeV².

according to the Deck amplitude squared. The results show that the program FIT obtains the general features of the important states up to a 3π mass of 1.4 GeV. There are however discrepancies in relative phases involving επ states for 3π masses above 1.4 GeV. Also for the $1^+S(\rho\pi)$ decay in the A_1 region the amplitude analysis gives a sharper peak than does FIT.

In the second part of our Deck model study[6], a large set of Monte Carlo events were generated according to the model and compared with events from the experimental data. In this part, an additional small term was added in the Deck model to include $\pi^-\pi^-$ scattering at the upper vertex. The Monte Carlo events were then compared to the experimental events by plotting various distributions and by comparing partial wave analyses for both sets of events. In fig.10, the 3π mass distribution comparison is shown. In this comparison there has been no normalization of the model. We see that the general agreement is good including the absolute magnitude. Our Deck model however produces an A_1 which is wider than the A_1 seen in the experimental data. On the 3π mass plot this is not immediately obvious since the combination of A_1 and A_2 in the experimental data simulate the wider A_1 in the Deck model. Thus our Deck model is too large in the A_2 region, also it does not give a large enough A_3 signal. In fig.11, the $\pi^+\pi^-$ mass distributions are compared for events in the A_1 region and in the A_3 region. Here the Deck model curves were normalized to the data to facilitate comparison. The agreement of the shape for the A_1 is good, however for the A_3 it is clear that the model does not produce enough f events.

Figure 12 gives some of the comparisons of the partial wave analysis applied to our Deck model events and to experimental events. The Deck model results are shown as smooth hand drawn curves, the experimental results are given by the points with errors. The Deck model gives more 0^- than does the data, and, as mentioned above, the 1^+ is wider in the model than in the data. The relative phase of 1^+S and 1^+P agrees well and a more detailed examination has shown that the Regge signature factor for the

exchanged pion trajectory is essential for this agreement[6]

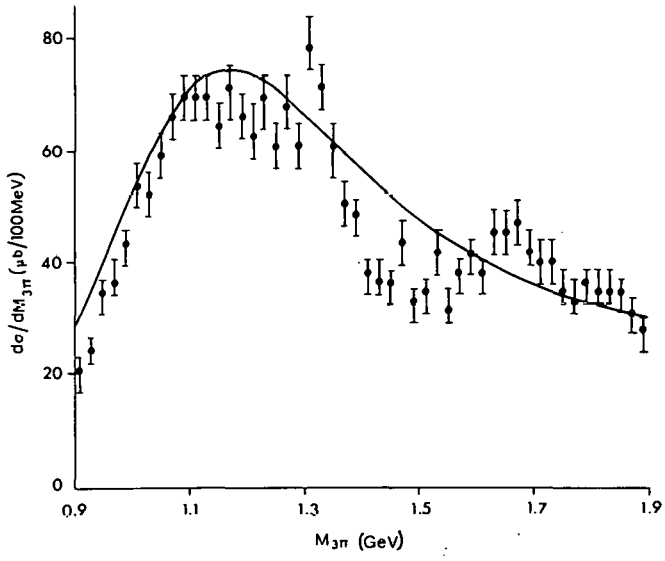

Fig. 10 Comparison of 3π mass distribution. The data points are combined data of ref. (1); the curve is calculated from the Deck model.

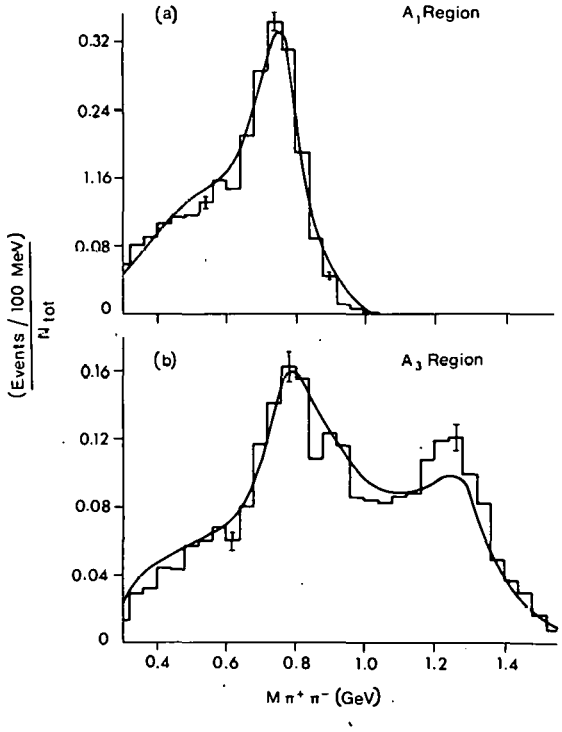

Fig. 11 Comparison of $\pi^+\pi^-$ mass distribution. The data points are from data of ref. (1); the curves calculated from the Deck model are normalized to the data (a) in A_1 region; (b) in A_3 region.

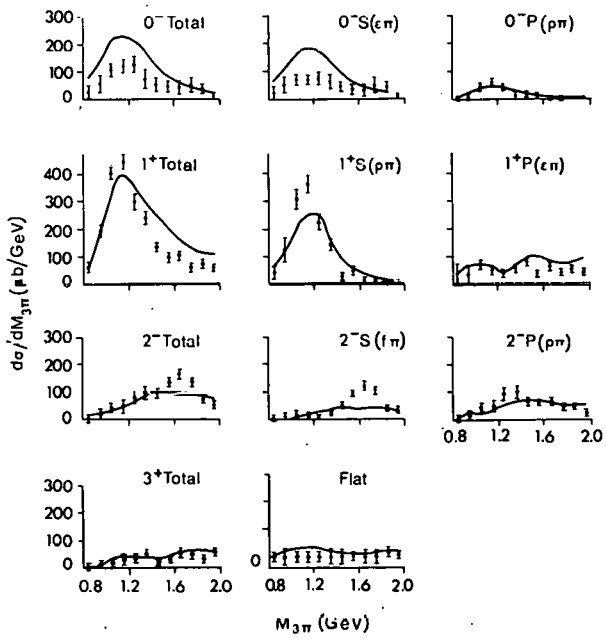

Fig. 12 Comparison of intensities of partial waves. The points are from application of FIT to the data of ref. (1); the curves are drawn by hand through results of FIT applied to the Deck model.

6. A_2 PRODUCTION AMPLITUDE

We have compared a simple Regge model for the A_2 production amplitude with the data[7]. The Regge model assumes Pomeron and f exchange for the natural parity part of the A_2 production. We thus used for the nucleon non-flip amplitude

$$M^{nf}(s,t) = -\sqrt{C}\sqrt{|t - t_{min}|}\cdot\left[e^{A_p t}\left(\frac{s}{s_0}\right)^{\alpha_p(t)} e^{-\frac{i\pi\alpha_p(t)}{2}} + K\, e^{A_f t}\left(\frac{s}{s_0}\right)^{\alpha_f(t)} e^{-\frac{i\pi\alpha_f(t)}{2}}\right]$$

with C, K, A_p and A_f as free parameters. We used $s_0 = 1$ GeV^2 and the trajectories $\alpha_p = 1 + 0.36t$, $\alpha_f = 0.56 + 0.86t$.

The differential cross section is related to the amplitude given above by

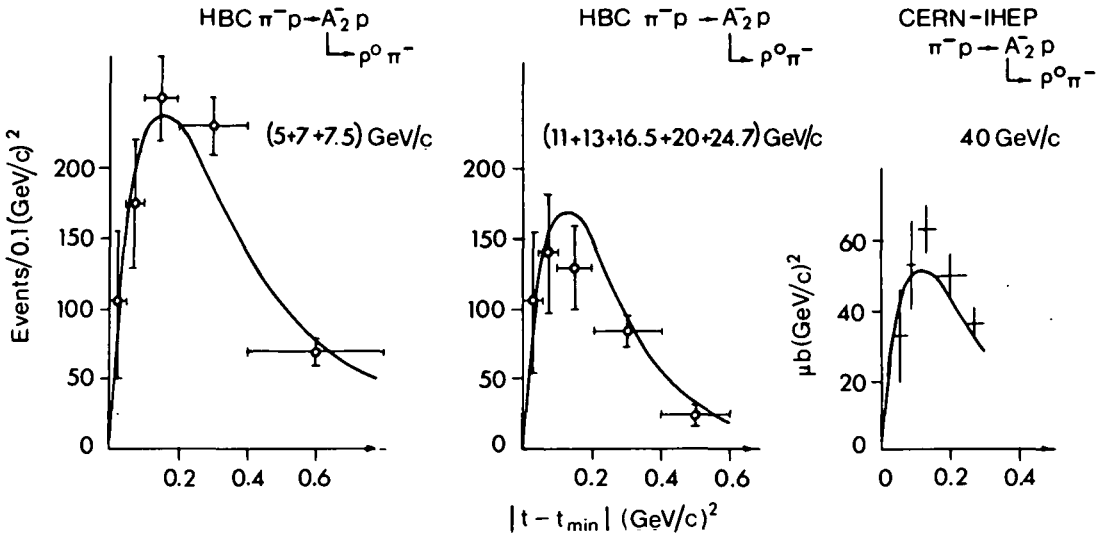

Fig. 13 Comparison of differential cross sections for $\pi^-p \to A_2^-p$. The points are from the data of ref. (1) and (2); the curves are from the Regge model fit described in text.

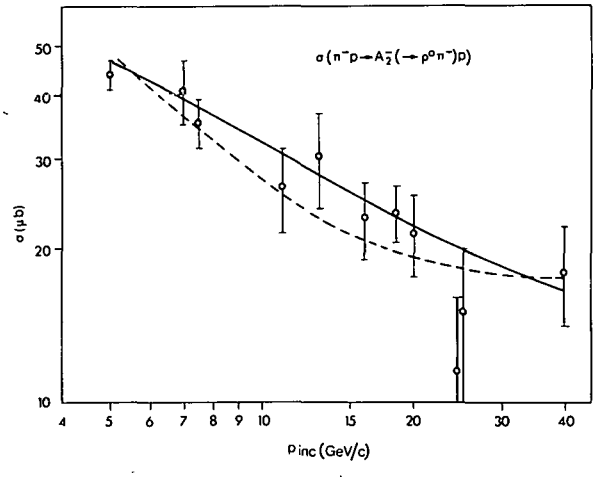

Fig. 14 Comparison of dependence of cross section on incident momentum. The points are from the data of ref. (1) and (2); the solid curve is for Regge model fit with K > 0; the dashed curve for fit with K < 0.

$$(\rho_{11} + \rho_{1-1}) \quad d\sigma/dt = \frac{|M^{nf}|^2}{s^2}$$

We fitted the $\pi^-p \to A_2^-p$ data from $\pi^-p \to \pi^+\pi^-\pi^-p$ (p_{lab} = 5-40 GeV). A satisfactory fit to the data (χ^2/NDF = 10.5/11) was obtained as shown in figs. 13 and 14.

The parameters of the fit are:

C = 1120 ± 300 mb A_p = 3.5 ± 0.5 GeV^{-2}

K = 1.5 ± 0.7 A_f = −0.5 ± 0.8 GeV^{-2}

In fig. 14, the solid curve represents the fit with K > 0 while the dashed curve represents a fit with K < 0.

We can compare the relative phase of the A_1 and A_2 amplitudes from the models with the relative phase found in the data. For the A_1 amplitude we take the results of the Reggeized Deck model shown in fig. 9 and for the A_2 amplitude we can consider the amplitudes with K > 0 and K < 0. The situation for K > 0 is shown in fig. 15 where the A_2 amplitude lies near 105° for 5 GeV/c incident momentum and moves towards 90° as the incident momentum increases and the f contribution becomes less important. For K < 0, the f contribution points in the opposite direction, hence the A_2 amplitude has phase less than 90° and this phase now increases towards 90° as the incident momentum increases. In fig. 16, the corresponding phase differences are shown; solid lines indicate the K > 0 choice, dashed lines the K < 0 choice, and

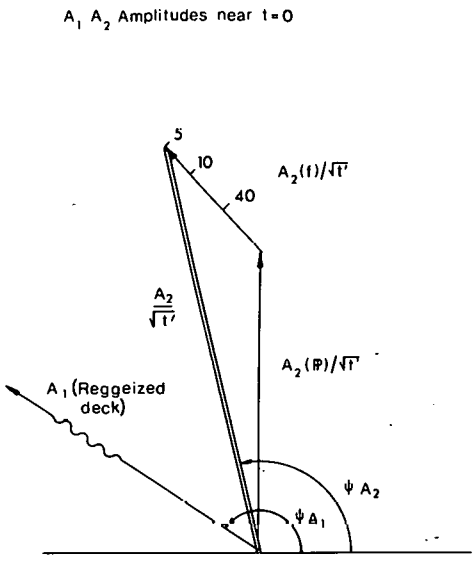

Fig. 15 *A_1 and A_2 amplitudes near $t = 0$. The A_1 amplitude is from Deck model (fig. 10); the A_2 amplitude corresponds to Regge model with $K > 0$.*

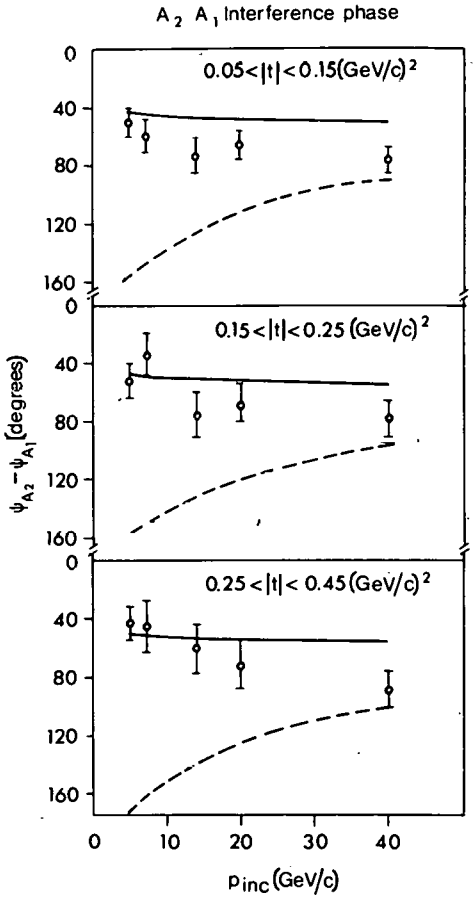

Fig. 16 *Comparison of phase difference between $2^+D(\rho\pi)$ and $1^+S(\rho\pi)$. The points are from data of refs. (1) and (2); the solid (dashed) curve uses the Deck model for A_1 and Regge model for the A_2 with $K > 0$ ($K < 0$).*

the points indicate the experimental data. The data favour the K > 0 choice where the overall agreement is reasonably good.

REFERENCES

1. G. Ascoli et al, Phys. Rev. D7, (1973) 669.
2. Yu.Antipov et al, Nucl. Phys. B63, (1973) 153.
3. G. Thompson et al, Phys. Rev. Letts. 32, (1974) 331.
4. G. Otter et al, Nucl. Phys. B80, (1974) 1.
5. G. Ascoli et al, Phys. Rev. D8, (1973) 3894.
6. G. Ascoli et al, Phys. Rev. D9, (1974) 1963.
7. G. Ascoli et al, Phys. Rev. Letts. 33, (1974) 610.

A SPIN-PARITY ANALYSIS OF THE $\pi^-\pi^+\pi^+$ SYSTEM PRODUCED COHERENTLY IN 4 GeV/c π^+d INTERACTIONS

A21

by

M.J. Emms, G.T. Jones, J.B. Kinson, B.J. Stacey†, M.F. Votruba and P.L. Woodworth,
University of Birmingham, UK,

I.G. Bell, M. Dale and J.V. Major
University of Durham, UK,

J.A. Charlesworth, D.J. Crennell and R.L. Sekulin,
Rutherford Laboratory, UK.

ABSTRACT

A spin-parity analysis of the low mass 3π system produced in the reaction $\pi^+d \to \pi^-\pi^+\pi^+d$ has been performed using data from an exposure of the CERN 2m bubble chamber to a π^+ beam of 4 GeV/c momentum. Unnatural parity states predominate, 1^+ being much more significant than 0^- and 2^-. The $J^P = 2^+$ contribution in the A_2 region was found to be (5 ± 2)%.

The three-body partial wave analysis technique developed at the University of Illinois[1,2] has been widely used to examine the properties of the 3π system recoiling off a proton[3,4] in the reactions

$$\pi^\pm p \to \pi^\pm\pi^\pm\pi^\mp p \qquad (1)$$

and produced off nuclei[5,6]. The spin-parity structure has been found to be similar in each case. The 3π system is produced mainly in unnatural parity states (0^-, 1^+, 2^- ...), being dominantly 1^+ with lesser contributions from the 0^- and 2^- states. However, there are differences in the production of the 2^+ state. Some 2^+ contribution is found in reaction (1) and in the coherent nuclear reactions of ref.(6), but none is seen [5] in the reaction

$$\pi^- C \to \pi^-\pi^-\pi^+ C^*(4.44) \qquad (2)$$

which proceeds via pure I = 0 exchange.

In this paper we present results on the spin-parity structure of the 3π system produced in the coherent deuteron reaction

$$\pi^+d \to \pi^-\pi^+\pi^+d \qquad (3)$$

at 4 GeV/c. Since the deuteron has isospin zero this reaction also proceeds by pure isospin zero exchange.

The data come from 700,000 pictures of 4 GeV/c π^+d interactions in the CERN 2m bubble chamber. A sample of 3847 four prong events fit reaction (3) with a chi-squared probability greater than 0.1%. At $t = t_{min}$, where t is the four momentum transfer squared between the target and recoil deuterons, the recoil deuteron will travel along the beam direction in the laboratory system with a momentum of less than 130 MeV/c when the 3π system has a mass of less than 1.0 GeV/c^2. In order to avoid any loss of slow deuterons which are not seen in the bubble chamber, we have therefore selected the 2321 events which fit the reaction

$$\pi^+d \to \pi^+\pi^+\pi^-n\,p_s \qquad (4)$$

with an unseen spectator proton and which have a p_sn effective mass less than 1.9 GeV/c^2. These have been refitted as coherent events with an unseen deuteron, yielding 763 acceptable fits. It is estimated[7] that the contamination from reaction (4) in our coherent sample is less than 10%.

Figure 1(a) shows the t' distribution, where $t' = t - t_{min}$, for all of the coherent events. Those with an unseen deuteron are shaded. By fitting a function of the form $Ae^{-b|t'|}$ to the distribution in the range $0.025 < |t'| < 0.1$ (GeV/c)^2, a value of (33.0 ± 1.4)(GeV/c)$^{-2}$ was obtained for the slope parameter b. When the events with an unseen deuteron are included this exponential function gives a good description of the data down to $|t'| = 0$, which would be expected for a coherent reaction which is dominated by diffraction processes.

Presented by B.J. Stacey.
†Now at Westfield College, London.

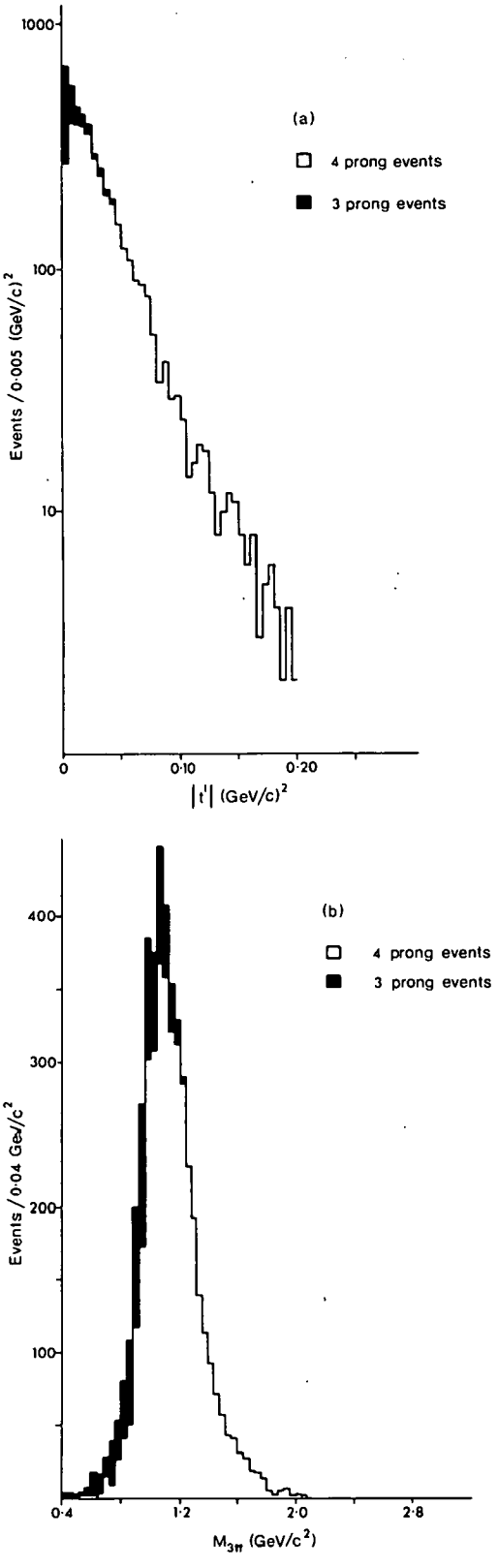

Fig. 1 (a) dσ/dt' for reaction (3). Events with an unseen deuteron are shaded. The fit is described in the text.

(b) $\pi^+\pi^+\pi^-$ effective mass distribution for all coherent events. Events with an unseen deuteron are shaded.

The effective mass distribution of the $\pi^+\pi^+\pi^-$ system for our total coherent sample of 4610 events is shown in fig.1(b).

The Illinois partial wave analysis was used to determine the spin-parity structure of the 3π system in the mass range 0.8 - 1.6 GeV/c^2, for events with $|t'| < 0.1$ (GeV/c)^2. In this analysis the decay distributions of the 3π system, assumed to decay via a dipion intermediate state, are fitted to sets of states $J^P L M^\eta$, where J^P represents the spin-parity of the 3π system, L is the relative angular momentum of the dipion and the third pion, and η is the naturality of the exchanged particle. In our analysis the Gottfried-Jackson frame was used to define the quantization axis, and the following basic set of states was fitted:

$$0^-S0^+(\varepsilon\pi), \quad 0^-P0^+(\rho\pi), \quad 1^+S0^+(\rho\pi),$$
$$1^+P0^+(\varepsilon\pi), \quad 2^-P0^+(\rho\pi), \quad 2^-D0^+(\varepsilon\pi).$$

and an incoherent isotropic background (FLAT). This set was chosen on the basis of the results obtained in analyses of reactions (1) and (2). In addition all other possible states with spin one or two and some spin three states were considered to see if they were required by the data.

The contributions of the various J^P states as functions of the 3π effective mass are shown by the crosses in fig.2. The continuous lines show the results[4] of the fits to reaction (1) and the black circles the results[5] from fits to reaction (2) both normalized to the total number of events used in our analysis. It is seen that the results for production off deuterons are similar to those obtained for production off carbon. The 3π system is produced almost entirely in unnatural parity states with 1^+ dominant and smaller contributions from 0^- and 2^-. For the 0^- state the επ contribution is dominant, whereas the 2^- state is mainly ρπ. In the case of $J^P = 1^+$ ρπ is more important than επ but there is an inherent ambiguity between these two contributions, particularly at small 3π effective mass[8].

The number of events in the $J^P = 2^+$ state in the A_2 region (1.2-1.4 GeV/c^2) is small, being (5 ± 2)% of the total, and is due almost entirely to the contribution of the $2^+D1^+(\rho\pi)$ state. All other states added to the basic set were found to be even less important than the 2^+ state.

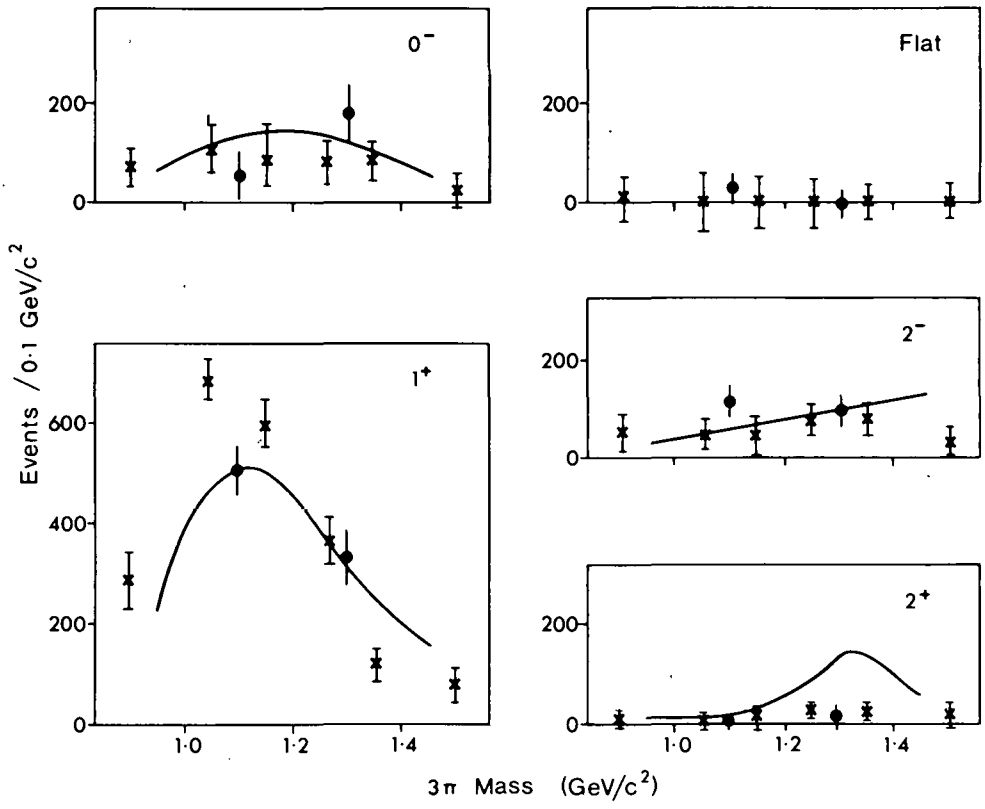

Fig. 2 Contributions of the various J^P states for the (3π)-mass region 0.8-1.6 GeV/c^2, for $|t'| < 0.1$(GeV/c)^2.

The results of the analysis were not significantly changed when

(i) events which could be affected by a $d\pi^+$ enhancement at about 2.2 GeV/c were removed,

(ii) the s-wave $\pi^-\pi^+$ system was parametrized by the CERN-Munich[9] phase shifts rather than a Breit-Wigner of mass 810 MeV/c^2 and width 550 MeV/c^2.

It has also been checked[7] that the small amount of 2^+ does not arise because of contamination from reaction (4). Additional selection criteria were imposed which reduced the contamination by a factor of about 4 and the fits repeated. The amount of 2^+ was found to be proportional to the number of coherent events, and not to the amount of background.

In conclusion, our analysis shows that the coherent production of 3π systems in I = 0 exchange reactions results almost entirely in states of unnatural parity, with 1^+ dominating over 0^- and 2^-. However, there is a contribution of (5 ± 2)% from the $J^P = 2^+$ state in the A_2 region.

We would like to thank Professor D.C. Colley and Dr. G. Kalmus for their support and encouragement.

REFERENCES

1. P.V. Brockway, Ph.D. Thesis, University of Illinois, Urbana, (1970).
2. J.D. Hanson, G.T. Jones, G. Otter and G. Rudolph, Nucl. Phys., B81, (1974) 403.
3. G. Ascoli, Phys. Rev. Letts. 25, (1970) 962.
4. G. Ascoli et al., Phys. Rev. D7, (1973) 669.
5. G. Ascoli et al., Phys. Rev. Letts. 31, (1973) 795.
6. U. Kruse et al., Phys. Rev. Letts. 32, (1974) 1328.
7. B.J. Stacey, Ph.D. Thesis, University of Birmingham, (1974).
8. B. Weinstein, G. Ascoli and L.M. Jones, Phys. Rev. D8, (1973) 2904.
9. G. Grayer et al., Nucl. Phys. B64, (1973) 134.

THIS PAGE

WAS INTENTIONALLY

LEFT BLANK

SESSION 3

Chairman: D. Morgan

THE DECK MODEL

Invited Talk

A CRITIQUE OF THE REGGEIZED DECK MODEL

E. Berger
Argonne National Laboratory

Contribution

DIFFRACTIVE PRODUCTION OF A_2 AND ITS GENERALIZATIONS

C.F. Cho
Max-Planck-Institut f. Physik u. Astrophysik, Munich

THIS PAGE

WAS INTENTIONALLY

LEFT BLANK

A CRITIQUE OF THE REGGEIZED DECK MODEL†

by

Edmond L. Berger
High Energy Physics Division
Argonne National Laboratory, Argonne, Illinois 60439
and
CERN, Geneva, Switzerland

ABSTRACT

A detailed analysis is presented of the Reggeized pion exchange Deck model for processes of the type $ap \to A^*N \to (a^*\pi)N$, where $a = \pi$, K, or nucleon and $a^* = \rho$, K^*, or Δ. Predictions of the model for both production and decay properties of the low mass system $A^* \to (a^*\pi)$ are derived and contrasted with data. Diffractive as well as charge exchange reactions are treated. The role of pion exchange in generating $(a^*\pi)$ enhancements near threshold and their properties is examined from several points of view. Characteristic exchange effects and quantum number properties (e.g. cross-overs) of the pion exchange Deck graph are shown to be verified in the data, but this graph alone is inadequate. The failures all point to the need for a second graph, having a* exchange properties. The contribution of a* exchange is roughly equal to that of the π-exchange graph.

1. INTRODUCTION

1.1 General

The apparent absence in nature of resonances with spin-parity $J^P = 1^+$ quantum numbers remains an outstanding mystery, and a source of malaise for quark model proponents[1]. Well-known enhancements are present in mass-distributions, for example the $A_1 \to 3\pi$ and $Q \to K\pi\pi$, which are candidates for the desired $J^P = 1^+$ nonet. These enhancements are known also to be dominantly, although not exclusively, in the $J^P = 1^+$ partial waves[2,3]. The difficulty with their acceptance as resonances is two-fold. First, the phase shift of a resonant wave should increase by 90° as the mass is varied through the resonance region. The existing 3 particle spin-parity analysis programs extract phases from the data which show essentially no variation with mass of the dominant $J^P = 1^+$ phase shift, relative to the other partial waves[2,3]. The strength of this conclusion depends, of course, on the competence of the phase-shift analysis programs to extract the true phase variation of a (perhaps) broad resonance located near threshold. Questions have indeed been raised regarding this competence, and also concerning the theoretical reliability of the isobar assumptions built into the programs[4].

The second argument against a resonance interpretation is that a substantial non-resonant $J^P = 1^+$ enhancement is expected from simple one pion-exchange Deck graphs[5,6]. This dynamical mechanism for producing a non-resonant $J^P = 1^+$ enhancement seems so straightforward that it undoubtedly contributes at least some of what is observed.

The Deck graph explanation is that the low mass enhancement results from the effect of exchanges, rather than as a manifestation of direct (s) channel dynamics.

It should be stressed from the start that the total observed $J^P = 1^+$ enhancement could well be a sum (including interferences) of a resonant and of a non-resonant Deck component. If the 1^+ Deck background is, say, 3 times as great in amplitude (10 times in cross section) as the 1^+ resonance, then the phase shift programs may well not be capable of extracting the resonance. Much greater statistical accuracy in the data and perhaps more clever methods of analysis would seem required to disentangle these options.

In this article I espouse the Deck (i.e. the exchange model) interpretation, and try to suggest

†Work performed under the auspices of the U.S.A.E.C.

tests of its suitability. However, it seems to me that the case is not closed against 1^+ resonances produced with cross sections of the size desired[1] (c.f. Section 4.3).

1.2 The Deck Model

The Deck model has appeared in different disguises in the literature[5,6]. Perhaps the best general context in which to place it is the framework of double-peripheral models for reactions in which two particles enter and three emerge[7]. Nevertheless, in keeping with the currently popular applications of the Deck model, I introduce the subject differently. I try to motivate the model by an invitation to examine the possible importance of pion-exchange in inelastic reactions. Although the pion exchange graph is only one of the candidates, if one thinks in the more general double-peripheral framework, its unique appeal is based partly on the belief that the pion's coupling is large, since the pion pole singularity is so near the physical region. Moreover, its propagator is presumed "well-known", so that momentum transfer dependences are approximately predictable. The greatest support is that the pion-exchange graph seems to work. Extensive analyses by the Illinois Group of the reaction $\pi p \to (3\pi)p$ conclude that essentially all aspects of the data they examined are reproduced[8]. However, in spite of this success, there are troubles for the π-exchange Deck model, both theoretical and phenomenological. Other graphs appear to be required to resolve these difficulties. In this exposé, I will examine the Deck model's successes and failures for several reactions, as well as some of the consistency problems faced on the theoretical side. Further experimental checks are proposed.

1.3 Reactions Studied

I will explain in some detail how the model is employed to describe the production and decay characteristics of A* in reactions of the form

$$ap \to A^*N \to a^*\pi N \qquad (1)$$

Here, a maybe any one of the set ($K^{\pm}$, $\pi^{\pm}$, K^0, $\overline{K^0}$, p, $\bar{p}$, n, and so forth). Correspondingly, a table can be made:

a	A*	a*
K	Q	K^*_{890}
K	L	K^*_{1420}
π	A_1	ρ
π	A_3	f
π	A_5	g
N	"N*(1300)"	N
N	"N*(1460)"	Δ

If N = p, these processes all fall into the general class of inelastic diffraction dissociation reactions. Their experimental characteristics are similar, so that it suffices to treat the general process (eqn.(1)), except that numerical calculations require specification of appropriate masses. I will also report on "charge exchange Deck model" calculations, for which N in eqn.(1) is a neutron. Detailed experimental study of these "charge-exchange reactions", including a spin-parity determination of their enhancements, is of critical importance.

It will be noted that all processes listed above are "beam dissociation" reactions, which means, in the pion-exchange Deck model, that the production of A* in $ap \to A^*p$ is a reflection of pion-target (e.g. pion-nucleon) elastic scattering. There are, of course, also "target dissociation" processes of the types

$$aN \to a(\pi N)$$

$$aN \to a(\pi\pi N)$$

in which a π elastic scattering plays a dominant role. I discuss such reactions also, but in much less quantitative detail.

From the Deck model point of view, the properties of the enhancement at low $(a^*\pi)$ mass in reaction (1) are reflections of the properties of exchanges. Thus, it is essential to be on the lookout for direct evidence in the data for characteristic features of exchanges, and for tests or indications of the quantum numbers of specific exchanges. My conclusions are that the data at small values of $(a^*\pi)$ mass do show evidence for exchange effects, particularly in the decay angular distributions, and that the quantum numbers of these exchanges may be determined by symmetry tests (e.g. polarizations, cross-overs) sim-

ilar to those previously used successfully in studies of much simpler reactions.

1.4 Outline

In Section 2, the Deck model amplitude is presented and criticized. Numerical parametrizations are given.

In Section 3, characteristic model predictions for the production of A* in ap → A*N are derived and compared with data. These include the enhancement generated near threshold in the πa* invariant mass distribution (Section 3.1); the magnitude and energy dependence of the integrated cross section (Section 3.2); the systematic behaviour of the slope of the production differential cross section $d\sigma/dt_{pN}$ as a function of s, the mass $M_{a^*\pi}$, and A* decay angles (Section 3.3); and polarizations (Section 3.4).

Section 4 is devoted to the decay aspects of A* → πa*. These include the spin-parity content of the A* system, for both "diffractive" and charge-exchange production (Section 4.1); a critique of the role of pion exchange (Section 4.2); the matter of whether t-channel or s-channel helicity conservation is preferred (Section 4.4); and the dependence on mass of the absolute and relative phases of the different J^P states (Section 4.5).

Inasmuch as some readers will be more interested in decay questions and little concerned by production properties, I have tried to write Section 4 so that it may be read independently of Section 3, and vice-versa. Nevertheless, it must be stressed that the Deck model does not "factorize". Production and decay are correlated, in that different regions of the "decay angular distribution of the object with mass M_{A^*}" have different production properties, and vice-versa. I try to spell-out what some of these correlations are, and how they may be seen by experimental selections not yet tried, to my knowledge. I am particularly fond of a selection on the s-channel azimuthal angle ϕ_c in A* decay, for reasons explained in Sections 3.3 and 4.2.

An Appendix is included in which I derive various useful kinematical relationships. Conclusions are gathered in Section 5.

2. DECK GRAPHS AND PARAMETRIZATION

The pion-exchange Deck graph is drawn in fig.1(a). It represents production of a system a* by π-exchange, followed by elastic scattering of the pion from the nucleon target. It is relatively well-known that this diagram generates an enhancement near (a*π) threshold in the mass distribution $d\sigma/dM_{a^*\pi}$.

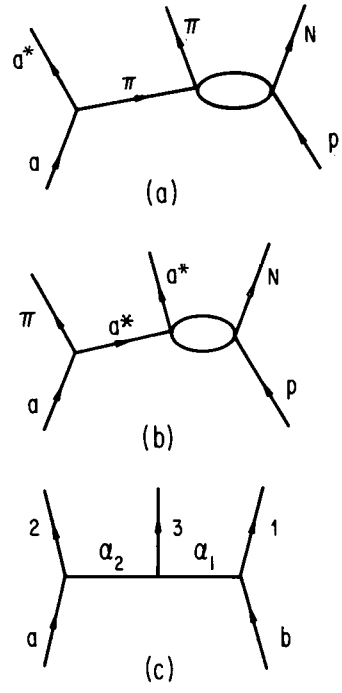

Fig.1 The pion exchange (a) and a exchange (b) Deck graphs for the reaction ap → a*πN. The ovals represent the full elastic scattering amplitudes. In (c), a general double peripheral graph is drawn for the reaction ab → 1 2 3. Symbols α_1 and α_2 denote trajectories.*

One of the more important conclusions of this investigation is that the threshold enhancements cannot be described successfully only in terms of pion exchange Deck amplitudes. Indeed, if one adopts the notion of an exchange model description of the low mass (πa*) enhancement in ap → (πa*)N, it appears necessary to use both π exchange and a* exchange graphs, as drawn in fig.1. In the usual parlance, this means both t-channel and u-channel exchanges in the scattering process a R → a*π, where "R" denotes some effective exchange at the pN vertex.

The π exchange graph is relatively easy to parametrize, although ambiguities do exist. The formalism of the a* exchange graph is much less certain. More-

over, once two graphs are involved, questions arise regarding interferences, double-counting, and so forth.

In this section, I discuss the detailed parametrization of the π exchange graph only. I will not write down any explicit forms for a* exchange. The conclusion that π exchange alone is insufficient is based on contrasting some salient predictions of the π exchange graph with data, in Sections 3 and 4. Most if not all of these discrepancies with data could be removed by inclusion of the a* exchange graph. This latter conclusion is based on the qualitative behaviour expected for a* exchange, as I will discuss.

2.1 The Illinois Graph

I treat the reaction $ap \to (a^*\pi)N$, which is only a selected portion of $ap \to (a\pi\pi)N$. Because a* resonance is a large fraction of the $(a\pi)$ scattering amplitude, I describe a correspondingly large fraction of the full reaction $ap \to (a\pi\pi)N$. To try to account for all, one could instead parametrize the graph shown in fig.2, in which the a* resonance is replaced by the full $(a\pi)$ scattering amplitude. This is what is done in the Illinois analyses of the π exchange Deck amplitude[8].

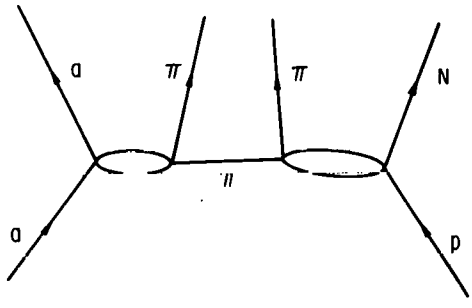

Fig.2 A pion exchange Deck graph for $ap \to a\pi\pi p$. The ovals represent the elastic scatterings $a\pi \to a\pi$ and $\pi p \to \pi N$.

Obviously the Illinois procedure results in a more complete fit to the data, but I believe the essential points of agreement and disagreement between the π exchange Deck graph and the data are not affected. Thus, instead of facing the full 2 to 4 body process $ap \to (a\pi\pi)N$, I restrict myself to the technically simpler 2 to 3 body reaction $ap \to (a^*\pi)N$.

2.2 Variables

Five independent kinematic variables are required in the description of a $2 \to 3$ body process, such as $ap \to a^*\pi N$. I select the set of invariants $s_{\pi a^*} = M^2_{\pi a^*}$; $s_{\pi N} = M^2_{\pi N}$; t_{pN}, t_{aa^*}, and s. These are illustrated in fig.3. I will introduce other related sets when I discuss decay properties in Section 4.

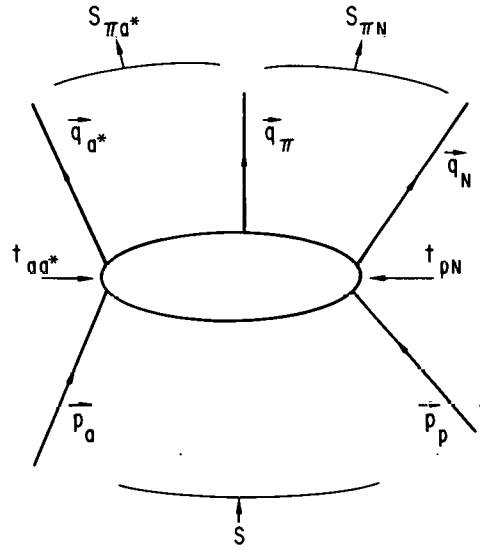

Fig.3 Diagram illustrating the kinematic variables for $ap \to a^*\pi N$.

2.3 Pion Exchange

Practical readers interested only in the answer are urged to skip to eqn.(8). The following is a detailed boring discussion of the content of eqn.(8).

The essential physics of the π exchange Deck graph drawn in fig.1(a) is represented by the amplitude

$$A_\pi = \frac{g}{(m_\pi^2 - t_{aa^*})} A_{\pi N}(s_{\pi N}, t_{pN}) \qquad (2)$$

where the coupling constant g at the πaa^* vertex is discussed below. The pion-exchange propagator accounts for the factor $(M_\pi^2 - t_{aa^*})^{-1}$, and the amplitude $A_{\pi N}(s_{\pi N}, t_{pN})$ represents the off-shell scattering $\pi p \to \pi N$.

Note that spin-indices are omitted here, but they may be reintroduced if one wants to discuss polarizations (Section 3.4).

As written above, the amplitude A_π shows no explicit dependence on either s or $s_{\pi a^*}$. Reggeization of the

pion introduces dependence on $s_{\pi a^*}$, as discussed below.

The use of exchanges to describe the dynamics at small values of $(a^*\pi)$ invariant mass is surely open to criticism. In the same spirit in which they are used in elastic phase-shift analyses, one might imagine employing exchanges at low $(a^*\pi)$ mass to describe the (small) high partial waves, and then try to extract the dynamically more interesting lower waves from data. This is a fine idea, but for the fact that in the inelastic reaction $ap \to a^*\pi p$, the peripheral pion exchange actually generates predominantly the large s wave system. This conversion of the pion's role from the highest to the lowest partial waves is a direct consequence of the inelastic kinematics, and of the fact that following its exchange, the exchanged pion undergoes diffractive scattering from the nucleon. This marvellous phenomenon is explained in Section 4.1.

I employ exchanges at low sub-energy without further apology.

Various prescriptions are possible for "taking the pion off-shell" in the amplitude $A_{\pi N}$. I adopted one method and did not investigate others. I construct $A_{\pi N}$ from on-shell πN elastic data. The off-shell pion is imagined to have only spin and helicity zero. The on-shell πN amplitude is evaluated from Saclay phase shifts[9] up to $M_{\pi N} = 2.6$ GeV, and from a multipole Regge fit[10] for higher $M_{\pi N}$. I obtain $A_{\pi N}$ at a given value of $M_{\pi N}$ and of the scattering angle θ_{pN} from the incident to final nucleon. In the on-shell case θ_{pN} is the usual c.m. scattering angle. For the inelastic process, θ_{pN} is the scattering angle from p to N in the final πN rest frame, calculated from the inelastic kinematics. Thus $\cos\theta_{pN}$ is always in the physical interval $[-1, +1]$, and the elastic amplitude $A_{\pi N}$ is never required in a domain which is nonphysical for elastic scattering.

As eqn.(2) is written, the exchanged pion is "bare"; there is no "form factor" in t_{aa^*}, nor any Regge factors.

Various prescriptions exist for altering the form of the pion propagator away from the pole. For example, nothing inhibits the introduction of a mild form factor

$$\exp(-a(m_\pi^2 - t_{aa^*})) \qquad (3)$$

with $a \simeq 1$ or 2 $(\text{GeV/c})^{-2}$. This serves to reduce the contribution of bare pion exchange at large $|t_{aa^*}|$. Similar suppression could be obtained if $(m_\pi^2 - t_{aa^*})^{-1}$ were replaced with a dual-model type propagator

$$\Gamma(-\alpha_\pi) \qquad (4)$$

where $\Gamma(x)$ is Euler's gamma function and

$$\alpha_\pi = \alpha_\pi'(t_{aa^*} - m_\pi^2) \qquad (5)$$

is the pion Regge trajectory, with slope α_π'.

Reggeization of the pion also introduces dependence on $s_{\pi a^*}$. At very large $s_{\pi a^*}$, this factor has the form $s_{\pi a^*}^{\alpha_\pi}$ in the amplitude. It is less clear what form should be used at low $s_{\pi a^*}$, or even whether Reggeization is justified at all. The specific form I use is

$$[(s_{\pi a^*} - u_{a\pi})/2]^{\alpha_\pi} \qquad (6)$$

where u_a is the momentum transfer from incident particle a to the final pion.

$$u_{a\pi} = -s_{\pi a^*} - t_{aa^*} + m_{a^*}^2 + m_a^2 + m_\pi^2 + t_{pN} \qquad (7)$$

This form (6) indeed fits data better than the simpler form $s_{\pi a^*}^{\alpha_\pi}$, for reasons which I will mention below, but the effects are more cosmetic than fundamental.

The explicit dependence on $s_{\pi a^*}$, whichever form is used, serves to sharpen the enhancement generated at low (πa^*) mass, but it does not create the enhancement[6]. The dependence on $s_{\pi a^*}$ shows up most clearly in the distribution $d\sigma/d\phi_t^{\pi N}$, where $\phi_t^{\pi N}$ is the t-channel aximuthal angle (Treiman-Yang angle) of the final πN system[6]. Dependence on $s_{\pi a^*}$ in the amplitude produces an asymmetry in $d\sigma/d\phi_t^{\pi N}$ in reasonable agreement with data[6].

Save for this Treiman-Yang angle distribution and for the issue of phase mentioned below, the agreement or lack thereof of the pion-exchange Deck model with data does not depend in a major way on Reggeization of the pion.

Reggeization provides the signature phase factor $e^{-i\pi\alpha_\pi/2}$ in the amplitude. At the pion pole, this phase is purely real. Thus, features depending on the presence of this phase factor require an examination of data at $|t_{aa^*}|$ values large enough for α_π to be non-negligible. Among the observational means for detecting the phase variation factor, two may be mentioned. One would be the interference of the pion-

exchange Deck graph with another amplitude of known phase structure. For example, the interference of $\pi p \to (3\pi)p$ with $\pi p \to A_2 p$, could be used, under the hypothesis that the A_2 production phase is known[11]. Second, in a spin-parity decomposition of the Deck amplitude in the πa^* sub-channel, at fixed $M_{\pi a^*}$, the relative phase of the different partial waves (e.g., s wave vs. p wave) depends on α_π' directly. This is discussed in Section 4.5. The Illinois group[8,11] argues that both methods are consistent with the assumption that the Regge phase factor is present, with slope $\alpha_\pi' \simeq 1$ (GeV/c)$^{-2}$.

The question of whether the pion is a Regge pole can presumably be answered directly with data on, say, $\pi p \to \rho^0 n$. In an analysis of such two-body data, Field and Sidhu[12] conclude that the absence of significant shrinkage of the differential cross section from 6 to 17 GeV/c puts a limit on α_π' of the type $\alpha_\pi' \lesssim 0.3$. Michael takes a more global view in arguing that strong evidence is lacking both for and against the assertion that the pion is a normal Regge pole with slope near unity[13]. The lesson for investigations in which the pion is used in inelastic processes is clear. Results which depend too strongly on the slope α_π' should be examined cautiously.

In summary, the full amplitude I use for numerical computations is

$$A_\pi = g \frac{[(s_{\pi a^*} - u_{a\pi})/2]^{\alpha_\pi}}{(m_\pi^2 - t_{aa^*})} e^{-i\pi\alpha_\pi/2} A_{\pi N}(s_{\pi N}, t_{pN}) \qquad (8)$$

with slope $\alpha_\pi' = 0.9$.

In addition to caveats already listed, eqn.(8) is further naive in that "absorption" effects are absent. I believe all these points of weakness do not affect the major conclusions reached in this article.

It should be noted that I treat both "diffractive" $ap \to A^*p$ and charge exchange $ap \to A^*n$ (or $an \to A^*p$) processes. Other than isospin constant factors, the difference between the diffractive and charge exchange reactions resides entirely in the amplitude $A_{\pi N}$.

At large $s_{\pi N}$, this difference may be expressed by the fact that the leading $s_{\pi N}$ dependence of $A_{\pi N}$ differs in the two cases:

$$\begin{aligned} &\text{CHEX} && A_{\pi N} \sim s_{\pi N}^{\alpha_\rho} \approx s_{\pi N}^{1/2} \\ &\text{Diffractive} && A_{\pi N} \sim s_{\pi N}^{\alpha_p} \approx s_{\pi N} \end{aligned} \qquad (9)$$

This simple difference in the $s_{\pi N}$ behaviour of $A_{\pi N}$ leads directly to the prediction of several important differences between diffractive and charge exchange inelastic processes, including their overall s dependence, shapes of mass distributions, decay angular distributions, spin-parity consent and so forth, as I will describe below.

2.4 Coupling Constants

The coupling constant g in eqn.(8) varies for different sets (a, a*). If (a, a*) = (p, n) or (n,p),

$$g^2 = 2 \cdot (4\pi)(14.5) \sqrt{-t_{aa^*}} \qquad (10)$$

If a* is a $J^P = 1^-$ vector state, then g is evaluated easily in terms of the width Γ of $a^* \to a\pi$

$$g^2 = 48\pi \Gamma m_{a^*}^3 / \{m_{a^*}^2 - (m_a + m_\pi)^2\}^{1/2} \{m_{a^*}^2 - (m_a - m_\pi)^2\}^{1/2} \qquad (11)$$

For a $J^P = 2^+$ object a*, the numerical factor 48 in eqn.(11) is replaced by 80.

The value of g must be further reduced by isospin factors appropriate to the charge states considered. For reaction $K^+p \to K^{*0}\pi^+p$, if only the charged decay mode $K^{*0} \to K^+\pi^-$ is accepted, the isospin factor is 4/9. For $K^0p \to K^{*+}\pi^-p$, with only $K^{*+} \to K^0\pi^+$ accepted, the factor is again 4/9. For $K^-p \to K^{*-}\pi^+n$, with only the mode $K^{*-} \to K^0\pi^-$ accepted, the factor is 2/9.

2.5 Normalization

Normalization is such that the integrated cross section in millibarns is

$$\sigma = \frac{0.3893}{F} \Phi_3 [\Sigma|A_\pi|^2] \qquad (12)$$

The flux factor F is

$$F = 4 m_p p_{inc.}^{lab} \qquad (13)$$

and $\Sigma|A|^2$ is the usual square of the absolute value of the invariant matrix element, summed over final spins and averaged over initial spins. The three

particle phase space element is

$$\Phi_3[1] = \frac{1}{(2\pi)^5} \prod_{i=1}^{3} \frac{d^3q_i}{2q_{io}} \delta^4(q_1 + q_2 + q_3 - p_1 - p_2) \tag{14}$$

The final and initial particle four-vector momenta are

$$q_i = (\underset{\sim}{q}_i, q_{io}) \quad \text{and} \quad p_j = (\underset{\sim}{p}_j, p_{jo}) \tag{15}$$

as illustrated in fig.3.

As discussed above, the quantity $\Sigma|A_{\pi N}|^2$ appearing in eqn.(8) is the (off-shell) $\pi p \to \pi N$ scattering amplitude, squared and summed, as usual. If the π were on-shell, the differential πp elastic cross section in millibarns would be

$$\frac{d\sigma}{d\Omega} = \frac{0.3893}{64\pi^2 s} \Sigma|A_{\pi N}|^2 \tag{16}$$

I computed distributions for the Reggeized Deck model using a standard Monte Carlo event generator. Results are described below.

3. PRODUCTION PROPERTIES

Because the full elastic amplitude $A_{\pi N}$ is embedded in the inelastic amplitude, eqn.(8), many production properties of $ap \to (a^*\pi)N$ are a direct reflection of observed features of $\pi p \to \pi N$. These include overall normalization, the s dependence of σ_{inel}, cross-over properties of the differential cross section $d\sigma/dt_{pN}$, the dominance of natural parity exchange in the t_{pN} channel, and polarization in the production. In this section I will discuss each of these issues. I begin first with a treatment of the character of the enhancement generated near threshold in the (πa^*) mass distribution.

3.1 The Low Mass Enhancement

In the reaction $ap \to a\pi\pi N$, the Deck model assumes the presence of resonances in the $(a\pi)$ and (πN) channels, but none in $(a\pi\pi)$ and $(\pi\pi N)$. It generates, nevertheless, pronounced non-resonant enhancements near threshold in the mass distributions $d\sigma/dM(a\pi\pi)$ and $d\sigma/dM(\pi\pi N)$.

These enhancements are present whatever the charge and isospin quantum numbers may be of $(\pi\pi a)$ and/or $(\pi\pi N)$, provided that the Deck graphs may be drawn. If the quantum numbers of $(\pi\pi a)$ or of $(\pi\pi N)$ allow, there may be genuine three body resonances in these channels, sitting on the Deck enhancements. As examples, the A_2 rides on the high mass side of the A_1 Deck enhancement in the (3π) channel; the K*(1420) is located on the high mass side of the Q(K$\pi\pi$) enhancement; and the N*(1688) is present in the $(N\pi\pi)$ or $(N\pi)$ channels. In principle, the Deck amplitude can interfere with the production amplitudes for these well established resonances, as well as with the amplitudes representing the production of bona fide $J^P = 1^+$ A_1, Q, and other resonances, so far not established. Here I will concentrate on the non-resonant pion-exchange Deck enhancement. In Section 4.3 I include some comments on resonance-Deck interference.

For general reactions of the type $2 \to 3$, enhancements near threshold in the invariant mass of a pair of the 3 final particles are a general consequence of double-peripheral dynamics[7], illustrated in fig. 1(c). Thus for a reaction mediated by fig.1(c), the distributions $d\sigma/dM_{13}$ and $d\sigma/dM_{23}$ may show peaks near threshold, while $d\sigma/dM_{12}$ peaks near the maximum $M_{12} = (\sqrt{s} - m_3)$. The precise shape and strength of the low mass enhancements depend strongly on the particular trajectories α_1 and α_2 exchanged. The π exchange Deck model is a special example of fig.1(c), in which α_2 = pion and α_1 = Pomeron plus (ρ,f), in the case of diffractive production, or $\alpha_1 = \rho$ in the case of charge exchange. The peak near threshold in the M_{23} distribution is more pronounced the greater is the difference $(\alpha_1(0) - \alpha_2(0))$. For example, the diffractive case provides sharper enhancements than for charge-exchange.

In the case of diffractive production, $ap \to a^*\pi p$, the pion-exchange Deck model provides a peak centred about 200 MeV above (πa^*) threshold, with full width at half maximum roughly 400 MeV wide. All reactions are thus very similar, save for a displaced threshold which is controlled by the mass of a*. A comparison with data is presented in fig.4. This is the Illinois calculation[8] of $\pi p \to (3\pi)p$, based on the diagram of fig.2. While generally acceptable, it is evident that the model does not follow the sharper fall of the data on the high mass side of the A_1 enhancement, and that it fails to generate a second peak in the A_3 region. Thus, the relative proportion of ρ and f present in $\pi\pi$ scattering does not translate properly into the relative strengths of A_1 and A_3.

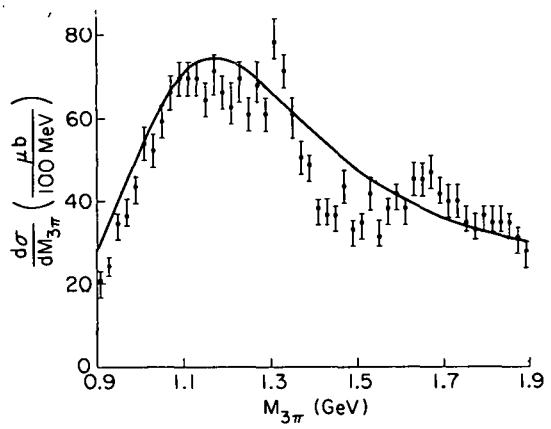

Fig. 4 The differential cross section $d\sigma/dM_{3\pi}$ from $\pi p \to (3\pi)p$. This figure is taken from ref. (8). Data points are combined 11 to 25 GeV/c data. The curve is the Illinois π exchange Deck model result, ref. (8).

A comparison of experiment[14] and theory for $Kp \to (K\pi\pi)p$ at 40 GeV/c is presented in fig.5. In the model, I computed $Kp \to K^*_{890}\,\pi p$ plus $Kp \to K^*_{1420}\,\pi p$. The theoretical curves are normalized absolutely, based on eqn.(8), but should be multiplied by the isospin factor (4/9) if exact comparison is to be made with the data. The relative proportion of Q and L production seems to be correctly reproduced. However, the theoretical curve rises from $(K^*_{890}\pi)$ threshold too steeply, peaks at a value of $(K\pi\pi)$ mass which is of order 50 MeV too low, and then tails off on the high side too gradually with respect to the data. Thus, the general agreement of the Deck enhancement with the experimentally observed enhancement is only qualitatively acceptable.

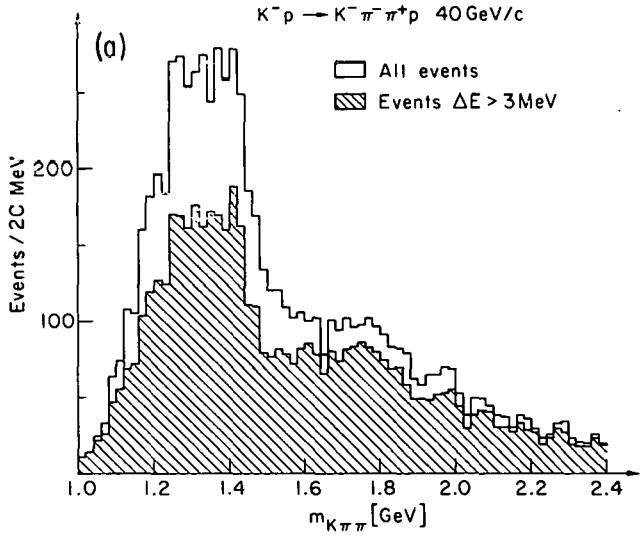

Fig. 5(a) Distribution of events as a function of $(K\pi\pi)$ mass from $K^-p \to (K\pi\pi)p$ at 40 GeV/c. Data are from ref. (14). The full histogram is for all events and the shaded portion for events in which there is no $K\pi$ ambiguity.

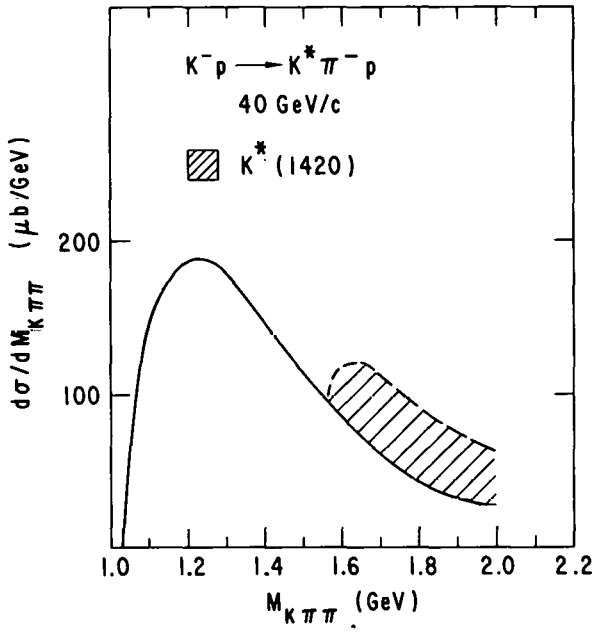

Fig. 6(b) Differential cross section $d\sigma/dM_{K^*\pi}$ calculated from the Reggeized pion exchange Deck amplitude at 40 GeV/c. The shaded portion is the contribution from $K^-p \to K^*_{1420}\,\pi^-p$ whereas the rest pertains to $K^-p \to K^*_{890}\,\pi^-p$. The curves are given in absolute units. If only the charged particle decay mode $K^{*0} \to K^-\pi^+$ is accepted, the normalization should be scaled down by the factor (4/9).

The discrepancy between theory and experiment on the high mass side of the A_1 and Q enhancements suggests the presence of some additional dynamical effect, not present in the model as it stands, which depresses the theoretical curve on the high mass side. One way to accomplish this is to remove some of the higher partial waves (i.e. waves above the dominant s wave $J^P = 1^+$), because it is these higher waves which feed the cross section at the larger values of $(a\pi\pi)$ mass. However, this "cure" seems not to be sufficient, because even the mass variation of the $J^P = 1^+$ component in the theory is incorrect[8], falling off too gradually as $(a\pi\pi)$ mass increases. Perhaps the lesson is that unitarity effects must be included in the model, as a form of rescattering in the (πa^*) channel.

3.2 Magnitude and Energy Dependence of σ

For a selected range of A* mass, the total cross section is obtained by integration of eqn.(12) over all kinematic variables. The prediction is "absolute" once a parametrization of eqn.(8) is adopted. Its magnitude is controlled by the magnitude of $\sigma_{el}^{\pi p}$ and by the width Γ_{a^*} for $a^* \to a\pi$. The energy dependence of σ_{A^*} follows that of $\sigma_{el}^{\pi p}$ (or, in case of charge-exchange, that of $\sigma(\pi^- p \to \pi^0 n)$). In fig.6, I present results obtained by the Illinois group[8] for $\pi^- p \to A_1^- p$, where A_1 is defined as $1.05 \leq M_{3\pi} \leq 1.25$ GeV. Agreement with the experimental cross section in the same energy and mass range is said to be good[8].

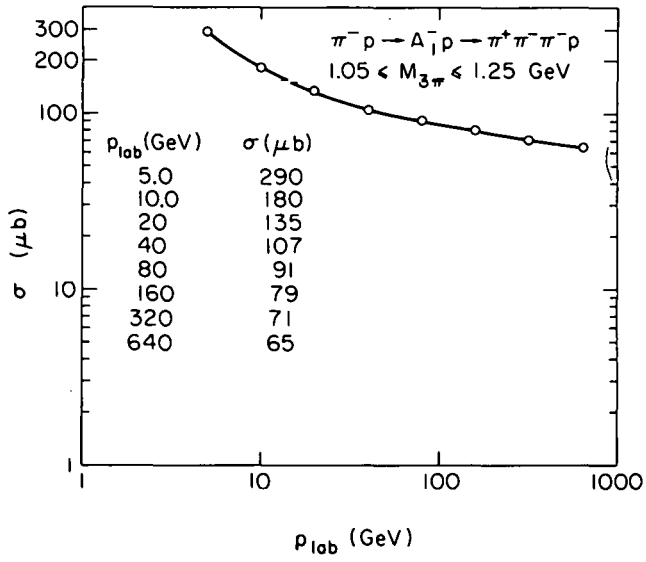

Fig.6 The integrated production cross section for $\pi^- p \to A_1^- p$ obtained by the Illinois group from their π exchange Deck model (ref.(8)). The A_1 is defined as $M_{3\pi}$ between 1.05 and 1.25 GeV.

A few comments may be made. On a purely technical level, keeping only the $\pi p \to (\pi\rho)p$ contribution rather than the full Illinois $\pi p \to (3\pi)p$ amplitude, I obtain 67% of the quoted Illinois cross sections at 10 and 20 GeV/c. A more serious reflection on the agreement with data is that use of $s_{\pi\rho}^{\alpha_\pi}$ rather than $[1/2(s_{\pi\rho} - u_{\pi\pi})]^{\alpha_\pi}$ in the amplitude (eqn.(8)) reduces the cross section by 30%. Moreover, where a "form factor" of the type $\exp(a(m_\pi^2 - t_{aa^*}))$ introduced in the amplitude, the cross section would be reduced by roughly $\frac{1}{2a}$. Values of $a \cong 2$ are hardly unreasonable. Thus, the "perfect" agreement with the experimental integrated cross section is not to be interpreted too strongly as an indication that the pion exchange graph saturates all the cross section. A choice of parameters were made.

Cross sections I computed for $K^{\pm} p \to K^{*0}_{890}\, \pi^{\pm} p$ and for $K^- p \to K^*_{890}\, \pi n$ are shown in fig.7. The charge-exchange cross section is an order of magnitude smaller at 6 GeV/c than the diffractive cross section, and it falls with energy much faster[15].

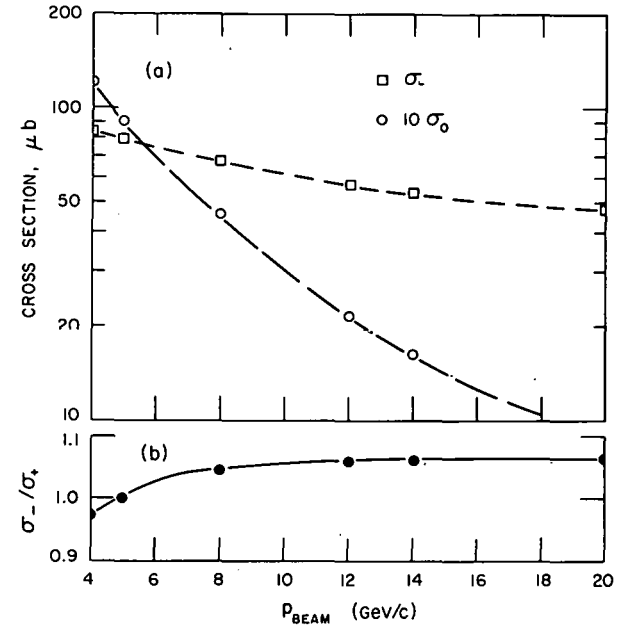

Fig.7 Cross sections $\sigma_\pm$ and σ_0 obtained from the Reggeized π exchange Deck model are presented as a function of incident kaon lab. momentum. σ_- is the cross section for $K^- p \to \bar{K}^{*0}_{890}\, \pi^- p$, with $\bar{K}^* \to K^0\pi^-$, only, or for $K^0 p \to K^{*+}_{890}\, \pi^- p$ $(K^{*+} \to K^0\pi^+)\sigma_+$ is the cross section for $K^+ p \to K^{*0}_{890}\, \pi^+ p$ $(K^{*0} \to K^+\pi^-)$ or for $K^0 p \to K^{*-}\pi^+ p$ $(K^{*-} \to \bar{K}^0\pi^-)$; and σ_0 is the cross section for the charge-exchange process $K^- p \to K^{*-}\pi^+ n \to K^0\pi^-\pi^+ n$. For all results, the two selections imposed are Mass $(K^*\pi) < 1.5$ GeV and Mass $(N\pi) > 1.34$ GeV, where N denotes the final nucleon.

In comparing these cross sections with data[16], I find that my diffractive results account for about half of the observed cross sections in the range 6 to 14 GeV/c. At 40 GeV/c, $\sigma(M_{K\pi\pi} \leq 1.6) = 188 \pm 9$ μb according to a Geneva-CERN-IHEP collaboration[14], whereas I obtain 37 μb. Scaling my result up by 1.5 to account for the full (Kπ) amplitude, rather than the K^*_{890} approximation, still leaves me short by a factor of 3. Since I helped myself to as much cross section as I could [no form factor on the π, $[1/2(s_{\pi K^*} - u_{K\pi})]^{\alpha_\pi}$,] I conclude that the agreement in absolute normalization is worse for Q production that it appears to be for A_1 production. Does this

imply need for a K^* exchange graph, and/or a contribution from $Kp \to \rho Kp$, or something else? Observation experimentally of an enhancement at low ($K\omega$) mass in $Kp \to \omega Kp$ suggests that $Kp \to \rho Kp$ might be a good fraction (e.g. 30%) of $Kp \to (K\pi\pi)p$, both experimentally and in the Deck description thereof. The relevant graph might have a K exchange followed by Kp off-shell elastic scattering, as shown in fig.8. Other features of data, discussed in Section 3.3.2 also suggest that the K^* exchange graph contributes to $Kp \to K^*\pi p$ a cross section roughly equal to that of π exchange.

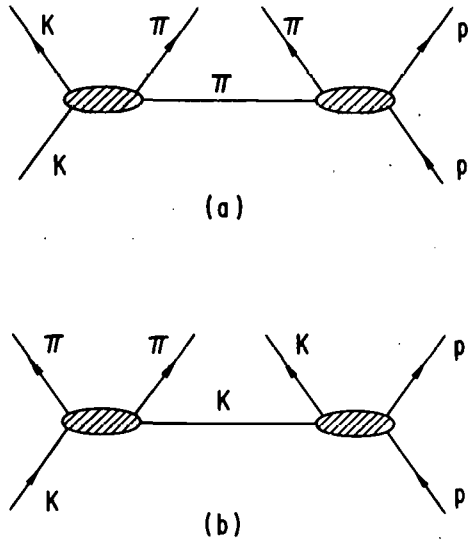

Fig.8 (a) Pion-exchange diagram for $Kp \to (K\pi)(\pi p)$. This graph is more complete in that the full $(K\pi)$ amplitude is retained, not just the $K^*(890)$.
(b) Kaon-exchange diagram for $Kp \to (\pi\pi)(Kp)$.

3.3 Production Differential Cross Sections

For $ap \to (a^*\pi)p$, we may try to parametrize the differential cross section as

$$\frac{d^2\sigma}{dt'dM_{a^*\pi}} = c \exp(bt'_{pp}) , \qquad (17)$$

Here t' is the difference $(t_{pp} - t^{max}_{pp})$, where t^{max}_{pp} is the smallest value of $|t_{pp}|$ for a given $M_{a^*\pi}$.

This parametrization is convenient, and it often allows a reasonable χ^2 (although not always). Slope b depends on s, $M_{a^*\pi}$, and also on the decay angles (θ,ϕ) in the $A^* \to \pi a^*$ rest frame. To first approximation b reflects the "input" slope from the elastic πN part of the amplitude. As a function of s, b therefore shows shrinkage, and it has other characteristic properties of πN scattering, such as cross-over behaviour.

3.3.1 Shrinkage

Values of b I computed from the π exchange Deck model for $K^{\pm}p \to K^{*0}\pi^{\pm}p$ are presented in fig.9, for the selection $M(K^*\pi) < 1.5$ GeV/c. I fitted theoretical distributions to eqn.(17) over the range $0.02 < |t'_{pp}| < 0.5$ $(GeV/c)^2$. The shrinkage is apparent, with b increasing logarithmically after a faster initial threshold rise. A comparison of the parts (a) and (b) of fig.9 shows that selections on the $(p\pi)$ mass may have a large effect on the measured slope. In $K^+p \to K^{*0}\pi^+p$, the Δ^{++} signal is strong in the final state at low incident momenta.

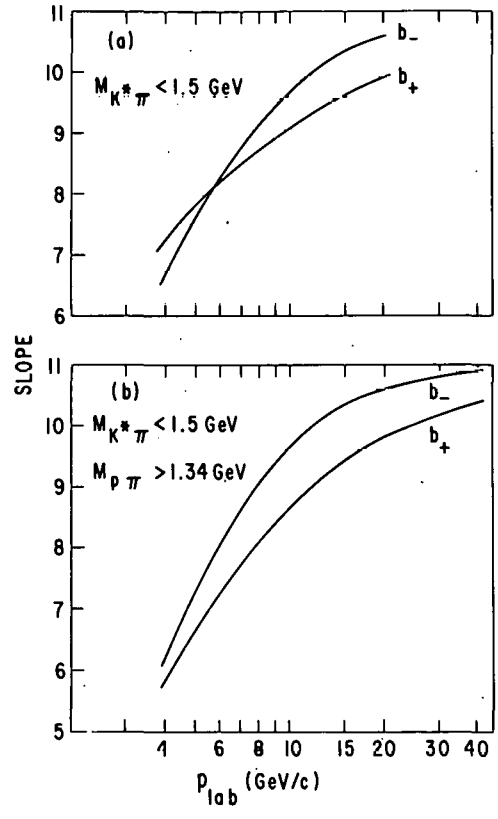

Fig.9 Slopes b for the differential cross section $d\sigma/dt' = c\exp(-bt')$ obtained from the Reggeized π exchange Deck model calculations described in the text, as a function of incident kaon lab. momentum. Slope b_- is for $K^-p \to K^{*0}_{890}\pi^-p$ or for $K^0p \to K^{*+}_{890}\pi^-p$. Slope b_+ is for $K^+p \to K^{*0}_{890}\pi^+p$ or $\bar{K}^0p \to K^{*-}_{890}\pi^+p$. In (a) and (b), the selection is made which restricts the $K^*\pi$ invariant mass to be below 1.5 GeV, in the "Q region". In (b), an additional selection restricts the final πp invariant mass to be greater than 1.34 GeV. All slopes are fitted over the range $0.02 < |t'| < 0.5$ $(GeV/c)^2$.

Because elastic πp scattering in the Δ regions has a large effective slope, this effect is transmitted to the inelastic reaction.

The values of $b_{\pm}$ given in fig.9(b) are roughly 0.7 larger than the experimental values in the range 6 to 14 GeV/c[17]. The rate of shrinkage seen is compatible with that observed in the data, as is the difference $(b_- - b_+)$. Inclusion of a K* exchange graph with weight comparable to that of π exchange would be expected to depress the net value of b_+.

3.3.2 Cross-Overs

It is observed experimentally that the slope b_- of $d\sigma/dt$ for $\pi^- p$ elastic scattering is larger than b_+ for $\pi^+ p$ elastic scattering. At high energy the value of the $\pi^- p$ differential cross section at $t = 0$ is larger than that of $\pi^+ p$, and its value at $|t| \gtrsim 0.4$ (GeV/c)^2 is smaller[18]. The cross-over occurs near $t \simeq -0.2$ (GeV/c)^2. These cross-over properties of πN elastic scattering should be reflected in inelastic processes if the pion exchange Deck model is relevant. Because I recently wrote a long article[15] on this subject, to which the interested reader may refer for details, I will confine my remarks here to a few brief comments.

The π exchange Deck graphs relevant for $\pi^{\pm} p \to (3\pi)^{\pm} p$ and $K^{\pm} p \to (K\pi\pi)^{\pm} p$ are sketched in fig.10. It will be noted that $d\sigma/dt'$ for the $\pi^{\pm}$ (and $K^{\pm}$) induced inelastic processes in controlled by $\pi^{\pm}$ elastic scattering. Thus we easily predict $b_{K^-} > b_{K^+}$ and $b_{\pi^-} > b_{\pi^+}$ for the above inelastic reactions, in fine accord with data[19,20].

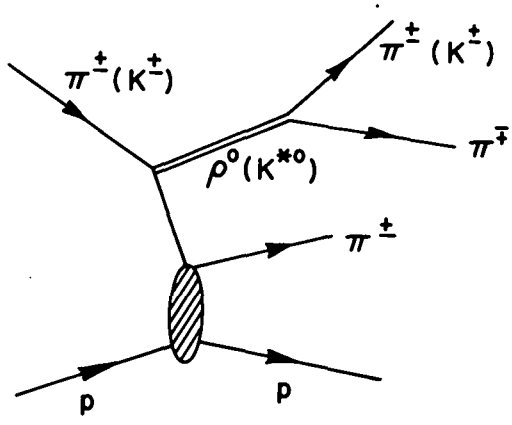

Fig.10 Pion-exchange Deck graphs for the processes $\pi^{\pm} p \to \rho^0 \pi^{\pm} p$ *and* $K^{\pm} p \to K^{*0} \pi^{\pm} p$.

The analogous expectation for neutral Q production does not agree with experiment[21]. As sketched in fig.11, the process $K^0 p \to Q^0 p$ is a reflection of $\pi^- p$ elastic scattering, whereas $\overline{K^0} p \to \overline{Q^0} p$ reflects $\pi^+ p$. Thus $b_{K^0} > b_{\overline{K^0}}$ is the π-exchange Deck model expectation. Data from a SLAC experiment show the opposite[21].

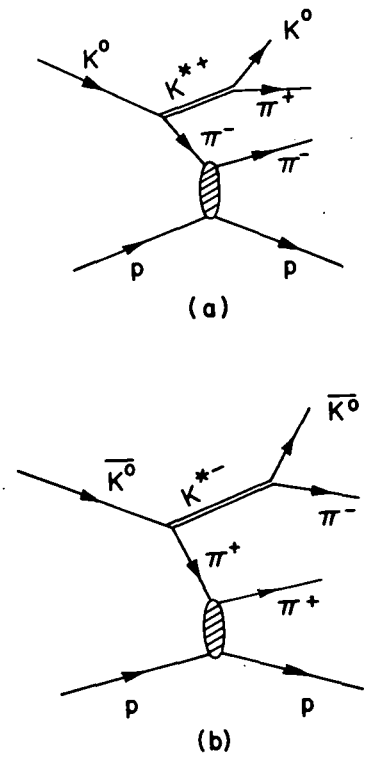

Fig.11 Pion-exchange Deck graphs for (a) $K^0 p \to K^{*+} \pi^- p$ *and* (b) $\bar{K}^0 p \to K^{*-} \pi^+ p$.

The SLAC $K^0 p \to Q^0 p$ results agree with the general systematics abstracted from elastic processes, which is the anti-particle induced reactions have larger values of $d\sigma/dt$ at $t = 0$ and larger slopes than their particle induced counterparts.

What are the implications of the disagreement with the SLAC data? One possibility is that the larger slope for $\overline{K^0}$ is a low-energy non-asymptotic effect, due to the presence of a Δ^{++} competing channel in the final state. While this guess should be checked more explicitly in the data, a careful reading of the publication suggests that the Δ region was excluded from the data sample before slopes were measured.

A more interesting conclusion within the Deck model context is that a K* exchange graph must be involved. The K*p (off-shell) elastic scattering presumably obeys canonical systematics, with $b_{\overline{K^*}} > b_{K^*}$. As a reflection, in the inelastic process $K^0 p \to Q^0 p$, we expect $b_{\overline{K^0}} > b_{K^0}$.

The π and K* exchange graphs both contribute to $Kp \to Qp$. For $K^{\pm}p \to Q^{\pm}p$, the π and K* exchange graphs give the same prediction $b_{K^-} > b_{K^+}$, in agreement with data. However, for $K^0p \to Q^0p$, the two graphs give opposite results. The K* exchange graph dominates the cross-over for $Kp \to Qp$, presumably because the cross-over effect is more pronounced in Kp elastic scattering than in πp elastic scattering.

The conclusion that the K* exchange graph contributes to $Kp \to Qp$ with weight roughly equal to that of the π exchange graph has far reaching consequences in Deck model investigations. It means that the π exchange graph might only be half the story also in all other processes to which the Deck model may be applied. A procedure to estimate the relative contributions is described in Section 3.3.3.

The reaction $K^0p \to Q^0p$ is not the only reaction for which the exchange Deck graph and the "other" exchange graph would predict opposite signs for cross-overs in $d\sigma/dt'$. In Table 1, I itemize a set of reactions and list the cross-over systematics expected. The overall cross-over in the data, if any, is determined by the relative weights of the two contributing exchange amplitudes.

Table 1

Pairs of inelastic reactions are listed in Column 1. One member of each pair is related to the other by line-reversal in the t-channel. In the remaining columns, I present predictions for the cross-over systematics of the production differential cross sections, based on the Deck model. Column 3 lists the asymptotic cross-over systematics of the differential cross sections $d\sigma/dt'$ for these pairs, according to the pion-exchange Deck model. The predictions are strictly valid only in the portion of phase-space where pion-exchange dominates (e.g. $\cos\phi_s > 0$; see Section 4.2.2), but, in certain cases, they may continue to be correct beyond. In Column 2 of parts (a) and (b), the πN charge states appearing in the Deck graph are noted; for the target a dissociation processes in parts (c) and (d), the a π charge states are presented.

Column 5 lists the asymptotic cross-over systematics for the portion of decay phase space ($\cos\phi_s < 0$) controlled by the a* exchange Deck graph. The net cross-over observed in the full data sample ($-1 \leq \cos\phi_s \leq 1$) depends upon the relative weights of the π-exchange and a* exchange graphs.

Table 1(a)

Projectile Dissociation; Proton Target

Process†	Pion Exchange Deck Graph $\cos\phi_s > 0$		The Other Graph $\cos\phi_s < 0$	
	Reflection of the Elastic Scattering of	Systematics for the Slopes of $d\sigma/dt'$ and Cross-over	Reflection of the Elastic Scattering of	Systematics for the Slopes of $d\sigma/dt'$ and Cross-over
$K^{\pm}p \to (K^*\pi^{\pm})p$	$\pi^{\pm}p$	$b_{K^-} > b_{K^+}$	K^*p $\bar{K}^*p$	$b_{K^-} > b_{K^+}$
$\pi^{\pm}p \to \rho^0\pi^{\pm}p$	$\pi^{\pm}p$	$b_{\pi^-} > b_{\pi^+}$	ρ^0p	$b_{\pi^+} = b_{\pi^-}$
$pp \to (n\pi^+)p$ $\bar{p}p \to (\bar{n}\pi^-)p$	π^+p π^-p	$b_{\bar{p}} > b_p$	np $\bar{n}p$	$b_{\bar{p}} > b_p$
$pp \to \Delta^{++}\pi^-p$ $\bar{p}p \to \overline{\Delta^{++}}\pi^+p$	π^-p π^+p	$b_p > b_{\bar{p}}$	$\Delta^{++}p$ $\overline{\Delta^{++}}p$	$b_{\bar{p}} > b_p$
$K^0p \to K^{*+}\pi^-p$ $\bar{K}^0p \to K^{*-}\pi^+p$	π^-p π^+p	$b_{K^0} > b_{\overline{K^0}}$	$K^{*+}p$ $K^{*-}p$	$b_{\overline{K^0}} > b_{K^0}$

†Predictions for $\pi^{\pm}p \to f^0\pi^{\pm}p$, for $\pi^{\pm}p \to g^0\pi^{\pm}p$ are the same as for $\pi^{\pm}p \to \rho^0\pi^{\pm}p$.

Table 1(b)

Projectile Dissociation; Neutron Target

Process	Pion Exchange Deck Graph $\cos\phi_s > 0$		The Other Graph $\cos\phi_s < 0$	
	Reflection of the Elastic Scattering of	Systematics for the Slopes of $d\sigma/dt'$ and Cross-over	Reflection of the Elastic Scattering of	Systematics for the Slopes of $d\sigma/dt'$ and Cross-over
$K^{\pm}n \to (K^{*}\pi^{\pm})n$	$\pi^{\pm}n$ (i.e. $\pi^{\mp}p$)	$b_{K^+} > b_{K^-}$	$K^{*}n$ $\bar{K}^{*}n$	$b_{K^-} > b_{K^+}$
$\pi^{\pm}n \to \rho^{0}\pi^{\pm}n$	$\pi^{\pm}n$ (i.e. $\pi^{\mp}p$)	$b_{\pi^+} > b_{\pi^-}$	$\rho^{0}n$	$b_{\pi^+} = b_{\pi^-}$
$pn \to (n\pi^{+})n$ $\bar{p}n \to (\bar{n}\pi^{-})n$	$\pi^{+}n$ (i.e. $\pi^{-}p$) $\pi^{-}n$ (i.e. $\pi^{+}p$)	$b_p > b_{\bar{p}}$	nn $\bar{n}n$	$b_{\bar{p}} > b_p$
$pn \to (\Delta^{\pm\pm}\pi^{\mp})n$ $\bar{p}n \to (\overline{\Delta^{++}}\pi^{+})n$	$\pi^{-}n$ (i.e. $\pi^{+}p$) $\pi^{+}n$ (i.e. $\pi^{-}p$)	$b_{\bar{p}} > b_p$	$\Delta^{++}n$ $\overline{\Delta^{++}}n$	$b_{\bar{p}} > b_p$
$K^{0}n \to (K^{*+}\pi^{-})n$ $\bar{K}^{0}n \to (K^{*-}\pi^{+})n$	$\pi^{-}n$ (i.e. $\pi^{+}p$) $\pi^{+}n$ (i.e. $\pi^{-}p$)	$b_{\bar{K}^0} > b_{K^0}$	$K^{*+}n$ $K^{*-}n$	$b_{\bar{K}^0} > b_{K^0}$

Table 1(c)

Target Dissociation; Proton Target

Process	Pion Exchange Deck Graph $\cos\phi_s > 0$		The Other Graph $\cos\phi_s < 0$	
	Reflection of the Elastic Scattering of	Systematics for the Slopes of $d\sigma/dt'$ and Cross-over	Reflection of the Elastic Scattering of	Systematics for the Slopes of $d\sigma/dt'$ and Cross-over
$K^{\pm}p \to K^{\pm}(n\pi^{+})$	$K^{\pm}\pi^{+}$	$b_{K^-} > b_{K^+}$ likely but depends on the unknown properties of $K\pi$ scattering. See text.	$K^{\pm}n$	$b_{K^-} > b_{K^+}$
$K^{\pm}p \to K^{\pm}(\Delta^{++}\pi^{-})$	$K^{\pm}\pi^{-}$	$b_{K^+} > b_{K^-}$ likely but depends on the unknown properties of $K\pi$ scattering. See text.	$K^{\pm}\Delta^{++}$	$b_{K^-} > b_{K^+}$
$\pi^{\pm}p \to \pi^{\pm}(n\pi^{+})$	$\pi^{\pm}\pi^{+}$	$b_{\pi^-} > b_{\pi^+}$ likely but depends on the unknown properties of $\pi\pi$ scattering. See text.	$\pi^{\pm}n$ ($\pi^{\mp}p$)	$b_{\pi^+} > b_{\pi^-}$
$\pi^{\pm}p \to \pi^{\pm}(\Delta^{++}\pi^{-})$	$\pi^{\pm}\pi^{-}$	$b_{\pi^+} > b_{\pi^-}$ likely but depends on the unknown properties of $\pi\pi$ scattering. See text.	$\pi^{\pm}\Delta^{++}$	$b_{\pi^-} > b_{\pi^+}$
$pp \to p(n\pi^{+})$ $\bar{p}p \to \bar{p}(n\pi^{+})$	$\pi^{+}p$ $\pi^{+}\bar{p}$ (i.e. $\pi^{-}p$)	$b_{\bar{p}} > b_p$	pn $\bar{p}n$	$b_{\bar{p}} > b_p$
$pp \to p(\Delta^{++}\pi^{-})$ $\bar{p}p \to \bar{p}(\Delta^{++}\pi^{-})$	$\pi^{-}p$ $\pi^{-}\bar{p}$ (i.e. $\pi^{+}p$)	$b_p > b_{\bar{p}}$	$p\Delta^{++}$ $\bar{p}\Delta^{++}$	$b_{\bar{p}} > b_p$

Table 1(d)

Target Dissociation; Neutron Target

Process	Pion Exchange Deck Graph cos $\phi_s > 0$		The Other Graph cos $\phi_s < 0$	
	Reflection of the Elastic Scattering of	Systematics for the Slopes of $d\sigma/dt'$ and Cross-over	Reflection of the Elastic Scattering of	Systematics for the Slopes of $d\sigma/dt'$ and Cross-over
$K^{\pm}n \to K^{\pm}(p\pi^-)$	$K^{\pm}\pi^-$	$b_{K^+} > b_{K^-}$ likely; see text.	$K^{\pm}p$	$b_{K^-} > b_{K^+}$
$K^{\pm}n \to K^{\pm}(\Delta^-\pi^+)$	$K^{\pm}\pi^+$	$b_{K^-} > b_{K^+}$ likely; see text.	$K^{\pm}\Delta^-$	$b_{K^-} > b_{K^+}$
$\pi^{\pm}n \to \pi^{\pm}(p\pi^-)$	$\pi^{\pm}\pi^-$	$b_{\pi^+} > b_{\pi^-}$ likely; see text.	$\pi^{\pm}p$	$b_{\pi^-} > b_{\pi^+}$
$\pi^{\mp}n \to \pi^{\pm}(\Delta^-\pi^+)$	$\pi^{\pm}\pi^+$	$b_{\pi^-} > b_{\pi^+}$ likely; see text.	$\pi^{\pm}\Delta^-$	?
$pn \to p(p\pi^-)$ $\bar{p}n \to \bar{p}(p\pi^-)$	π^-p $\pi^-\bar{p}$ (i.e. π^+p)	$b_p > b_{\bar{p}}$	pp $\bar{p}p$	$b_{\bar{p}} > b_p$
$pn \to p(\Delta^-\pi^+)$ $\bar{p}n \to \bar{p}(\Delta^-\pi^+)$	π^+p $\pi^+\bar{p}$ (i.e. π^-p)	$b_{\bar{p}} > b_p$	$p\Delta^-$ $\bar{p}\Delta^-$	$b_{\bar{p}} > b_p$

3.3.3 How to deal with the "Other" Graph

While the π exchange amplitude was relatively easy to parametrize, the "other" graph is less so. If ρ or K* exchange is used, the particle is far off-shell even at overall negative momentum transfer. Moreover, there are no measured cross sections for ρN or K*N elastic scattering. For $pp \to pn\pi^+$, the "other" graph requires nucleon exchange, whose parametrization is a great deception[22].

In any case, before attempting detailed parametrizations, it is preferable to seek as direct evidence as possible in the data for the characteristic features of the π exchange and of the K*, ρ or nucleon exchange graphs. There appears to be a good way to accomplish this, by studying the distribution $d\sigma/d\phi_s$, where ϕ_s is the "s-channel" helicity or azimuthal angle of the $A^* \to a^*\pi$ decay, in the A^* rest frame, as sketched in fig.12.

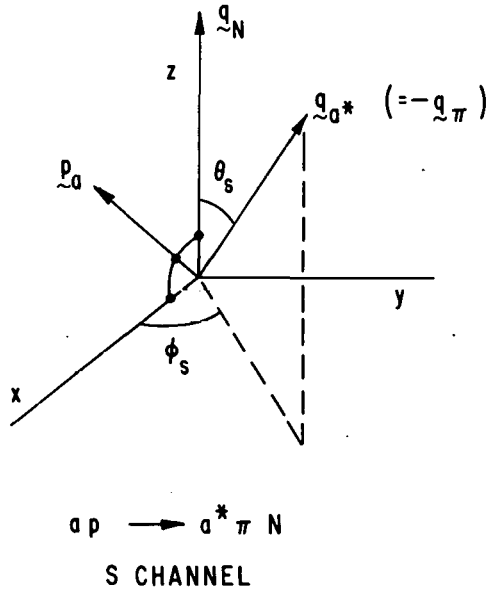

Fig.12 Diagram in which the s-channel decay angles (θ_s, ϕ_s) of $A^* \to (a^*\pi)$ are defined.

We may choose as a set of independent kinematic variables the 5 quantities (s, t_{pN}, $M_{a^*\pi}$, θ_s, and ϕ_s). The variable ϕ_s is "conjugate" to t_{aa^*} because

$$|t_{aa^*}| = A - B\cos\phi_s \qquad (18)$$

where A and B are positive valued functions of the other 4 invariants. In the absence of any dependence on t_{aa^*} (or on $t_{a\pi}$) in the amplitude for $ap \to a^*\pi N$, the distribution $d\sigma/d\phi_s$ should be flat, regardless of whatever dependence is present in the amplitude on the other 4 invariants. My numerical

calculations show that the pion-exchange graph gives a sharp peaking of $d\sigma/d\phi_s$ towards cos ϕ_s = + 1. An example is shown in fig.13. The a* exchange graph will peak towards cos ϕ_s = - 1. The sum of the two could be flat, or show various other structure depending upon the relative weights of the two graphs. A glance at $d\sigma/d\phi_s$ should therefore be instantly instructive.

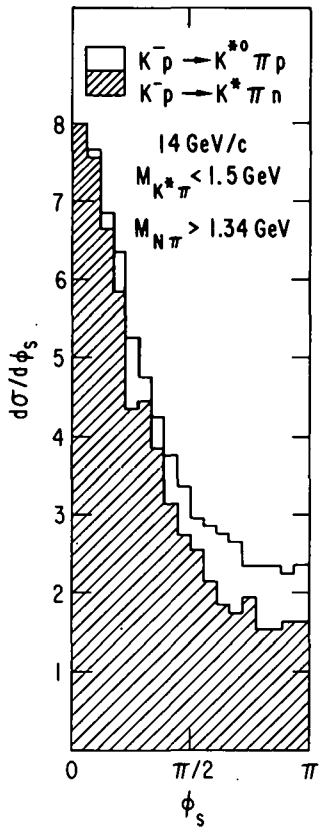

Fig.13 The distribution $d\sigma/d\phi_s$ for $K^-p \to K^*_{890}\,\pi N$ as obtained from the π exchange Deck model at 14 GeV/c. The selections Mass $(K^*\pi) \leq 1.5$ GeV and Mass $(N\pi) \geq 1.34$ GeV were imposed. The full distribution is for the "diffractive" reaction (in which N = proton), whereas the shaded distribution is for the charge-exchange process. The normalization is in arbitrary units for both reactions, adjusted so that the cross sections at $\phi_s = 0$ are equal. Results are presented in histogram form, as obtained from the Monte Carlo event generator.

Selections on ϕ_s should be especially useful. If events are chosen with cos ϕ_s > 0, the contribution from the π exchange Deck graph is enhanced. Correspondingly, cos ϕ_s < 0 selects the a* exchange graph.

Returning to the cross-over situation in $K^0p \to Q^0p$, I predict that events in the cos ϕ_s > 0 segment should have the non-canonical cross-over behaviour $b_{K^0} > b_{\overline{K^0}}$, controlled by the π exchange graph, whereas events with cos ϕ_s < 0 should follow the K* exchange systematics, $b_{\overline{K^0}} > b_{K^0}$. If this prediction fails, the Deck model is in serious difficulty.

A second reaction for which there are data is $\pi^\pm p \to \pi^\pm(\pi^-\Delta^{++})$ at 16 GeV/c[19]. No cross-over is observed in the total sample. Here ϕ_s is the helicity angle of the Δ^{++} in the $(\pi^-\Delta^{++})$ rest frame. Events with cos ϕ_s > 0 should have a cross-over determined by $(\pi^\pm\pi^-)$ elastic scattering, namely $b_{\pi^+} > b_{\pi^-}$. If cos ϕ_s < 0, the Deck graph incorporates $(\pi^\pm\Delta^{++})$ elastic scattering, for which $b_{\pi^-} > b_{\pi^+}$ is expected. The overall absence of a cross-over suggests equal compensating contributions from the π and Δ exchange graphs. These predictions[15] were checked in the data by making the ϕ_s selections and examining the cross-over properties of the t-distributions in the two segments. The predictions are confirmed[23]. The same predictions apply to $K^\pm p \to K^\pm(\pi^-\Delta^{++})$, for which data exist at 8 GeV/c.

The success of the cross-over predictions for $\pi^\pm p \to \pi^\pm(\pi^-\Delta^{++})$ confirms the utility of the cos ϕ_s selection procedure. It also helps to establish that the cos ϕ_s > 0 region shows quantum number characteristics (symmetry properties) of π exchange, whereas the cos ϕ_s < 0 region has baryon exchange properties. Thus, the validity of using exchanges of specific type to describe the low mass $(\pi^-\Delta^{++})$ enhancement is supported. Note, in passing, that the data show also that production and decay of $(\pi^-\Delta^{++})$ do not factorize, in that different portions of the decay angular distribution have different production characteristics.

3.3.4 Mass-Slope correlation

A general feature of inelastic data is that the slope b of $d^2\sigma/dt'dM_{a^*\pi}$ at fixed s decreases systematically as $M_{a^*\pi}$ increases. Data on $Kp \to (K\pi\pi)p$ at 40 GeV/c are shown in fig.14, along with results of my calculation. The agreement is excellent.

The interpretation of this anti-shrinkage with increasing $M_{a^*\pi}$ is intriguing. Regarding the process as $ap \to A^*p$, we might conclude that the production dynamics depend intrinsically on the mass of A* (or on the "size" of A*), in such a way that slope b is an explicit function of $M_{a^*\pi}$. The Deck model provides a different interpretation, essentially a

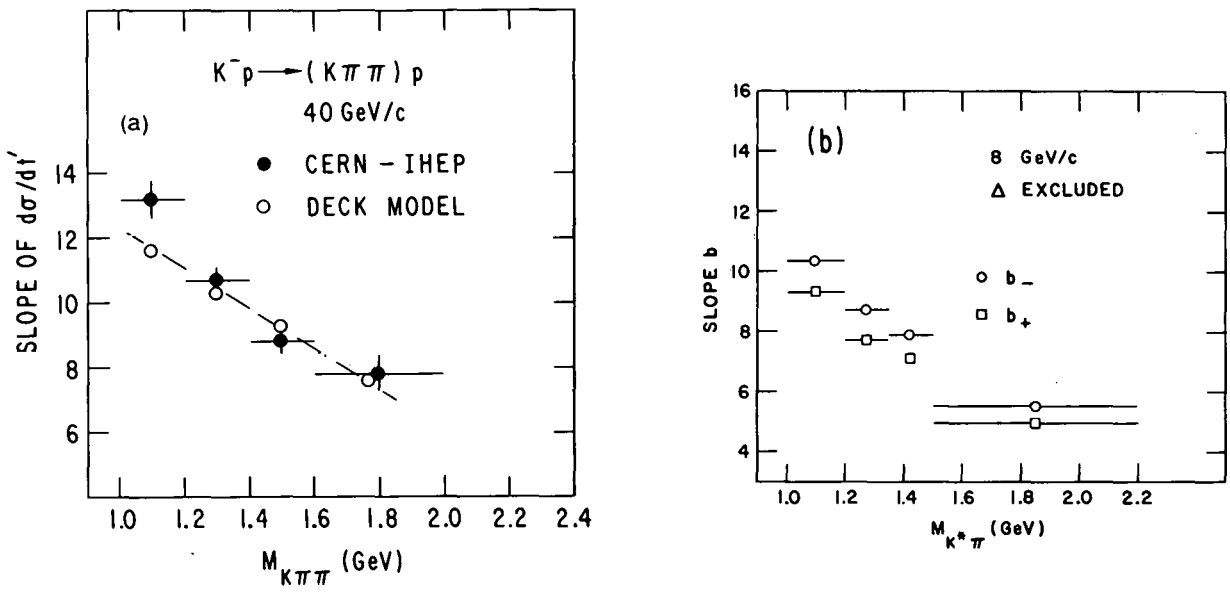

*Fig. 14 (a) The slope b of the production differential cross section for $\bar{K}p \to K^*_{890}\,\bar{\pi}p$ at 40 GeV/c is plotted versus the mass of the (K*π) system, for 4 selected intervals of (K*π) mass. Results of the π exchange Deck model are compared with Serpukhov data (ref. (14)). The dashed line is drawn to aid the eye.*
*(b) Slopes $b_\pm$ of dσ/dt' predicted by the Reggeized π exchange Deck model for $\bar{K}p \to (K^{*0}\pi^\pm)p$ [or, equivalently, for $K^0_L p \to (K^{*\mp}\pi^\pm p)$] are shown as a function of (K*π) invariant mass at 8 GeV/c. The selection Mass (pπ) > 1.34 GeV is imposed.*

kinematic correlation explanation.

At the threshold $M_{a^*\pi} = (m_{a^*} + m_\pi)$, the momentum transfers t_{aa^*} and t_{pN} are related by the equation (see Appendix)

$$t_{aa^*} = \left\{ \frac{m_{a^*}\, t_{pN}}{(m_{a^*} + m_\pi)} + \text{constant} \right\} \approx t_{pN} \qquad (19)$$

The essential t dependence of the pion exchange Deck amplitude is expressed as

$$A \simeq \frac{1}{m_\pi^2 - t_{aa^*}} \exp(\lambda\, t_{pN}) \qquad (20)$$

Near threshold, therefore,

$$A \simeq \frac{1}{k_1 - t_{pN}} \exp(\lambda\, t_{pN}) \simeq \exp(k_2\, t_{pN}) \qquad (21)$$

where $k_2 > \lambda$. Thus, we expect a large slope $b(\approx 2k_2)$ for low M_{A^*}, significantly larger than the "input" elastic slope 2λ. Much above threshold, the kinematic coupling no longer operates and, for a sum of reasons, $b < 2\lambda$.

The π-exchange Deck model results I present in figs. 14(a) and (b) illustrate these arguments, and appear to agree with experiment.

The a* exchange graph will also give a similar mass-slope correlation, although perhaps less pronounced.

There is an obvious way to check whether the Deck explanation is correct. Because the model's explanation depends on the kinematic coupling between t_{pN} and t_{aa^*} (or $t_{a\pi}$), it should suffice to re-do the analysis, but in more dimensions. Thus, one should investigate the three dimensional distribution

$$\frac{d^3\sigma}{dt'_{pN}\, dM_{\pi a^*}\, dt_{aa^*}} \qquad (22)$$

for fixed t_{aa^*} and determine whether the slope in t'_{pN} still falls systematically as $M_{a^*\pi}$ is increased. If so, the Deck explanation is wrong.

Sadly, present statistics do not allow such precision.

An attempt to study the mass-slope correlation effect in greater detail was made by Pirila and Miettinen[24] with data on $pp \to p(n\pi^+)$ at 19 GeV/c. Suffering from poor statistics, they adopted a complicated maximum likelihood fit technique. They

conclude that the pion-exchange Deck model explanation is not correct. Their method appears to be reliable, but its conclusions are really limited to a denial that the pion-exchange graph is the whole story. They cannot rule out the possibility that a combination of pion and baryon exchange amplitudes would work. Their analysis should not be misunderstood either as "proving" that slope b must have intrinsic dependence on the mass $M_{a^*\pi}$.

A preliminary investigation of $K^{\pm}p \to K^{*0}\pi^{\pm}p$ at 8 GeV/c was reported by the Athens-Bruxelles-CERN-Democritos-Liverpool-Mons-Vienna collaboration[25], using the Pirila technique. This paper concludes also that the pion exchange Deck graph alone is insufficient to explain the mass-slope correlation.

3.4 Polarizations

Problems encountered in spin-parity analysis of the A_1 and Q regions include that of coherence. Among others, a source of incoherence is the fact that different nucleon spin-amplitudes contribute to $ap \to A^*p \to (\pi a^*)p$. In an attempt to measure the relative sizes of the spin non-flip and spin-flip amplitudes, it should be valuable to determine the polarization in the production. On a more general level, polarization data would appear to be as crucial to the detailed understanding of inelastic reactions as they have been in elastic scattering. Finally, as I will detail here, they should provide another excellent test of exchange model ideas. These tests have both qualitative and quantitative aspects.

Imagine production from a polarized proton target at rest in the lab. and define $\hat{N}$ as the normal to the $ap_{in} \to A^*p_f \to (a^*\pi_f)p_f$ production plane. Its sense is determined as usual by

$$\underset{\sim}{N} = \underset{\sim}{a} \times \underset{\sim}{A^*} = \underset{\sim}{p}_f \times \underset{\sim}{a} \qquad (23)$$

where $\underset{\sim}{a}$, $\underset{\sim}{A^*}$, and $\underset{\sim}{p}_f$ are lab. system momentum vectors. I am interested in the correlation between the direction of target polarization and $\hat{N}$. Other components of polarization may be measured in inelastic reactions, but I confine my attention here to this normal component, denoted P_{inel}.

According to the π exchange Deck model, this polarization is predictable from that measured in π-N elastic scattering[26]. However, two points must be mentioned. First, in computing $P(t_{pN}, M_{\pi a^*})$, as a function of momentum transfer and mass, it is necessary to average over a wide interval in the πN final sub-energy. This means an average of the elastic polarization over a wide energy range. Second, the normals to the $ap \to A^*p$ and final πp production planes do not point in the same direction. The input elastic polarization is that measured along the normal $\underset{\sim}{n} = \underset{\sim}{p}_f \times \underset{\sim}{\pi}_f$, in the polarized target lab. frame.

After working things through in detail, I find the following π exchange Deck model prediction for inelastic polarization[27]:

$$\sigma_{inel} P_{inel} = \frac{0.3893}{F} \Phi_3 \left[\hat{n} \cdot \hat{N} P_{el} \Sigma |A_{\pi p}|^2 \right] \qquad (24)$$

where $\Phi[\ ]$ stands for an integral over phase space.

This should be compared with eqn.(12) of Section 1. The factor $\hat{n} \cdot \hat{N}$, which is easily re-expressed in terms of invariants, takes care of the difference in reaction plane normals. The value of $\hat{n} \cdot \hat{N}$ varies over phase space, but peripheral events at high energy have $\hat{n} \cdot \hat{N} \simeq 1$. Thus, the elastic polarization is not washed out.

Some results of my explicit calculations are presented in figs.15 through 18. The mean effective πN lab. momentum contributing to $ap \to a^*\pi N$ turns out to be roughly one-fourth of the incident particle a lab momentum. Although the results are shown for $K^{\pm}p \to K^{*0}\pi^{\pm}p$, the same curves apply for any processes of the type $ap \to a^*\pi^{\pm}p$ (e.g. $\pi^{\pm}p \to (3\pi)^{\pm}p$) at the momenta indicated, and with $M(a^*\pi)$ selected correspondingly.

Inasmuch as the magnitude of elastic πN polarization falls with energy roughly as $1/\sqrt{s}$, so it does with that of P_{inel}. However, the effective threshold is much higher ($\times$ 4) in the inelastic case. The explicit calculations show that polarizations are expected to be substantial even at 40 GeV/c.

The "mirror-symmetry" of πN elastic polarization is evident in the predictions shown in figs.16 - 18; i.e. $P_+ \simeq -P_-$. Since this prediction is closely tied to π exchange, it is strictly true only for the π exchange region $\cos\phi_s > 0$, discussed in Section 3.3.3. The "double-zero" of π-N elastic polarization near $|t| \simeq 0.6$ (GeV/c)^2 is also evident. I

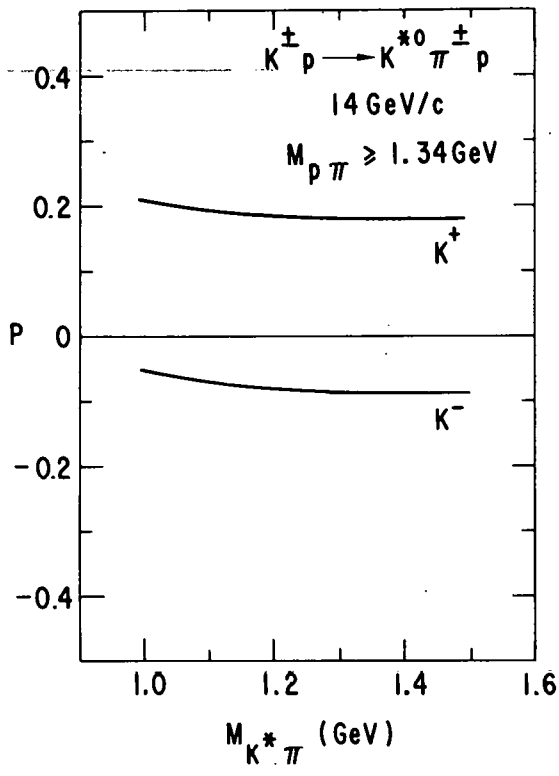

Fig. 15 Polarizations predicted by the π exchange Deck model for $K^{\pm}p \rightarrow (K^{*0}_{890}\ \pi^{\pm})p$ at 14 GeV/c are plotted against mass of the $(K^*\pi)$ system.

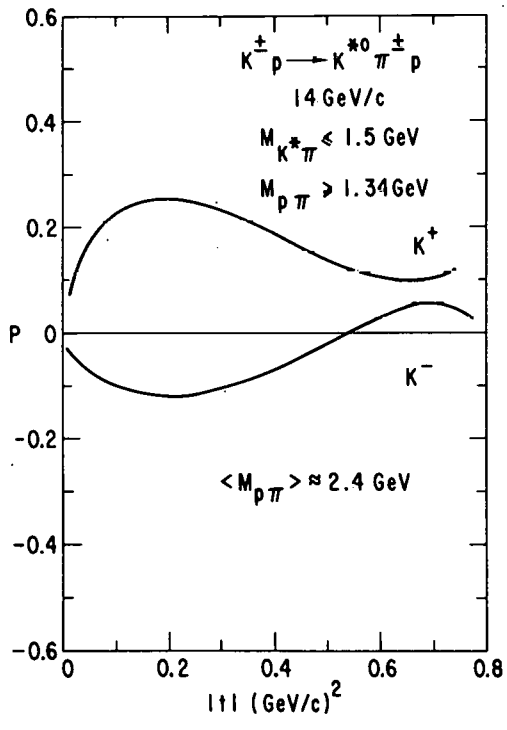

Fig. 17 Same as fig. 16, but for incident kaon momentum of 20 GeV/c.

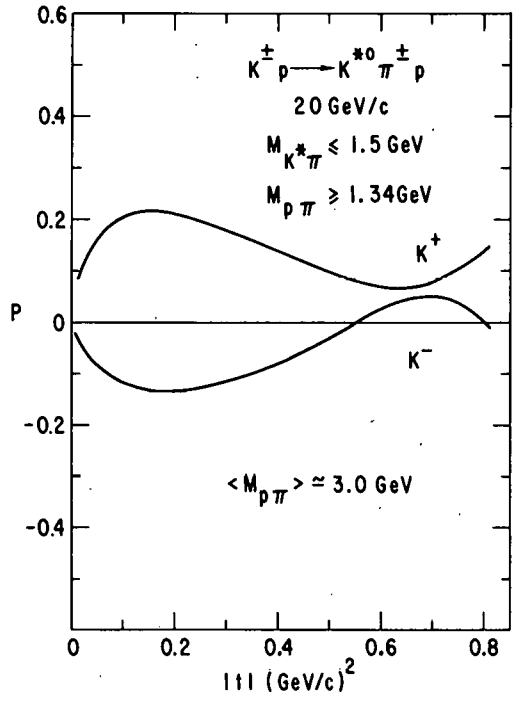

Fig. 16 Polarizations predicted by the π exchange Deck model for $K^{\pm}p \rightarrow (K^{*0}_{890}\ \pi^{\pm})p$ at 14 GeV/c are plotted as a function of momentum transfer from the initial to final proton. The mass $(K^*\pi)$ is integrated from threshold up to 1.5 GeV, and the mass $(p\pi^{\pm})$ is restricted to be greater than 1.34 GeV. Noted on the figure is the fact that the final pπ mass spectrum covers a broad range, with mean value roughly 2.4 GeV.

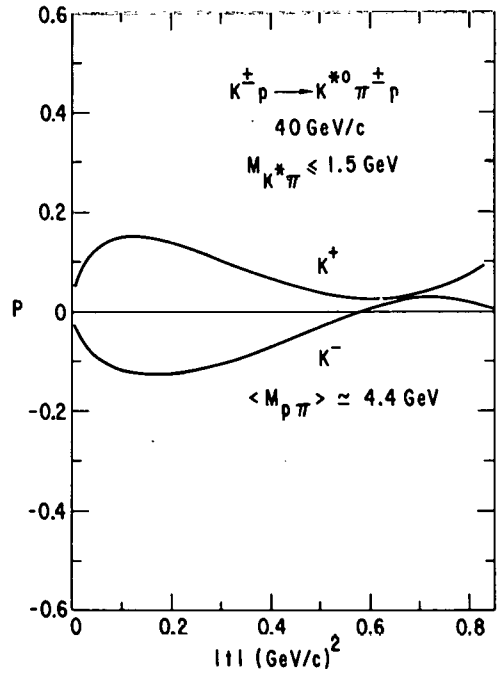

Fig. 18 As for fig. 17, but at 40 GeV/c.

doubt this will show up in the inelastic reactions because other exchanges and spin amplitudes will probably have complicated the story at these larger t values.

The influence of the "other" exchange graph deserves comment. For example, in $Kp \to (K^*\pi)p$, the K^* exchange graph, with K^*p elastic scattering, will doubtlessly not give polarizations having the mirror symmetric property characteristic of πN scattering. Comparisons with data should bear this in mind, and selections on $\cos \phi_s$ are always advisable. If the polarizations in K^*p and $\overline{K^*}p$ elastic scattering are similar to those of $K^{\pm}p$ elastic scattering, then the $\cos \phi_s < 0$ region dominated by K^* exchange should show positive polarizations for both $Q^{\pm}$ production.

If one thinks of $K^{\pm}p \to Q^{\pm}p$ as a quasi-elastic process with properties similar to Kp elastic scattering, the expected polarizations should be positive for both Q^+ and Q^-, for all values of $\cos \phi_s$, as they are for $K^{\pm}p$ elastic scattering. The contrast of this expectation with the results given in figs. 15-18 is striking.

3.5 Quantum Numbers at the Nucleon Vertex

Because the natural parity exchanges dominate in meson-baryon elastic scattering (i.e. $\mathbb{P}$, ρ, f, ω, A_2), by reflection they are also predicted by the Deck model to control the reactions $ap \to (a^*\pi)N$.

In the region of phase space dominated by π exchange ($\cos \phi_s > 0$), the exchanges at the pN vertex must have positive G parity ($\mathbb{P}$, ρ, f) as well.

4. PROPERTIES OF THE DECAY $A^* \to a^*\pi$

The Deck amplitude provides a potentially complete description of both the production and decay aspects of the system $A^*(\to a^*\pi)$ in the reaction $ap \to a^*\pi N$. In the previous section, properties of production were described. The present chapter deals with decay. However, I should stress from the start that production and decay do not factorize. For instance, different regions of the decay phase space of $A^* \to a^*\pi$ are produced with different momentum transfer distributions.

4.1 Spin-Parity Content

The first question of interest is the spin-parity content of A^*. The model provides definite predictions. The results are very different for diffractive and charge-exchange production.

Complicated numerical programs exist for determining the partial wave content of $A^* \to (a\pi\pi)$, whether A^* is generated from a model amplitude or is actual data[23]. However, the essential physical ideas are trivial, and simple analytic arguments suffice for understanding the predictions of the model.

The model amplitude is presented in eqn.(8) in terms of invariants. To obtain the partial wave content of the low-mass A^* enhancement generated by this amplitude, we must re-express the amplitude in terms of a more appropriate (or transparent) set of variables. In the rest system of A^*, this set should include the two decay angles of A^*, (θ, ϕ), with respect to some set of axes. The partial wave content is then obtained by projecting $A(s, t_{pN}, M_{A^*}, \theta, \phi)$ onto a set of angular momentum functions $Y_{L,M}(\theta, \phi)$:

$$A_\pi \sim \sum_{L,M} a_{L,M} Y_{L,M}(\theta, \phi) \qquad (25)$$

The "constants" $a_{L,M}$ are functions of s, t_{pN}, and M_{A^*}. If the enhancement is purely an s-wave, then only a_0 is non-zero.

The s-channel set of angles (θ_s, ϕ_s) is defined in fig.12, whereas the t-channel (Gottfried-Jackson) set (θ_t, ϕ_t) is presented in fig.19.

We may try to guess the spin-parity content of the π exchange Deck amplitude by regarding the graph of fig.1(a) as a quasi-two body process $aR \to a^*\pi$, where R is some effective exchange at the pN vertex. This quasi-two body process in fig.1(a) is mediated by pion-exchange, whose amplitude behaves as $(m_\pi^2 - t_{aa^*})^{-1}$. In terms of $\cos \theta_t$, we therefore have an amplitude of the form

$$A_\pi \sim \frac{1}{k_1 - k_2 \cos \theta_t} \qquad (26)$$

where k_1 and k_2 are positive constants. The naive guess then would be that $d\sigma/d\cos \theta_t$ is very peaked towards $\cos \theta_t \simeq +1$, and, consequently, that the partial wave decomposition shows a broad spectrum of high partial waves, and very little s-wave. This

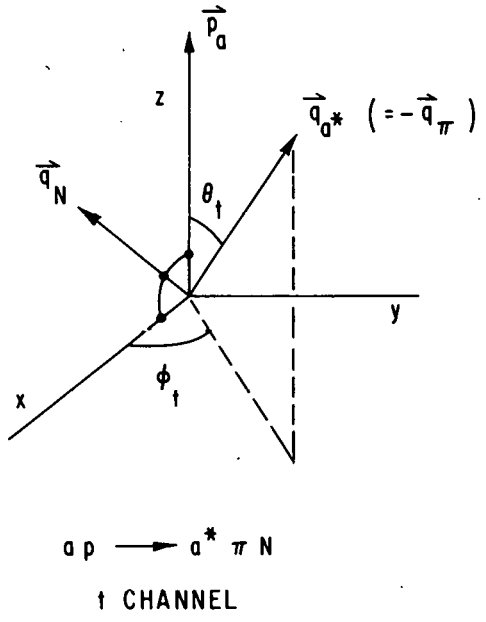

Fig. 19 Diagram in which the t-channel decay angles (θ_t, ϕ_t) of $A^* \to (a^*\pi)$ are defined.

indeed is what happens for simple 2 → 2 amplitudes, but it is not true of the Deck 2 → 3 amplitude.

The essential point missing from the above argument is that there are <u>two</u> important sources of dependence on cos θ_t in the Deck amplitude. The first is indeed the propagator $(m_\pi^2 - t_{aa^*})^{-1}$, but the second is the dependence on $s_{\pi N}$ present in the amplitude $A_{\pi N}(s_{\pi N}, t_{pN})$.

An aside: the Appendix may be consulted for details; the relevant kinematic conclusion is the relationship (eqn. (A.31))

$$s_{\pi N} \sim (m_\pi^2 - t_{aa^*}) \qquad (27)$$

at small t_{pN}.

In the π exchange Deck amplitude, the essential dependence on $s_{\pi N}$ and on t_{aa^*} <u>in the diffractive case</u> ap → a*πp is expressed by eqns. (2) and (9)).

$$A_\pi^{Diff} \sim s_{\pi N} / (m_\pi^2 - t_{aa^*}) \qquad (28)$$

According to eqn. (27), therefore, the cos θ_t dependences cancel each other and

$$A_\pi \to a_0(s, t_{aa^*}, M_{A^*}) \qquad (29)$$

i.e. a function independent of θ_t and ϕ_t; d /dcos θ_t should be flat from cos θ_t = -1 to +1. This means expressly that the dominant J^P content of the diffractive enhancement is s wave[6]. With a $J^P = 1^-$ a*, the J^P of A* is 1^+. If a* is 2^-, A* is 2^+.

In the charge-exchange case, $A_{\pi N} \sim s_{\pi N}^{1/2}$. Thus,

$$A_\pi^{Cex} \sim s_{\pi N}^{1/2} / (M_\pi^2 - t_{aa^*}) \sim (k_1 - k_2 \cos\theta_t)^{-1/2} \qquad (30)$$

The charge-exchange process ap → a*πn is therefore expected to show a full spectrum of partial waves, not a dominant s-wave.

In fig. 20, I present results of my calculation of

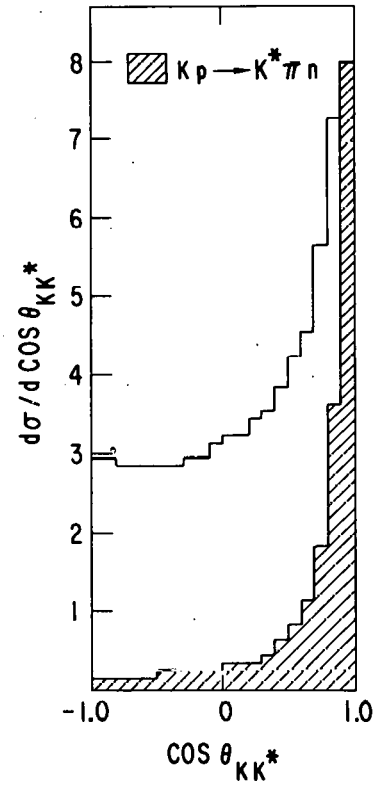

Fig. 20 The differential cross section dσ/dcos θ_{KK^*} as a function of the t-channel angle cos θ_{KK^*} between incident K and final K for the reactions $K^- p \to K^*_{890}$ πN at 14 GeV/c, as predicted by the π^- exchange Deck model. The selections imposed are Mass (K*π) ≤ 1.5 GeV and Mass (Nπ) ≥ 1.34 GeV. The full distribution is for the "diffractive" reaction (in which N = proton), whereas the shaded portion is for the charge-exchange process (N = neutron). The normalization is in arbitrary units (for integrated cross sections, see fig. 7). Results are presented in histogram form, as obtained from the Monte Carlo event generator.*

$d\sigma/d\cos\theta_t$ for $K^-p \to K^*\pi N$ at 14 GeV/c, for the mass interval $M_{K^*\pi} < 1.5$ GeV. The diffractive case $Kp \to K^*\pi p$ shows a rather flat (s-wave) distribution from $\cos\theta_t = -1$ to $\cos\theta_t \sim 0.5$, and then a rising tail of high partial waves. This basically agrees with the analytic argument given above. The tail of high partial waves near $\cos\theta_t \simeq +1$ arises in part from the fact that I use the full amplitude $A_{\pi N}$ in my calculations, not just the leading diffractive ($\sim s_{\pi N}$) part.

The distribution $d\sigma/d\cos\theta_t$ for the charge-exchange process $Kp \to K^*\pi n$ in fig.20 shows a very small s-wave component, but a large forward peak of high partial waves, again as advertised in the analytic discussion above. The difference between the diffractive and charge-exchange angular distributions $d\sigma/d\cos\theta_t$ is obviously very marked in the model.

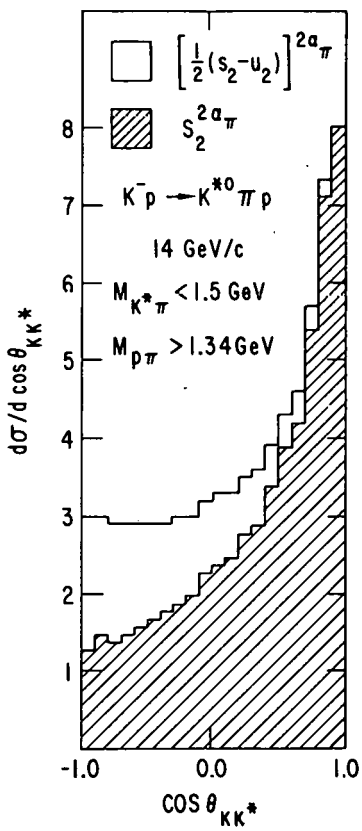

Fig.21 An examination of the sensitivity of the predicted distribution $d\sigma/d\cos\theta_{KK^*}$ to alterations of the π exchange Deck amplitude. The full distribution was obtained from the amplitude given in eqn.(8), whereas the shaded portion resulted after the factor $1/2(s_{\pi K^*} - u_{K\pi})$ was replaced by $s_{\pi K^*}$. Results are given for $K^-p \to K^{*0}\pi^-p$ at 14 GeV/c with the selections noted.

A series of comments follows.

1. Sensitivity of results to details of parametrization. To evaluate this sensitivity, I made some calculations with $s_{\pi K^*}$ instead of $1/2(s_{\pi K^*} - u_{K\pi})$ as the Regge sub-energy factor in eqn.(8). A comparison of results is shown in fig.21. The choice of $1/2(s_{\pi K^*} - u_{K\pi})$ obviously enhances the s-wave component substantially.

2. The Illinois group[8] made a very careful partial wave decomposition of their π exchange Deck amplitude for $\pi p \to (3\pi)p$. The results are shown in fig.22, as the intensity of the various contributing waves versus mass of the 3π system[8]. In comparing these results with data, they find that the $J^P = 1^+$ intensity peaks at about the correct value of (3π) mass, but that its full width at half maximum is too broad. Their predicted ratio of $0^-/1^+$ intensity is too large to agree with the data.

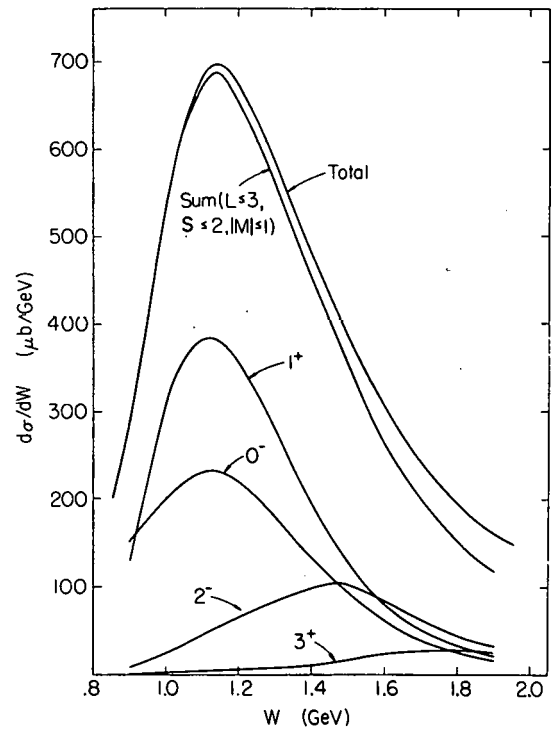

Fig.22 Cross sections for the dominant J^P states present in the low mass (3π) enhancement, as predicted by the Illinois π exchange Deck model for $\pi p \to (3\pi)p$ at 16 GeV/c, are given as a function of (3π) invariant mass; from ref.(8).

3. While by no means a perfect description of the data, it is clear that the π exchange Deck graph provides a threshold enhancement which resembles the data for the diffractive reactions $ap \to a^*\pi p$, not only in overall production aspects, but also in J^P content. The substantial difference expected by the

model for the J^P content of the low-mass enhancement in the charge-exchange process $ap \to a^*\pi n$ argues strongly for a detailed experimental J^P analysis of such data. If the s-wave $J^P = 1^+$ signal found in the charge-exchange data is much stronger than that foreseen in the model, this fact in itself would argue for resonance interpretation of the enhancement in charge exchange (c.f. also Section 4.3).

4.2 A Critique of the Role of Pion Exchange

The J^P analysis discussed in the previous section is based entirely on the exchange Deck graph, fig.1(a). The results agree rather well with data, and thus one might suppose that this agreement supports keeping only the π exchange graph. Indeed, the cancellation between the diffractive $s_{\pi N}$ dependence and the pion pole propagator to give a dominant $J^P = 1^+$ enhancement would almost appear to rely crucially on pion exchange[6]. Unfortunately, the case is not so simple.

4.2.1 The a* Exchange Graph

Although the parametrization of the a* exchange propagator for fig.1(b) is not as simple as that for pion exchange, the essential momentum transfer and sub-energy dependences of the amplitude will resemble (for $ap \to a^*\pi p$)

$$A_{a^*} \sim s_{a^*p}\, \exp(\lambda t_{pN}) \,/\, (m^2_{a^*} - t_{a\pi}) \qquad (31)$$

to first approximation. The kinematical derivations of the Appendix show that the same cancellation of $\cos\theta_t$ dependence occurs here, as for π exchange (eqn.(A.32)). Thus, to first order again, the a* exchange graph also provides basically a flat distribution $d\sigma/d\cos\theta_t$, and an s-wave πa^* enhancement. Doubtlessly the contributions to higher partial waves of a* and π exchange will be different, but both should contribute significantly to the s-wave.

The J^P content and the distribution $d\sigma/d\cos\theta_t$ are therefore obviously not very useful means for establishing the presence of π and/or a* exchange contributions. The distribution $d\sigma/d\cos\theta_t$ is furthermore inappropriate for attempts to estimate the relative size of π and a* exchange contributions. Just as the π exchange graph gives a peak near $\cos\theta_t \simeq 1$ in $d\sigma/d\cos\theta_t$ (fig.20), the a* exchange graph will tend to peak near $\cos\theta_t \simeq -1$. However, the "background" from the π exchange graph extends all the way to $\cos\theta_t \simeq -1$, and its magnitude in the region $\cos\theta_t < 0$ is very sensitive to the choice of parametrization of the π exchange amplitude (compare figs.20 and 21). Thus from the plot of $d\sigma/d\cos\theta_t$ it remains unclear how much cross section to assign to the π and a* exchanges. The only exception to this rule is a situation in which quantum numbers forbid one of the exchanges. For example, in $K^-p \to K^*\pi^+n$, K* exchange is forbidden, and the distributions reflect the π exchange graph directly.

4.2.2 The Distribution $d\sigma/d\phi_s$

Fortunately, the distribution $d\sigma/d\phi_s$ should provide direct evidence for exchange effects and allow direct estimation of the relative size of π and a* exchange contributions. Here ϕ_s is the s-channel azimuthal angle of the $A^* \to a^*\pi$ decay, as defined in fig.12. The great virtue of this angle is based on the kinematic fact (see Appendix) that

$$|t_{aa^*}| = A - B\cos\phi_s \qquad (32)$$

where A and B are positive valued functions of the other four independent invariants (s, M_{A^*}, t_{pN}, $s_{\pi N}$) in the amplitude[28].

If the $ap \to a^*\pi N$ amplitude does not depend explicitly on t_{aa^*}, $t_{a\pi}$, or on ϕ_s, then the distribution $d\sigma/d\phi_s$ is necessarily flat from 0 to 2π (to π if folded). The only invariants which introduce dependence on ϕ_s into the amplitude are t_{aa^*} and $t_{a\pi}$. An amplitude (π exchange) which is large for small t_{aa^*} results in a peak of $d\sigma/d\phi_s$ near $\phi_s = 0$, whereas an amplitude which favours small $t_{a\pi}$ (a* exchange) causes a peak in $d\sigma/d\phi_s$ near $\phi_s = \pi$. Note that $t_{aa^*} + t_{a\pi} = -s_{\pi a^*} + t_{pN} + M^2_{a^*} + M^2_{\pi} + M^2_{a}$.

An explicit example is presented in fig.13, from which it is seen how strongly the π exchange Deck graph populates the region $\phi_s < \pi/2$. Introduction of a form factor in eqn.(8) to suppress large $|t_{aa^*}|$ will favour the region $\phi_s < \pi/2$ even more strongly. Seen also in fig.13 is the fact that the π exchange Deck graph generates a similar $d\sigma/d\phi_s$ distribution for the diffractive and charge exchange reactions. This latter point illustrates my argument that it is the t_{aa^*} structure of eqn.(8), and not dependence on other invariants, which is reflected directly in the $d\sigma/d\phi_s$ distribution.

Note that the peak in $d\sigma/d\phi_s$ near $\phi_s = 0$ is the π exchange peak. The pion-pole is not cancelled in this variable, and it was in the $d\sigma/d\cos\theta_t$ plot, by the $s_{\pi N}$ dependence of the inelastic amplitude. This should put an end to the loose talk in some recent literature regarding cancellation of the pion

singularity. The compensation occurs only in the cos θ_t distribution.

Experimental data on $d\sigma/d\phi_s$ are not as generally available as would seem appropriate given the power of this distribution. A peak in $d\sigma/d\phi_s$ near $\phi_s = 0$ signals presence of a π exchange graph, whereas a peak near $\phi = \pi$ gives evidence of an a* exchange graph. The total distribution could be flat, forward peaked, backward peaked, or otherwise, depending on the relative strengths of the two graphs. The relative number of events in the regions cos $\phi_s > 0$ and cos $\phi_s < 0$ can be used to estimate the relative strengths of π and a* exchange. A preliminary view of data in the Q region from $K^{\pm}p \to K^* \pi^{\pm}p$ at 8 GeV/c[17] and for $K^-p \to \overline{K^*} \pi^-p$ at 16 GeV/c[29] show rather flat $d\sigma/d\phi_s$ distributions. This result supports the conclusion that, in these reactions, the π and K* exchange graphs are of roughly equal importance, as was suggested in Section 3.3.2. This is the first direct evidence that the pion exchange Deck graph alone is incapable of reproducing the data in the Q region. Within the context of an exchange model interpretation of the Q enhancement, both "t-channel" (i.e., π) and "u-channel" (i.e., K*) exchange graphs are required in roughly equal proportion. In studies of $pn \to p(p\pi^-)$ at 19 and 28 GeV/c, the Brookhaven-Vanderbilt collaboration[30] finds a ϕ_s distribution in the low-mass $(p\pi^-)$ system which shows roughly a 2 to 1 ratio of events favouring π over baryon exchange.

4.3 Resonance-Deck Interference

As described in Section 4.1, the Deck amplitude provides a low mass enhancement whose partial wave content covers a series of spin-parity states. In nature, there may also be, in addition, resonances in some or all of these waves, whose production is coherent with that of the non-resonant (Deck) background. For instance, in $\pi p \to (3\pi)p$, there is the $J^P = 2^+$ A_2 resonance (d wave $\rho\pi$), which may interfere with the Deck 2^+ wave[11].

It is interesting to inquire about possible resonances in the s wave (πa^*) system, which would interfere with the dominant s wave produced in the Deck model. Cross section estimates for the production of such resonances run in the 10 to 20 μb range[1], whereas the Deck background is of order 100 μb. Thus, the resonances would not stand out clearly in standard plots of invariant mass. Moreover, existing three particle phase shift analysis programs may find it particularly hard to disentangle such a weak resonance signal from the Deck background.

The resonances might well show up more transparently if the mass distribution $d\sigma/dM_{\pi a^*}$ were plotted for events from a partial segment of the decay angle phase space. Specifically, one might consider displaying events in the two dimensional decay space defined by (cos θ_t, ϕ_t) [or by (cos θ_s, ϕ_s)]. The events could be divided into four (eight) samples and plots of $d\sigma/dM_{\pi a^*}$ made for each:

I. $-1 \leq \cos\theta \leq 0$ $\quad \pi \geq \phi \geq \pi/2$

II. $-1 \leq \cos\theta \leq 0$ $\quad \pi/2 > \phi \geq 0$

III. $0 < \cos\theta \leq 1$ $\quad \pi \geq \phi > \pi/2$

IV. $0 < \cos\theta \leq 1$ $\quad \pi/2 > \phi \geq 0$

A single resonance would populate all four (eight) segments equally, whereas the π exchange and a* exchange Deck graphs concentrate events towards specific corners, as shown in fig.24. The character of the resonance-Deck interference should be sufficiently different in the four sectors. If events taken, for example, from the two non-Deck corners of the (cos θ, ϕ) plot were to show statistically significant, relatively narrow structure, the case for resonance interpretation would be correspondingly strengthened. Background graphs do not create narrow peaks.

In searching for resonance effects in the $Q(K\pi\pi)$ region, careful comparisons of K^+p and K^-p data may be particularly illuminating. Because the K^+p channel is exotic whereas K^-p is not, the relative phase of resonance and Deck background should be different in two cases. This phase difference might explain the different mass structure[20] observed for the Q^+ and Q^-.

4.4 Helicity Conservation

At issue is knowledge of the value of helicity of the A* object produced in $ap \to A^*N \to (\pi a^*)N$, with respect to a given axis of quantization. The favourite axes of reference are the t-channel (fig.19) and s-channel (fig.12) frames.

From the point of view of the Deck model, there are two aspects to the prediction of the s- or/and t-channel helicities of A*. Since the production

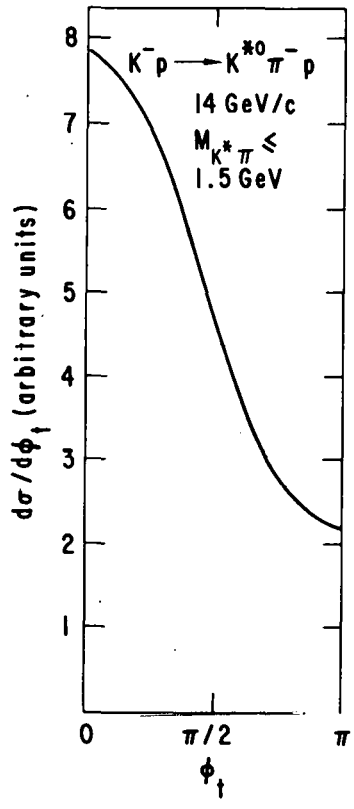

Fig.23 The distribution $d\sigma/d\phi_t$ as a function of the t-channel azimuthal angle ϕ_t. The curve was obtained from the π^- exchange Deck amplitude, eqn.(8), for $K^- p \to K^{*0}_{890} \pi^- p$ at 14 GeV/c. The selections imposed were Mass ($K^*\pi$) < 1.5 GeV and Mass ($p\pi^-$) > 1.34 GeV.

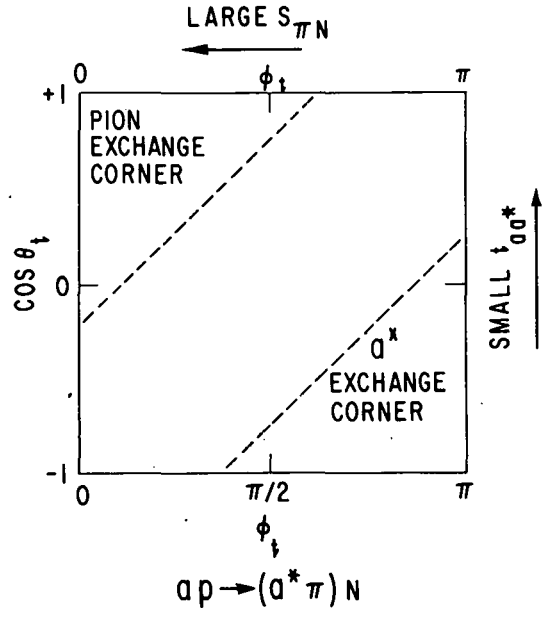

Fig.24 The two-dimensional decay phase-space of $A^* \to a^*\pi$ in terms of the t-channel decay angles, as defined in fig.19. At high energy the π^- exchange and a^* exchange Deck graphs of fig.1 concentrate events into the two corners noted in the figure.

amplitude is an amplitude for $ap \to a^*\pi N$, one must first decide the helicity state of a^* and then the net helicity of the combined system (πa^*). The helicity state of a^* is a question of how exchanges couple at the respective vertices. The helicity contributed by the re-combination of (πa^*) is easily expressed in terms of the azimuthal angles ϕ_s and ϕ_t.

To illustrate this latter point, suppose that a^* is produced with helicity zero in the t-channel. Then the helicity of A^* is also zero in the t-channel if and only if the amplitude for $ap \to a^*\pi N$ does not depend on ϕ_t. If there is ϕ_t dependence, then the t-channel helicity of A^* cannot be zero. It must contain a sum of different helicity states.

Consider now the π exchange Deck amplitude, eqn.(8). It shows important dependence on t_{aa^*} and on $s_{\pi N}$. When re-expressed in terms of s-channel decay angles in the A^* rest frame, as detailed in the Appendix,

$$|t_{aa^*}| = A - B \cos\phi_s \qquad (33)$$

where A and B are functions of the other four invariants. When re-expressed in terms of t-channel decay angles

$$s_{\pi N} = C + D \cos\phi_t \qquad (34)$$

Because the amplitude contains this important dependence on ϕ_s and on ϕ_t, the π-exchange Deck model conserves neither s nor t channel helicity for the full low-mass enhancement. In fact, the violations of both are rather strong. Distributions $d\sigma/d\phi_s$ and $d\sigma/d\phi_t$ I computed from the π exchange model are presented in figs.13 and 23. These would both be flat if no ϕ dependence were present in the amplitude A_π. The asymmetries predicted are rather obvious. I argued above that the pronounced peak near $\phi_s = 0$ in $d\sigma/d\phi_s$ owes its existence to π exchange. The experimental distributions $d\sigma/d\phi_s$ for $Kp \to K^*\pi p$ is more nearly flat[17,28] in disagreement with the pure π exchange model, and suggestive that an important K^* exchange graph must also be included.

As explained above, the π exchange Deck model provides generally neither s nor t channel helicity conservation for the full low mass (πa^*) enhancement. However, suppose we confine our attention to the s-

wave component of the (πa^*) enhancement. For the s wave partial amplitude, there obviously can be no ϕ dependence. Thus, the issue of s or t-channel helicity conservation reverts simply to a statement about the helicity of a^*. The pion exchange coupling at the $\pi\rho$ vertex of $\pi p \to \rho\pi N$ or at the KK^* vertex of $Kp \to K^*\pi N$ is known to populate preferentially t-channel helicity zero ρ and K^*. Thus, the prediction is clear[31]: the π exchange Deck model favours t-channel helicity conservation in $\pi p \to A_1 p$ and $Kp \to Qp$.

Statements about helicity expectations for the a^* exchange graphs are yet to be worked out in detail.

Experimentally, the $J^P = 1^+$ $K^*\pi$ component of $Kp \to K^*\pi p$ shows t-channel helicity conservation, consistent with the π exchange Deck model. The low-mass (ρK) and (ωK) diffractive enhancements found in $K^-p \to \rho Kp$ and $K^-p \to \omega Kp$ appear to have zero helicity in the s-channel[32]. It should be determined what these facts imply for the relevant ω, ρ and K exchange Deck graphs.

4.5 Phases

The complex phase behaviour of the π exchange Deck amplitude eqn.(8) comes from two sources: first, the phase of the πN off-shell elastic amplitude $A_{\pi N}$, which varies with $s_{\pi N}$ and t_{pN}; second, the phase of the Reggeized pion propagator $e^{-i\pi\alpha_\pi/2}$, which varies only as a function of t_{aa^*}. The Illinois group[8] made a detailed analysis of these phase variations and of their relationship to data. I will confine myself to a few pedagogical remarks.

Take a fixed small value of t_{pN} and a fixed value of $M_{a^*\pi}$, and large s. Then the phase of $A_{\pi p}$ is roughly i, and the phase dependence of A_π for $ap \to a^*\pi p$ is approximately

$$i \exp[-i\pi\alpha_\pi/2] \;\tilde{\propto}\; i \exp[-i\pi\alpha'_\pi t_{aa^*}/2] \qquad (35)$$

Because $\langle|t_{aa^*}|\rangle \simeq 0.15$ (GeV/c)^2, the average phase of the amplitude differs from i by about 15^0, when $\alpha'_\pi \simeq 0.9$ (GeV/c)$^{-2}$.

This average phase varies only gradually as $M_{a^*\pi}$ changes, since changes of M_{a^*} in the low mass region produce only gradual changes in $\langle t_{aa^*}\rangle$ and $\langle s_{\pi N}\rangle$. Thus, no dramatic resonance like phase variation can be expected from the model as $M_{a^*\pi}$ is altered, in agreement with data.

One important phase feature of the model is its prediction of the relative phase between different J^P states at small $M_{a^*\pi}$. This relative phase is not zero because the s, p, d. ... waves sample the $\exp(+ i\alpha' t_{aa^*})$ distribution in different ways. Re-expressing the phase dependence on t_{aa^*} as a dependence on $\cos\theta_t$ ($t_{aa^*} \propto k_1 + k_2 \cos\theta_t$), the phase of the s wave is proportional to an integral.

$$\int_{-1}^{+1} f(\cos\theta_t)\, d\cos\theta_t \qquad (36)$$

whereas that of the p-wave is proportional to a different integral, of the form

$$\int_{-1}^{+1} f(\cos\theta_t)\cos\theta_t\, d\cos\theta_t \qquad (37)$$

According to the Illinois paper[8], a 90^0 phase difference is thus obtained between the 1^+ $s(\rho\pi)$ and 1^+p ($\varepsilon\pi$) partial waves, when the slope $\alpha'_\pi \simeq 0.9$ (GeV/c)$^{-2}$. No phase difference is obtained if $\alpha'_\pi = 0$, of course, since then the π exchange phase is purely real. This 90^0 phase difference agrees with the phase extracted from data[2], and is interpreted by the Illinois group as supportive of the Regge nature of the pion.

If all relative phases predicted by the model agreed with data, this conclusion might be compelling. However, the 1^+s to 0^-s relative phase does not agree well with data[8]. Moreover, support for the idea that $\alpha'_\pi \simeq 1$ (GeV/c)$^{-2}$ is hard to reconcile with the apparent absence of shrinkage[12] mentioned in Section 2. Finally, from the necessity for K^* exchange in $Kp \to Qp$, as concluded above, it appears that a ρ exchange graph might be required in a more complete treatment of $\pi p \to (3\pi)p$. The inclusion of this graph is expected to modify phases, but it is hard to gauge its quantitative impact.

5. CONCLUSIONS

As a result of the detailed analysis by the Illinois group[8], the Reggeized pion exchange Deck model[6] has been shown to reproduce data on $\pi p \to (3\pi)p$, at small values of (3π) invariant mass, to a far more successful degree than previously believed. Never-

theless, several aspects of the pion exchange amplitude are uncertain. These include the absence of a form factor, and the issue of whether Reggeization is justified. If reasonable alterations are made in the amplitude, the agreement with data, including the crucial J^P content, worsens considerably.

In this article I have concentrated more on $Kp \to (K\pi\pi)N$. The pion exchange Deck model reproduces these data much less well.

I identified two important characteristic features of the pion exchange Deck amplitude. First, that the amplitude produces a distribution $d\sigma/d\phi_s$ which peaks sharply towards $\phi_s = 0$ (Sections 3.3 and 4.2). This property is intimately associated with the t-channel exchange property of Deck graphs. A "u-channel" graph, having a ρ or K* exchange provides a peak towards $\phi_s = \pi$. Angle ϕ_s is the s-channel azimuthal angle of a* in the decay $A^* \to (a^*\pi)$.

The second characteristic feature of the pion-exchange graph is associated with quantum number or symmetry properties. These can be tested by features in data, such as cross-overs[15] of differential cross sections (c.f. Table 1) or polarizations, whose signs carry the signature of specific quantum numbers.

Predictions were made and experimental investigations suggested to pursue both points listed above. In particular, selections on $\cos\phi_s$ for $ap \to a^*\pi p$ were proposed to separate the regions of phase space in which the pion exchange and a* exchange Deck graphs dominate. The quantum number characteristics of π exchange (a* exchange) should prevail only in the region $\cos\phi_s > 0$ ($\cos\phi_s < 0$).

Data on several reactions show that although $d\sigma/d\phi_s$ peaks near $\phi_s = 0$, as expected for the π exchange Deck graph, the overall distribution is much more symmetric than would be consistent with π exchange only. The need for a substantial contribution from a* exchange seems demanded. For $Kp \to K^*\pi p$, the K* exchange graph appears to have weight roughly equal to that of π exchange.

The inclusion of a K* exchange graph in the Deck model description of $K^0p \to Q^0p$ and $\overline{K^0}p \to \overline{Q^0}p$ resolves also the erroneous prediction of the cross-over systematics, obtained from the π exchange Deck graph only. This proposal can be tested in detail with the SLAC K_L^0p data, by means of the $\cos\phi_s$ selections described above. The incorporation of a K* exchange graph further improves agreement of the model with experimental values of the integrated cross section and the slope b of the production differential cross section.

The reactions $\pi^\pm p \to \pi^\pm(\pi^-\Delta^{++})$ are described by a sum of pion and baryon exchange Deck graphs, whose characteristic cross-over systematics differ in sign[15]. This prediction of the Deck model was verified at 16 GeV/c[23]. The success confirms both the utility of the $\cos\phi_s$ selection procedure and the fact that quantum number characteristics of both Deck model graphs are evident in the data.

It remains unclear whether a resonant $J^P = 1^+$ signal is present in the A_1 and Q region data. A possible method for separating the resonances from the large Deck background was discussed in Section 4.3. Charge-exchange processes, such as $K^-p \to (K\pi\pi)n$ and $Kp \to (3\pi)\Lambda$, deserve special experimental emphasis because the s-wave Deck background in these reactions is much reduced from its level in diffractive processes.

REFERENCES

1. A.J.G. Hey, Introductory Talk, these proceedings. G.C. Fox and A.J.G. Hey, Nucl. Phys. B56, (1973) 386.

2. G. Ascoli et al, Phys. Rev. D7, (1973) 669; R. Klanner, CERN-NP Internal report 73-9 (1973).

3. Yu.M. Antipov et al, (K^-p at 40 GeV/c) Report COO-1194-290, Sept. 1974; Aachen-Berlin-CERN-London-Vienna Collaboration, M. Deutschmann et al. Phys. Letts. 49B, (1974) 388.

4. I.J.R. Aitchison, these proceedings.

5. S.D. Drell and K. Hiida, Phys. Rev. Letts. 7, (1961) 199; R.T. Deck, ibid. 13, (1964) 169; U. Maor and T.A. O'Halloran, Phys. Letts. 15, (1965) 281; U.Maor, Ann. Phys. (N.Y.) 41, (1967) 456; L. Stodolsky, Phys. Rev. Letts. 18, (1967) 973; M.Ross and Y.Yam, ibid. 19, (1967) 546;

M.L.Good and W.D.Walker, Phys.Rev. 120, (1960) 1857.

6. E.L.Berger, Phys. Rev. 166, (1968) 1525, and ibid 179, (1969) 1567; E.L.Berger, Regge Pole Conference, Irvine (1969), Argonne National Laboratory Report, ANL/HEP 6927; E.L.Berger, et al. Phys. Rev. Letts. 20, (1968) 964; ibid 22, (1969) 731; and ibid 21, (1968) 701.

7. H.M.Chan, K.Kajantie and G.Ranft, Nuovo Cim. 49A, (1967) 157; F.Zachariasen and G.Zweig, Phys. Rev. 160, (1967) 1326; N.Bali, G.F.Chew and A.Pignotti, Phys. Rev. 163, (1967) 1572.

8. G.Ascoli, et al. Phys. Rev. D8, (1973) 3894 and ibid D9, (1974) 1963.

9. R.Lacaze, private communication. I am grateful to Dr. Lacaze for assistance with the numerical program for reconstructing amplitudes from phase shifts.

10. V.D.Barger and R.J.N.Phillips, Phys. Rev. 187, (1969) 2210.

11. G.Ascoli, et al. Phys. Rev. Letts. 33, (1974) 610.

12. R.D.Field and D.Sidhu, Phys. Rev. D10, (1974) 89 (c.f. fig.16).

13. C.Michael, parallel session contribution XVII Int. Conf. on High Energy Physics, London, 1974, p.I-180.

14. Yu.M. Antipov, et al. ibid.

15. E.L.Berger, Argonne National Laboratory Report ANL/HEP 7464, to be published in Phys. Rev.

16. Aachen-Berlin-CERN-London-Vienna Collaboration, D.R.O.Morrison, Rapporteurs talk, XVth Int.Conf. on High Energy Physics, Kiev, 1970, K^-p at 10 GeV/c.
T.Ludlam, J.Sandweiss and A.J.Slaughter, Phys. Rev. D2, (1970) 1234, K^-p at 12.6 GeV/c.
Birmingham-Glasgow-Oxford Collaboration, K.Barnham, et al. Nucl. Phys. B25, (1970) 49, K^+p at 10 GeV/c.
Plus articles listed under ref.(20) of the present paper.

17. S.Stergiou, TC Division, CERN, private communication.

18. I.Ambats, et al. Phys. Rev. D9, (1974) 1179.

19. Aachen-Berlin-Bonn-CERN-Heidelberg Collaboration, J.V.Beaupre, et al. Phys. Letts. 41B, (1972) 393.

20. Athens-Bruxelles-CERN-Democritos-Liverpool-Mons-Vienna Collaboration, A.Stergiou, et al. CERN Report, CERN/D.Ph.II/PHYS. 73-1, ($K^{\pm}p$ at 8 GeV/c); P.J.Davis, et al. Phys. Rev. D5, (1972) 2688, ($K^{\pm}p$ at 12 GeV/c); R.Barloutaud, et al. Nucl. Phys. B59, (1973) 374, (K^-p at 14 GeV/c).

21. G.W.Brandenburg, et al. Nucl. Phys. B45, (1972) 397.

22. E.L.Berger and G.C.Fox, Nucl. Phys. B26, (1971) 1.

23. Aachen-Berlin-Bonn-CERN-Heidelberg Collaboration, to be published.

24. P. Pirila and H. Miettinen, Phys. Letts. 40B, (1972) 127.

25. Athens-Bruxelles-CERN-Democritos-Liverpool-Mons-Vienna Collaboration, to be published.

26. G.C.Fox, Phys. Rev. D9, (1974) 3196; E.L.Berger and G.C.Fox, Proc. 2nd Int. Conf. on Polarized Targets (Berkeley, California, 1971), Ed. by G. Shapiro.

27. J.P.Ader, R.Lacaze and R.Peschanski, obtained an independent derivation of this expression.

28. I am grateful to P.Pirila for conversations regarding the usefulness of this variable.

29. Aachen-Berlin-CERN-London-Vienna Collaboration, to be published.

30. J.Handon, et al. Vanderbilt Report VAND-HEP 74(2).

31. J.Donohue, Nucl. Phys. B35, (1971) 213.

32. Aachen-Berlin-Bonn-CERN-Heidelberg-London-Vienna Collaboration, G.Otter, et al. Nucl. Phys. B87, (1975) 189.

APPENDIX

KINEMATICS

The process treated is $ap \to a^*\pi N$. Momentum vectors of the initial and final state particles are denoted by p and q, respectively, and masses by m.

The invariants of interest are

$$s = (p_a + p_p)^2 = (q_{a^*} + q_\pi + q_N)^2 , \quad (A.1)$$

$$s_{\pi N} = (q_\pi + q_N)^2 \equiv M^2_{\pi N} , \quad (A.2)$$

$$s_{\pi a^*} = (q_\pi + q_{a^*})^2 \equiv M^2_{A^*} , \quad (A.3)$$

$$s_{a^*N} = (q_{a^*} + q_N)^2 , \quad (A.4)$$

$$t_{aa^*} = (q_{a^*} - p_a)^2 , \quad (A.5)$$

$$t_{pN} = (q_N - p_a)^2 , \quad (A.6)$$

$$t_{a\pi} = (q_\pi - p_a)^2 . \quad (A.7)$$

Note that

$$s_{\pi a^*} + t_{aa^*} + t_{a\pi} = m_a^2 + m_{a^*}^2 + m_\pi^2 + t_{pN} \quad (A.8)$$

and

$$s_{\pi a^*} + s_{\pi N} + s_{a^*N} = s + m_{a^*}^2 + m_\pi^2 + m_N^2 . \quad (A.9)$$

A.1.1 t-Channel Variables; A* Rest Frame

A set of interesting independent kinematic variables is s, $M^2_{A^*}$, t_{pN}, θ_L and ϕ_L, where θ_L and ϕ_L are the t-channel scattering angles defined in fig.9, in the rest frame of A* ($\underset{\sim}{q}_{A^*} \equiv \underset{\sim}{q}_{a^*} + \underset{\sim}{q}_\pi = 0$).

In terms of these variables, the energies and magnitudes of the three-vector momenta of a, N, a*, and π are

$$E_a = \frac{(M^2_{A^*} + m_a^2 - t_{pN})}{2M_{A^*}} , \quad (A.10)$$

$$|p_a| = \frac{\lambda^{1/2}(M^2_{A^*}, m_a^2, t_{pN})}{2M_{A^*}} , \quad (A.11)$$

$$E_N = \frac{(s - m_N^2 - M^2_{A^*})}{2M_{A^*}} , \quad (A.12)$$

$$|q_N| = \frac{\lambda^{1/2}(s, m_N^2, M^2_{A^*})}{2M_{A^*}} , \quad (A.13)$$

$$E_{a^*} = \frac{(M^2_{A^*} + m^2_{a^*} - m_\pi^2)}{2M_{A^*}} , \quad (A.14)$$

$$|q_\pi| = |q_{a^*}| = \frac{\lambda^{1/2}(M^2_{A^*}, m^2_{a^*}, m_\pi^2)}{2M_{A^*}} , \quad (A.15)$$

$$E_\pi = M_{A^*} - E_{a^*} . \quad (A.16)$$

Note that

$$t_{aa^*} = (q_{a^*} - p_a)^2 = m^2_{a^*} + m_a^2 - 2E_{a^*}E_a + 2|q_{a^*}||p_a| \cos\theta_t . \quad (A.17)$$

Thus, we can express

$$t_{aa^*} = g_1(M_{A^*}, t_{pN}) + \cos\theta_t \, g_2(M_{a^*}, t_{pN}) , \quad (A.18)$$

where functions g_1 and g_2 depend on no invariants other than those listed explicitly. Moreover,

$$s_{\pi N} = (q_\pi + q_N)^2 = m_\pi^2 + m_N^2 + 2E_\pi E_N + 2|q_\pi||q_N| \{\cos\theta_t \cos X + \sin\theta_t \sin X \cos\phi_t\} . \quad (A.19)$$

The angle X between vectors $\underset{\sim}{q}_N$ and $\underset{\sim}{p}_a$ is defined through

$$t_{aN} = -s - t_{pN} + m_a^2 + M^2_{A^*} + m_N^2 + m_p^2 = m_a^2 + m_N^2 - 2E_aE_N + 2|p_a||q_N| \cos X . \quad (A.20)$$

Therefore,

$$s_{\pi N} = g_3(s, M_{A^*}) + g_4(s, M_{A^*}, t_{pN}) \cos\theta_t + g_5(s, M_{A^*}, t_{pN}) \sin\theta_t \cos\phi_t , \quad (A.21)$$

where functions g_3, g_4, and g_5 depend on the three invariants listed (plus masses).

$$s_{a^*N} = m^2_{a^*} + m_N^2 + 2E_{a^*}E_N - 2|q_{a^*}||q_N| \{\cos\theta_t \cos X + \sin\theta_t \sin X \cos\phi_t\} \quad (A.22)$$

In the limit of high s ($>> M_{A^*}^2$),

$$E_N \rightarrow s/2M_{A^*} \quad , \tag{A.23}$$

$$|q_N| \rightarrow s/2M_{A^*} \quad . \tag{A.24}$$

Moreover, for high s and (typical) forward production ($t_{pN} \rightarrow 0$),

$$E_a \rightarrow (M_{A^*}^2 + m_a^2)/2M_{A^*} \quad , \tag{A.25}$$

$$|p_a| \rightarrow (M_{A^*}^2 - m_a^2)/2M_{A^*} \quad , \tag{A.26}$$

$$\cos X \rightarrow -1 + \text{terms of order } s^{-1} \quad . \tag{A.27}$$

In this limit, the ϕ dependence in eqns.(A.21) and (A.22) drops out leaving

$$s_{\pi N} \rightarrow \frac{s}{M_{A^*}} \{E_\pi - |q_\pi| \cos \theta_t\} \quad , \tag{A.28}$$

$$s_{a^*N} \rightarrow \frac{s}{M_{A^*}} \{E_{a^*} + |q_{a^*}| \cos \theta_t\} \quad . \tag{A.29}$$

We observe that large $s_{\pi N}$ is intimately correlated with the region $\cos \theta_t \simeq -1$.

In the limit $t_{pN} \rightarrow 0$ (no restriction on s), we can re-write eqn.(A.17) as

$$(t_{aa^*} - m_\pi^2) = \frac{(M_{A^*}^2 - m_a^2)}{M_{A^*}} (-E_\pi + |q_\pi| \cos \theta_t) \tag{A.30}$$

Combining eqns.(A.28) and (A.30), we observe

$$s_{\pi N} \rightarrow s \frac{(m_\pi^2 - t_{aa^*})}{(M_{A^*}^2 - m_a^2)} \tag{A.31}$$

when $t_{pN} \rightarrow 0$, and s is large. The only restriction on M_{A^*} is that $s >> M_{A^*}$ (and $s >>$ all other masses in the reaction).

An identical algebraic manipulation results in

$$s_{a^*N} \rightarrow s \frac{(m_{a^*}^2 - t_{a\pi})}{(M_{A^*}^2 - m_\pi^2)} \quad . \tag{A.32}$$

The expressions (A.31) and (A.32) are crucial for analyses of the J^P structure of the Deck amplitude in the A* rest system.

A.1.2 s-Channel Variables; A* Rest Frame

An alternative set of variables are s, $M_{A^*}^2$, t_{pN}, θ_s and ϕ_s, where θ_s and ϕ_s are s-channel scattering angles, defined in fig.12, in the rest frame of $A^*(q_{A^*} \equiv q_{a^*} + q_\pi = 0)$. Angle ϕ_s has the same value in the overall c.m. frame.

The equations (A.10) through (A.16) still apply. However, now

$$s_{\pi N} = m_N^2 + m_\pi^2 + 2E_N E_\pi + 2|q_N||q_\pi| \cos \theta_s \tag{A.33}$$

$$= g_3(s, M_{A^*}^2) + g_6(s, M_{A^*}^2) \cos \theta_s \quad . \tag{A.34}$$

As fixed s and M_{A^*}, the distribution in $\cos \theta_s$ reflects directly any structure associated with the variables $s_{\pi N}$ and s_{a^*N}.

$$s_{a^*N} = m_N^2 + m_{a^*}^2 + 2E_N E_{a^*} - 2|q_N||q_{a^*}| \cos \theta_s \tag{A.35}$$

The momentum transfer variable

$$t_{aa^*} = m_a^2 + m_{a^*}^2 - 2E_a E_{a^*} + 2|p_a||q_{a^*}| \{\cos \theta_s \cos X + \sin \theta_s \sin X \cos \phi_s\} \tag{A.36}$$

$$\equiv g(M_{A^*}, t_{pN}) + g_7(s, M_{A^*}, t_{pN}) \cos \theta_s + g_8(s, M_{A^*}, t_{pN}) \sin \theta_s \cos \phi_s \quad . \tag{A.37}$$

$$\equiv G_3(s, M_{A^*}, t_{pN}, s_{\pi N}) + G_4(s, M_{A^*}, t_{pN}, s_{\pi N}) \cos \phi_s \quad . \tag{A.38}$$

In the limit of high s,

$$s_{\pi N} \rightarrow \frac{s}{2M_{A^*}} (E_\pi + |q_\pi| \cos \theta_s) \quad , \tag{A.39}$$

$$s_{a^*N} \rightarrow \frac{s}{2M_{A^*}} (E_{a^*} - |q_{a^*}| \cos \theta_s) \quad . \tag{A.40}$$

A.1.3 Threshold Limits of A*

It is useful to remark that in the limit $M_{A^*} \to (m_{a^*} + m_\pi)$, eqn.(A.17) reduces to

$$t_{aa^*} = \frac{(m_{a^*} t_{pN} + m_\pi m_a^2)}{(m_{a^*} + m_\pi)} - m_{a^*} m_\pi \qquad (A.41)$$

and

$$t_{a\pi} \to \frac{(m_\pi t_{pN} + m_{a^*} m_a^2)}{(m_{a^*} + m_\pi)} - m_{a^*} m_\pi \quad . \qquad (A.42)$$

The values of t_{aa^*} and $t_{a\pi}$ are fixed once t_{pN} is given. Corrections to these expressions above threshold are proportional to the pion momentum in the A* rest system.

DIFFRACTIVE PRODUCTION OF A_2 AND ITS GENERALIZATIONS

by

C.F. Cho and L. Stodolsky
Max-Planck-Institut f. Physik u. Astrophysik, Munich

Abstract

Diffractive dissociation of spin-0 particles which violates the Morrison rule are studied using the Drell-Hiida-Deck type model. An example of this type of process is $\pi + p \to A_2 + p$. Rules for the helicity structure of the dissociated system are derived. In particular, in the diffractive dissociation $0^- \to 1^-, 2^+, \ldots$, when the virtual particle which is dissociated from the incident particle and elastically scattered from the target nucleon is a spin-0 particle, then the dissociated system has spin projection $|J,1\rangle + |J,-1\rangle$ in its Gottfried-Jackson frame. In general, if one assumes spin-independence in the elastic scattering of the virtual particle-target elastic scattering, the same conclusion holds. Other implications of the Drell-Hiida-Deck type model on diffractive dissociation processes are discussed and testable predictions made.

Presented by C.F. Cho.

THIS PAGE

WAS INTENTIONALLY

LEFT BLANK

SESSION 4

Chairman: E. Gabathuler

Invited Talk

MULTIPARTICLE SPECTROMETERS AND THEIR USE IN MESON SPECTROSCOPY

R.J. Cashmore
Nuclear Physics Laboratory, University of Oxford

THIS PAGE

WAS INTENTIONALLY

LEFT BLANK

MULTIPARTICLE SPECTROMETERS AND THEIR USE IN MESON SPECTROSCOPY

by

R.J. Cashmore
Nuclear Physics Laboratory, University of Oxford,
Keble Road, Oxford OX1 3RH

EH/A22

1. INTRODUCTION

The whole field of $\pi\pi$ and $K\pi$ scattering has been revolutionized by spectrometer experiments[1,2] studying the reactions

$$\pi^- p \to \pi^+\pi^- n \qquad (1)\ \text{(CERN-MUNICH)}$$

$$K^+ p \to K^+\pi^-\Delta^{++} \qquad (2)$$
$$K^- p \to K^-\pi^+ n \qquad (3)\ \Big\}\ \text{(SLAC)}$$

The reasons for such an improvement are the following:

(a) the spectrometer, with its good resolution and particle identification, can be used at high beam momenta, thus allowing penetration to smaller values of t for a given resonance and hence observation of a bigger component of the pion exchange cross section;

(b) the numbers of events are enormous compared with previous bubble chamber experiments.

After success in these 2 meson systems, the next states to be studied will be the 3 particle states produced in

$$\pi^- p \to \pi^-\pi^+\pi^- p \qquad (4)\ \text{(CIBS at 25/40 GeV/c)}$$

$$K^\pm p \to K^\pm\pi^+\pi^- p \qquad (5)\ \text{(SLAC at 13 GeV/c)}$$

$$\pi^- A \to \pi^-\pi^+\pi\, A \qquad (6)\ \text{(BNL at 24 GeV/c)}\ \text{(CERN at 9/15 GeV/c)}$$

Of these experiments I will concentrate on reaction (5); the others are dealt with in other talks at this conference[3,4].

2. RELEVANT PROPERTIES OF SPECTROMETERS

As already mentioned the two principle properties which are important are

(a) enormous increase in statistics (> × 10) with good measurement resolution; and

(b) particle identification.

But they do not have uniform acceptance. The major question is therefore whether this matters, i.e. Can we still extract the physics?

The answer to the question is very definitely yes. This is apparent for 2 particle final states (the 3^- g, and 3^- K^* are only convincingly demonstrated in spectrometers) as we have seen, and it will be shown that it is equally apparent for 3 particle final states.

We can thus look forward to the revolutionary effect of spectrometers on the 3 meson systems; in particular, studies of non-diffractive production reactions with their small cross sections now becomes feasible with appreciable statistics, e.g.

$$\pi^- p \to \pi^+\pi^-\pi^0 n \qquad (7)$$

$$\gamma p \to \pi^+\pi^+\pi^- n \qquad (8)$$

$$\to \pi^+\pi^-\pi^0 p \qquad (9)$$

3. AN ILLUSTRATION - 13 GeV/c K^+p SCATTERING

In order to bring out the features of spectrometers I will use as an example the SLAC experiment on $K^\pm p$ scattering at 13 GeV/c[2]. This experiment was designed to study

(i) $K\pi$ scattering
(ii) $K\pi\pi$ systems in reaction (5)
(iii) Elastic scattering
(iv) Any other reactions you might pick up in a multiparticle trigger.

The apparatus is shown in fig.1 and is a conventional multiparticle spectrometer. The only feature I particularly want to draw attention to is the large

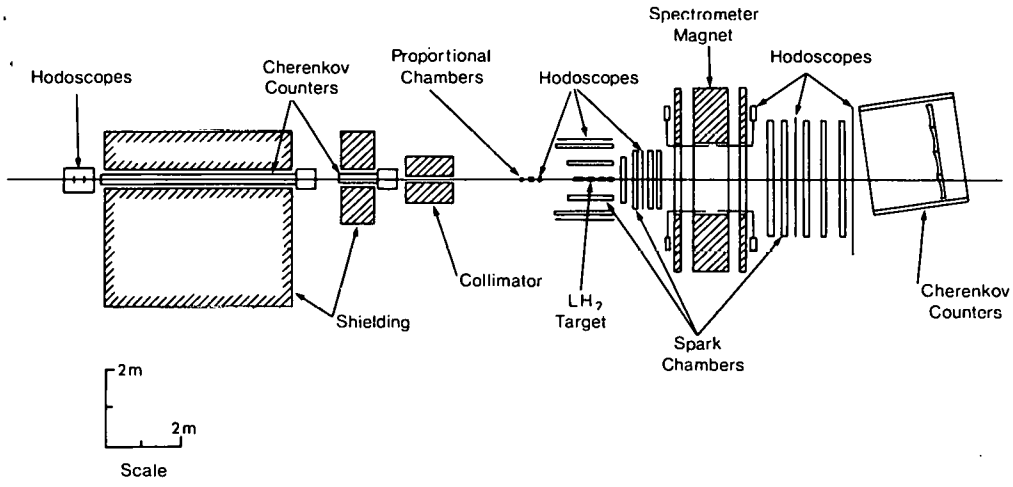

Fig. 1 The SLAC spectrometer.

Cherenkov counter at the end of the spectrometer. This has eight separate mirrors each viewed by its own photo-tube and thus provides the ability to identify a number of particles in the final state.

At SLAC, due to the duty cycle, we use a general trigger. However we also have an r.f. separated beam giving approximately 10^3 kaons/s.

The trigger actually used is:

Beam = $(xy = 1) \cdot \bar{R} \cdot C_K \cdot C_\pi$ ($K^\pm$ beam)

Mesons = Beam $\cdot$ T $\cdot$ $(A \geq 2) \cdot (B \geq 2) \cdot \bar{M}$

where T is a hodoscope before the magnet, A and B hodoscopes afterwards and M veto counters inside the magnet covering all faces. Thus we essentially require ≥ 2 particles through the magnet together with no vetoes firing.

The final data samples will correspond to $\sim 10^9$ incident K^+'s and $\sim 7.5 \times 10^8$ incident K^-'s both at 13 GeV/c. The resulting event samples will be

$K^+p \to K^+\pi^-\Delta^{++}$	130,000	$K^-p \to K^-\pi^+n$	65,000
$\to K^+\pi^+n$	16,000	$\to K^-\pi^-\Delta^{++}$	30,000
$\to K^0\pi^+p$	12,000	$\to \bar{K}^0\pi^-p$	10,000
$K^+p \to K^0\Delta^{++}$	14,000	$K^-p \to \bar{K}^0n$	6,500
		$\to \phi[\Lambda,\Sigma^0]$	5,500
$K^+p \to K^+\pi^+\pi^-p$	75,000	$K^-p \to K^-\pi^+\pi^-p$	60,000
$\to K^+\phi p$	4,000	$\to K^-\phi p$	3,000
$K^+ \to \pi^+\pi^+\pi^-$	250,000	$K^- \to \pi^-\pi^+\pi^-$	200,000

(The τ decays are particularly useful for monitoring the apparatus and beam).

4. FEATURES OF THE DATA AND EXPERIMENTAL POINTS

(a) Statistics: In order to ensure that the numbers quoted above are appreciated, fig.2 shows the raw mass spectrum for $K^+\pi^+\pi^-$. The smudge at the bottom of the plot is the previous best single experiment on this reaction[5].

(b) Resolution: Figure 3 contains the missing mass spectrum while fig.4 shows some effective mass spectra. It is clear that we can easily identify reaction (5). In all further plots we select events for which 700 < M < 1100 MeV. It is important to state that these results come from raw measurements. We have not indulged in any kinematic fitting.

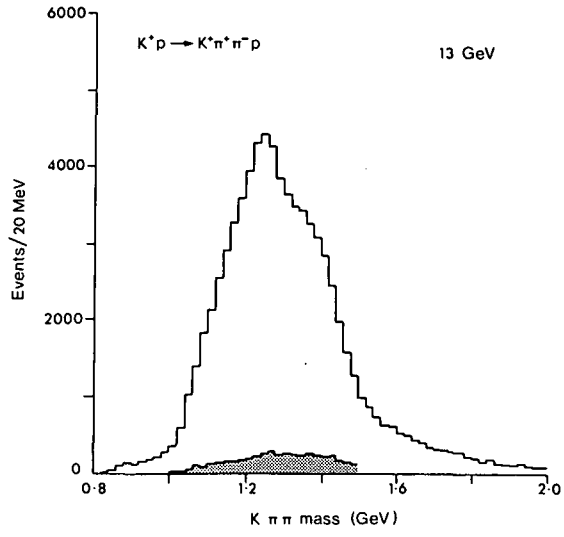

Fig. 2 The mass spectrum of $K^+\pi^+\pi^-$ after identification of the final state particles.

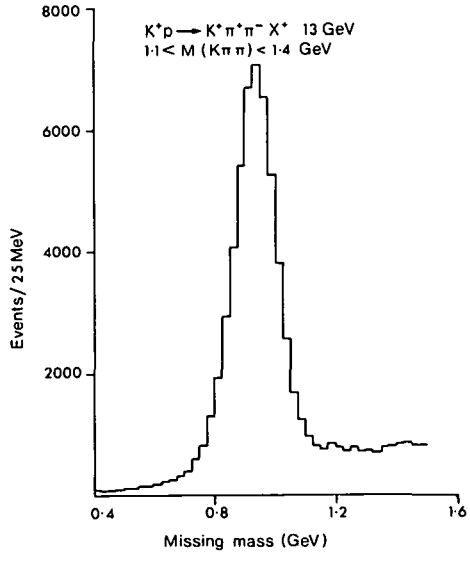

Fig. 3 The missing mass (mm) spectrum in the reaction $K^+p \to K^+\pi^+\pi^-$ (mm)

(c) Identification: Figure 5 shows the effective mass spectrum of X^+X^- in

$$K^+p \to X^+X^- \quad \Delta^{++} \tag{10}$$

where we have assumed X^+ and X^- to be pions. We clearly see a K^0 peak superimposed on a background due to reaction (2) where we have mislabelled the K^+ as a π^+. If we now use the Cherenkov counter to

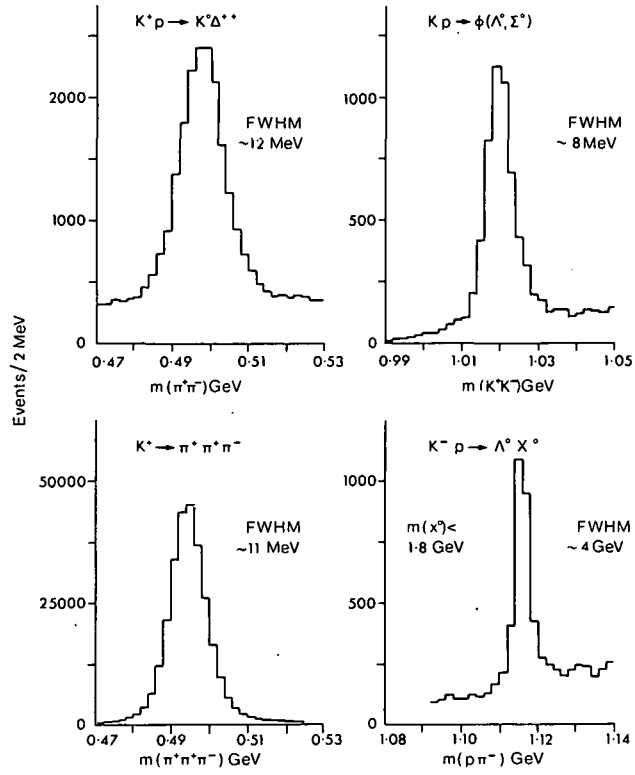

Fig. 4 Experimental effective mass resolutions.

label the positive particle as a π^+ or K^+ the two lower spectra result. We now see a very clean K^0 signal with the flat background due to misidentification of a K^+ clearly demonstrated.

In analyzing reaction (5) we can identify three categories:

(i)	where we identify both positives	$K^+\pi^+$
(ii)	where we identify only the K^+	K^+X
(iii)	where we identify only the π^+	π^+X

We use all three categories in our analysis. The last two categories are subject to backgrounds, although these are small, e.g. the major contamination in (ii) is from

$$K^+p \to K^+\phi p \tag{11}$$

which is explicitly rejected by a ϕ mass cut, while (iii) will have a background from

$$K^+p \to K^0 \quad \pi^+p \qquad K^0 \to \pi^+\pi^- \tag{12}$$

which is similarly rejected with a K^0 mass cut.

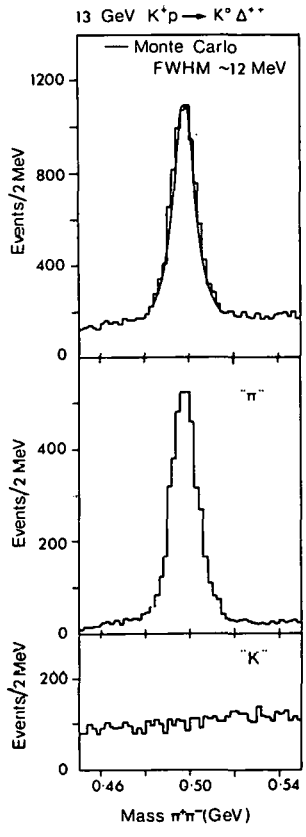

Fig. 5 The use of the Cherenkov counter in identifying $K^+p \to K^0\Delta^{++}$. The upper figure shows the $M(X^+X^-)$ mass spectrum while the lower two figures demonstrate the results when identification of the positive particle as a π^+ or K^+ in the Cherenkov counter is demanded.

The Cherenkov counter was set with a π threshold at p ~ 2.5 GeV/c resulting in K's giving light at a momentum ~ 8 GeV/c.

5. HOW TO EXTRACT THE PHYSICS?

All we need to know is

(i) How particles propagate in free space and pass through magnets[6].

(ii) The properties of the Cherenkov counter.

(iii) The efficiencies of counters, chambers and track finding (all measured in a good spectrometer experiment)

(iv) The absorption and interaction of particles passing through matter.

Thus there is nothing magical in analyzing data from a good spectrometer. All it requires is care and the application of well known laws of physics.

6. WHAT ARE THE EFFECTS OF GEOMETRICAL APERTURES AND PARTICLE IDENTIFICATION?

As the spin parity of the Kππ system is a function of effective mass we have to understand the effects of finite acceptance on particular partial waves.

(i) What happens to a partial wave?

In figs.6 and 7 we see the effects on the 1^+0^+ s-wave πK* (the major Q wave). The angles are defined from vectors in the $(K^+\pi^+\pi^-)$ rest frame by

$$\underset{\sim}{z} = \underset{\sim}{p}_{\pi^+} \qquad \underset{\sim}{y} = \underset{\sim}{p}_{\pi^-} \wedge \underset{\sim}{p}_{k^+} \qquad \hat{\underset{\sim}{x}} = \hat{\underset{\sim}{y}} \wedge \hat{\underset{\sim}{z}}$$

($\hat{\underset{\sim}{y}}$ and $\hat{\underset{\sim}{z}}$ normalized vectors)

$$\cos\beta = \hat{\underset{\sim}{p}}_{beam} \cdot \hat{\underset{\sim}{z}}$$

$$\tan\alpha = \frac{\underset{\sim}{p}_{beam} \cdot \hat{\underset{\sim}{y}}}{\hat{\underset{\sim}{p}}_{beam} \cdot \hat{\underset{\sim}{x}}}$$

β_i α and the polar angles of the beam in x y z

For orientation fig.8 shows the corresponding angular distributions for the raw data in the mass range 1.24 to 1.26 GeV/c^2. It is clear that the 1^+0^+ s-wave πK^* is a major component.

(ii) Acceptance of $1^+0^+\pi K^*$ as a function of mass and t

In fig.9 we see the mass dependence of this wave for two t' values ($t' = t - t_{min}$) together with the t dependence at a given mass. All variations are smooth.

(iii) Acceptance for other waves

Figure 10 shows similar mass and t dependence for a selection of other waves. As we might have expected the acceptance does indeed depend on the angular distributions involved. The most important remark however is that these acceptances vary smoothly and do not show sudden discontinuities!

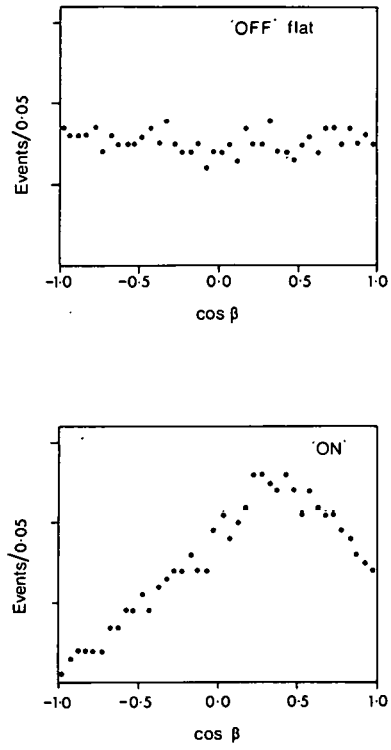

Fig.6 The effects of the spectrometer and of particle identification on the cos β distribution for the 1^+0^+ πK^* s-wave.

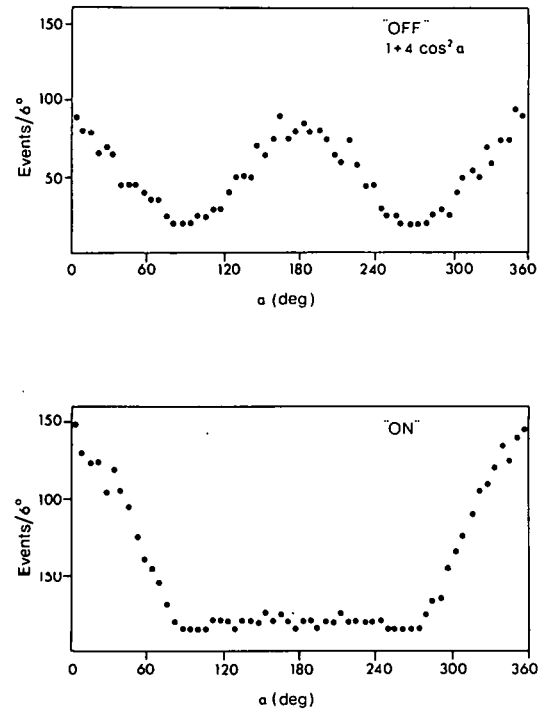

Fig.7 The effects of the spectrometer and of particle identification on the α distribution for the 1^+0^+ πK^* s-wave.

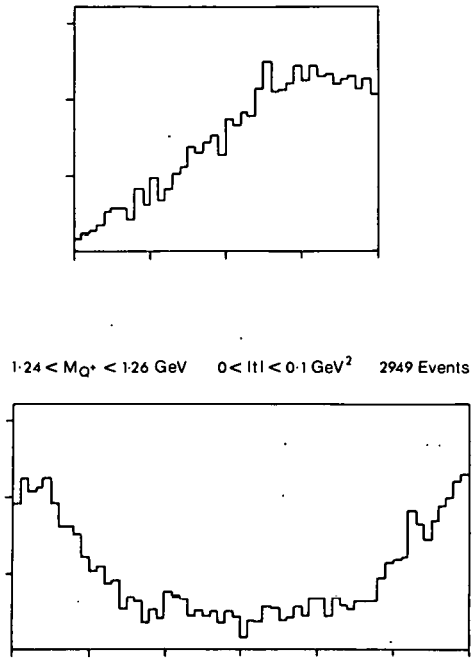

Fig.8 Raw data for the angular distributions cos β and α.

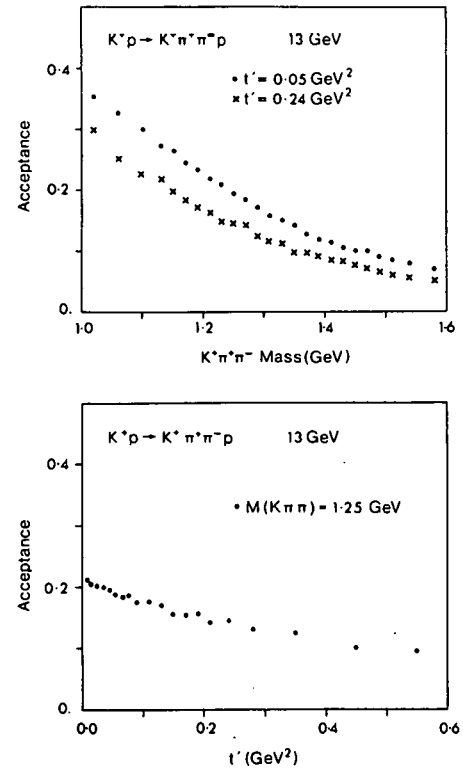

Fig.9 The mass and t' dependence for the acceptance of the 1^+0^+ s-wave πK^*

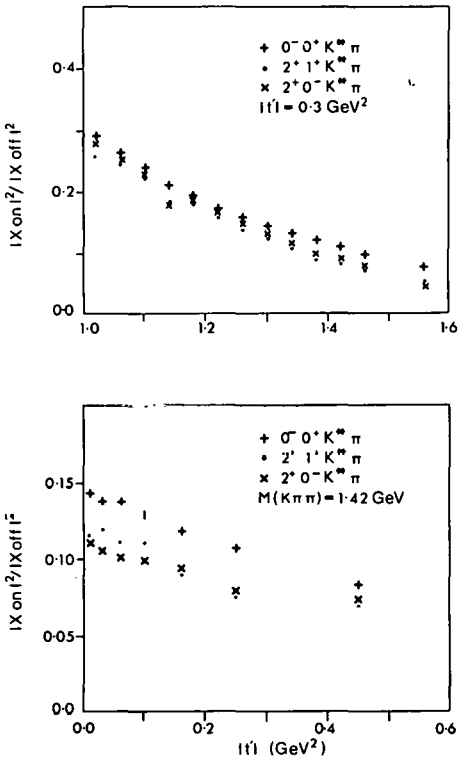

Fig. 10 The mass and t dependence for the acceptance of a variety of other waves.

7. HOW TO ANALYSE THE DATA?

(i) Not weighting

This would require a knowledge of the acceptance over a five dimensional grid (α, β, γ, ω_1^2, ω_2^2) at each mass and t value, together with sufficient data in each volume of this space to make weighting a statistically sound procedure. It is impossible even with our statistics. The most deadly sin that one can commit is to attempt to do it in an inferior way (this in the past has resulted in a bad name for spectrometers).

(ii) The 'Correct Way'

This means that we make some theoretical model for the distribution of events, pass it through a spectrometer, and then compare with the data. (For 2 particle cases this 'model' is that the angular distribution may be expressed as a sum of spherical harmonics, for the 3 particle case we use the isobar model.)

Perfect acceptance:

In general the kinematical distributions depend on 7 variables M, t, (α, β, γ, ω_1^2 and ω_2^2). We will perform the analysis at a given bin in M and t. Then

$$\frac{d^5\sigma}{d\underset{\sim}{y}} = \left|\sum_\alpha P_\alpha X_\alpha(\hat{y})\right|^2 \qquad (13)$$

where $\underset{\sim}{y}$ are the kinematical variables (α, β, γ, ω_1^2, ω_2^2)

X_α the decay matrix elements for a given partial wave α. These contain the angular momentum decomposition, barrier factors, Breit-Wigners etc[7].

P_α the partial wave amplitudes we wish to determine at each value of M and t.

Then

$$\sigma = \int \left|\sum_\alpha P_\alpha X_\alpha(\underset{\sim}{y})\right|^2 d\underset{\sim}{y} = \sum_{\alpha_1\alpha_2} P_{\alpha_1} P^*_{\alpha_2} N_{\alpha_1\alpha_2} \qquad (14)$$

where

$$N_{\alpha_1\alpha_2} = \int X_{\alpha_1} X^*_{\alpha_2}\, d\underset{\sim}{y} \qquad (15)$$

We then use the maximum likelihood method to give the values of P_α by maximizing the function

$$\log \mathscr{L} = \sum_{i=1}^{N_{\text{events}}} \log \frac{d^5\sigma(i)}{d\underset{\sim}{y}} - \int \frac{d^5\sigma}{d\underset{\sim}{y}}\, d\underset{\sim}{y} \qquad (16)$$

Turn on a spectrometer:

We now have that

$$\frac{d^5\sigma_{\text{obs}}}{d\underset{\sim}{y}} = \frac{d^5\sigma}{d\underset{\sim}{y}} A(\underset{\sim}{y}) \qquad (17)$$

where $A(\underset{\sim}{y})$ is the acceptance, a function of $\underset{\sim}{y}$.

The likelihood function then becomes

$$\log \mathscr{L} = \sum_{i=1}^{N_{\text{events}}} \log \frac{d^5\sigma(i)}{d\underset{\sim}{y}} + \sum_{i=1}^{N_{\text{events}}} \log A(\underset{\sim}{y}_i) - \int \frac{d^5\sigma}{d\underset{\sim}{y}} A(\underset{\sim}{y})\, d\underset{\sim}{y} \qquad (18)$$

We first note that the second term in (18) is a constant for all fits and thus we may ignore it. (It does not depend on P_α in any way.) We may also write

$$\int \frac{d^5\sigma}{d\underset{\sim}{y}} A(\underset{\sim}{y})\, d\underset{\sim}{y} = \int \left|\sum_\alpha P_\alpha X_\alpha\right|^2 A(\underset{\sim}{y})\, d\underset{\sim}{y} = \sum_{\alpha_1\alpha_2} P_{\alpha_1} P^*_{\alpha_2} W_{\alpha_1\alpha_2} \qquad (19)$$

where

$$W_{\alpha_1\alpha_2} = \int X_{\alpha_1} X^*_{\alpha_2} A(\underset{\sim}{y})\, d\underset{\sim}{y} \qquad (20)$$

Thus in fitting we use a likelihood function

$$\log \mathcal{L} = \sum_{i=1}^{N_{events}} \log \left| \sum_{\alpha} P_\alpha X_\alpha(y_i) \right|^2 - \sum_{\alpha_1\alpha_2} P_{\alpha_1} P^*_{\alpha_2} W_{\alpha_1\alpha_2} \quad (21)$$

and maximize this to give the parameters P_α.

Finally we can then obtain the numbers of events at production from the P_α with

$$\sigma_{production} = \sum_{\alpha_1\alpha_2} P_{\alpha_1} P^*_{\alpha_2} N_{\alpha_1\alpha_2} \quad (22)$$

It is important to note that the integrals $W_{\alpha_1\alpha_2}$ and $N_{\alpha_1\alpha_2}$ can be calculated once and for all using Monte Carlo techniques. They do not have to be recalculated at each step.

(iii) Derivative Calculations

This point is of importance for the practitioner of the method. Simple calculation shows that the derivatives of the log likelihood function with respect to the fitting parameters are

$$\frac{\partial \log \mathcal{L}}{\partial \, \mathrm{Re}\, P_R} = \sum_i \left\{ \frac{1}{\sigma_i} \, 2 \, \mathrm{Re}[X^*_k (\sum_j P_j X_j)] \right\} - 2 \, \mathrm{Re}(\sum_j P_j W_{jk}) \quad (23)$$

$$\frac{\partial \log \mathcal{L}}{\partial \, \mathrm{Im}\, P_R} = \sum_i \left\{ \frac{1}{\sigma_i} \, 2 \, \mathrm{Im}[X^*_k (\sum_j P_j X_j)] \right\} - 2 \, \mathrm{Im}(\sum_j P_j W_{jk}) \quad (24)$$

where

$$\sigma = \left| \sum_j P_j X_j \right|^2 \quad (25)$$

This implies that the derivatives are easily calculated at each step with little increase in computer time.

(iv) How to calculate the decay amplitudes?

The simplest way to do this is to use one of the two major programs:

(a) Illinois (Ascoli, Kruse ...)

This has been used with great success in many analyses of 3 meson (0^-) systems[3].

(b) SLAC/LBL[8]

This system is much more oriented towards amplitude analysis and has a very good pedigree being initially used in analysis of

$$\pi N \to \pi\pi N \quad (26)$$

and later adapted to analyse 3 meson systems[9-11] in

$$\pi^+ p \to \pi^+\pi^+\pi^- p$$
$$K^+ p \to K^\pm \pi^+ \pi^- p$$
$$\pi^+ p \to \pi^+\pi^-\pi^0 \Delta^{++}$$

Indeed the program is general enough to cope with all results, and may be easily adapted and plugged into any minimizer. All the work now described has used this program.

8. HOW TO OBTAIN THE PARTIAL WAVES IN A FIT

Throughout this section and in the next the SLAC $K\pi\pi$ analysis is taken as an example and demonstration. However these results are still preliminary.

(i) The data: We will use the data shown in fig.11 where we have used a t' selection $0.1 < t' < 0.5$. We will return to the cross hatched data later.

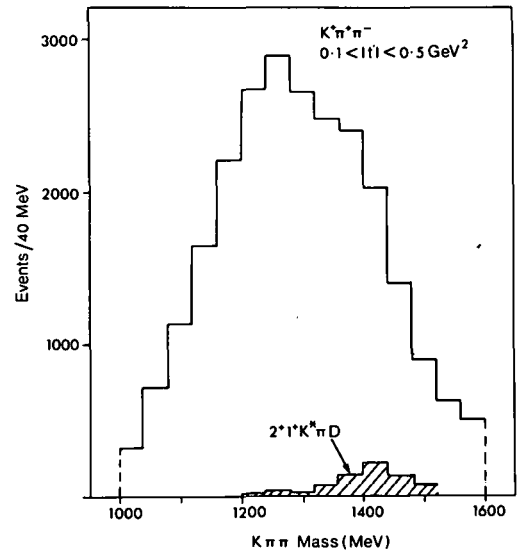

Fig.11 The $K\pi\pi$ mass distribution for $0.1 < t' < 0.5$. The cross hatched histogram represents the contribution of the 2^+1^+ πK^*D wave in the raw data.

(ii) Numbers of events

From our experience of $\pi N \to \pi\pi N$ we felt we needed at least 1000 events per M, t bin in order to obtain good solutions. As we wished to analyse the $K\pi\pi$ mass region 1.0 - 1.5 GeV in 25 MeV mass bins with at least two t bins this meant a total of 150,000 events, approximately what we obtained.

(iii) The Wave Set and our present (preliminary) solution

The process of reaching a solution is laborious and iterative (you stop when either exhausted or stability is reached). Let me list the various stages

(a) Select some sensible t' bin (e.g. 0.05 → 0.3) in which you are sensitive to all waves which might be present (remember natural parity exchange M > 1 states often go to zero at t' = 0) and a set of mass bins, e.g. 40 MeV.

(b) Choose a starting set of waves (e.g. 0^-, 1^+, 2^-, 2^+ - a good selection of what might be present - obviously prejudice is involved).

(c) Take random starts (~ 10) in each bin and then maximize. In our case this leads to 1, 2 or 3 distinct maxima at each mass.

(d) Propagate solutions from adjacent mass bins. In our case most of these propagated to already existing solutions and we were left with a few ($\lesssim 3$) solutions at each mass.

(e) Remove waves consistent with zero and remaximize.

(f) Throw out solutions which are poorer (we want always to reduce the numbers we have to consider). This can be done in the following way[12]. We wish to compare two solutions A and B and find out if A is systematically better than B. Define the following quantity on an event by event basis

$$\mathscr{L}^i_{AB} = \mathscr{L}^i_A - \mathscr{L}^i_B \qquad (26)$$

where $\mathscr{L}$ is the log likelihood function. Now $\mathscr{L}_{AB}$ will have some distribution function with mean $\bar{\mathscr{L}}_{AB}$, with $\delta\mathscr{L}_{AB}$ and error on the mean $\delta\bar{\mathscr{L}}_{AB}$. Now $\delta\mathscr{L}_{AB}$ will be the same whatever the sample of events, whereas $\delta\bar{\mathscr{L}}_{AB}$ decreases the bigger the sample.

$$\delta\bar{\mathscr{L}}_{AB} \sim \frac{1}{\sqrt{N}}\,\delta\mathscr{L}_{AB} \qquad (27)$$

We may then expect A to be systematically better than B if

$$\bar{\mathscr{L}}_{AB} > k\,\delta\bar{\mathscr{L}}_{AB} \qquad (28)$$

where k is in the range ~ 0.3 to 1. Indeed we can empirically determine k if we have some partial wave which must be present in the data, e.g. K*(1400). We can compare the two solutions with and without it present.

(g) We now have a basic set of waves S and a few solutions at each mass.

At this point we add on new groups of waves to each solution, beginning with random starts in these new waves and looking to see if any are necessary. By this technique one eventually obtains a new set of waves S'

(h) We then begin the whole process over again (starting from step (c)) and look for new solutions and the stability of the wave set S'.

We then repeat the process until we are happy with the stability.

We now have our basic set of waves and our basic set of solutions (in our case 1 or 2 at each mass).

(iv) Checks on the fit

(a) We generate a Monte Carlo experiment with our fit parameters and compare projections of this with the data looking for any wild discrepancy.

(b) We follow an alternative procedure to (iii) i.e. choose a large mass bin and perform a t-sweep looking for new waves.

(v) Basic set of waves and solution

With this final set of waves and solutions we are ready to study any physics topics, e.g. to identify a very small wave we might resort to both large M and t bins.

9. RESULTS

Our analysis is still at a preliminary stage and we are not entirely satisfied that we have completed the process described in sect.8 as thoroughly as we would like. Thus I cannot present any results for the Q region of Kππ mass.

(i) The partial wave set

The partial wave set we are presently using is listed below:

(a) natural parity exchange non-flip amplitudes

$0^-0^+\pi K^*p$, $1^+0^+\pi K^*s$, $1^+1^+\pi K^*s$, $2^-0^+\pi K^*p$, $2^+1^+\pi K^*d$

0^-0^+ $K\rho p$, 1^+0^+ $K\rho,s$

$0^-0^+\pi\kappa$ s, 1^+0^+ $\pi\kappa$ p

0^-0^+ $K\varepsilon s$, 1^+0^+ $K\varepsilon$ p

(b) unnatural parity exchange

2^+0^- πK^*d

(c) natural parity exchange flip amplitudes

1^+0^+ πK^*s

0^-0^+ $K\varepsilon$ s (although this wave may not be necessary)

(In principle at a given value of M and t we cannot

identify flip and non-flip amplitudes at the nucleon vertex. However we use this terminology both from prejudice and observation of the t-distribution of these waves).

(ii) The K*(1400)

In order to demonstrate the success of the methods outlined we shall concentrate on this resonance. It is expected in the two waves

2^+1^+ πK^*d - natural parity exchange interfering with many other waves.

2^+0^- πK^*d - unnatural parity exchange (π) incoherent with all the other waves.

(a) Mass spectra

Figure 12 shows the mass dependence of these two waves. A beautiful K*(1400) signal is seen in the 2^+1^+ wave with mass and width consistent with the accepted values. (I might add that this is usually a one bin effect in most conventional analyses.)

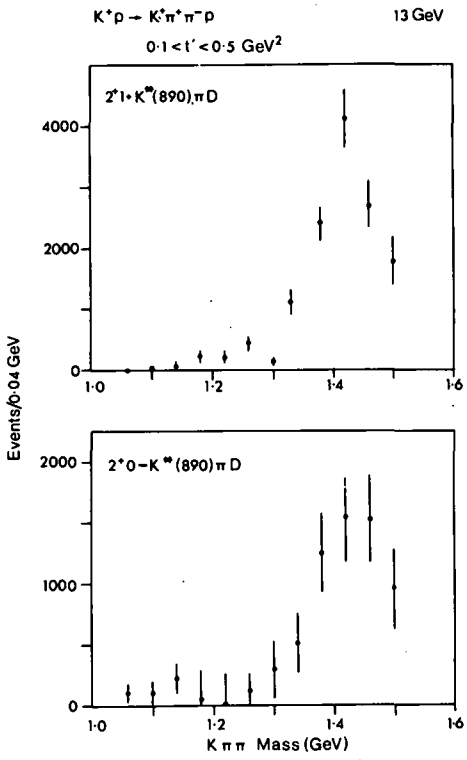

Fig. 12 Mass dependence of the intensity at production (i.e. corrected for acceptance) of the 2^+1^+ and 2^+0^+ πK^* waves.

The 2^+0^- is even more remarkable - such an observation has never been previously made in this type of reaction and analysis. It is only by virtue of the high statistics that we are able to pick up such a small signal which is incoherent with all the other states.

(b) Sensitivity of the experiment

In fig.11 we see the contribution of the 2^+1^+ πK^*d wave to the raw data ($\lesssim$ 10%). We can use the mass bin 1320 - 1360 MeV to gain an idea of the sensitivity of the experiment. There we see ~ 3% effect in the raw data is measured as a six standard deviation effect. Thus we can conclude that it will be possible to observe ~ 1% effects in the data (we are pushing the isobar model - is it really that good?)

(c) t distributions

Figure 13 shows the t dependence for these two K*(1400) waves using a large $K\pi\pi$ mass bin $1360 < M(K\pi\pi) < 1480$. We observe differential cross sections consistent with natural parity exchange (dip in the forward direction) and unnatural parity exchange (pion exchange). Thus we find the K*(1400) production mechanisms we might expect.

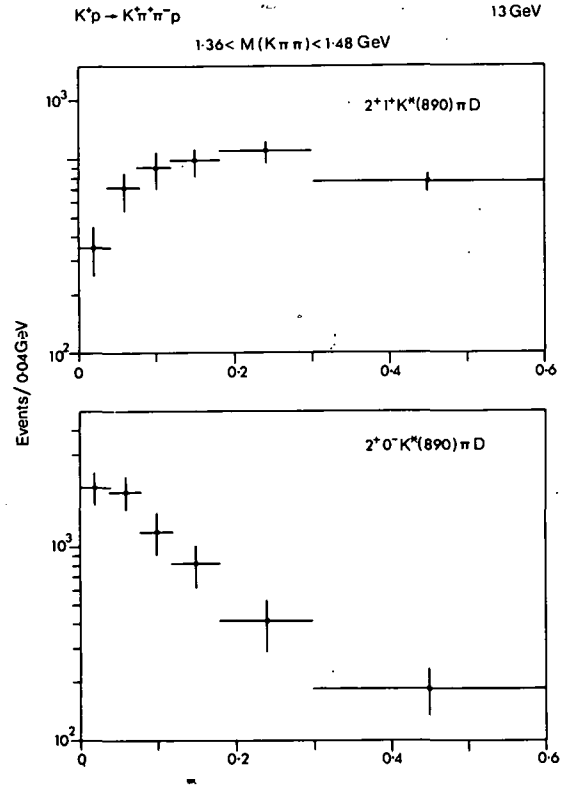

Fig. 13 The t dependence of the intensity at production (i.e. corrected for acceptance) of the 2^+1^+ and 2^+0^- πK^* waves.

(d) Other waves

We have searched for other waves. In particular 2^+2^+ and 2^+2^- waves are both zero while the 2^+1^- πK^*, 2^+1^+, and 2^+0^- $K\rho$ are all small and await a large M and large t bin for their reliable observation.

Thus we can conclude that the method we apply appears

to be successful when we test our expectations of the observation of the $K^*(1400)$.

10. CONCLUSIONS

We can draw the following conclusions from this demonstration.

(a) Acceptance problems are well defined and tractable.

(b) The increased statistics make the observation of smaller and smaller effects possible, e.g. the 2^1O πK^* wave.

(c) We can look forward to a very detailed description of the Q region from our 13 GeV/c $K^{\pm}p$ experiment at SLAC (both in mass and t).

(d) The future looks exceedingly bright for other experiments - for example those which will unravel the A_1 enigma in reactions such as (7),(8) and (9).

REFERENCES

1. G. Grayer et al, Nucl. Phys. B75, (1974) 189.

2. G. Brandenburg et al, (SLAC) Contribution to the XVII Int. Conf. on High Energy Physics, London, 1974. (SRC, Rutherford Laboratory, 1974) Paper 235.

3. U. Kruse - These proceedings.

4. V. Chaloupka - These proceedings.

5. P.J. Davis et al, Phys. Rev. D5, (1972) 2688.

6. I. Newton and H. Lorentz.

7. See G.T. Jones - These proceedings and references quoted therein.

8. D.J.Herndon, P. Söding and R.J. Cashmore, LBL-543/SLAC-PUB-1108. To be published in Phys. Rev.

9. M. Tabak et al, Proc. 4th Int. Conf. on Experimental Meson Spectroscopy, Boston (1974). APS No.21, p.46 and LBL-3010.

10. R.J. Cashmore, T. Lasinski - Private Communication.

11. F. Wagner, M. Tabak, and D. Chew, LBL-3395; and F. Wagner - These proceedings.

12. D.J. Herndon et al, LBL-1065(Rev.)SLAC-PUB-1108. To be published in Phys. Rev.

SESSION 5

Chairman: C. Michael

THE ISOBAR MODEL

Invited Talk

CORRECTIONS TO THE ISOBAR MODEL FOR THREE HADRON FINAL STATES

I.J.R. Aitchison
Department of Theoretical Physics, University of Oxford

Contribution

RE-ARRANGEMENT EFFECTS IN THREE-BODY FINAL STATES

D. Morgan
Rutherford Laboratory

THIS PAGE

WAS INTENTIONALLY

LEFT BLANK

CORRECTIONS TO THE ISOBAR MODEL FOR THREE HADRON FINAL STATES

by

I.J.R. Aitchison
Department of Theoretical Physics,
University of Oxford.

A 21

1. WHY THE ISOBAR MODEL NEEDS TO BE CORRECTED (1): UNITARITY IN FINAL STATE TWO-PARTICLE (SUB-ENERGY) CHANNELS.

In the analysis of systems decaying into three mesons one deals, after the angular momentum decomposition, with amplitudes of the form $T^J_{LS}(s_1,s_2,m^2)$ where J is the total angular momentum of the decaying system, S is the angular momentum of one dimeson pair, say (23), and L is the orbital angular momentum of the third meson (1) relative to that pair; and where, if p_i is the four-momentum of the i^{th} final state meson,

$$m^2 = (p_1 + p_2 + p_3)^2, \qquad s_1 = (p_2 + p_3)^2,$$

$$s_2 = (p_1 + p_3)^2.$$

Such an amplitude is represented by fig.1. There are

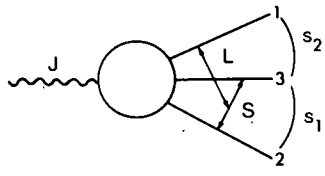

Fig.1 Three-meson decay amplitude.

analogous amplitudes for the other two pairings, in general. Suppose first that only the pair (23) interacts strongly in the final state. In the <u>isobar model approximation</u> one then writes

$$T^J_{LS}(s_1,s_2,m^2) = C^J_{LS}(m^2) \times \frac{1}{D_1(s_1)} \times \text{barrier factors} \qquad (1)$$

where D_1 is the denominator function of the (23) scattering amplitude (usually only those cases are considered in which D_1 is resonant or nearly so), and the $C^J_{LS}(m^2)$ are complex functions of m^2 to be determined by fitting to the data. This decomposition is illustrated in fig.2.

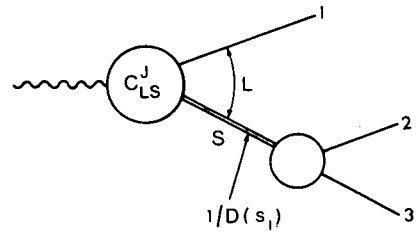

Fig.2 Isobar model approximation to the decay amplitude of fig.1, for the case in which only the pair (23) interacts strongly in the final state.

In the case in which several pairs interact strongly, one can make a suitable generalisation. The complete amplitude for the decay is then a <u>sum</u> of terms of the form (1), suitably symmetrised if necessary. <u>Such an amplitude does not satisfy two body unitarity in the final state</u>. In order to demonstrate this basic fact, and the reason for it, as simply as possible, I shall now consider a highly simplified model: one in which all angular momentum effects are absent, so J = L = S = 0, and in which only <u>two</u> final state pairs interact strongly (as in $K^+\pi^+\pi^-$ for instance). Our basic assumption[1] is that the complete decay amplitude may be written as

$$F(s_1,s_2,m^2) = \frac{\phi_1(s_1,m^2)}{D_1(s_1)} + \frac{\phi_2(s_2,m^2)}{D_2(s_2)} \qquad (2)$$

The first term on the right hand side of eqn.(2) corresponds to the term of eqn.(1), and the second is the contribution from the other pair, (13); but in the isobar model for this simple case the functions ϕ_i are taken <u>to be independent</u> of s_i, $\phi_i(s_i,m^2) \approx C_i(m^2)$, as indicated by fig.3, whereas in eqn.(2) we are allowing a more general behaviour in the functions ϕ_i, <u>which will be determined from the constraint of sub-energy unitarity</u>. Let us consider then the constraint of two body unitarity in the (23) channel. This constraint may be written

as a discontinuity relation[2]:

$$F(s_{1+},s_2,m^2) - F(s_{1-},s_2,m^2)$$
$$= 2i\,\rho(s_1)\cdot\frac{1}{2}\int_{-1}^{1} dx_1\, F(s_{1+},s_2(s_1,x_1,m^2),m^2)\cdot M_1(s_{1-}) \qquad (3)$$

where +(-) means that the variable s_1 is taken above (below) the cut starting from the branch point at $s_1 = (m_2 + m_3)^2$, $\rho(s_1)$ is the phase space factor for the two body channel (23), $M_1(s_1)$ is the elastic (23) scattering amplitude, and x_1 is the angle between particle 1 particle 2 in the (23) c.m.s. The variable s_2 depends linearly on x_1 for fixed s_1 and m^2, and the x_1 integration can be viewed as a line on the s_1 - s_2 Dalitz plot, for fixed s_1 and m^2 - see fig.4. Eqn.(3) is illustrated in fig.5.

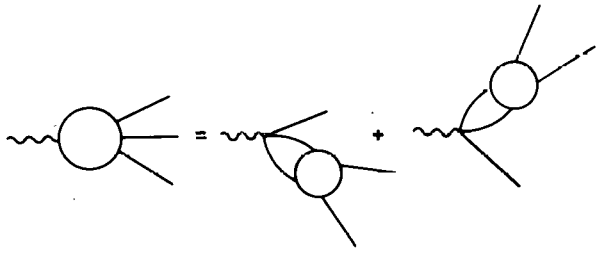

Fig.3 Isobar model approximation to the model amplitude $f(s_1,s_2,m^2)$.

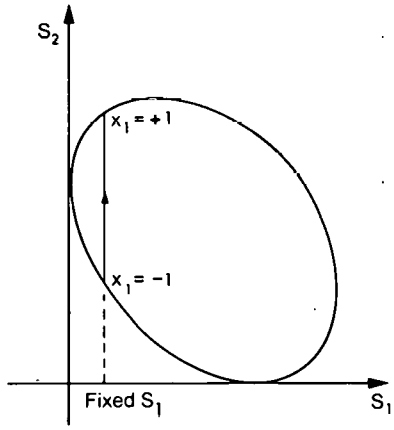

Fig.4 The x_1 integration in the discontinuity relation for F.

Relation (3) is the natural generalisation of the discontinuity relation for the elastic (23) amplitude,

$$M_1(s_{1+}) - M_1(s_{1-}) = 2i\,\rho(s_1)\,M_1(s_{1+})\,M_1(s_{1-}) \qquad (4)$$

pictured in fig.6. If this seems unfamiliar, note that $M_1(s_{1-}) = M_1^*(s_{1+})$ so that eqn.(4) is indeed equivalent to the ordinary relation $\mathrm{Im}(M_1) = \rho|M_1|^2$.

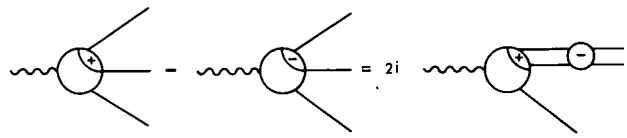

Fig.5 The discontinuity relation for F.

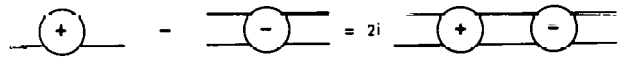

Fig.6 The discontinuity relation for the elastic two-particle amplitude M_1.

Let us now see if expression (2) satisfies eqn.(3). First note that if we write, as usual,

$$M_1(s_1) = N_1(s_1)/D_1(s_1) \qquad (5)$$

eqn.(4) implies that

$$D_1^{-1}(s_{1+}) - D_1^{-1}(s_{1-}) = 2i\,\rho(s_1)\,N_1(s_1)/(D_1(s_{1+})\,D_1(s_{1-})) \qquad (6)$$

From eqn.(2) we obtain

$$\begin{aligned} F(s_{1+},s_2,m^2) &= F(s_{1-},s_2,m^2) \\ &= \frac{\phi_1(s_{1+},m^2)}{D_1(s_{1+})} - \frac{\phi_1(s_{1-},m^2)}{D_1(s_{1-})} \\ &= \phi_1(s_{1+},m^2)\,(D_1^{-1}(s_{1+}) - D_1^{-1}(s_{1-})) \\ &\quad + D_1^{-1}(s_{1-})\,(\phi_1(s_{1+},m^2) - \phi_1(s_{1-},m^2)) \\ &= \frac{\phi_1(s_{1+},m^2)}{D_1(s_{1+})}\cdot\frac{2i\,\rho(s_1)\,N_1(s_1)}{D_1(s_{1-})} \\ &\quad + D_1^{-1}(s_{1-})\,(\phi_1(s_{1+},m^2) - \phi_1(s_{1-},m^2)) \\ &= \frac{\phi_1(s_{1+},m^2)}{D_1(s_{1+})}\cdot 2i\,\rho(s_1)\,M_1(s_{1-}) \\ &\quad + D_1^{-1}(s_{1-})\,(\phi_1(s_{1+},m^2) - \phi_1(s_{1-},m^2)) \end{aligned} \qquad (7)$$

On the other hand, eqn.(3) gives, using eqn.(2),

$$F(s_{1+},s_2,m^2) - F(s_{1-},s_2,m^2)$$

$$= 2i\,\rho(s_1)\cdot\frac{1}{2}\int_{-1}^{1} dx_1\, M_1(s_{1-}) \left[\frac{\phi_1(s_{1+},m^2)}{D_1(s_{1+})} + \frac{\phi_2(s_2,m^2)}{D_2(s_2)}\right] \qquad (8)$$

$$= \frac{\phi_1(s_{1+},m^2)}{D_1(s_{1+})}\cdot 2i\,\rho(s_1)\,M_1(s_{1-}) + 2i\,\rho(s_1)\,M_1(s_{1-}) \cdot\frac{1}{2}\int_{-1}^{1} dx_1\,\phi_2(s_2,m^2)/D_2(s_2)$$

Comparing (8) with (7) we deduce the fundamental relation[3]

$$\phi_1(s_{1+},m^2) - \phi_1(s_{1-},m^2) = 2i\,\rho(s_1)\,N_1(s_1)\cdot\frac{1}{2}\int_{-1}^{1} dx_1\,\frac{\phi_2(s_2,m^2)}{D_2(s_2)} \qquad (9)$$

A similar relation holds for ϕ_2.

Eqn.(9) shows immediately that <u>the ϕ functions have non-zero discontinuities across the normal threshold sub-energy cuts</u> - that is, they are <u>not</u> regular functions of their sub-energy variables, but rather have branch points at the sub-energy thresholds, and discontinuities given by eqn.(9) across the associated cuts. Yet in the isobar model (for this simple case) they are approximated by functions which are <u>independent</u> of the sub-energy variables, $\phi_i(s_1,m^2) \quad C_i(m^2)$. This is one good reason why the isobar model is open to criticism, particularly if the <u>phase</u> of the ϕ_i functions is important, as in the analysis of three hadron decays, since functions with a branch point have a habit of developing a varying phase.

A typical term responsible for the cut in ϕ_1 is shown in fig.7. This shows a "first rescattering correction to the isobar model", in which the pair (13) is first produced with amplitude C_2, particle 3 then interacting finally with particle 2. Such a process has a normal threshold branch point in s_1 associated with elastic two body intermediate states in the final amplitude M_1, as indicated by the dotted line labelled (1); this branch point is taken care of by the factor D_1^{-1} in (2). But there is <u>also</u> a branch point associated with the two body intermediate state corresponding to the dotted line labelled (2), and it is intuitively clear that the contribution from these latter states involves the amplitude in the s_2 channel, as in eqn.(9)

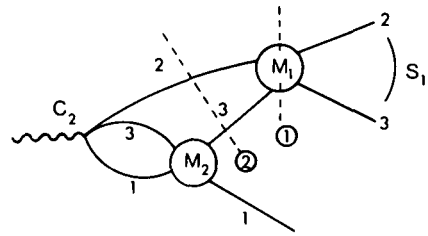

Fig.7 First rescattering correction to the isobar approximation, showing the branch point associated with elastic scattering (cut (1)) and the branch point associated with rescattering (cut (2)).

We now turn to the question of how to implement the requirement (9).

2. IMPLEMENTATION OF THE SUB-ENERGY UNITARITY REQUIREMENT

(a) <u>The K-matrix method</u>

By considering the contribution of graphs like fig.7, one can see that the integral term in eqn.(9) does <u>not</u> have the normal threshold branch point at $s_1 = (m_2 + m_3)^2$; neither, by definition, does $N_1(s_1)$. But, of course, the phase space factor $\rho(s_1)$ does, since it is proportional to

$$\{[s_1 - (m_2 + m_3)^2][s_1 - (m_2 - m_3)^2]\}^{1/2}/s_1^{1/2} \qquad (10)$$

- in fact, $\rho(s_1)$ has a square root branch point at $s_1 = (m_2 + m_3)^2$. Now the discontinuity of the function $z^{1/2}$ across the cut $z > 0$ is simply $2z^{1/2}$; hence one <u>minimal</u> way of satisfying eqn.(9) is to take

$\phi_1(s_1,m^2) =$

function with no branch point at $s_1 = (m_2 + m_3)^2$

$$+ i\,\rho(s_1)\,N_1(s_1)\cdot\frac{1}{2}\int_{-1}^{1} dx_1\,\frac{\phi_2(s_2,m^2)}{D_2(s_2)} \qquad (11)$$

The first term on the RHS of eqn.(10) is of course not determined by the relation (9) since its discontinuity vanishes. Dividing eqn.(11) by $D_1(s_1)$ we therefore find that the function $\phi_1(s_1,m^2)/D_1(s_1)$ which enters into eqn.(2) for the complete decay

amplitude is given by

$$\frac{\phi_1(s_1,m^2)}{D_1(s_1)} = \frac{C_1}{D_1(s_1)} + i\,\rho(s_1)\,M_1(s_1)\cdot\frac{1}{2}\int_{-1}^{1} dx_1\ \frac{\phi_2(s_2,m^2)}{D_2(s_2)} \qquad (12)$$

where C_1 has no sub-energy cut in s_1; there is a similar equation for ϕ_2/D_2. We may immediately identify the first term on the RHS of eqn.(12) with the isobar model, in which $C_1 = C_1(m^2)$, while the second term embodies the rescattering corrections. If we introduce the functions

$$\Phi_i(s_i,m^2) \equiv \phi_i(s_i,m^2)/D_i(s_i) \qquad i = 1,2$$

we have two coupled integral equations for the Φ_i, of the form

$$\Phi_1 = C_1/D_1 + \int_1^1 k_{12}\,\Phi_2\,dx_1$$
$$\Phi_2 = C_2/D_2 + \int_{-1}^{1} k_{21}\,\Phi_1\,dx_2 \qquad (13)$$

where k_{ij} are certain kernel functions. The complete amplitude F is then $\Phi_1 + \Phi_2$, which does satisfy the sub-energy unitarity constraint (9) (and the analogous one for the s_2 cut).

This method of implementing eqn.(9) may be understood simply, as follows, by considering an analogous procedure carried out on the elastic amplitude $M_1(s_1)$. From eqn.(4) we obtain

$$M_1^{-1}(s_{1+}) - M_1^{-1}(s_{1-}) = -2i\,\rho(s_1) \qquad (14)$$

which can be very simply satisfied by taking (c.f. eqn.(9) and (11))

$$M_1^{-1}(s_1) = K_1^{-1}(s_1) - i\,\rho(s_1) \qquad (15)$$

where K_1 is a function which is free of the normal threshold branch cut in s_1. But eqn.(15) is simply the relation between the K-matrix K_1 and the scattering amplitude M_1. We suspect then that eqn.(12) can be derived by generalising the idea of the K-matrix to a decay process, and this is indeed the case.

To see this, consider the amplitude for a particle of mass m to scatter from a particle of mass m_1 so as to produce two particles of masses m_2, m_3 in the final state, where $m < m_1 + m_2 + m_3$; this is illustrated in fig.8. The requirement of elastic unitarity in the (23) channel is satisfied[4] by the decomposition shown in fig.9, where intermediate lines are put on shell, the amplitude =□= is just the elastic (23) K-matrix, and the amplitude =□= is free of the normal threshold branch point in s_1.

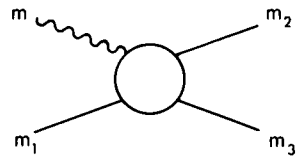

Fig.8 The amplitude for the process $m + m_1 \to m_2 + m_3$.

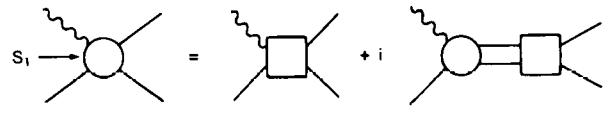

Fig.9 The K-matrix decomposition for the amplitude of fig.8.

Now increase m so that it ends up greater than $m_1 + m_2 + m_3$: in that case we are in the decay situation, and fig.9 becomes fig.10, where we have included two terms in the RHS, one for each of the interacting pairs of our model. It can be shown[5] that this decomposition leaves ~□≡ free of normal threshold branch points in each of the sub-energy variables s_1, s_2. Figure 10 is clearly an integral equation for the decay amplitude, which can be given content once ~□≡ is specified. The first detailed treatment of this integral equation, by Taha[5], proposed that ~□≡ should be taken to be a constant, but Graves-Morris pointed out[6] that this leads to a difficulty in the case of resonances in the final state, the decay amplitude developing zeros at the resonance positions. A more sensible choice is to take[7]

$$\sim\!\square\!\equiv = C_1(m^2)\,K_1(s_1) + C_2(m^2)\,K_2(s_2) \qquad (16)$$

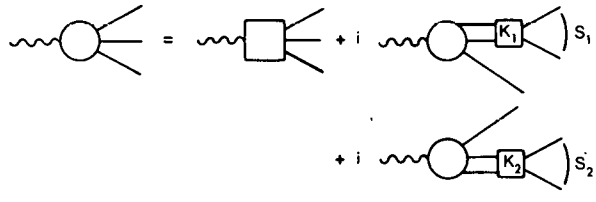

Fig.10 The K-matrix decomposition for the decay amplitude.

since then the resonance poles in the K's cancel the unphysical zeros. The K's, we repeat, do not have the normal threshold branch point, and so eqn.(16) is a perfectly legitimate choice for ~□≡ . Inserting eqn.(16) into fig.10 one obtains F in the form of eqn.(2) with the ϕ's obeying precisely eqn.(12), or (13).

This approach has been recently applied by Ascoli and Wyld[8], and independently by Goradia et al[8], to the $A_1 \to 3\pi$ problem. We shall discuss the results of their calculations in Section 3 below. First, we present an alternative way to implement eqn.(9).

(b) Dispersion relation method

We assume that ϕ_1 is an analytic function of s_1 except for the normal threshold branch point at $s_1 = (m_2 + m_3)^2$, from which extends the cut $s_1 \geq (m_2 + m_3)^2$; the discontinuity across this cut is given by (9). If ϕ_1 tends to zero at infinity as $1/s_1$ or faster, we can then write a dispersion relation for ϕ_1:

$$\phi_1(s_1,m^2) = \text{function free of the cut } s_1 \geq (m_2 + m_3)^2 + \frac{1}{2\pi i}\int_{(m_2+m_3)^2}^{\infty} ds_1' \,[\phi_1(s_{1+}',m^2) - \phi_1(s_{1-}',m^2)]/(s_1' - s_1 - i\,\varepsilon) \qquad (17)$$

When we insert eqn.(9) in eqn.(17) we obtain again an integral equation for ϕ_1, the inhomogeneous term being, as in eqn.(12), identified with the amplitude $C_1(m^2)$. Equation (17) embodies both unitarity and analyticity.

We note that, using $1/(x_1' - x_1 - i\,\varepsilon)$ = principal value $(1/(x' - x)) + i\,\pi\,\delta(x' - x)$ eqn.(17) reduces precisely to eqn.(12) with the addition of "off-energy shell" contributions associated with the principal value integral; these contributions are required by analyticity. Equation (17) was first derived[9] starting from the Khuri-Treiman representation for a decay amplitude[10]; but since that representation is also based simply on sub-energy unitarity and analyticity the present approach is equivalent.

(c) Theoretical remarks on the comparison between the K-matrix and dispersion relation approaches.

(i) K-matrix methods are well-adapted to parametrising an amplitude in an economical way so as to incorporate unitarity constraints; they tend not to be so suitable for unitarising a given dynamical input. For instance, in the case of the elastic (23) amplitude $M_1(s_1)$, suppose we were given the function $N_1(s_1)$. One way of generating a unitary $M_1(s_1)$ would be to write

$$M_1(s_1) = N_1(s_1)/(1 - i\,N_1(s_1)\,\rho(s_1)) \qquad (18)$$

which identifies N_1 with the K-matrix K_1. However, if we use analyticity, we write $M_1 = N_1/D_1$ and obtain a dispersion relation for D_1,

$$D_1(s_1) = 1 - \frac{1}{\pi}\int_{(m_2+m_3)^2}^{\infty} \rho(s_1')\,\frac{N_1(s_1')\,ds_1'}{(s_1' - s_1 - i\,\varepsilon)} \qquad (19)$$

taking $D_1 \to 1$ at infinity. Again, the on-shell part of (19) agrees with the denominator of (18), but there are principal value additions. From (19) and (17) we see that in general the dispersion relation method integrates over the discontinuity; this has a smoothing effect, which means, conversely, that if we take only the on-shell contributions (as in a K-matrix unitarisation) we shall tend to get an amplitude which has some unwanted rapid variation. Indeed, there are singularities (in the s_i variables) in the functions ϕ_i generated by eqns.(13) which are not present in the perturbation theory diagrams of the form of fig.7[11]. The singularities of the ϕ_i satisfying equations of the type (17), however, agree with perturbation theory. This point may be relevant to an understanding of the rather disappointing results of Ascoli and Wyld[8], as we shall see in Section 3.

(ii) However, the dispersion relation method apparently leads to an integral equation that has two integrations, which is a substantially tougher numerical proposition than the single variable integral equation (12). Fortunately, this difficulty can be overcome analytically; it is possible to transform eqn.(17) into an equation involving only a single integration[9]:

$$\Phi_1(s_1,m^2) = \frac{G(m^2)}{D_1(s_1)} + \frac{1}{D_1(s_1)}\int_{-\alpha}^{(m-m_2)^2} \Delta_{12}(s_1,m^2,s_2')\,\Phi_2(s_2',m^2)\,ds_2' \qquad (20)$$

where Δ_{12} is a certain kernel function[12]. We have used $\Phi_1 = \phi_1/D_1$ as before, and Φ_2 satisfies a similar equation with $1 \leftrightarrow 2$.

The equation (20) has an interesting non-relativistic limit[9]: it reduces precisely to the Faddeev equations appropriate to the problem of final state interactions among three particles interacting via δ-function forces. Thus it has a potential theory analogue.

(iii) On the other hand, the range of integration in (20) is infinite, while that in (12) is finite; and, more seriously, the kernel function Δ_{12} is singular on the boundary of the Dalitz plot for the variables $s_1 - s_2'$ (and similarly for Δ_{21}). This is a numerical analysis problem, experience in dealing with which has been obtained in other three body problems[13].

(iv) Finally, we allude here to something we shall take up again in Section 4: the fact that eqn.(20) has a potential theory analogue leads us to suspect that the amplitudes ϕ_i may even satisfy unitarity in the three particle channel also, since, of course, unitarity is built in to the Schrödinger equation (with real potentials). This is indeed the case[14], in a certain sense, as we shall see in Section 4. The three particle → three particle amplitude that is implicitly contained in eqn.(20) is simply the sum of all pair-wise scatterings, as illustrated in fig.11. On the other hand, while amplitudes generated by eqns.(13) also formally satisfy three body discontinuity relations, the 3 → 3 amplitude implicit in eqns.(13) has all internal particle propagators in fig.11 replaced by δ-functions (since, in a K-matrix approach, internal lines are always on-shell). This is a somewhat pathological amplitude, which is a cause for worry, particularly since in the applications of current interest it is precisely the variation of the amplitudes as a function of the three body mass m that is of interest.

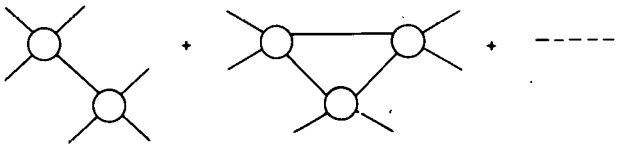

Fig.11 The pairwise scattering contribution to the connected 3 → 3 amplitude.

Having said all this, however, I would not like my partiality for eqn.(20) to detract from the very considerable effort made by Ascoli and Wyld[8], and Goradia et al[8], using eqns.(13); to this work we now turn, since it is, at the very least, a most useful first step in applying unitarity corrections to the isobar model.

3. APPLICATION OF THE K-MATRIX SUB-ENERGY UNITARISATION APPROACH TO THE A_1 PROBLEM

The A_1 is a broad enhancement observed in the 3π mass distribution, just above the ρπ threshold, in reactions $\pi N \to 3\pi N$. Consider in particular the reaction

$$\pi^- p \to \pi^+\pi^-\pi^- p \qquad (21)$$

The enhancement is predominantly in the $J^P = 1^+$ state. Let us label the π^+ as particle 3, and the two identical π^-'s as 1 and 2; the complete decay amplitude must then be symmetrical under $1 \leftrightarrow 2$. In the notation of Section 1, we are concerned with amplitudes $T^J_{LS}(s_1,s_2,m^2)$ where J = 1, and L and S are as defined in Section 1. In order not to introduce too much complexity at the start, we follow Goradia et al[8] and consider only two possible dimeson states: the ε meson (T = 0, S = 0) and the ρ meson (T = 1, S = 1). The former couples with the third pion to $J^P = 1^+$ by having L = 1, the latter has L = 0. The T = 2 interaction in the $\pi^-\pi^-$ channel (s_3) is neglected, as is the f meson, and the L = 2 coupling of the ρπ system.

The structure of the integral equations describing the rescattering corrections can be arrived at by considering the possible types of process which contribute. We focus attention on all rescattering processes which end in an interaction between particles 2 and 3: these will correspond to the term $\phi_1(s_1,m^2)/D_1(s_1)$ of eqn.(2), except that here since both the ε and ρ states enter, we shall have both $\phi_\varepsilon/D_\varepsilon$ and ϕ_ρ/D_ρ to consider. Such processes will be multiplied by appropriate angle-dependent functions $Z^{J^P=1^+}_{\rho \text{ or } \varepsilon}$, and the full amplitude obtained by symmetrisation. Clearly, the first two terms are as shown in fig.12(a) and 12(b), which are the usual isobar model terms,

$$\phi_\varepsilon(s_1,m^2) = C_\varepsilon(m^2), \qquad \phi_\rho(s_1,m^2) = C_\rho(m^2).$$

The first rescattering corrections to the ε channel (i.e. to ϕ_ε) are shown in figs.12(c) and (d), and we see that they involve integrations over both a ρ re-

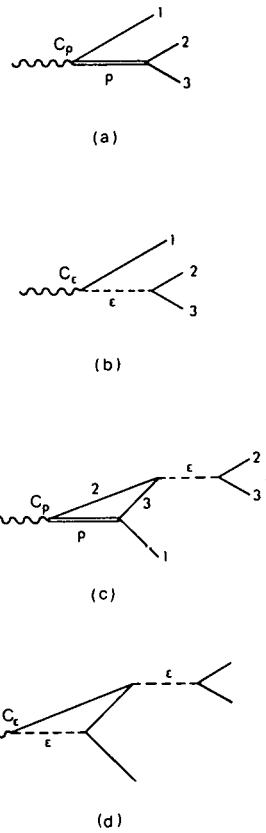

Fig. 12 Terms contributing to ϕ_ε and ϕ_ρ. (a) Isobar model term in ϕ_ε. (b) Isobar model term in ϕ_ρ. (c) and (d):- First rescattering corrections in ϕ_ε.

sonance and an ε state in the (13) channel; similarly the corrections to ϕ_ρ involve both ρ and ε in the parallel channel. Thus the equations for ϕ_ρ and ϕ_ε are coupled, and have the structure (c.f. eqns. (12) and (13)

$$\left.\begin{aligned}\phi_\varepsilon(s_1,m^2) &= C_\varepsilon(m^2) + \int \frac{k_{\varepsilon\varepsilon}\,\phi_\varepsilon}{D_\varepsilon} + \int \frac{k_{\varepsilon\rho}\,\phi_\rho}{D_\rho}\\ \phi_\rho(s_1,m^2) &= C_\rho(m^2) + \int \frac{k_{\rho\varepsilon}\,\phi_\varepsilon}{D_\varepsilon} + \int \frac{k_{\rho\rho}\,\phi_\rho}{D_\rho}\end{aligned}\right\} \qquad (22)$$

or $\quad \phi_i = C_i + \sum_{j=\varepsilon,\rho} K_{ij}\,\phi_j, \quad (i,j = \varepsilon,\rho),$

where K_{ij} is an integral operator.

Equations (22) may be solved by replacing the integrations by sums over a discrete mesh, so that they become matrix equations, which may be inverted.

Goradia et al[8] call the inverse matrix $\underline{\underline{H}}(s_1,m^2)$ and write the solution as

$$\begin{pmatrix}\phi_\varepsilon(s_1,m^2)\\ \phi_\rho(s_1,m^2)\end{pmatrix} = \begin{pmatrix}H_{\varepsilon\varepsilon}(s_1,m^2) & H_{\varepsilon\rho}(s_1,m^2)\\ H_{\rho\varepsilon}(s_1,m^2) & H_{\rho\rho}(s_1,m^2)\end{pmatrix}\begin{pmatrix}C_\varepsilon(m^2)\\ C_\rho(m^2)\end{pmatrix} \qquad (23)$$

The amplitude in the (23) channel for $A_1 \to \pi\rho$ is then proportional to $\phi_\rho/D_\rho = (C_\varepsilon H_{\rho\varepsilon} + C_\rho H_{\rho\rho})/D_\rho$ and similarly for $A_1 \to \pi\varepsilon$. In the isobar model, there would only be the graphs of figs. 12(a) and 12(b), and we should have $H_{\rho\varepsilon} = H_{\varepsilon\rho} = 0$, $H_{\varepsilon\varepsilon} = H_{\rho\rho} = 1$. Deviations from these values will therefore be a measure of the effect of the rescattering corrections. Figure 13, taken from Goradia et al[8] shows the real and imaginary parts of $\underline{\underline{H}}$ as a function of $s_1 (\equiv s_{\pi\pi})$ for various values of $m^2 (\equiv W)$, taking the T = 0 s-wave π-π scattering length (in the ε channel) to be $a_0^0 = 0.58\ m_\pi^{-1}$. Note that $H_{\rho\varepsilon}$ and $H_{\rho\rho}$ both appear multiplied by D_ρ^{-1}, which peaks at $s_1 \approx 0.6$ GeV^2, while $H_{\varepsilon\rho}$ and $H_{\varepsilon\varepsilon}$ are multiplied by D_ε^{-1} which is large for $0.4\ \text{GeV}^2 \lesssim s_1 \lesssim 1\ \text{GeV}^2$. Figure 13 shows that in the regions of interest deviations from the isobar approximation, as calculated by this K-matrix method, are quite substantial, in both magnitude and phase; the corrections are functions with a strong dependence on both s_1 and m^2.

These calculations therefore cast doubt on the results of analyses which claim to extract m^2-dependence of complex quantities such as C_ε, C_ρ by using the isobar model. What one should do, presumably, is a re-analysis of the data using the functions ϕ_ε, ϕ_ρ which include rescattering corrections. This is what Ascoli and Wyld[8] have done. For this purpose, however, eqns. (22) as they stand are not at all suitable; the reason is that the C_i's are fitting parameters, and thus if we use eqns. (22) we have different equations to solve each time we search on new values of the C_i's! We can, of course, use the matrix $\underline{\underline{H}}$ following Goradia et al[8], since this depends only on the two-body parameters (which are input) and not on the C_i. An alternative, due to Ascoli and Wyld[8], will be convenient in discussing three-body unitarity, so we shall describe it now.

To understand the basic point, imagine writing down the full amplitude for $J^P = 1^+$ to go to 3π, including just the $\rho\pi(L = 0)$ and $\varepsilon\pi(L = 1)$ states; it will have the form

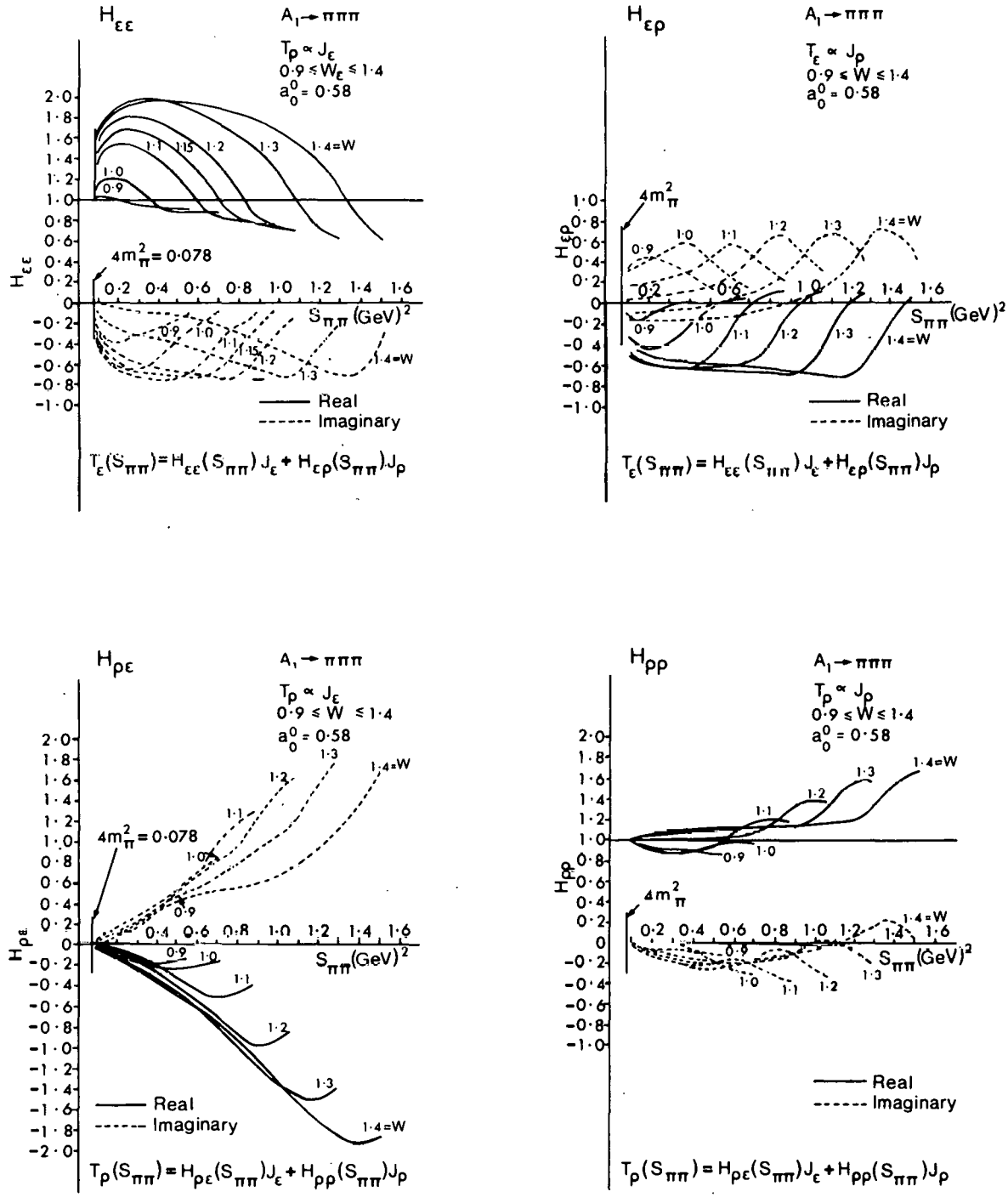

Fig. 13 The real and imaginary parts of the overlap matrix $\underline{H}$ of Goruda et al[8] as a function of $s_1 (\equiv s_{\pi\pi})$, for various values of the three particle mass $m (\equiv W)$. The $T = 0$ S-wave π–π scattering length is taken to be $a_0^0 = 0.58\ m_\pi^{-1}$.

$$\frac{\phi_\varepsilon(s_1,m^2)}{D_\varepsilon(s_1)}\ Z^{1+}_{L=1,S=0}\ (\text{angles}) \tag{24}$$

$$+\ \frac{\phi_\rho(s_1,m^2)}{D_\rho(s_1)}\ Z^{1+}_{L=0,S=1}\ (\text{angles})\ +\ (1 \leftrightarrow 2)$$

where

$$\left.\begin{aligned}\phi_\varepsilon &= C_\varepsilon + \int K_{\varepsilon\varepsilon}\,\phi_\varepsilon + \int K_{\varepsilon\rho}\,\phi_\rho\\ \phi_\rho &= C_\rho + \int K_{\rho\varepsilon}\,\phi_\varepsilon + \int K_{\rho\rho}\,\phi_\rho\end{aligned}\right\} \tag{25}$$

Now in eqn.(24) there will appear, as we see by iterating (25), a collection of terms multiplying C_ε and another collection multiplying C_ρ. If we can obtain equations directly for these quantities which multiply C_ε and C_ρ we shall be able to do the fitting quite simply in terms of these quantities and the C_i's.

If we iterate eqn.(25) we find that they can be rewritten as follows:

$$\left.\begin{aligned}\phi_\varepsilon &= C_\varepsilon\,\phi_{\varepsilon\varepsilon} + C_\rho\,\phi_{\varepsilon\rho}\\ \phi_\rho &= C_\varepsilon\,\phi_{\rho\varepsilon} + C_\rho\,\phi_{\rho\rho}\end{aligned}\right\} \tag{26}$$

where

$$\left.\begin{aligned}\phi_{\varepsilon\varepsilon} &= 1 + \int K_{\varepsilon\varepsilon}\,\phi_{\varepsilon\varepsilon} + \int K_{\varepsilon\rho}\,\phi_{\rho\varepsilon}\\ \phi_{\rho\varepsilon} &= \int K_{\rho\varepsilon}\,\phi_{\varepsilon\varepsilon} + \int K_{\rho\rho}\,\phi_{\rho\varepsilon}\end{aligned}\right\} \tag{27}$$

and

$$\left.\begin{aligned}\phi_{\varepsilon\rho} &= \int K_{\varepsilon\rho}\,\phi_{\rho\rho} + \int K_{\varepsilon\varepsilon}\,\phi_{\varepsilon\rho}\\ \phi_{\rho\rho} &= 1 + \int K_{\rho\rho}\,\phi_{\rho\rho} + \int K_{\rho\varepsilon}\,\phi_{\varepsilon\rho}\end{aligned}\right\} \tag{28}$$

We have introduced four new functions $\phi_{ij}(i,j = \varepsilon,\rho)$ whose physical meaning is as follows: ϕ_{ij}/D_i is the amplitude for producing resonance i in the final state given that resonance j was produced at the beginning of the rescattering chain. Naturally, then, $\phi_{\varepsilon\varepsilon}$ and $\phi_{\rho\varepsilon}$ go with the production amplitude C_ε while $\phi_{\varepsilon\rho}$ and $\phi_{\rho\rho}$ go with C_ρ. This way of writing the corrections focuses attention on the first interaction rather than on the last, since for the purposes of fitting to data it is the initial amplitudes C_i that are the important variable parameters. A typical term in $\phi_{\rho\varepsilon}$ is shown in fig.14(a), and one in $\phi_{\varepsilon\varepsilon}$ is shown in fig.14(b). The general amplitude $\phi_{\rho\varepsilon}$, for example, is shown in fig.14(c).

The full amplitude in $J^P = 1^+$ is now, symbolically,

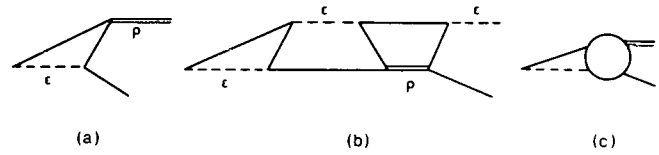

Fig.14 (a) A term in $\phi_{\rho\varepsilon}$. (b) A term in $\phi_{\varepsilon\varepsilon}$. (c) The general amplitude $\phi_{\rho\varepsilon}$.

$$C_\varepsilon^{1+}\left(\frac{\phi_{\varepsilon\varepsilon}}{D_\varepsilon}\ Z_\varepsilon^{1+} + \frac{\phi_{\rho\varepsilon}}{D_\rho}\ Z_\rho^{1+}\right) + C_\rho^{1+}\left(\frac{\phi_{\varepsilon\rho}}{D_\varepsilon}\ Z_\varepsilon^{1+} + \frac{\phi_{\rho\rho}}{D_\rho}\ Z_\rho^{1+}\right) \tag{29}$$

$$+\ (1 \leftrightarrow 2)$$

The quantity (29) is now in a form suitable for fitting to data since the ϕ_{ij}'s are independent of the C_i's and are determined by the two body input. In the isobar model, $\phi_{ij} = \delta_{ij}$ simply.

Ascoli and Wyld[8] have set up the equations analogous to (27) and (28), and solved them, retaining five amplitudes:

$\varepsilon\pi$ L = 1, $\rho\pi$ L = 0, $\rho\pi$ L = 2, $f\pi$ L = 1, $f\pi$ L = 3.

(We are implicitly absorbing kinematic barrier factors into the C_i whereas Ascoli and Wyld[8] retain them in (27) and (28)). In the region of the A_1, only the first two are important. Unfortunately, the only results of the work of Ascoli and Wyld that I am in possession of are those presented at the 1974 Meson Spectroscopy Conference. They reported as follows. Firstly, for m ∿ 1.1 GeV the amplitudes ϕ_{ij}, as a function of the $\pi\pi$ sub-energy, deviated quite markedly from the isobar model values, especially for the case of $\phi_{\rho\varepsilon}$ (as Goradia et al[8] found). Secondly, Ascoli and Wyld used the functions ϕ_{ij} in a refit to their data, and found that the fits were significantly worsened. Figure 15 shows the difference between the χ^2 values obtained using the unitarised amplitudes ϕ_{ij} and the non-unitarised isobar amplitudes. This is undoubtedly a very disappointing result, after a lot of hard work. There is one interesting feature of the unitarised fits, however; in both the $J^P = 0^-$ and 1^+ cases, Ascoli and Wyld reported that the unitarised fits required more of both $\varepsilon\pi$ and $\rho\pi$ waves than the non-unitarised fits. The data, on the other hand, does not require much

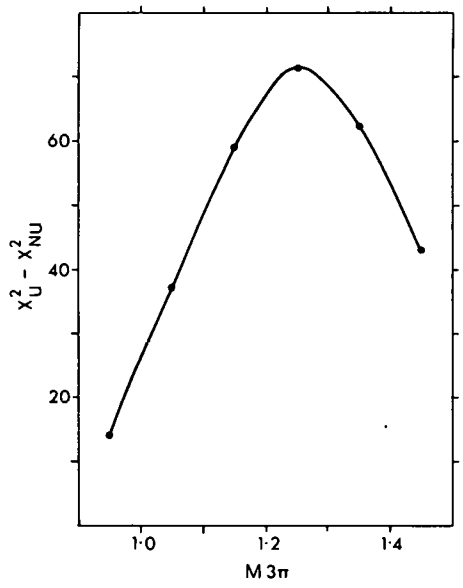

Fig. 15 The difference in X^2 values, as given by Ascoli and Wyld[8], obtained in fitting the A_1 data using the unitarised amplitudes ϕ_{ij} and the non-unitarised isobar amplitudes.

επ in the final state. Thus, they say, what is happening is that the rescattering from ρπ to επ produces more επ in the final state than there is in the data: the fitting procedure then arranges to cancel this excess επ off by including a large επ production amplitude C_ε, with the phases conspiring suitably. It finds this a hard job, so the X^2 is worse, presumably. They suggest that the trouble may be that the ρπ → επ rescattering is <u>too</u> strong. As we remarked in Section 2(c)(i), the K-matrix unitarisation method is likely to produce more rapid variations, in general, than a dispersion relation approach, which involves a further integration. Clearly the next thing to try, I believe, is the dispersion relation integral equations, analogous to eqn.(20), for this case. A student at Oxford, Richard Golding, is now working on these equations. If, when <u>these</u> functions are used, the fit is <u>still</u> worse, I shall be worried!

4. WHY THE ISOBAR MODEL NEEDS TO BE CORRECTED (2): THREE BODY UNITARITY

We have emphasised so far the fact that the isobar model does not satisfy the sub-energy (two body) discontinuity relations, and we have seen how to make it do so by means of the correction functions ϕ, which satisfy certain integral equations (K-matrix or dispersion-theoretic). This is only one aspect of the physical problem of three hadron decays, however. <u>What about unitarity in the three body channel, m^2</u>? We might, for instance, worry that our corrections ϕ violate three body unitarity - they do after all introduce a strong m^2 dependence, as we have seen - in which case their phenomenological use would be suspect; also, the isobar model itself does not manifestly satisfy three body unitarity, yet in the applications we are here considering it <u>is</u> the three body channel that we are really interested in.

In fact, the situation with regard to three body unitarity and the functions ϕ is a rather happy one. Consider what corrections the integral equations sum up: they are all pairwise rescatterings, as shown in fig.16 (reverting to the model of Sections 1 and 2). We might well expect that, because all these processes involve three meson intermediate states in the m^2 channel (cut them vertically by lines such as (1)), they do include at least <u>some</u> three body effects already - namely, as much of the full 3 meson → 3 meson amplitude as is given by pairwise interactions of the form of fig.11. And indeed this

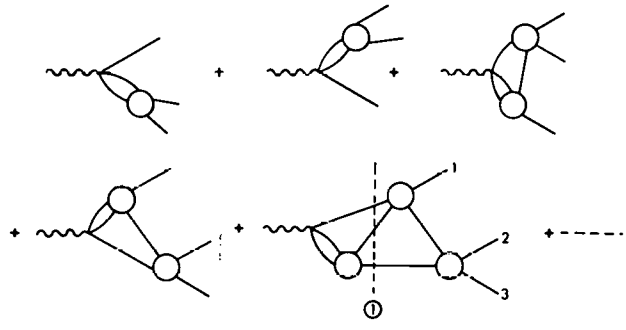

Fig. 16 Pairwise rescattering term in an amplitude ϕ showing the three-meson intermediate state cut, (1).

is so: it can be shown[14] that the integral eqns. (20), and the analogous one with 1 ↔ 2, <u>with C_i independent of m^2</u>, do define a decay amplitude $F = \Phi_1 + \Phi_2$ satisfying the three body discontinuity relation pictured in fig.17, with the 3 → 3 amplitude being composed of the series in fig.11[15]. In other words, the constraint of three body unitarity is satisfied by such amplitudes F even if the production amplitudes C_i are independent of m^2.

Just the same would also be true of the F generated from the K-matrix equations (13), but in this case the 3 → 3 amplitude, as we mentioned in

Fig.17 Three-body discontinuity relation for the decay amplitude.

Section 2(c)(iv), has all intermediate particles on shell i.e. it contains a lot of δ-functions, and is thus unphysical.

Before proceeding further, we follow the steps leading from (25) to (28) working this time with the Φ's where $\Phi_i = \phi_i/D_i$, and with the dispersion equations (20). We find, for the simple model of Section 2, that $F = \Phi_1 + \Phi_2$ where

$$\left.\begin{aligned}\Phi_1(s_1,m^2) &= C_1(m^2)\ \Phi_{11}(s_1,m^2) + C_2(m^2)\ \Phi_{12}(s_1,m^2)\\ \Phi_2(s_2,m^2) &= C_2(m^2)\ \Phi_{22}(s_2,m^2) + C_1(m^2)\ \Phi_{21}(s_2,m^2)\end{aligned}\right\} \quad (30)$$

and where $\Phi_{ij}(s_i,m^2)$ is the amplitude for ending in a scattering between the i^{th} pair having begun with a scattering between the j^{th} pair; the Φ_{ij}'s satisfy

$$\left.\begin{aligned}\Phi_{11}(s_1,m^2) &= \frac{1}{D_1(s_1)} + \frac{1}{D_1(s_1)} \int_{-\infty}^{(m-m_2)^2} ds_2'\ \Delta_{12}(s_1,m^2,s_2')\ \Phi_{21}(s_2',m^2)\\ \Phi_{21}(s_2,m^2) &= \frac{1}{D_2(s_2)} \int_{-\infty}^{(m-m_1)^2} ds_1'\ \Delta_{21}(s_2,m^2,s_1')\ \Phi_{11}(s_1',m^2)\end{aligned}\right\} \quad (31)$$

$$\left.\begin{aligned}\Phi_{12}(s_1,m^2) &= \frac{1}{D_1(s_1)} \int_{-\infty}^{(m-m_2)^2} ds_2'\ \Delta_{12}(s_1,m^2,s_2')\ \Phi_{22}(s_2',m^2)\\ \Phi_{22}(s_2,m^2) &= \frac{1}{D_2(s_2)} + \frac{1}{D_2(s_2)} \int_{-\infty}^{(m-m_1)^2} ds_1'\ \Delta_{21}(s_2,m^2,s_1')\ \Phi_{12}(s_1',m^2)\end{aligned}\right\} \quad (32)$$

The Φ_{ij}'s have the resonance propagator D_i^{-1} included, so we illustrate a typical term in Φ_{11}, for example, by fig.18. We therefore have, in this model,

$$\begin{aligned}F(s_1,s_2,m^2) &= C_1(m^2)[\Phi_{11}(s_1,m^2) + \Phi_{21}(s_2,m^2)]\\ &\quad + C_2(m^2)[\Phi_{12}(s_1,m^2) + \Phi_{22}(s_2,m^2)]\end{aligned} \quad (33)$$

with which we can compare eqn.(29). The Φ_{ij}'s are determined again by the input two body parameters, and can be computed once and for all; the C_i's are the fitting parameters. The m^2 dependence in the Φ's is such as to guarantee three body unitarity in the sense described, so that the functions $C_i(m^2)$ are not required by three body unitarity to vary in m^2.

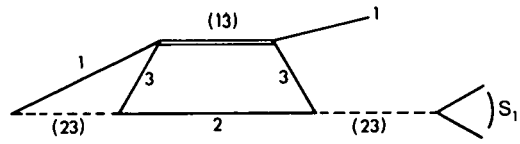

Fig.18 Typical term in Φ_{11}.

What is the implication of this for the analysis of three hadron decays? Suppose, for the sake of argument, that one sets up equations like (31) and (32) for the $J^P = 1^+ \to \varepsilon\pi$, $\rho\pi$ system, and that one discovered an m^2 dependence in the Φ_{ij}'s that was resonance-like around the A_1 mass. This would say that the A_1 system was generated by rescattering effects among the επ, ρπ channels. Indeed, just this result is tentatively claimed by Pasquier in recent work[16]. Now, the original analysis of Ascoli et al[17] showed that if the decay amplitude is parametrised as in the non-unitarised isobar model then the production amplitudes $C^{J^P = 1^+}$ have a rather slow phase variation in m^2, which is not characteristic of a resonance. Thus if Pasquier's result is right, and there is a pronounced m^2 - dependent phase variation in the Φ's, it must somehow get washed out by a compensating correction coming from the s_i dependence of the Φ's (which also, of course, differs from the isobar model). It is difficult to see how this might happen, and we shall just have to await the results of calculations based on eqns.(31) and (32).

There is a further possibility to be considered also. The pairwise interactions of fig.11 are not the only

possible three body interactions; for example, a process such as fig.19(a) is not included in any term of fig.11. Figure 19(a) is a contributor to a whole class of diagrams depicted by fig.19(b), which contains all $\rho\pi$ interactions other than the pairwise rescattering ones. Amplitudes such as fig.19(b) will possess a three body cut. Now, we have seen that our decay amplitudes C_i could be taken to have no three body (m^2) cut insofar as the $3\pi \to 3\pi$ amplitude is given purely by the pairwise rescatterings. This suggests that any three body cut in the C_i's will be related to the rest of the $3\pi \to 3\pi$ amplitude i.e. to amplitudes such as fig.19(b).

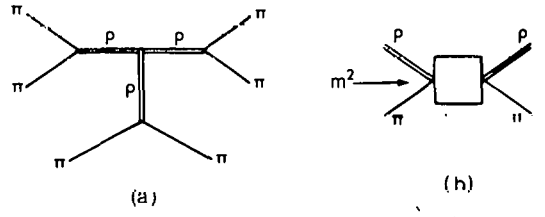

Fig. 19 (a) Example of a $\rho\pi$ interaction which is not contained in any one of the pairwise rescattering series.
(b) General $\rho\pi$ amplitude including everything except the rescattering graphs.

The way to formalize this is indicated by some recent and very interesting work by Gustafson[18]; he works with a non-relativistic, and static, model, but the integral equations we are dealing with are the natural generalisation of his dynamical framework. Referring to eqn.(33), let us define

$$\left.\begin{aligned}\psi_1(s_1,s_2,m^2) &\equiv \Phi_{11}(s_1,m^2) + \Phi_{21}(s_2,m^2)\\ \psi_2(s_1,s_2,m^2) &\equiv \Phi_{12}(s_1,m^2) + \Phi_{22}(s_2,m^2)\end{aligned}\right\} \qquad (34)$$

so that $F = C_1\,\psi_1 + C_2\,\psi_2$: the ψ_i's are the quantities which multiply the production parameters C_i. It may be shown[19] that

$$\psi_1(s_1,s_2,m^2) = \frac{1}{D_1(s_1)} + \int_{-\infty}^{(m-m_1)^2} ds_1'\,\Psi^r_{11}(s_1,m^2,s_1') + \int_{-\infty}^{(m-m_1)^2} ds_1'\,\Psi^r_{21}(s_2,m^2,s_1') \qquad (35)$$

and similarly for $\psi_2(s_1,s_2,m^2)$, where Ψ^r_{ij} is the connected three particle → three particle amplitude generated by pairwise scatterings which begin with pair j and end with pair i. The form of eqn.(35) is easy to understand: whereas the decomposition $F = \Phi_1 + \Phi_2$ focuses attention on the last rescattering, the decomposition $F = C_1\,\psi_1 + C_2\,\psi_2$ focuses on the first scattering, which goes with the amplitudes C_i. Thus ψ_1 receives contributions from graphs which begin with a (23) interaction and end with a (23) interaction - i.e. Ψ_{11} - and from graphs which begin with a (23) interaction but end with a (13) interaction, i.e. Ψ_{21}. The reason for the s_1' integrations in eqn.(35) is simply that the ψ functions contain contributions of the form shown in fig.18, which clearly involves an integration of a Ψ_{11} amplitude over the first sub-energy variable. We may represent ψ_1 and ψ_2 pictorially by figs.20(a) and 20(b).

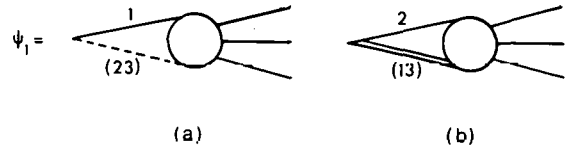

Fig. 20 (a) Diagrammatic representation of the function ψ_1, which sums up all pairwise rescatterings beginning with an interaction between the pair (23).
(b) Diagrammatic representation of ψ_2.

The form of eqn.(35), and the analogous one with $1 \leftrightarrow 2$, is now convenient for investigating three body unitarity. Following the idea of Gustafson[18], we write the full three particle → three particle amplitude, in this simple model, as

$$\Psi(s_1',s_2',m^2,s_1,s_2) = \Psi^r_{11} + \Psi^r_{21} + \Psi^r_{12} + \Psi^r_{22} + \Psi^{int} \qquad (36)$$

where Ψ^{int} is the "intrinsic" three body part, not contained in the pairwise contributions Ψ^r_{ij}. We now assume that Ψ^{int} may be approximated in "unitarised isobar form" as

$$\Psi^{int} = \sum_{i,j=1}^{2} \psi_i(s_1',s_2',m^2)\,A_{ij}(m^2)\,\psi_j(s_1,s_2,m^2) \qquad (37)$$

where $A_{ij}(m^2)$ is the "intrinsic" amplitude for isobar j to scatter off the third particle producing isobar i and a third particle. The approximation lies in neglecting the sub-energy dependence of the A_{ij} - all the sub-energy cuts being in the ψ_i. In a simple isobar model, the ψ_i in eqn.(37) would be replaced by their first order contributions, D_i^{-1} (c.f. eqn.(35)). A term $\psi_1\,A_{12}\,\psi_2$ from (37) corres-

ponds to the diagram of fig.21. Eqn.(37) is the natural extension of the decomposition $F = C_1 \psi_1 + C_2 \psi_2$ to the three particle → three particle case: the ψ's in eqn.(37) will guarantee sub-energy unitarity and three body unitarity in the pairwise rescattering approximation. We expect that the three body discontinuity of the $C_i(m^2)$ functions will be related to the "intrinsic" isobar amplitudes $A_{ij}(m^2)$.

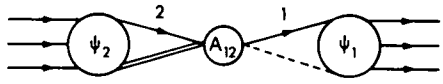

Fig.21 The 'unitarised isobar ansatz' for the 'intrinsic' 3 → 3 amplitude ψ_{12}^{int}

This turns out to be so. Applying the m^2 - discontinuity relation shown in fig.17, with the decay amplitude given by $\sum_{i=1}^{2} C_i \psi_i$ and the three particle → three particle amplitude given by eqns.(36) and (37), one finds the following discontinuity relations for the $C_i(m^2)$ across the three body cut:

$$C_i(m_+^2) - C_i(m_-^2) = 2i \sum_{j,k=1}^{2} A_{ik}(m_+^2)\, \rho_{k_j}(m^2)\, C_j(m_-^2) \qquad (38)$$

where (with appropriate normalisations)

$$\rho_{ij}(m^2) = \iint \psi_{i+}(s_1,s_2,m^2)\, \psi_{j-}(s_1,s_2,m^2)\, ds_1\, ds_2 \qquad (39)$$

the integration being over the Dalitz plot for the decay. Similarly, applying the same idea to the three particle → three particle amplitude itself, one finds

$$A_{ij}(m_+^2) - A_{ij}(m_-^2) = 2i \sum_{k,\ell} A_{ik}(m_+^2)\, \rho_{k\ell}(m^2)\, A_{\ell_j}(m_-^2) \qquad (40)$$

Relations (38) and (40) are very similar to ordinary coupled channel two body discontinuity relations: eqn.(38) is similar to a discontinuity relation for a final state interaction problem involving two coupled "two-body" channels, labelled 1 and 2, while eqn.(39) is similar to a discontinuity relation for the coupled "two-body" amplitudes themselves. The only noteworthy difference is the presence of off-diagonal terms in the phase space matrix ρ_{ij}.

Such terms are in fact easy to understand. Consider the lowest order contribution to $\rho_{12}(m^2)$ say: in eqn.(39) we replace $\psi_{1+}(s_1,s_2,m^2)$ by $D_1^{-1}(s_1)$ and $\psi_{2-}(s_1,s_2,m^2)$ by $D_2^{-1*}(s_2)$ and integrate over the Dalitz plot. This produces a diagram shown in fig.22(a), the dotted line symbolizing the three body phase space integration over s_1,s_2. This is a "bubble graph", which is singular in the physical region when m^2 is above the threshold for producing isobars 1 and 2, since the decays and recombinations are then allowed physically; that is, the three particles in the intermediate state exposed by the dotted line cut can all be on-shell, which is the signal that this process contributes to a phase-space term. The general form of ρ_{12} is shown in fig.22(b). Such off-diagonal phase space terms appear to have been discussed first by Mandelstam et al[20]: our work complements theirs by including all sub-energy unitarity effects as well, via the functions ψ_i.

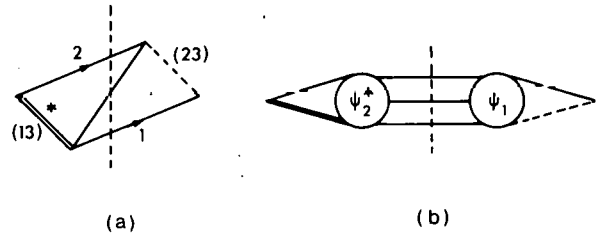

Fig.22 (a) Lowest order contribution to the off-diagonal phase space element ρ_{12}. *(b) General term in* ρ_{12}.

One can now take up the implementation of eqns.(38) and (40)! Once again we have a choice of methods; we can apply a K-matrix technique, or use dispersion relations. Note, however, that this time we are operating in the m^2 (three body channel) and not in the s_i (sub-energy) channels. The K-matrix technique would be similar to the usual many-channel many-resonance formalism[21], with the difference that the generalised phase space ρ_{ij} must be used. Such a K-matrix formalism was used by the SLAC - Berkeley group[22] in their analysis of the phases of baryon resonances decaying to $\pi\Delta$ and ρN. In this work, however, the full functions ψ_i were not used: instead $\psi_i(s_i,s_j,m^2)$ was replaced by the simple isobar denominator $D_i^{-1}(s_i)$ - that is, the amplitudes

failed to satisfy sub-energy unitarity, though they did satisfy three body unitarity.

Gustafson himself has used discontinuity relations of the form of eqns.(38) and (40) to write dispersion relations which provide a dynamical scheme for generating baryon resonances in $\pi N \to \pi N$, and $\pi N \to \pi\pi N$[23]. The results are really rather encouraging. Equally, the coupled scheme of eqns.(38) and (40) could be put into dispersion relations for the final state interaction problem. In such an approach, of course, as in any dynamical scheme, one will have to make assumptions about the forces which drive the amplitudes A_{ij}. We would here be moving away from phenomenological analysis towards a dynamical theory. Perhaps the best approach for the f.s.i. problem would be to start with a K-matrix parametrisation of both eqns.(38) and (40), after the style of ref.(22); after this one could perhaps try using a K-matrix parametrisation for the A_{ij} while feeding eqn.(38) into a dispersion relation (in m^2) for the $C_i(m^2)$. In either case, one will then have a general parametrisation which embodies correctly three body unitarity (both for the pairwise rescattering contributions and for the intrinsic three body part), as well as sub-energy unitarity.

5. CONCLUSIONS

I shall sum up with what I think is the present state of our theoretical understanding of the analysis of three hadron final states, using the simple model I introduced in Section 2. The decay amplitude $F(s_1,s_2,m^2)$ may be written as

$$F(s_1,s_2,m^2) = C_1(m^2)\ \psi_1(s_1,s_2,m^2) + C_2(m^2)\ \psi_2(s_1,s_2,m^2) \qquad (41)$$

where the ψ_i functions sum up all pairwise rescatterings starting with pair i. Such a representation satisfies all the requirements of sub-energy unitarity, and could be used for numerical work in fitting data, since the ψ_i's are determined solely from input two-body amplitudes. It also satisfies three body unitarity if the C_i's are taken to be constant (or, more generally, without the three body cut in m^2), provided the three particle → three particle amplitude is given purely by pairwise scattering terms. If one wishes to include other three body processes, still within the general framework of the isobar model, one can introduce "intrinsic" isobar scattering amplitudes A_{ij}; the functions C_i then have a three body cut in m^2, their discontinuities across which are related to the A_{ij}. The A_{ij} themselves also satisfy quite simple discontinuity relations across the three body cut. These m^2 discontinuity relations can be implemented in a phenomenological way by a K-matrix parametrisation, or, used in dispersion relations, as the basis of a dynamical model of the three body system.

We have moved a long way from the simple isobar model in which the ψ_i are just the isobar enhancement factors D_i^{-1}. That model is in principle inadequate because of three body effects. The representation (41) distinguishes between two different three body effects. The ψ_i factors sum up all pairwise rescatterings among the three particles, and could have quite strong dependences on m^2 and on the sub-energy variables. There is no reason *a priori* to think that the s_i dependence in the ψ's factorises from the m^2 dependence, so that the latter might be incorporated into the $C_i(m^2)$ to give back something which resembles the factorised form of the isobar model. In addition to this three body effect, the $C_i(m^2)$ can also acquire a cut in m^2 associated with intrinsic (non pairwise) three body scattering. It is even conceivable that these two different m^2 dependences could conspire to average out to something slowly varying! There is a lot of work to be done.

REFERENCES

1. We neglect any simultaneous dependence on the variables s_1 and s_2. This amounts to assuming that the two body interactions in the final state occur in only a finite number (in practice, small) of partial waves. See R.F.Peierls and J.Tarski, Phys. Rev. 129, (1963) 981; and G.Bonnevay, Nuovo Cim. 30, (1963) 1325. See also R.Pasquier and J.Y.Pasquier, Phys. Rev. 170, (1968) 1294, especially footnote 18.

2. R.J. Eden, P.V. Landshoff, D.I. Olive and J.C. Polkinghorne, The Analytic S-Matrix (Cambridge, C.U.P., 1966) 232.

3. Our derivation is inspired by that of R.Aaron and R.D.Amado, Phys. Rev. Letts. 31, (1973) 1157, who first emphasised the importance of this result in the analysis of three hadron final states. An early reference for the necessity of having recoupling (or rescattering) terms in order to satisfy the two body discontinuity relations is:- G.N. Fleming, Phys. Rev. 135B, (1964) 551.

4. See ref.2, p.231.

5. M.O.Taha, Nuovo Cim. 42A, (1966) 201.

6. P.R.Graves-Morris, Nuovo Cim. 50A, (1967) 681.

7. This is the generalisation of the choice recommended in I.J.R.Aitchison, Nucl. Phys. A189, (1972) 417; it is used by Y.Goradia, T.Lasinski, M.Tabak and G.Smadja in their work on the unitarised isobar model for 3π systems (preliminary version); see also G.Smadja, LBL-382 (unpublished): It is also used by G.Ascoli and H.W.Wyld (preliminary version, Illinois; and talk presented by G. Ascoli at the 4th Int. Conf. on Experimental Meson Spectroscopy, Boston, 1974, APS No.21).

8. Cited in ref.7.

9. I.J.R.Aitchison, Phys. Rev. 137, (1965) B1070.

10. N.N.Khuri and S.B.Treiman, Phys. Rev. 119, (1960) 1115.

11. I.J.R.Aitchison, Nuovo Cim. 51A, (1967) 249.

12. For simplicity we suppress here other kernels whose support is $-\infty \leq s'_2 \leq 0$.

13. J.H.Hetherington and L.H.Schick, Phys. Rev. 135, (1965) B935; I.J.R.Aitchison, Cavendish Laboratory preprint, June 1966 (unpublished); K.M.Watson and J.Nuttall, Topics in Several Particle Dynamics (San Francisco, Holden-Day, 1967); R.T.Cahill and I.H.Sloan, Proc. First Int. Conf. on the Three Body Problem in Nuclear and Particle Physics, 1969 (Amsterdam, North-Holland, 1970) p.265.

14. I.J.R.Aitchison and R.Pasquier, Phys. Rev. 152, (1966) 1274.

15. We are glossing over the question of the symmetry of $3 \to 3$ amplitude. See R.Pasquier and J.Y.Pasquier, Phys. Rev. 170, (1968) 1294.

16. R.Pasquier, Thèse, Université Paris-Sud, Centre d'Orsay, 1973.

17. Yu.M.Antipov et al, Nucl. Phys. B63, (1973) 153.

18. G.Gustafson, Nucl. Phys. B63, (1973) 325.

19. This result is a simple extension of eqn.(20) of ref.14. See also Appendix B of the work cited in ref.15.

20. S.Mandelstam, J.E.Paton, R.F.Peierls and A.Q.Sarker, Ann. Phys. 18, (1962) 198.

21. I.J.R.Aitchison, Nucl. Phys. A189, (1972) 417.

22. R.J.Cashmore, contribution to the 14th Scottish Universities Summer School in Physics, 1973; D.Herndon, P.Söding and R.J.Cashmore, LBL-543 (1973); A.H.Rosenfeld et al, SLAC-PUB-1386 (1974); R.J.Cashmore et al, SLAC-PUB-1387 (1974); R.S.Longacre et al, SLAC-PUB-1390 (1974); see also R.S.Longacre, Thesis, University of California, Berkeley, LBL-948 (1973).

23. G.Gustafson, Nucl. Phys. B63, (1973) 347; Nucl. Phys. B66, (1973) 182; and other references cited in these articles.

THIS PAGE

WAS INTENTIONALLY

LEFT BLANK

RE-ARRANGEMENT EFFECTS IN THREE-BODY FINAL STATES

by

D. Morgan
Rutherford Laboratory

A21

The question of re-scattering corrections is a lurking uncertainty in the discussion and interpretation of isobar analyses of production processes[1]. Among other things, the apparent phase behaviour of three-body resonances will in general be modified by re-arrangement collisions in the final state. Are such effects significant, especially for problematic situations such as the $I = 1\ 1^+$ state of the 3π system?

A scheme is proposed for estimating these effects, on the lines of the Khuri-Treiman approximation, but with the integrations confined to the physical Dalitz plot. Although the quantities describing the resulting modifications of the isobar amplitudes are functions of the sub-energies, it is useful to introduce suitably averaged quantities (with the average over the Dalitz plot weighted according to the modulus squared of the final state interaction amplitude).

Invoking these averages suggests a simplified approximate version of the re-scattering equations in which all the functions appearing are replaced by their averages, reducing the equations to algebraic ones. The resulting averaged production amplitudes possess an extra re-arrangement phase in addition to their conventional quasi-two-body phase shift (this separation of phase contributions is not utterly without ambiguity but should be sustainable for short-range variations). The extra phase is calculable from the re-arrangement Born approximation. Calculations are in progress for the $I = 1\ 3\pi$ partial waves.

When the production process admits the same exchange as occurs in the 3 - 3 re-arrangement process, a grouping of contributions is found very similar to that described by Bowler and Game[2]. As with their work, additional phase modifications can arise if the production Born approximation is itself allowed to have a phase. The notion of Reggeised exchange contributions might seem to sanction such phases but it is difficult to see to what physical processes the resulting discontinuities correspond.

REFERENCES

1. See I.J.R. Aitchison's review in these proceedings.

2. M.G. Bowler and M.A.V. Game, Oxford University Preprint 38/74; see also M.G. Bowler's talk in these proceedings.

THIS PAGE

WAS INTENTIONALLY

LEFT BLANK

SESSION 6

Chairman: R.J. Cashmore

THE AXIAL VECTOR MESON CRISIS

Invited Talk

DIFFRACTIVE PRODUCTION OF RESONANCES AND THE DECK MECHANISM

M.G. Bowler
Nuclear Physics Laboratory, University of Oxford

Contributions

AN AMPLITUDE ANALYSIS FOR THE REACTION $\pi^+ p \to \pi^+\pi^-\pi^0\Delta^{++}$ AT 7 GeV/c

F. Wagner
Lawrence Berkeley Laboratory

A PARTIAL WAVE ANALYSIS OF THE 3π SYSTEM IN THE REACTION $\pi^+ d \to \pi^+\pi^-\pi^0 pp_s$

D.J. Crennell
Rutherford Laboratory

THIS PAGE

WAS INTENTIONALLY

LEFT BLANK

DIFFRACTIVE PRODUCTION OF RESONANCES AND THE DECK MECHANISM

by

M.G. Bowler
Nuclear Physics Laboratory, University of Oxford.

A21

1. INTRODUCTION

This paper is concerned with the singular properties of the amplitude $B\, e^{i\delta} \cos\delta + A/k \sin\delta\, e^{i\delta}$ where δ is a two body phase shift and B is a diffractive production amplitude of the Drell-Hiida-Deck kind. Operationally we characterize diffractive production by the following features:-

(1) No exchange of internal quantum numbers.
(2) Marked peripherality.
(3) Cross section only slowly falling as a function of incident energy.
(4) Relatively low mass for the diffractively produced systems.

We suppose the interaction leading to diffractive production to be mediated by the Pomeron which, whatever it may be, is responsible for the absorbtive part of elastic scattering, and hence associated with the Pomeron leg (see fig.1) is a phase factor of $\pi/2$. The blob representing what goes on between the absorbtion of the Pomeron at the production vertex and the explosion into particles may of course have associated with it additional internal phase factors. It is the internal structure of this blob that I am concerned with in this paper, in the specific reactions

$$\pi \to 3\pi$$
$$K \to K\pi\pi$$
$$N \to N\pi, \quad N\pi\pi$$

diffractively.

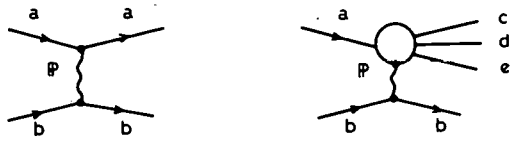

(a) (b)

Fig.1 (a) Absorbtive elastic scattering.
(b) Diffractive dissociation.

All these reactions have a large enhancement just above an appropriate threshold and for 10 years an argument has raged over whether such bumps are to be associated with diffractive production of resonances (fig.2(a)) or with the Deck effect (fig.2(b)). With small momentum transfer in both legs of fig.2(b) a low mass diffractive enhancement certainly results.

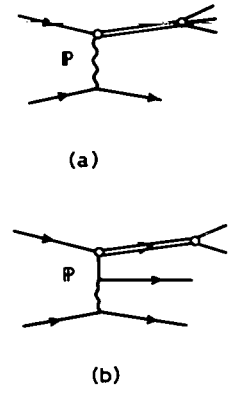

Fig.2 (a) Diffractive resonance production.
(b) The Deck mechanism.

It is important to understand what is going on not only to settle a detail of strong interaction dynamics but because $J^P = 1^+$ bumps in 3π and $K\pi\pi$ are the only candidates for some members of the families of 1^+ mesons that the quark model leads us to expect. The 3π (A_1) system has so far received the most attention and as everyone knows the situation has been revolutionised by the three particle PWA programs. The application of these programs to the 3π system produced without charge exchange has allowed the extraction not only of the intensity in each PW as a function of mass, but also has yielded the relative phases of the waves. The phase of the 2^+ $\rho\pi$ d-wave goes through 90° over the width of the A_2 resonance, but the relative phases of all other waves are only slowly varying - say $\lesssim 40^\circ$ over $\sim$ 500 MeV[1]. Ascoli and his collaborators have accounted successfully for surprisingly detailed features of the J^P structure of the A_1 enhancement with a Reggeised Deck model[2].

All this would seem to have settled the hash of the A_1. The 1^+ intensity does not have a Breit-Wigner shape, the phase variation is small, (whereas if there is a resonance we expect the 1^+ $\rho\pi$ amplitude to pick up a factor $e^{i\delta}$ through Watson's theorem, even if the resonance is not directly produced) and the Deck model explains an awful lot. I have been concerned to see whether, nonetheless, there could still be a real A_1 resonance, coupling more or less elastically to s-wave $\rho\pi$. The reasons for this attempt are

(1) Innate conservatism. I cannot believe that the enormously successful quark model could fail over such a detail.

(2) While the shape of 1^+ intensity does not look like a resonance, it doesn't look like a Deck effect either - in fig.3 I show the data with the highest statistical weight I know[3].

(3) The peculiar behaviour of the ratio of $K\rho$ to $K^*\pi$ in 1^+ $K\pi\pi$ - the ρ is produced preferentially around threshold, which argues for at least one resonance in the Q region[4].

(4) Misbehaviour of certain $\Delta\pi$ and $N\pi$ diffractive amplitudes, in a way very reminescent of the A_1[5,6]. In these channels we know where the resonances are.

The problem is to determine the properties of diffractive amplitudes when the Deck mechanism is important and there exists a resonance in the channel fed by the Deck mechanism.

2. RESCATTERING CORRECTIONS TO DECK AMPLITUDES

If there exists a resonance in the channel fed by the Deck effect, it is likely that this resonance can be produced directly in diffractive dissociation, implying the addition of both terms in fig.2. However, the existence of a resonance means that the Deck amplitude must be modified to take into account the effects of rescattering. Diagramatically there are three terms to be added, as shown in fig.4. Note that each of the three diagrams has its own internal blob phases. Suppose then, that we have a Deck amplitude B. How must this be modified for rescattering through an elastic phase shift δ?

We can rule out a form

$$B \to B\, e^{i\delta} \sin\delta$$

because if there is no rescattering we expect the unmodified Deck amplitude. I was led to consider the form

$$B \to B\, e^{i\delta} \cos\delta$$

for the result of the Deck amplitude plus rescattering and hence wrote for the full amplitude

$$F = B\, e^{i\delta} \cos\delta + \frac{A}{k} \sin\delta\, e^{i\delta} \qquad (1)$$

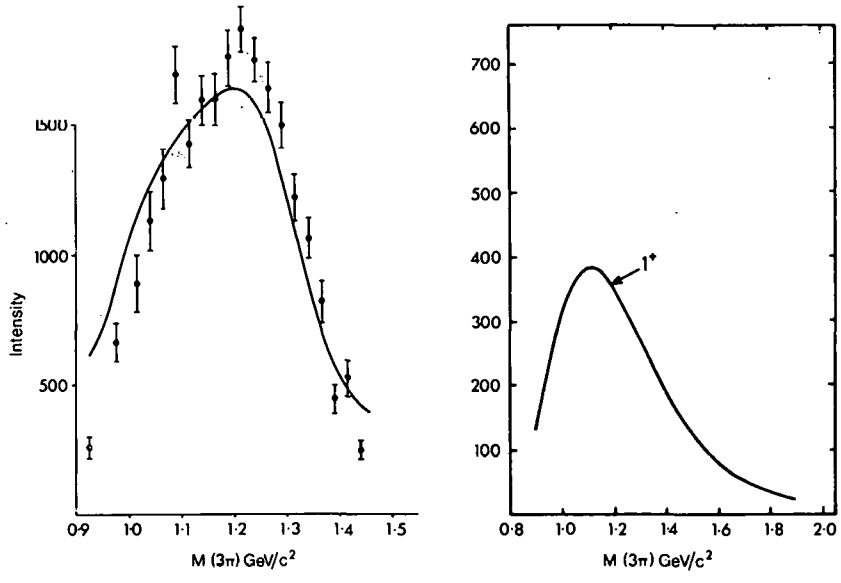

Fig.3 The data points on (a) give the 1^+s intensity extracted by Ascoli and Klanner from the combined 25 GeV/c and 40 GeV/c data of the CIBS collaboration. The curve through the points is the weighted sum of the curves obtained for the 25 GeV/c data and the 40 GeV/c data. (b) shows the 1^+ intensity calculated from the Ascoli Deck model.

where the second term represents the direct diagram of fig.4(c).

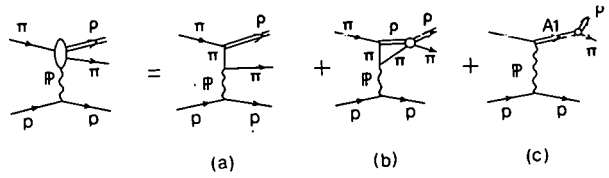

Fig.4 Diffractive ρπ production terms for a π exchange Deck background when a resonance exists in the 1^+ ρπ channel.

While the full amplitude can certainly be written in this form, the specific interpretation of B as the unmodified Deck amplitude is much more dubious. There are plenty of production processes where only terms in $e^{i\delta} \sin\delta$ contribute. However, this interpretation may be justified for the case of Deck-type amplitudes, which are characterized by a relatively narrow enhancement in the mass of the produced system, say ρπ. This means a relatively sharp peak in the relative momentum of the ρ and π: Fourier transforming into configuration space we have rescattering taking place with two diffuse waves passing through each other. This suggests that the correct thing to do is to multiply the Deck term B by the ρπ S-matrix rather than the T-matrix which is appropriate for a contact background (flat in momentum space). Thus

$$B \to B\, e^{2i\delta} = B \cos\delta\, e^{i\delta} + i\, B \sin\delta\, e^{i\delta}$$

The second term may be absorbed into the direct production term and is usually a small correction. The whole procedure has been justified within the context of conventional final state interaction theory using the Omnès equation. This is discussed in the Appendix.

While it is obvious that the expression (1) for F will yield intensities which look like neither a Deck mechanism nor a resonance, each term picks up a phase factor $e^{i\delta}$. Nonetheless, this expression does contain the possibility of a slowly varying overall phase. This may be seen by considering an extreme case. Suppose that

$$\frac{A}{k} \approx -i\, B$$

Then

$$F \to B(\cos\delta - i \sin\delta)e^{i\delta} = B$$

The condition which is necessary for phase suppression is that the intrinsic phases of A and B are not the same: and we have seen that there is no reason for them to be the same. Then

$$\phi_F = \delta + \tan^{-1}\left(\frac{\text{Im } B \cos\delta}{\text{Re } B \cos\delta + \frac{A}{k}\sin\delta}\right)$$

relative to the phase of A.

3. FITS TO A_1 DATA

We first confronted the model amplitude (1) with the extensive data obtained by the CIBS collaboration at 40 GeV/c. The theoretical intensity was compared with the 1^+ intensity extracted by Ascoli and Klanner using the Illinois PWA programme, and the theoretical phase with the 1^+s - 0^-s relative phase[7]. We assumed that the 0^-s phase and the phase of the 1^+s term B are constant, and gave B an exponential dependence on ρπ mass. The result of the

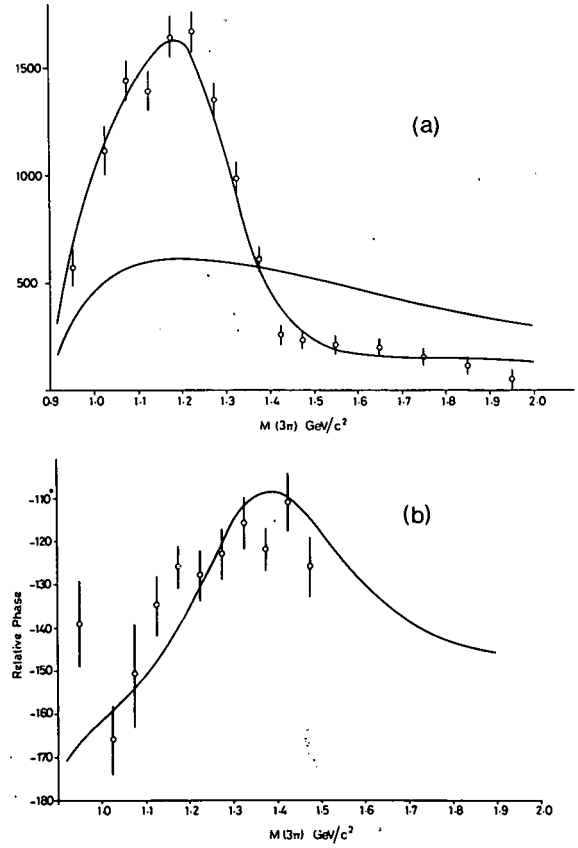

Fig.5 The first fit of the model to A_1 data. The data are from the 40 GeV/c CIBS spectrometer experiment. The Deck background was parametrised as an exponential in 3π mass with constant phase. (a) shows the intensity distribution: the lower curve shows $|B|^2 k$ where B is the fitted Deck background. (b) shows the phase of 1^+s relative to 0^-s; the fit was made under the assumption that the phase of 0^-s is constant.

fit is shown in fig.5: not only is the phase variation δ substantially suppressed, but the peculiar shape of the 1^+s intensity is incredibly well fitted, but with an A_1 mass of $\sim$ 1.3 rather than $\sim$ 1.1. There is a further interesting result: the intrinsic phase of B is $\approx 40^0$ ahead of the intrinsic phase of A. Now Ascoli and his collaborators have calculated the intrinsic phase of B: it is slowly varying and at a mass of $\sim$ 1.3 GeV/c^2 has a value $\sim 150^0$. Of this, $\approx 90^0$ may be attributed to the phase associated with the Pomeron leg of the Deck diagram: the extra 60^0 is claimed to be due to the signature factor of the Reggeised pion in the other leg of the Deck diagram[2]. Now we expect the intrinsic phase of A to be $\approx 90^0$, associated with the exchanged Pomeron and hence expect the intrinsic phase of B to be $\approx 60^0$ ahead of A - in astonishingly good agreement with the results obtained by fitting our model to the data[8].

In our subsequent work we have taken all the available diffractive A_1 data and fitted with a more elaborate model. First, we used the Omnès equation to calculate explicitly the contribution of rescattering to the term in sin δ. Secondly we used for the Deck terms the results of the Illinois Deck calculation, although we did not constrain the amount of 1^+s Deck amplitude. We fitted seven sets of data simultaneously: the quality of fit obtained is displayed for two sets in figs.6 and 7. The best we could achieve with Deck amplitudes only is shown in figs.8 and 9[9].

The Ascoli amplitudes, while not necessarily authenticated by the Almighty, are very reasonable things to use in view of their success in getting not only the relative amounts of different waves about right but also because they get a number of relative phases about right. Both these properties are due primarily to the signature factor of the Reggeised pion trajectory.

In an OPE model the dependence of the amplitude on the pion propagator is

$$\sim \frac{1}{t_R - m_\pi^2}$$

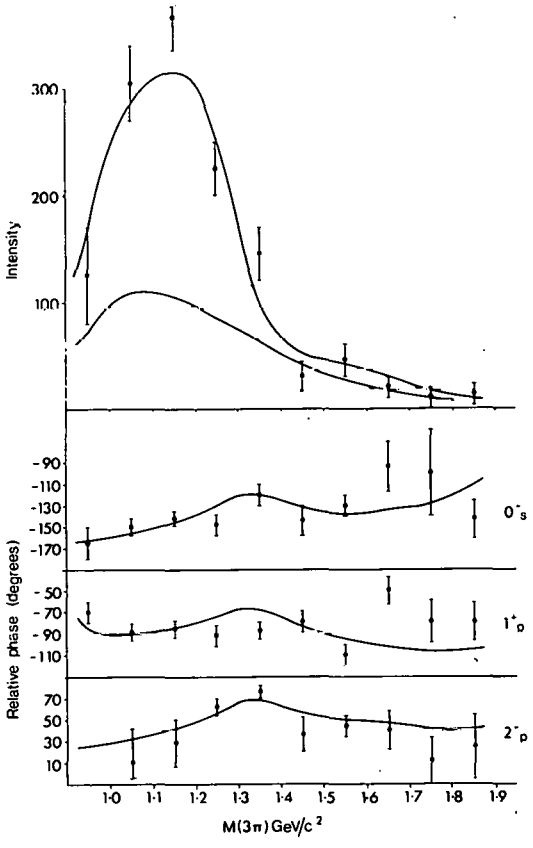

Fig.6 Comparison of the results of the full fit with the Ascoli compilation of 11 - 25 GeV/c π^- data.

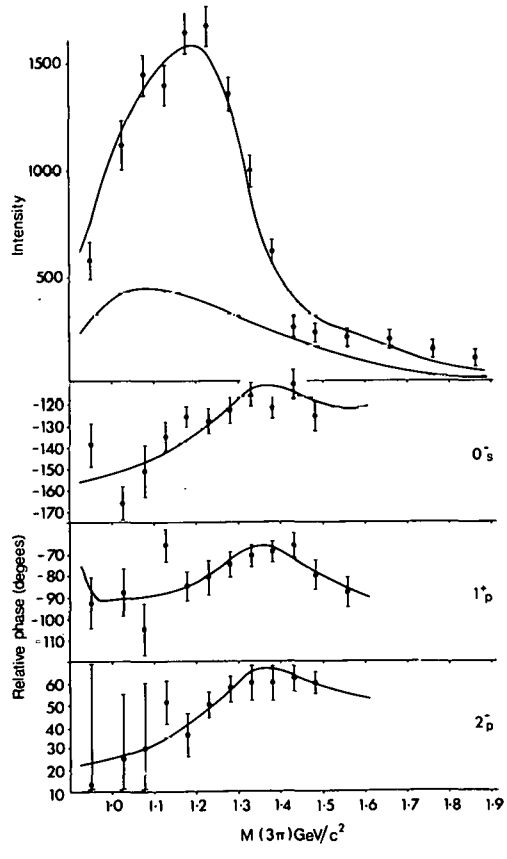

Fig.7 Comparison of the results of the full fit with the 40 GeV/c CIBS data.

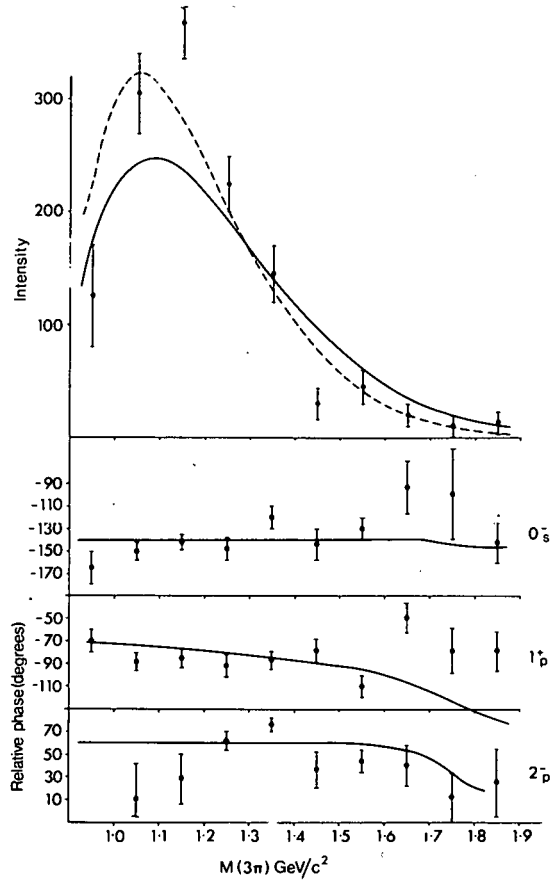

Fig.8 The best fits obtained with the parametrised Deck background alone, displayed for the Ascoli compilation. The solid intensity curve represents our best estimate of the background shape, the broken curve the best fit.

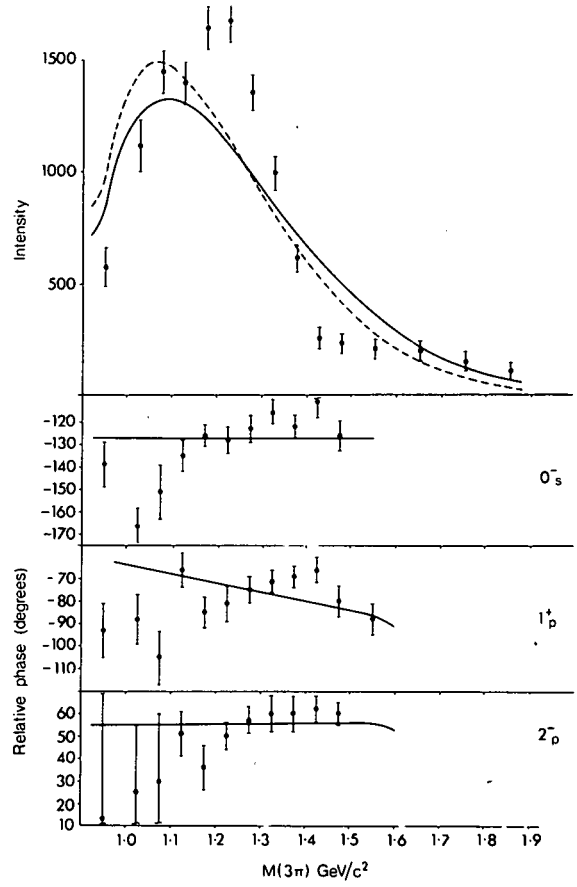

Fig.9 The best fits obtained with the parametrised Deck background alone, displayed for the Ascoli compilation. The solid intensity curve represents our best estimate of the background shape, the broken curve the best fit.

which is cancelled by a term at the πN vertex, leaving an amplitude that does not depend on t_R and hence does not depend on cos θ, where θ is the Jackson polar angle. With a Reggeised pion

$$\frac{1}{t_R - m_\pi^2} \to \frac{e^{-i\pi\alpha(t_R)/2}}{t_R - m_\pi^2}$$

so the amplitude depends on t_R through

$$e^{-i\pi\alpha(t_R)/2} \qquad \alpha \sim t_R = m_\pi^2 + M_{\pi\pi}^2 - 2E_{in}E_{\pi\pi} + 2p_{in}p_{\pi\pi}\cos\theta$$

where $E_{\pi\pi}$, $p_{\pi\pi}$ are the energy and momentum of the dipion system in the 3π centre-of-mass, E_{in} and p_{in} are the energy and momentum of incoming pion in the 3π centre-of-mass. The amplitude is thus like

$$e^{i\frac{\pi}{2}\{2E_{in}E_{\pi\pi} - m_\pi^2 - M_{\pi\pi}^2\}} \qquad e^{-i\pi p_{in}p_{\pi\pi}\cos\theta}$$

The first factor gives an overall phase which increases with $E_{3\pi}$. The second factor may be partial wave analyzed to give

$$\text{s-wave} \sim 1$$
$$\text{p-wave} \sim -i\pi p_{\pi\pi}p_{in}$$

This tells us in elementary terms why 1^+s and 0^-s are in phase and 90° different from 1^+p. The details could be changed, for example by including a form factor $e^{\alpha t_R}$, but the qualitative conclusions seem quite sound. However, we do need an explanation for the apparent lack of ρ exchange terms.

We conclude that the lack of 1^+ phase variation in diffractive production is no evidence against the

existence of a real A_1 meson, coupling elastically to $\rho\pi$, and that the shape of the observed 1^+ enhancement may be explained by virtue of such a meson provided it has mass and width

$$M_{A_1} \approx 1.3 \text{ GeV/c}^2$$

$$\Gamma_{A_1} \approx 250 \text{ MeV/c}^2$$

We have also concluded[9] that the diffractive data make it most unlikely that the A_1 has a mass of 1.1 GeV/c^2. Phase suppression can still be achieved, but the shape is quite wrong, (fig.10).

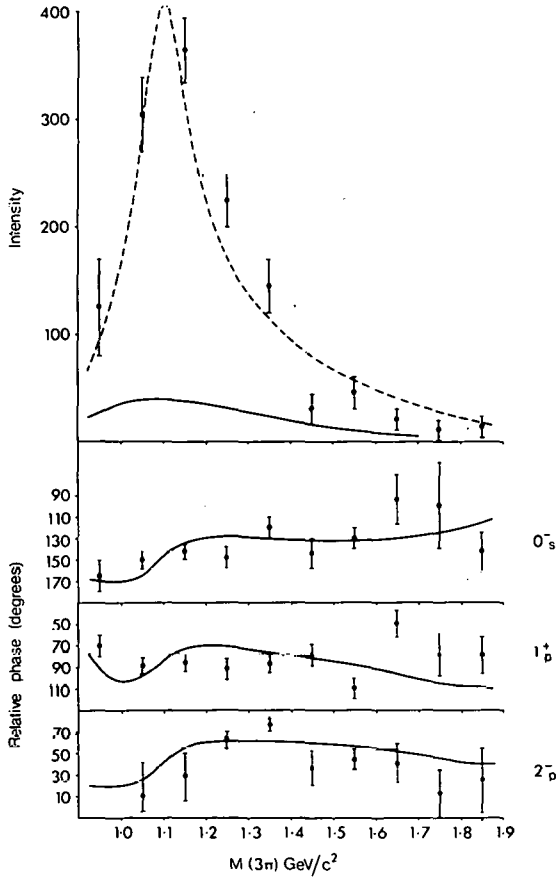

Fig. 10 (a) The best fit achieved with M_{A_1} = 1.1 GeV/c^2, for the Ascoli compilation data.

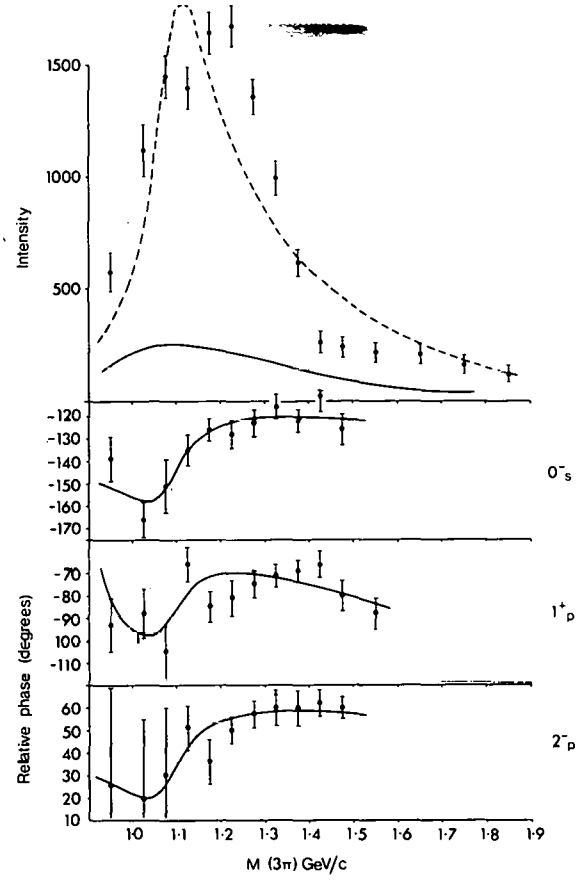

Fig. 10 (b) The best fit achieved with M_{A_1} = 1.1 GeV/c^2, for the CIBS 40 GeV/c data.

4. THE 1^+ K$\pi\pi$ SYSTEM (Q)

This is the analogue of the A_1 system, and is expected to be complicated if all the 1^+ states predicted by the quark model are realised in nature. There should be two strange 1^+ states in the mass region $\approx 1.3 - 1.4$ GeV/c^2, the strange analogues of the A_1 and the B. Breaking of SU3 can mix them and so the Q could consist of two diffractively produced resonances as well as Deck amplitudes for $K^*\pi$ and ρK, all these amplitudes coherent[4].

Two channel, two resonance analogues of the expression (1) can be written down through a K-matrix formulation[10] and the results of fitting them to K^+ data at 10 GeV/c[11] are shown in figs.11 and 12. The shape of the Q and the peculiar fact that ρK is only produced around threshold are well accounted for in this model[12]. A comparison of our calcu-

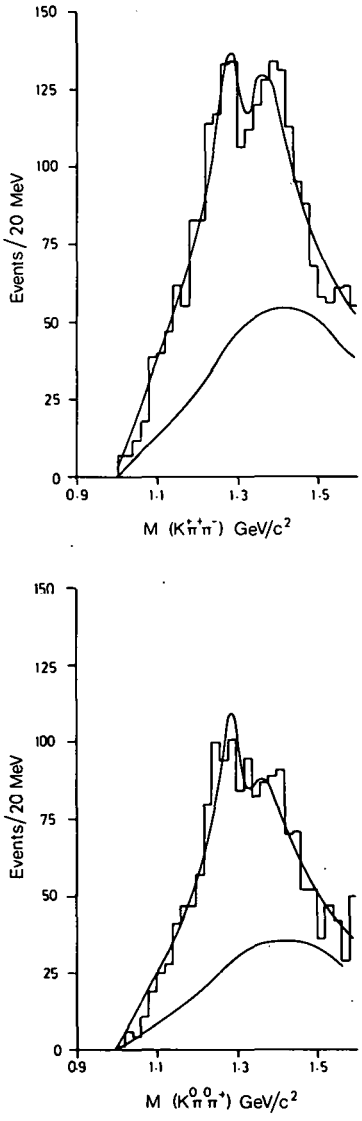

Fig. 11 The Kππ mass spectra obtained by fitting a two channel - two resonance model to the data of the BGO collaboration. The lower curve is the assumed background in waves other than 1^+

lated 1^+ intensity with the 1^+ intensity extracted by PWA of 10 and 16 GeV/c K^- data[13] is shown in fig.13: the agreement is excellent even at high mass where we are extrapolating our fitted K^+ amplitude.

We may conclude that the Q fits nicely into this framework, but the quality of the present data on the Q is not good enough for us to say more: we eagerly await results from the SLAC spectrometer which should resolve many questions about the Q.

It is amusing that with the A_1 at about 1.3 GeV/c^2 and the (unmixed) Q_A at about 1.34 GeV/c^2 we find

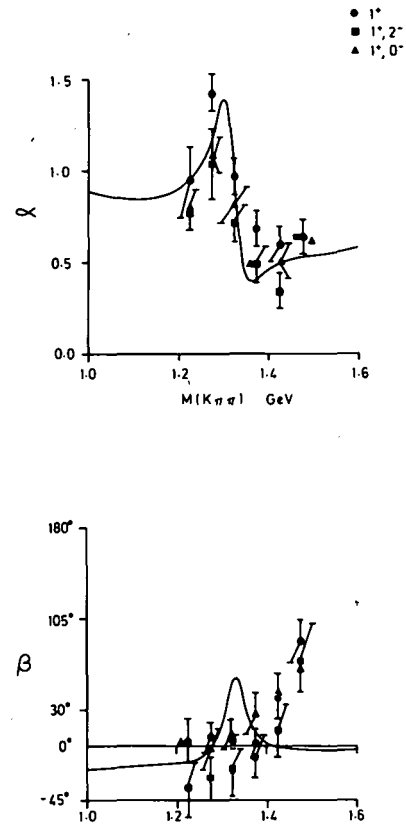

Fig. 12 The modulus (α) and phase (β) of the ρK amplitude relative to the $K^*\pi$ amplitude in the Q (10 GeV/c BGO data).

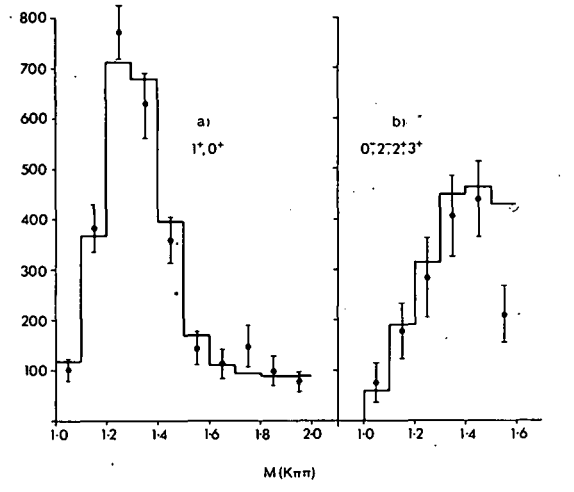

Fig. 13 (a) The 1^+ intensity extracted from the fits to the Q^+ at 10 GeV/c between 1.0 and 1.6 GeV/c is compared with the 1^+ intensity extracted from 10 and 16 GeV/c K^- data with the Ascoli program.

(b) The assumed background in fitting the 10 GeV/c K^+ data is compared with the intensity of waves other than 1^+s extracted by PWA of 10 and 16 GeV/c K^- data. Normalisation of (a) and (b) is common.

the D and E to be approximately ideally mixed - if the E really is the missing C = +1 isoscalar 1^+. This ties in with the approximate degeneracy of the D and our A_1 and with the apparent $\pi\delta$ decay mode of the D. We thus have a pleasing picture of the A_1 nonet, but the foundations are built on sand.

5. DIFFRACTIVE PRODUCTION OF N*'s

In our model for the A_1 the peak in the 1^+ intensity is shifted down some 200 MeV/c^2 and the phase variation is suppressed. Very similar features appear in two papers[5,6] on the diffractive production of $\Delta\pi$ and $N\pi$ systems. The $1/2^+$ $p\pi^-$ system peaks around 1.2 GeV/c^2 and there is a well known resonance somewhere between 1.4 and 1.47 GeV/c^2 - we have a downward shift of $\sim$ 200 MeV/c^2. The $3/2^-$ $p\pi^-$ system (d-wave) is in about the right place, but does not show up in $\Delta\pi$, which is s-wave and so expected to be fed strongly by the Deck mechanism.

A further puzzle is that the phase of $1/2^+$ $p\pi^-$ is slowly varying between 105^0 and 130^0 between 1.3 GeV/c^2 and 1.5 GeV/c^2, measured with respect to an assumed BW phase for $3/2^-$. We expect from the Deck mechanism with rescattering a variation like $e^{2i\delta}$ and so perhaps > 180^0 over this region.

The data are poor but these peculiarities seem to have a natural explanation within our model. We must however employ a one resonance but two or more channel formulation in an attempt to reproduce these features.

6. DIFFRACTIVE ρ PHOTOPRODUCTION

The one place where diffractive production of resonances is well established is distinguished by the operation of a mechanism very like the one we have proposed. Diffractive photoproduction of vector mesons occurs strongly and in the case of the relatively broad ρ the shape is distorted so that the peak is moved down by $\sim$ 20 MeV/c^2 and is steeper on the high mass side than the low[14]. So far as I know phase information is not available, but the shape of the ρ is explained by interference between the direct ρ photoproduction term of fig.14(a) and the Drell-Hiida mechanism of fig.14(b) - the photo-

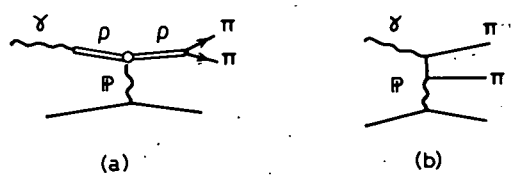

Fig.14 Diffractive ρ photoproduction (a) and the Drell-Hiida mechanism (b).

production analogue of Deck. This model for the is known as the Söding model[15] - the people who applied it at SLAC multiplied the Drell-Hiida amplitude by cos δ $e^{i\delta}$[14].

Rho production is also the only place I know of where the phase associated with the Pomeron has been directly checked. This was done by interfering e^+e^- from the decay of diffractively produced ρ (fig.15(a)) with the pure QED diagram of fig.15(b). The phase associated with the Pomeron leg is within about 10^0 of π/2 - the difference is readily attributable to the exchange of other things along with the Pomeron[16].

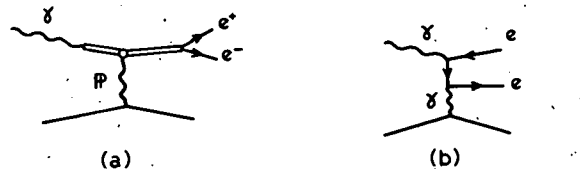

Fig.15 Production of e^+e^- pairs through diffractive ρ photoproduction (a) and pure QED (b) allowed the measurement of the production phase of the ρ.

7. CONCLUSIONS

We have demolished the widespread belief that in production processes a two particle channel picks up a dominant phase factor $e^{i\delta}$ automatically and have shown that in production processes severe resonance distortion may occur and may be accompanied by phase variation wildly different from $e^{i\delta}$. All that is required is a background amplitude not completely dominated by direct resonance production. The specific model we have constructed seems to deal successfully with ρ distortion in photoproduction and seems to be capable of explaining observations on diffractive production of N* systems that had

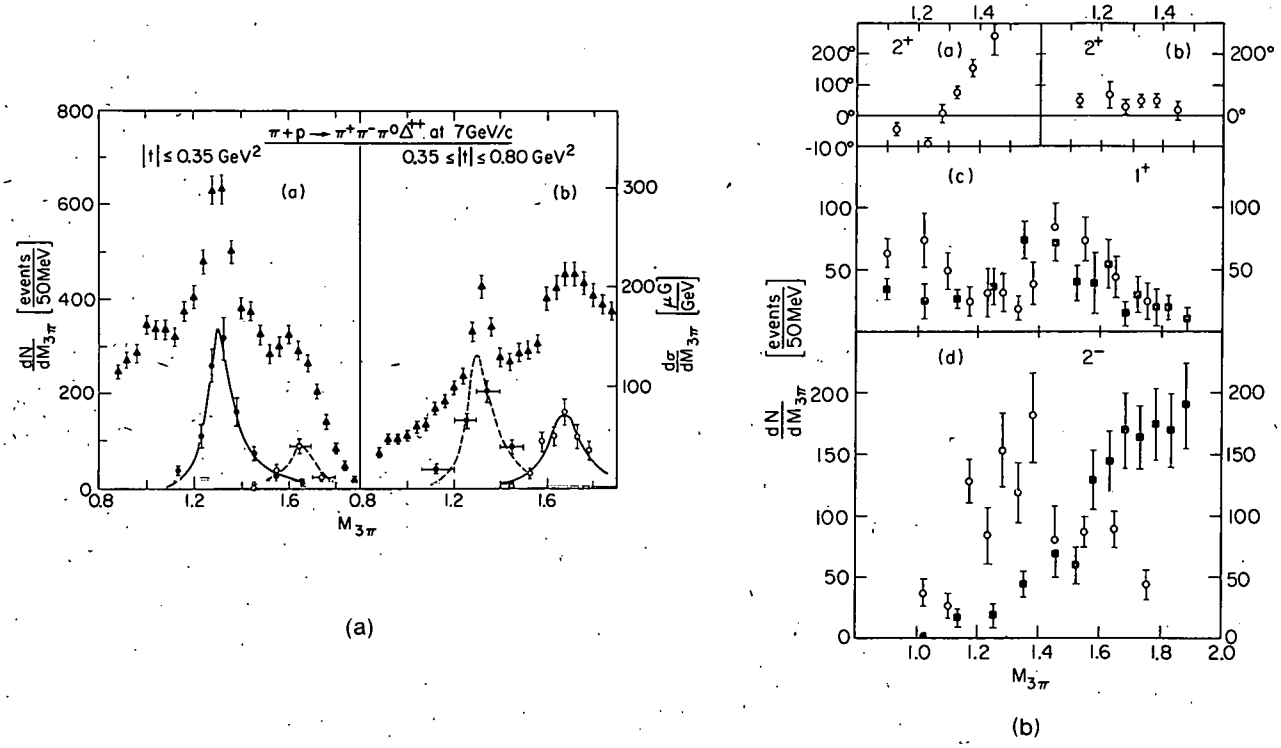

Fig. 16 Results of an analysis of $\pi^+\pi^-\pi^0$ produced against Δ^{++} at 7 GeV/c. (a) Mass spectra, 2^+ I = 1 and 3^- I = 0 signals. (b) Section (a) Relative phase between 2^+ D and 2^-s at low $|t|$. Section (b) Relative phase between natural and unnatural exchange for 2^+ production at low $|t|$. Section (c) I = 1 1^+ intensity at low $|t|$ (open circles) and high $|t|$ (solid squares) section (d) I = 1 2^- intensity for low and high $|t|$.

previously received no explanation. The data on A_1 and Q (where there is no independent evidence for resonances) fit very nicely into this framework.

Indeed I was very confident that my colleagues and I had found the solution to the A_1 enigma until I received from Fritz Wagner at LBL the data shown in fig.16[17]. He has been analyzing $\pi^+p \to \Delta^{++}\,\pi^+\pi^-\pi^0$ at 7 GeV/c. If there is an A_1, it should show up. He sees a beautiful A_2 with a cross section $\sim$ 60 μb, made mostly by B exchange (not ρ exchange) but there is no evidence for an A_1 resonance. I doubt if this demolishes the A_1: the predicted cross section in this reaction for natural spin-parity exchange is only 7 μb[18] and at this level a substantial double Regge exchange background may conspire to confuse the situation, but I must admit my confidence to have been shaken. This meeting being held at an electron accelerator, it is appropriate that the best place to establish or destroy the A_1 unambiguously appears to be through photoproduction, fig.17.

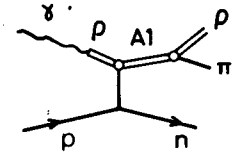

Fig. 17 A_1 photoproduction by π exchange.

The work described in this paper has been carried out in collaboration with I.J.R. Aitchison, J.B. Dainton and M.A.V. Game.

REFERENCES

1. See the review by R.Diebold, Proc. XVI Int. Conf. on High Energy Physics (1972) Vol.3; the review by G.Ascoli, Proc. XVII Int. Conf. on High Energy Physics, London, 1974, (SRC, Rutherford Laboratory, 1974) p.II-8, and refs.(2),(3) and (7).

2. G.Ascoli et al, Phys. Rev. D8, (1973) 3894; Phys. Rev. D9, (1974) 1963.

3. Yu.M.Antipov et al, Nucl. Phys. B63, (1973) 153.

4. K.W.J.Barnham et al, Nucl. Phys. B25, (1970) 49; H.H.Bingham et al, Nucl. Phys. B48, (1972) 589; P.J.Davis et al, Phys. Rev. D5, (1972) 2688; M.G.Bowler et al, Nucl. Phys. B74, (1974) 493.

5. D.C.Colley et al, Nucl. Phys. B55, (1973) 1.

6. D.Lissauer et al, Phys. Rev. D6, (1972) 1852.

7. Yu.M.Antipov et al, Nucl. Phys. B63, (1973) 141.

8. M.G.Bowler and M.A.V.Game, Oxford University Preprint, 38/74, (1974).

9. M.G.Bowler, M.A.V.Game and I.J.R.Aitchison, submitted to Nucl. Phys. B.

10. I.J.R.Aitchison, Nucl. Phys. A189, (1972) 417.

11. K.W.J.Barnham et al, Nucl. Phys. B25, (1970) 49.

12. M.G.Bowler and J.B.Dainton, Oxford University Preprint, 61/74, submitted to Nucl. Phys. B.

13. M.Deutschman et al, Phys. Letts. B49, (1974) 388; S.N.Tovey et al, Rutherford Laboratory Preprint, RL 74-073, (1974).

14. J.Ballam et al, Phys. Rev. D5, (1972) 545.

15. P. Söding, Phys. Letts. 19, (1965) 702.

16. H.Alvensleben et al, Nucl. Phys. B25, (1971) 342.

17. F.Wagner, These proceedings and LBL-3395.

18. G.C.Fox, private communication. See also G.C.Fox and A.J.G.Hey, Nucl. Phys. B56, (1973) 386.

APPENDIX

FINAL STATE INTERACTION THEORY (See Ref.(9))

This material is due to I.J.R.Aitchison. The rescattering corrections to an amplitude B are given by the Omnès equation:

$$F(m^2) = B(m^2) + \frac{1}{\pi}\int_{m_{min}}^{\infty} \frac{g^*(m'^2)\,F(m'^2)\,d\,m'^2}{m'^2 - m^2 - i\,\epsilon}$$

where m_{min} is the two body threshold ($m\pi + m_p$ for the A_1) and

$$g = e^{i\delta}\sin\delta$$

is the two body scattering amplitude. B is thus the driving term in an inhomogeneous equation: the solution can be written as

$$F_I = B\,e^{i\delta}\cos\delta + \frac{e^{i\delta}\sin\delta}{k}\frac{1}{N}\frac{P.V.}{\pi}\int\frac{N'k'B'd\,m'^2}{m'^2 - m^2}$$

where k is phase space and N the numerator function in

$$\frac{N}{D} = \frac{e^{i\delta}\sin\delta}{k}$$

To this solution F_I of the inhomogeneous equation we may add with arbitrary phase a solution F_H of the homogeneous equation

$$F_H = \frac{p}{N}\frac{e^{i\delta}\sin\delta}{k}$$

where p is a polynomial. In the region of a resonance N is approximately constant and the final form we used for the A_1 is

$$F_{1+} = B\,e^{i\delta}\cos\delta + \frac{e^{i\delta}\sin\delta}{k}\left\{R + \frac{P.V.}{\pi}\int\frac{B'k'd\,m'^2}{m'^2 - m^2}\right\}$$

We have verified by numerical calculation with a reasonable N function that the approximation N = constant makes only small differences for a B which is localised in momentum space, although for a constant B the integral eats away the cos δ term and the residuum behaves as $\sin\delta e^{i\delta}$. Indeed for the Deck amplitudes we have used the principal value integral is only a small correction to the dominant rescattered Deck term which is $B\,e^{i\delta}\cos\delta$.

Theoretically the one thing that is not clear is the role that duality might play in all this.

AN AMPLITUDE ANALYSIS FOR THE REACTION $\pi^+p \to \pi^+\pi^-\pi^0\Delta^{++}$ AT 7 GeV/c *

by

F. Wagner†, M. Tabak and D.M. Chew§
Lawrence Berkeley Laboratory
University of California
Berkeley, California 94720

ABSTRACT

An amplitude analysis for the reaction $\pi^+p \to \pi^+\pi^-\pi^0\Delta^{++}$ at 7 GeV/c has been performed using the isobar model for the 3π system. The 3π-mass covers the range from 0.82 to 1.90 GeV. We observe strong A_2 production. The spin parity of the $\omega^*(1700)$ is determined to be 3^-. No significant A_1 production can be seen.

The interest in 3π final states lies in the fact that the constituent quark model predicts the existence $I(J^P) = 1(2^+)$, $0(3^-)$ as well as $J^P = 1^+$ resonances in both isostates I[1]. Analysis of the reaction

$$\pi^{\pm}p \to \pi^{\pm}\pi^+\pi^-p \qquad (1)$$

have yet confirmed only the 2^+ state[2], because I = 0 cannot contribute to reaction (1) and the 1^+ states may be hidden under diffractive dissociation of the π and/or production of 3π by the Deck mechanism. For both reasons a neutral 3π system seems to be more suitable for detection of these possible resonances. Therefore we studied the reaction

$$\pi^+p \to \pi^+\pi^-\pi^0\Delta^{++}. \qquad (2)$$

The conventional approach to analyze the 3π system in (1) or (2) is to use the so-called isobar model[3,4]. It has been applied in two ways. Ascoli and his disciples[5] ignore the baryon spin and fit the 3π density matrix to the data. Spin coherence of the initial and final proton in reaction (1) is compatible with the data[5,6], giving an *a posteriori* justification of this procedure. Another method has been proposed by Tabak et al[6], where the production amplitudes are used as parameters. In reaction (2), in contrast to reaction (1), additional information about the production mechanism can be obtained by studying the Δ-decay into π^+p. Therefore we are bound to use the latter method.

In an analysis of $KN \to K\pi\pi N$ a striking similarity between the diffractive and charge exchange reaction has been found, both reactions being dominated by unnatural spin parity states produced via natural exchange[7], as also found for reaction (1). It is interesting to know whether reaction (2) follows the same pattern. In addition one can test the quark model prediction[8] for the $p\Delta^{++}$ vertex, predictions that are in remarkable agreement with the data for several quasi two body reactions[9-11]. After a description of the data and generalization of the isobar formalism to include the Δ decay, we discuss the fitting procedure and describe the results obtained in these fits.

The measurements are based on a 700,000 picture exposure of the 82" SLAC bubble chamber at 7 GeV/c[12]. Of all events, 85,856 fitted the reaction $\pi^+p \to \pi^+\pi^-\pi^0\, p\pi^+$ corresponding to a cross section of 2.16 ± 0.09 mb. To select reaction (2) we imposed a mass cut on either π^+p combination of $1.16 \leq M_{\pi^+p} \leq 1.28$ GeV. Depending on the 3π mass $M_{3\pi}$, 5-12% of the events had both π^+ in this mass band. In these cases we took both combinations with a relative weight according to a Breit-Wigner mass distribution for the Δ. After this cut we have 6790 events for $|t_{p\Delta}| \leq 0.35$ GeV^2 (hereafter called the low $|t|$ interval) and 5998 events for $0.35 \leq |t_{\Delta p}| \leq 0.80$ GeV^2 (high $|t|$ interval) in the mass range $0.82 \leq M_{3\pi} \leq 1.90$ GeV. We checked that the Δ decay moments $\langle Y_L^M \rangle$ are zero for $L \geq 3$ and that there is little N* production visible in any Δπ channels in this kinematic region.

Presented by F. Wagner.

*Work supported by the auspices of the U.S. Atomic Energy Commission.

†Also at Max-Planck-Institut für Physik, München, Germany (after 1st January, 1975).

§On leave of absence from the Université de Paris VI, Paris, France.

The isobar model[4] describes any 3π state with spin parity J^P, helicity m referring to a quantization axis in the production plane, and isospin I as being the sum of $\pi\pi$ (isobar) states with spin ℓ in an orbital angular momentum state L with the third π. Using amplitudes satisfying the constraints from parity we replace m by $|m|,\eta$ where $\eta = +1(-1)$ is related to natural (unnatural) parity exchange[4]. The amplitude for reaction (2) can be written as

$$T_{s\mu} = \sum_{Km\eta} D_{Km\eta}\, T^{\eta m}_{s\mu}\,(K, M_{3\pi}, t). \qquad (3)$$

In this equation the spins of the Δ and p are characterized by their exchanged spin $s(s = 1,2)$ and the corresponding z-component $\mu(\mu = 0,1,2)$, which is equal to the helicity flip at the $p\Delta$ vertex[9]; η takes care of negative values of μ; K abbreviates all 3π quantum numbers except η and m; that is, by K we mean $I(J^P\ \varepsilon\pi/\rho\pi/f\pi)$; the known function D contains the angle dependent part and the $\pi\pi$ phases describing the isobars ρ, ε, f. The isobar model assumes that the amplitudes T do not depend on any $\pi\pi$ submasses. Parity conservation at the Δp vertex implies[9] vanishing of T^{1m}_{10} and T^{-1m}_{20}.

Due to the lack of polarization measurements and limited statistics, we want to make the following additional assumption: We neglect all amplitudes with an helicity flip of 2 units at either vertex ($m = 2$ and/or $\mu = 2$). This assumption depends on the co-ordinate system we are going to describe now. For reaction (1) and several other two body reactions, it has been shown[9] that the vector

$$\underset{\sim}{c} = \underset{\sim}{q}_\eta + \frac{t - m_\pi^2}{2s}\,(\underset{\sim}{q}_p + \underset{\sim}{q}_\Delta) \qquad (4)$$

taken as z-axis in the meson rest frame leads to helicity conservation for the meson system. Similarly we use for the Δ the vector c'

$$\underset{\sim}{c}' = \underset{\sim}{q}_p + \frac{t - m_p^2}{2s}\,(\underset{\sim}{q}_\pi + \underset{\sim}{q}_{3\pi}) \qquad (5)$$

in the Δ rest frame as z axis. Theoretically the choice of eqns.(4) and (5) is motivated by the coupling of vector mesons to a conserved current[13]. Since the angle between $\underset{\sim}{c}$ (or $\underset{\sim}{c}'$) and the corresponding t-channel direction is small, there is little difference between neglecting helicity flip of two units (however, not of one unit) in the t-channel helicity system and in the systems defined by eqns.(4,5).

With this assumption, the unpolarized differential cross section W including the Δ decay is given by

$$W = \sum D_{Km\eta} \cdot D^{*}_{Km\eta} \cdot A^{\eta\bar{\eta}}_{ss\mu\bar{\mu}}(\hat{p}) \cdot T^{\eta m}_{s\mu}(K) \cdot T^{\bar{\eta}\bar{m}*}_{s\bar{\mu}}(\bar{K}) \qquad (6)$$

The matrix A depends on the unit vector $\hat{p}$ of the proton from the Δ decay and is given explicitly in the Appendix. Apart from the simplicity of eqn.(6), one other reason to use s and μ to characterize the Δp vertex is that the quark model[8] predicts vanishing[9] of any $T^{\eta m}_{s\mu}$ with $s = 2$.

The amplitudes T in eqn.(6) are parameters in a maximum likelihood fit[14] to the data, which were binned in $M_{3\pi}$ and t. We allowed for all waves up to $J^P = 3^+$ with $\ell + L \leq 3$ and $I \leq 2$ plus the $O(3^-F\rho\pi)$ wave in their various isospin and spin combinations. Together with the $p\Delta$ quantum numbers, this gives 473 real parameters, an impossible number to fit simultaneously. Consequently, we adopted the following procedure: First, we varied only those waves which were present in the charged 3π system as determined in previous analyses[5,6] for both $I = 0$, and only $s = 1$ amplitudes at the $p\Delta$ vertex. Then, in succeeding fits, we added parameters with the aim of significantly increasing both the likelihood and the energy continuity of the solutions. We rejected those parameters which did not meet these criteria. This procedure was iterated until the major waves stopped changing. The results presented here come from this final set, but share their major features with earlier fits. For details of the analysis see ref.(15).

The experimental mass distributions in the two t-intervals show two significant peaks at $M_{3\pi} \sim 1.3$ GeV and $M_{3\pi} \sim 1.7$ GeV respectively (fig.1). The fitted total contributions for $T([1(2^+D\rho\pi)]$ and $T[O(3^-F\rho\pi)]$ show that the peaks are caused by these amplitudes. The first peak must be attributed to the A_2. The relative phase between the dominant A_2 amplitude $T^{-10}_{10}[1(2^+D\rho\pi)]$ and the background wave $T^{10}_{20}[1(2^-f\pi)]$ exhibits (fig.2(a)) the variation expected for a Breit-Wigner resonance. A fit with a Breit-Wigner distribution to the points for this 2^+ amplitude at low $|t|$ (fig.1(a)) gives a mass of (1.298 ± 0.008) GeV and a width of (0.122 ± 0.012) GeV, which agree well with the world average[16].

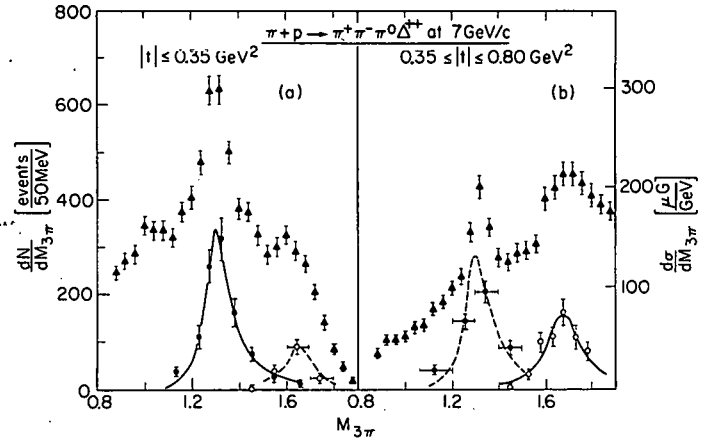

Fig. 1 The experimental 3π mass spectrum for $\pi^+ p \to (3\pi)^0 \Delta^{++}$ as function of $M_{3\pi}$ (▲), left hand scale in Events/ 30 MeV right hand scale in μb/GeV, Fig. 1(a) for $|t| \leq 0.35$ GeV^2 and Fig. 1(b) for $0.35 \leq |t| \leq 0.80$ GeV^2. The total intensity going into $1(2^+ D\rho\pi)$ (●) and into $0(3^- F\rho\pi)$ (○) are also given. Solid curves are Breit-Wigner fits to the 2^+ intensity at low $|t|$ and to the 3^- intensity at high $|t|$. Dashed curves are the same fits normalized to the number of events in the $|t|$-bin.

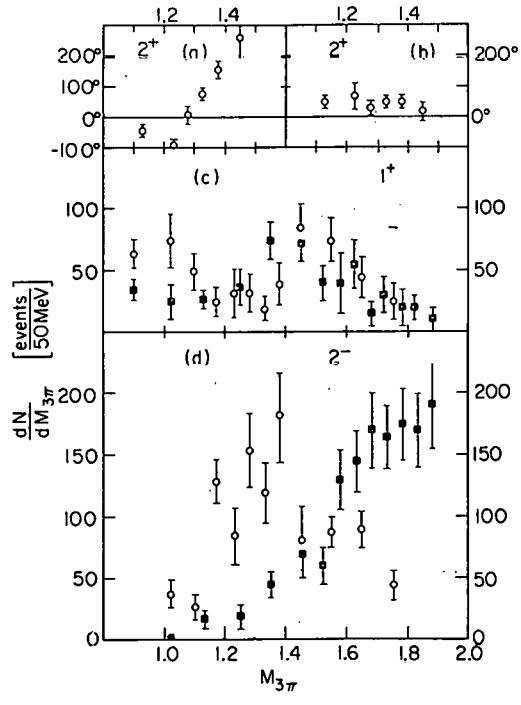

Fig. 2 (a) Relative phase between $T_{10}^{-10}[1(2^+ D\rho\pi)]$ and $T_{20}^{10}[1(2^- sf\pi)]$ as function of $M_{3\pi}$ at low $|t|$.

(b) Relative phase between the natural exchange and the unnatural exchange amplitude T_{10}^{-10} for $[1^+(2^+ D\rho\pi)]$ as function of $M_{3\pi}$ at low $|t|$. The straight line gives the prediction of Regge ρ and B exchange.

(c) Total intensity going into $1(1^+)[1(2^-)]$ as function of $M_{3\pi}$ for low $|t|$ (○) and for high $|t|$ (●).

If we identify the second peak with the $\omega^*(1700)$ found earlier in its (3π) and (5π) decay[17], this $\omega^*(1700)$ is found by us to have the spin parity assignment of $J^P = 3^-$. The fit with Breit-Wigner to the points for this 3^- amplitude present in the high t mass distribution of fig.1(b) gives the following result: (1.669 ± 0.011) GeV for its mass and for its width (0.173 ± 0.019) GeV; these values are similar to the mass and width of the g-meson[16]. A phase variation is more difficult to obtain, mainly due to the lack of a reliable single background wave. Nevertheless most solutions are compatible with a phase increase of 100^0 for a mass of the (3π) system between 1.625 and 1.725 GeV. This fact and the observed Breit-Wigner shape make a resonance interpretation very likely. After the recent spin parity assignment of 3^- to the $K^*(1800)$[18], the only missing member of the 3^- nonet is the ϕ; ideal mixing predicts its mass to be ≈ 2 GeV.

By integrating the above Breit-Wigner fits, the $A_2(1310)$ and $\omega^*(1700)$ production cross sections are found to be (53 ± 7) μb and (33 ± 12) μb, respectively, for $|t| \leq 0.8$ (GeV/c)^2. The relative phase of about 50^0 between the amplitudes T_{11}^{11} (natural exchange) and T_{10}^{-10} (unnatural exchange) for the A_2 as shown in fig.2(b), at low $|t|$ agrees with Regge ρ and B exchange. Regarding the relative intensity of these two exchanges, it appears that both resonances are produced predominantly by unnatural (B) exchange. For the A_2 this fact has been predicted by Fox and Hey[19]. By semi-inclusive duality arguments[20], the following scaling law holds for the ratio R between natural and unnatural parity exchange production for a resonance x

$$R_x = \frac{m_\omega^2}{m_x^2} R_\omega. \qquad (7)$$

Using the value $R_\omega = 0.8$[11,12], eqn.(7) leads to the prediction of $R_{A_2} = 0.28$ and $R_{\omega'} = 0.22$ in excellent agreement with our observed ratios of $R_{A_2} = 0.32 \pm 0.05$ and $R_{\omega'} = 0.14 \pm 0.07$ at low t. For both resonances we found contributions less than 5% to the non-quark amplitudes $T_{2\mu}^{nm}$. That is production of the natural spin parity resonances (for the ω see ref.(11) in reaction (2) has only pΔ couplings allowed by the quark model[8].

No other amplitudes with a resonant like behaviour have been found. In particular the $1(1^+)$ wave (A_1) remains small as one can see from fig.2(c). An A_1 hiding under the A_2 as proposed in ref.(21) is certainly excluded. For a width less than 150 MeV we estimate $\sigma(A_1) < 2$ μb. The $1(2^-)$ wave, although large (fig.2(d), does not exhibit a resonance-like structure as claimed in ref.(22). The peaks differ in the two t bins and also differ from that observed in reaction (1). Apart from the strong $1(0^-\varepsilon\pi)$ wave below 1.4 GeV, the remaining background is shared by many different amplitudes. Even if we are not sure about any individual wave, the following general features about the background appear:

i) All background waves belong to unnatural spin parity:

$$0^-, \quad 1^+, \quad 2^-, \quad 3^+.$$

ii) The background is produced almost entirely by natural exchange. Column 1 of Table 1 gives the ratios of natural to unnatural background production for the various mass bins in both t intervals.

iii) In contrast to the resonances, the background waves are produced dominantly by the non-quark amplitudes $T_{2\mu}^{10}$. The ratio between quark and non-quark background cross section is approximately equal to 0.6 (see column 2 of Table 1).

iv) The data bear out helicity conservation for the background along the direction $\underset{\sim}{c}$ of eqn.(4) for the 3π system up to the level 5%, as column 3 of Table 1 shows. This fact is non-trivial, especially at high t.

v) No such helicity conservation occurs at the Δp vertex. In fact, επ and fπ waves prefer s = 2, μ = 0, while ρπ waves are mainly in s = 1, μ = 1 states. Together with the resonance couplings at least five different proton-Δ spin combinations are significantly non-zero. Points (i) and (ii) have been observed also in reaction (1)[5,6] and for $K^-p \to \bar{K}\pi\pi N$ in both the charged and the neutral $\bar{K}\pi\pi$ system[7]. Our result supports the suggestion of ref.(7) that the background in diffractive and charge exchange reactions differ only by its energy dependence.

Table 1

Ratios of non-resonant background cross sections

	1		2		3	
$M_{3\pi}$ (GeV)	Low $\|t\|$	High $\|t\|$	Low $\|t\|$	High $\|t\|$	Low $\|t\|$	High $\|t\|$
0.82 - 0.98	0.02 ± 0.02	-	0.64 ± 0.10	0.73 ± 0.14	0.15 ± 0.07	-
0.98 - 1.06	0.16 ± 0.06	-	0.61 ± 0.09	0.56 ± 0.16	0.12 ± 0.06	-
1.06 - 1.20	0.07 ± 0.03	0.03 ± 0.03	0.61 ± 0.06	0.71 ± 0.09	0.05 ± 0.03	0.05 ± 0.03
1.20 - 1.30	0.03 ± 0.02	0.07 ± 0.03	0.64 ± 0.10	0.38 ± 0.11	0.02 ± 0.02	0.06 ± 0.03
1.30 - 1.40	0.09 ± 0.05	0.04 ± 0.02	0.54 ± 0.08	0.42 ± 0.17	0.08 ± 0.04	0.06 ± 0.02
1.40 - 1.50	0.05 ± 0.02	0.02 ± 0.02	0.42 ± 0.07	0.77 ± 0.16	0.04 ± 0.02	0.04 ± 0.02
1.50 - 1.60	0.03 ± 0.02	0.07 ± 0.04	0.65 ± 0.12	0.76 ± 0.08	0.09 ± 0.03	0.10 ± 0.03
1.60 - 1.70	0.01 ± 0.01	0.03 ± 0.02	0.36 ± 0.13	0.48 ± 0.06	0.02 ± 0.03	0.11 ± 0.03
1.70 - 1.80	0.03 ± 0.03	0.03 ± 0.02	1.28 ± 0.18	0.55 ± 0.05	0.05 ± 0.04	0.03 ± 0.01
1.80 - 1.90	-	0.02 ± 0.02	-	0.72 ± 0.06	-	0.03 ± 0.02

Column 1 gives the ratio of background produced via natural exchange to that via unnatural exchange.
Column 2, the ratio of intensity in the background of s = 1 quark coupling to s = 2 at pΔ vertex.
Column 3, the ratio of helicity nonconserving to helicity conserving background.

In conclusion, in the $(3\pi)^0$ mass distribution between 1.0 and 2.0 GeV, we have observed the A_2 and a peak due to the production of a $3^-\omega^*$ state with the same mass as the g-meson. No significant A_1 production has been found. Resonance production agrees with the predictions of the quark model and semi-inclusive duality. The background waves behave very similarly to the corresponding ones found in other 3π or $K\pi\pi$ systems.

We are very indebted to the members of Group A at LBL for allowing us to use the DST of the events in this analysis. We are very grateful to Professor A. Rosenfeld for his continuous interest and encouragement in the present work. We thank Dr. T. Lasinski for helpful discussions and Dr. P. Eberhard regarding the use of the fitting program OPTIME.

REFERENCES

1. See, for example, J.L. Rosner, Proc. XVII Int. Conf. on High Energy Physics, London (1974). (SRC, Rutherford Laboratory, 1974) II-171.

2. See, for example, F. Wagner, Proc. XVII Int. Conf. on High Energy Physics, London (1974). (SRC, Rutherford Laboratory, 1974) II-27 and LBL-3091 (July 1974).

3. D.J. Herndon, P. Söding and R.J. Cashmore, To be published in Phys. Rev. D (1974), and LBL-543.

4. For details on the meson formalism, see J.D. Hansen, G.T. Jones, G. Otter and G. Rudolph, CERN D.Ph.II/73-74, to be published in Nucl. Phys. (1974).

5. Y.M. Antipov, G. Ascoli, R. Busselo, M.N. Focacci, W. Kienzle, R. Klanner, A. Lebedev, P. Leconte, V. Roinishvili, A. Weitsch and F.A. Yotch, Nucl. Phys. B63, (1973) 153; R. Klanner, Thesis, Munich (1973), CERN, NP 73-9 (1973).

6. M. Tabak, E.E. Ronat, A.H. Rosenfeld, T.A. Lasinski and R.J. Cashmore, Proc. 4th Int. Conf. on Experimental Meson Spectroscopy, Boston (1974) APS No.21, p.46 and LBL-3010 (May 1974).

7. Aachen-Berlin-CERN-London-Vienna and Athens-Liverpool-Vienna Collaborations, Proc. XVII Int. Conf. on High Energy Physics, London 1974. (SRC, Rutherford Laboratory, 1974) paper No.422.

8. A.Bialas and K.Zalewski, Nucl. Phys. B6, (1968) 449, 465.

9. F.Wagner, LBL-3611 (December 1974), in preparation.

10. R.D.Field, CALTEC preprint CALT-68-466, (1974).

11. D.M.Chew, M.Tabak and F.Wagner, LBL-3396 (November 1974), to be published.

12. For details and further references see W.F.Buhl, G. Gidal, D.F.Grether, W.Ko, M.Alston-Garnjost, A.Barbaro-Galtieri, G.R.Lynch and F.T.Solmitz, Phys. Letts. 48B, (1974) 388, and references quoted therein.

13. C.F.Cho and J.J.Sakurai, Phys. Letts. 30B, (1969) 119;
C.F.Cho, Phys. Rev. D4, (1971) 194.

14. We used the program OPTIME of P.E.Eberhard and W.O.Koellner, Comp. Phys. Commun. 3, (1972) 296, and 5, (1973) 163.

15. M.Tabak, Ph.D. Thesis, LBL-3397, in preparation.

16. Particle Data Group, Phys. Letts. 50B, (1974) 91.

17. J.A.J. Matthews, J.D. Prentice, T.S. Yoon, J.T. Carroll, M.W. Firebaugh and W.D. Walker, Phys. Rev. D3, (1971) 561, and references quoted in ref.(16).

18. G.W.Brandenburg, et al. Proc. XVII Int. Conf. on High Energy Physics, London, 1974. (SRC, Rutherford Laboratory, 1974) paper No.235.

19. G.C.Fox and A.J.G.Hey, Nucl. Phys. B56, (1973) 386.

20. P.Hoyer, R.G.Roberts and D.P.Roy, Nucl. Phys. B56, (1973) 173.

21. M.G.Dowler and M.A.V.Game, Oxford University Report, 38/74, (1974).

22. G.Thompson, R.C.Badewitz, J.A.Gaidos, R.L.McIlwain, K.Paler and R.B.Willman Nucl. Phys. B69, (1974) 381;
G.Otter, G.Rudolph, H.Wieczorek, H.Böttcher, W.Novak, K.Böckmann, H.Plothow, V.Cocconi, M.Counihan, A.Kotanski, D.Morrison, D.Sotiriou, R.Stroynowski, H.Wahl, T.Hirose, and E.Leitner, Nucl. Phys. B80, (1974) 1.

APPENDIX

Following ref.(9) we order the Δp spin combinations into a vector $x_i = (T^1_{11}, T^{-1}_{10}, T^{-1}_{11}, T^{-1}_{21}, T^1_{20}, T^1_{21})$. The Δ decay distributions can be written in terms of $\vec{p} = (\sin\theta\cos\phi, \sin\theta\sin\phi, \cos\theta)$ as $W = \Sigma x_i\, A_{in}(\vec{p}) x^*_n$, where the symmetric matrix A is given by (see ref.(9)).

$$A = \begin{pmatrix}
\frac{3}{2}p_y^2 + \frac{1}{2} & & & & & \\
\frac{3}{2}p_z p_y & \frac{3}{2}p_z^2 + \frac{1}{2} & & & & \\
-\frac{3}{2}p_x p_y & -\frac{3}{2}p_x p_z & \frac{3}{2}p_x^2 + \frac{1}{2} & & & \\
\frac{\sqrt{3}}{2}p_x p_y & -\frac{\sqrt{3}}{2}p_z p_x & \frac{\sqrt{3}}{2}(p_y^2 - p_z^2) & \frac{3}{2}(1 - p_x^2) & & \\
-\frac{3}{2}p_z p_x & 0 & -\frac{3}{2}p_z p_y & -\frac{\sqrt{3}}{2}p_z p_y & \frac{3}{2}p_z^2 + \frac{1}{2} & \\
\frac{\sqrt{3}}{2}(p_x^2 - p_z^2) & \frac{\sqrt{3}}{2}p_z p_y & \frac{\sqrt{3}}{2}p_x p_y & \frac{3}{2}p_x p_y & -\frac{\sqrt{3}}{2}p_x p_z & \frac{3}{2}(1 - p_y^2)
\end{pmatrix}$$

A PARTIAL WAVE ANALYSIS OF THE 3π SYSTEM IN THE REACTION $\pi^+ d \to \pi^+\pi^-\pi^0 pp_s$

by

M.J. Emms, G.T. Jones, J.B. Kinson, B.J. Stacey[§], M.F. Votruba, and P.L. Woodworth,
University of Birmingham, UK,

I.G. Bell, M. Dale, and J.V. Major,
University of Durham, UK,

J.A. Charlesworth[†], D.J. Crennell, G.E. Kalmus, and R.L. Sekulin,
Rutherford Laboratory, UK.

A21

We present here preliminary results for a partial wave analysis of the charge exchange reaction:-

$$\pi^+ d \to \pi^+\pi^-\pi^0 pp_s \qquad (1)$$

The data came from an exposure of the CERN 2m deuterium bubble chamber to a separated beam of 4 GeV/c π^+ mesons. The exposure of about 16 events per microbarn yields approximately 41,000 events best described by reaction (1).

The obvious features seen in this reaction are the ω^0, some Δ production and an enhancement in the $\pi^+\pi^-\pi^0$ effective mass distribution in the A_2 (1310) region as seen in fig.1. Only those events with $|t'|(t' = t - t_{min}) < 0.5$ GeV^2 are shown in the figure.

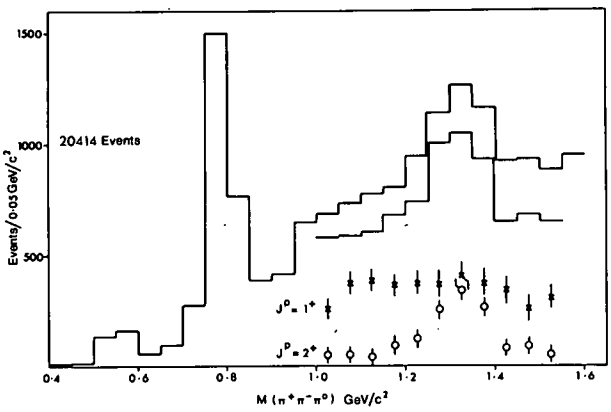

Fig.1 $\pi^+\pi^-\pi^0$ effective mass distribution for reaction (1) with $|t'| < 0.5$ GeV^2. The lower histogram shows the same sample after all Δ production has been removed. The crosses show the $J^P = 1^+$ and the circles the 2^+ contributions to the reaction.

This $|t'|$ cut is introduced to enhance peripherally produced states and its main effect is to reduce the $J^P = 0^-$ contribution. We have used the Illinois partial wave analysis program[(1)] to analyze this reduced sample in the 3π mass region from 1.0 to 1.55 GeV/c^2. This program allows the removal of the pπ effective mass regions corresponding to Δ^{++}, Δ^0 and Δ^+, and calculates the number of events expected if Δ were not present. This is shown as the lower histogram in fig.1.

The 3π system is now analyzed in terms of quasi two-body decays of partial wave components $J^P L M^\eta$ in the Gottfried-Jackson frame. Here, J^P is the spin-parity and M the helicity of the 3π state, L is the angular momentum of the two-body intermediate state and η the naturality of the exchange.

In this analysis we have tried many states of $J \leq 2$ decaying in the επ ρπ and fπ modes. Most of these are present in some mass or t bins, but no fπ decay modes are needed. The states that are always necessary are $J^P = 0^-$, 1^+ and 2^- with 2^+ required in the A_2 region. Of these the 0^- decays principally by επ and the 2^- has mostly $M^\eta = 0^+$ and shows a slowly rising intensity across the mass band. The contributions of $J^P = 1^+$ and 2^+ are shown in fig.1 and are discussed in more detail below.

The 2^+ wave decays by the ρπ mode only and is only present in the isotopic spin = 1 state. A_2 is produced most strongly with helicity 0 by unnatural parity exchange (fig.2(a)), but is also clear in the natural and unnatural parity exchange helicity 1 states (fig.2(b) and (c)). There is no evidence of helicity 2 production in this $|t'|$ range.

Paper presented by D.J. Crennell.

[§]Now at Westfield College, London.

[†]Now at Dept. of Civil Engineering, University of Newcastle.

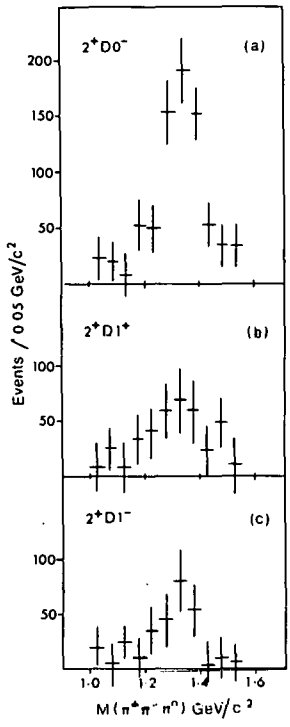

Fig.2(a),(b),(c) The $J^P = 2^+$, $M^\eta = 0^-$, 1^+ and 1^- contributions to the reaction.

The relative phase of the A_2 to the background 0^- and 2^- waves can only be determined for states produced by the same exchange naturality; since the $J^P = 0^-$ and most of the 2^- require $\eta = +$ which contributes little to A^0_2 production, the phase is poorly determined, but nevertheless is in agreement with the Breit-Wigner prediction.

Various theories[2] have made predictions for the ratio R of unnatural to natural parity exchange in the production of different particles by the same exchange mechanisms. Thus we have compared the ω^0[3] and A^0_2 production in this experiment with the prediction

$$\frac{R(A_2)}{R(\omega)} \sim \frac{(M(A_2))^2}{(M(\omega))} = 2.80 .$$

We find a value for

$$\frac{R(A_2)}{R(\omega)} = \frac{2.7 \pm 0.4}{0.90 \pm 0.08} = 3.0 \pm 0.45$$

in agreement with the theory.

The $J^P = 1^+$ partial wave populates all three helicity states and decays principally by the $\rho\pi$ mode in both isotopic spin 0 and 1 combinations. We have not yet satisfactorily separated these six independent states, but the total 1^+ contribution (crosses in fig.1) is large and quite sufficient to accommodate the I = 1 $\rho\pi$ resonance predicted by the A_1 model of Bowler and Game[4].

In the A_2 (1310) mass region the 1^+ contribution is of similar magnitude to the 2^+, in contrast with the 3π system produced at 7 GeV/c in the reaction[5]

$$\pi^+ p \to \pi^+\pi^-\pi^0 \Delta^{++},$$

where the $J^P = 1^+$ state has only 10% of the 2^+ intensity.

The results presented here are preliminary; however we believe that they will not change significantly. The data are currently being examined in more detail and we hope shortly to publish our final conclusions. In addition we shall be studying the higher mass region ($M > 1.5$ GeV/c^2).

REFERENCES

1. P.V.Brockway, Ph.D. Thesis, University of Illinois, Urbana. (1970);
J.D.Hansen, G.T.Jones, G.Otter and G.Rudolf, Nucl. Phys. B81, (1974) 403.

2. P.Hoyer, R.G.Roberts and D.P.Roy, Nucl. Phys. B56, (1973) 173;
C.Michael, Nucl. Phys. B63, (1973) 431.

3. M.J.Emms et al submitted to the XVII Int. Conf. on High Energy Physics, London, 1974.
A more detailed study of ω^0 production is in preparation for publication.

4. M.G.Bowler and M.A.V.Game, Oxford University Report 38/74, (1974).

5. F.Wagner, M.Tabak and D.M.Chew, These proceedings and LBL-3395, (November, 1974).

SESSION 7

Chairman: A. Donnachie

FURTHER DEVELOPMENTS

Invited Talk

SOME REMARKS ON ANALYSES OF MULTI-MESON SYSTEMS

V. Chaloupka
C.E.R.N.

Contribution

EVIDENCE FOR DIFFERENT POLARIZATION OF THE 1^+S $K^*\pi$ AND 1^+S $K\rho$ SYSTEMS

J.D. Hansen
Niels Bohr Institute

THIS PAGE

WAS INTENTIONALLY

LEFT BLANK

SOME REMARKS ON ANALYSES OF MULTI-MESON SYSTEMS

by

V. Chaloupka
C.E.R.N.

A21

1. THE ASSUMPTIONS AND LIMITATIONS OF PRESENT MULTI-MESON ANALYSIS

The first part of my contribution consists of a brief review of some of the assumptions and limitations of the presently used analyses of multi-meson systems:

1.1 The use of an isobar model, with its assumptions, poses problems for unitarity. This point was discussed in detail at this meeting.

1.2 Our knowledge of some isobars (e.g. ε, κ) is far from sufficient.

1.3 Coherence is often assumed both in analysis (e.g. coherence of states with given J^P) and in the interpretation of the results. Let me stress once more that

$$\text{Phase } (\rho_{ab}) \neq \text{Phase (b)} - \text{Phase (a)}$$

for

$$\frac{\rho_{ab}}{\sqrt{\rho_{aa}\,\rho_{bb}}} \neq 1$$

1.4 The input to an analysis should be a data sample corresponding to production of a 3-meson system. This is not easily achieved (especially in non-diffractive reactions) and is difficult to verify (e.g. the absence or cutting off of the meson-baryon isobars is not enough).

1.5 Even with limitations on maximum J^P, the problem usually has too many free parameters to be determined in the fit. Various "procedures" used lead in principle only to a solution (at best to the "simplest solution compatible with the data"). Limited statistics also limit the possibilities of investigating the (presumably non-resonant) contributions of states with $I > 1$. As an example, we give a table with isospin characteristics of the currently available 3π production reactions:

Reaction	$I(3\pi)$
1) $\pi^{\pm}p \to p\pi^{\pm}\pi^{+}\pi^{-}$	1, 2
2) $\pi^{+}n \to p\pi^{+}\pi^{-}\pi^{0}$	0, 1, 2
3) $\pi^{-}p \to n\pi^{+}\pi^{-}\pi^{0}$	0, 1, 2
4) $\pi^{+}p \to n\pi^{+}\pi^{+}\pi^{0}$	2
5) $\pi^{+}p \to \Delta^{++}\pi^{+}\pi^{-}\pi^{0}$	0, 1, 2, 3
6) $K^{-}p \to \Lambda\pi^{+}\pi^{-}\pi^{0}$	0, 1

Note the possibility of getting some information on the $I = 2$ 3π system for reaction (3) from reaction (4).

1.6 Although in principle unique for a given set of waves, the resolving power of a density matrix approach may be very weak in unfavourable cases. Thus, it is difficult to get a unique solution for the 3π system below and near the $\rho\pi$ threshold, because of the similarity of the 1^+ S-wave ($\rho\pi$) and 1^+P wave ($\varepsilon\pi$)[1]. This may be illustrated also by preliminary results from an analysis of the 3π system coherently produced on nuclei[2], which in the A_1 region show a solution with a Breit-Wigner variation of the phase of the $1^+\rho$ wave in respect to the 0^-P wave. Up to now, this solution could not be discarded in favour of the solution with a constant phase.

1.7 Finite experimental resolution is not accounted for adequately. The full treatment of this problem is hopelessly complicated:

$$W^{obs}(\underset{\sim}{x}) = \int W^{theor}(\underset{\sim}{x}^1)\ \mathrm{Res}(\underset{\sim}{x} - \underset{\sim}{x}^1)\ d\underset{\sim}{x}^1$$

where:

$W^{obs}(\underset{\sim}{x})$ is the observed distribution in variables $\underset{\sim}{x}$ (e.g. $\underset{\sim}{x} = \{\alpha, \beta, \gamma, s_1, s_2\}$)

$W^{theor}(\underset{\sim}{x})$ is the theoretical distribution

$\mathrm{Res}(\Delta\underset{\sim}{x})$ is the experimental resolution function (including correlations).

To illustrate the possible effect of ignoring the finite experimental resolution, we consider the reaction $\pi^- p \to p\pi^+\pi^+\pi^-$ and make some simplifying assumptions:

a) consider the experimental resolution only in $m(\pi^+\pi_1^-)$ and $m(\pi^+\pi_2^-)$, taken as independent variables,

b) assume a Breit-Wigner shape of the resolution function (with FWHM = R)

Then, one can easily show that

$$|BW(\Gamma)|^2 \to |BW(\Gamma + R)|^2$$

$$\begin{matrix}\mathrm{Re}\\ \mathrm{Im}\end{matrix} BW(\Gamma) \to \sqrt{\frac{\Gamma}{\Gamma + R}} \begin{matrix}\mathrm{Re}\\ \mathrm{Im}\end{matrix} BW(\Gamma + R)$$

Therefore, a typical symmetrical term

$$|A_{12} + A_{21}|^2 \to |A_{12}|^2 + |A_{21}|^2 + 2k\ \mathrm{Re}\ A_{12}\bar{A}_{21}$$

where $k = \frac{\Gamma}{\Gamma + R}$ is a coherence factor due to the finite experimental resolution.

Note that even in the case of $\rho(760)$ (Γ = 100, R = 10), the coherence is only k = 90%. This may distort a fit which assumes complete coherence, especially in the case of a destructive interference. The effect is of course even more serious for narrower resonances (e.g. $K^*(890)$); in the case of the $\omega(780)\pi$ system, it prevented us from measuring the imaginary part of the density matrix[3].

1.8 Conclusion:

It may be that the A_2 with its destructive signature is not sensitive to the deviations from the simplifications listed above. Also, none of these features can be reasonably expected to fake the observed Breit-Wigner behaviour of the 2^+ state.

On the other hand, we might not have been so lucky in other cases, and "unexpected results" (e.g. absence of a Breit-Wigner phase variation) should be interpreted with extreme care.

2. "DENSITY MATRIX" AND/OR "AMPLITUDE" APPROACH TO MULTI-MESON ANALYSIS

In the second part of my talk, I would like to discuss the relations between the density matrix and "amplitude" approaches for analysis of produced multi-meson systems, when the baryon polarizations are not measured.

Consider a multi-meson system R produced by a π or K beam on baryon B, with recoil baryon B':

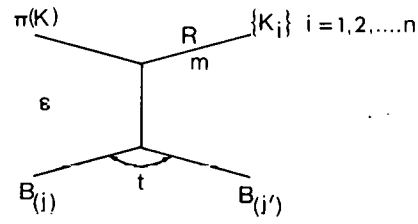

Here j(j') are spins of B(B'), K is a set of quantum numbers describing the system R (e.g. $K_i = (J^P \mu M^\eta)$; - see G.T. Jones' talk, these proceedings and s,t,m are the total c.m. energy squared, the four-momentum transfer squared and the mass of R, respectively.

The density matrix approach describes the system R with an n-dimensional Hermitian positive-definite density matrix with n^2 real free parameters (for simplicity, we do not consider the trace condition, nor the parity conservation in the production process).

The amplitude approach uses the definition of the density matrix in terms of the production amplitudes:

$$\rho_{ab}(s,m,t) = \sum_{K=1}^{r} P_k^a(s,m,t)\ \overline{P_k^b(s,m,t)}$$

where r is the rank of the density matrix (in our case r = (2j + 1)(2j' + 1)). This parametrization has therefore 2nr real free parameters.

It is however well known that it is not possible to determine the amplitudes without measuring the baryon polarizations. Formally:
if $\rho = P P^+$ $P' = U P \Rightarrow P' P'^+ = \rho$ for any unitary U (i.e. P' gives the same density matrix ρ and therefore the same experimental distribution $W = M\rho\bar{M}$, where M is the vector of the decay amplitudes).

Still, by conveniently fixing the r^2 free parameters of the unitary matrix U, we can describe the problem in terms of $(2nr - r^2)$ independent parameters. The way to do it is to use a "minimal parametrization"

of an Hermitian, positive-definite, n-dimensional matrix of rank r.

a) Chung and Trueman[4] use a parametrization

$$\rho = VV^+$$

with

$$V_{ij} = 0 \quad \text{for} \quad j > i$$

$$V_{ij} = \xi_\ell e^{i\alpha_\ell} \qquad \ell = n(j-1) + i - \frac{j(j-1)}{2}$$

$$\alpha_\ell = 0 \quad \text{for} \quad i = j$$

$$\xi_\ell \geq 0 \qquad 0 \leq \alpha_\ell \leq 2\pi$$

The rank condition is imposed by setting

$$\xi_\ell = 0, \quad \alpha_\ell = 0 \quad \text{for} \quad \ell > nr - \frac{r(r-1)}{2}$$

(We use a modified definition of ℓ in respect to ref.(3)).

It is easy to check that this parametrization indeed gives $(2nr - r^2)$ free parameters.

b) An alternative parametrization is actually used in the Illinois program[5], when the positivity constraint is needed (for connoisseurs: subroutine HUDDLE calling VTOB, BTOU, TAUTOX etc.):

The density matrix is parametrized by its eigenvalues and by a unitary matrix constructed from its eigenvectors:

$$\rho = U \rho_D U^+ \qquad \rho_D = \begin{pmatrix} \lambda_1 & & & \\ & \lambda_2 & & \\ & & \ddots & \\ & & & \lambda_n \end{pmatrix}$$

The minimal parametrization of U is

$$U = \prod_{\substack{i=1,n-1 \\ j=i+1,n}} S_{ij}$$

where $(S_{ij})^{ab} = \delta_{ab}$, except for

$$(S_{ij})^{ij} = -(S_{ij})^{ji} = B_{ij}$$

$$(S_{ij})^{ii} = (S_{ij})^{jj} = \sqrt{1 - |B_{ij}|^2} \qquad |B_{ij}| \leq 1$$

The rank condition (not applied in the Illinois program) can be imposed by fixing:

$$\lambda_i = 0 \qquad \text{for} \quad i > r.$$

$$B_{ij} = 0$$

Again, we get $(2nr - r^2)$ free parameters describing a general Hermitian, positive-definite n-dimensional matrix of rank r.

The use of a parametrization like (a) or (b) (there are other possibilities) is the most which can be done without using the baryon polarizations. The number of free parameters is linear in terms of a number of waves, as in an amplitude analysis, and not quadratic as in the density matrix approach, but it is not a partial wave analysis; I call it "rank analysis". A genuine partial wave analysis can only be performed with the information on the polarization of baryons (initial: polarized target, or recoil : secondary scattering, or weak decay of a hyperon). The actual formalism is rather simple; it depends on the reaction investigated. I limit myself only to a few remarks:

(i) the polarization can be usefully used even in the unmodified density matrix approach[6];

(ii) the full use of polarization will (besides the amplitudes themselves) provide additional constraints, enabling one to check various assumptions of the isobar model etc.;

(iii) using the polarizations may be the only way to get the phase variation, e.g. of B(1230) → ωπ (see discussion of the experimental resolution above).

For my concluding remarks let me return to the "rank analysis": Finite bins in s, m(R) and t which have to be used in the actual analysis of the data, may cause violation of the rank condition: in general, the "averaged density matrix"

$$\rho_{ab} = \int_{s,m,t} \sum_{k=n}^{r} p_k^a(s,m,t) \; \overline{p_k^b(s,m,t)}$$

may have any rank up to n equal to the dimension of ρ. The rank condition (and even the positivity constraint) may be violated also by an inadequate parametrization of the data (wrong set of waves, isobar model, etc.) or due to some error, e.g. in the acceptance calculation.

In addition, the uniqueness of the density matrix approach (formally quadratic in parameters) is related to the rank and positivity constraints: if these are satisfied by the data, there is a one-to-one correspondence to the (in principle) unique solution of the rank approach (linear in parameters).

Therefore, an analysis combining the rank approach and the density matrix approach in successive steps would seem very useful; we are actually working on such a project at CERN.

REFERENCES

1. B.Weinstein et al, Phys. Rev. D8, (1973) 2909.

2. J.Pernegt, (ETH, Zurich - now at CERN). Private communication.

3. V.Chaloupka et al, Phys. Letts. 51B, (1974) 907.

4. S.U.Chung and T.L.Truemann, Brookhaven National Laboratory preprint, BNL-19311 (1974).

5. G.Ascoli et al, the PWA program (in FORTRAN) and some development notes.

6. E.g., in reaction $K^-p \to \Lambda\, \pi^+\pi^-\pi^0$ (Amsterdam-Nijmegen-CERN-Oxford Collaboration). We investigate separately the properties of $\pi^+\pi^-\pi^0$ system with given spin orientation of the Λ; we of course intend to perform an amplitude analysis as well.

EVIDENCE FOR DIFFERENT POLARIZATION OF THE 1^+S $K^*\pi$ AND 1^+S $K\rho$ SYSTEMS

by

J.D. Hansen
The Niels Bohr Institute, Copenhagen, Denmark.

A21

1. INTRODUCTION

I would like to present new results on the study of the Q-enhancement using the reactions

$$K^-p \to K^-\pi^-\pi^+p \qquad (1)$$

$$K^-p \to \bar{K}^0\pi^-\pi^0p \qquad (2)$$

The data presented comes from a collaboration of Rutherford, École Polytechnique, and Saclay using a beam of 14.3 GeV/c kaons[1]. The number of events in reactions (1) and (2) are 16000 and 4000, respectively. Two points concerning the 1^+S contribution to the Q-enhancement are discussed:

1) That the isospins of the 1^+S $K^*(890)\pi$ and 1^+S $K\rho$ systems are $\frac{1}{2}$.

2) That the 1^+S $K^*(890)\pi$ and 1^+S $K\rho$ systems are produced with different polarization i.e. they are not decay modes of a single Q.

Previous partial wave analysis can be found in refs.(2-5).

2. ISOSPIN

Figure 1 shows the effective mass of the $K^-\pi^-\pi^+$ and $\bar{K}^0\pi^-\pi^0$ systems. Except for a possible narrow peak in reaction (2) between 1.2 and 1.3 GeV the two distributions agree both in shape and magnitude. This is expected if the $K\pi\pi$ system is dominated by a $K^*\pi$ sub-system and the isospin is $\frac{1}{2}$. The $K\rho$ is twice as big in reaction (2) as in reaction (1) if, again, the isospin is $\frac{1}{2}$. The narrow peak suggests therefore a $K\rho$ enhancement in that region. To study this further we show in fig.2 the 1^+S $K^*\pi$ and 1^+S $K\rho$ "amplitudes" for three different mass ranges. The magnitude of the amplitude is taken to be the square root of the corresponding density matrix element with M = 0 and the phase is given from the phase of

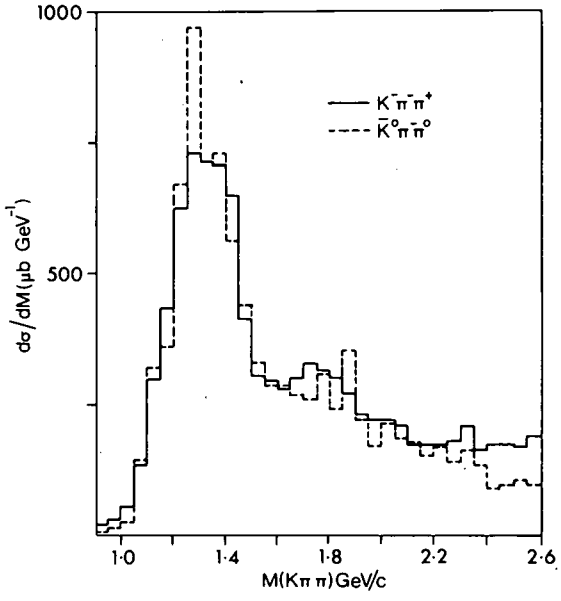

Fig.1 The differential cross section as function of the $K\pi\pi$ mass for reactions (1) and (2).

the interference density matrix elements. The amplitudes are normalized so that the amplitude 1^+S $K^{*0}\pi^-(K^-\pi^+)$ is always equal to $-\sqrt{2}$ and so that the 1^+S $K^{*0}\pi^-(\bar{K}^0\pi^0)$ points along the positive real axis. The phase between two final states with different charges can naturally not be measured. Figure 2(a) shows what is expected if the isospin is $\frac{1}{2}$. If both the $K^*\pi$ and the $K\rho$ comes from a SU(3) multiplet with C = +1, (-1) then the relative phase of $K^{*0}\pi^-(K^-\pi^+)$ and $K^-\rho^0$ should be $0(\pi)$, otherwise this phase is free to vary (as it is suggested in the figure).

Good agreement with isospin $\frac{1}{2}$ prediction is observed both in magnitude for the $K\rho$ and $K^*\pi$ systems as well as the phase of the latter. This proves that the isospins of the 1^+S systems are $\frac{1}{2}$. In addition the existence of the $K\rho$ sub-system is clearly demon-

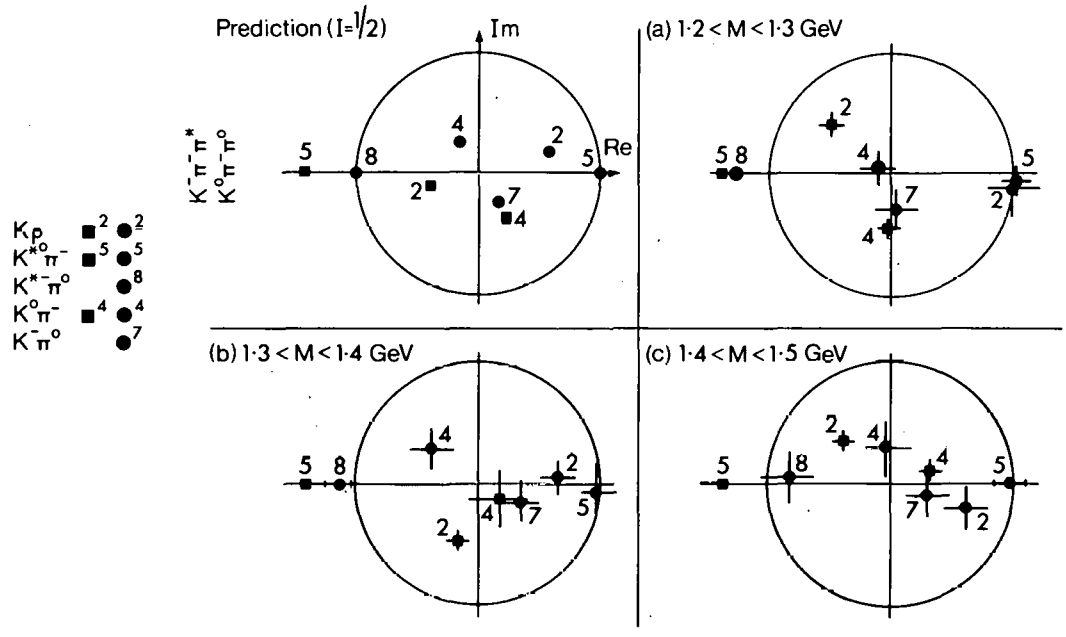

*Fig. 2 Fitted decay amplitude of the $J^P M^\eta = 1^+0^+$ state in the complex plane. The diagram in the top left corner defines the notation and illustrates the predictions of SU(2) for a I = 1/2 state (there is no prediction for the relative phase of K*π, Kρ, Hπ which were chosen at random here.*

strated. This has been in doubt[5] because of the ambiguity in the mass determination of the two negative tracks in reaction (1). However no such ambiguity exists in reaction (2) and the correct ratio of the Kρ contributions to the two channels as well as the correct phase relation show that the ambiguity problems have been handled correctly.

3. POLARIZATION

It was found[6] that the double moments of the Euler angles, angles which are used in the fits, vary over the Dalitz plot in a manner not well described by the usual partial wave fits in the case of the D^2_{00} and D^2_{10} moments. The latter comes from interference between states of different M. The usual fits use assumption 4 of ref.(7), which states that:

$$h^{J^P\eta,\ell jn}_{M\lambda_b\lambda_4} = T^{J^P\eta}_{M\lambda_b\lambda_4} \cdot C^{J^P\ell jn} \qquad (3)$$

which implies among other things that the ratio of two states with the same J^P does not depend on the polarization.

If eqn.(3) is replaced by

$$h^{J^P\eta,\ell jn}_{M\lambda_b\lambda_4} = T^{J^P\eta}_{M\lambda_b\lambda_4} \cdot C^{J^P\ell jn}_{M} \qquad (4)$$

then fits of the same quality in terms of likelihood can be obtained as the fit without any assumption. Actually the fits are very similar. The great advantage of eqn.(4) is that the number of parameters is only slightly increased to obtain the same likelihood as the fits without this assumption. Both agree in the results very well and are both typically 40 units of likelihood better in the experiments presented here[1,6]. It is the allowance of a different dependence on M which produces the improvement in the fit. A possible different dependence on the proton helicities can not be detected with the present statistics. Note that the M dependence

implies the existence of at least two different 1^+ systems, i.e. two Q's.

In the following, results are presented using eqn.(4). Using eqn.(4) or no assumption give consistent results. Figure 3 shows the partial wave decomposition for reactions (1) and (2). The biggest state in the Q-region is the 1^+ state in both reactions. The cross sections are similar for the 1^+S state in both reactions. The slight excess of events in reaction (2) over reaction (1) might come from the 1^+S Kρ contribution.

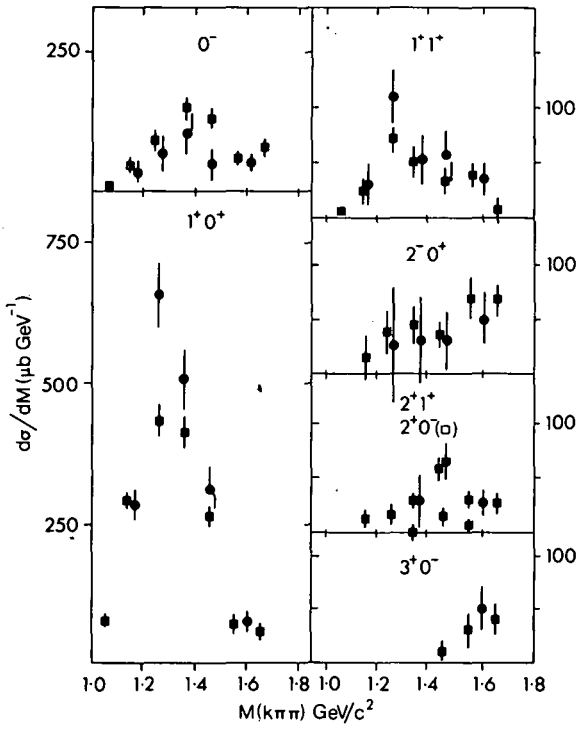

Fig.3 The differential cross section, dσ/dM, for each partial wave measured in reactions (1) and (2), plotted as squares and circles, respectively.

Figure 4 shows the intensity of the various 1^+S $K^*\pi$ and 1^+S Kρ polarization states versus mass in reactions (1) and (2). No evidence for unnatural spin parity exchange was observed. The fits were performed both in the t-channel and in the s-channel. Firstly, the results in the two reactions agree very well, when the cross section of $\bar{K}^0\rho^-$ has been reduced by a factor 2, which stems from the isospin being $\frac{1}{2}$, and agree with previous experiments including the fact that the Kρ system peaks at threshold in in contrast to the 1^+S $K^*(890)\pi$ which peaks about 200 MeV above its threshold.

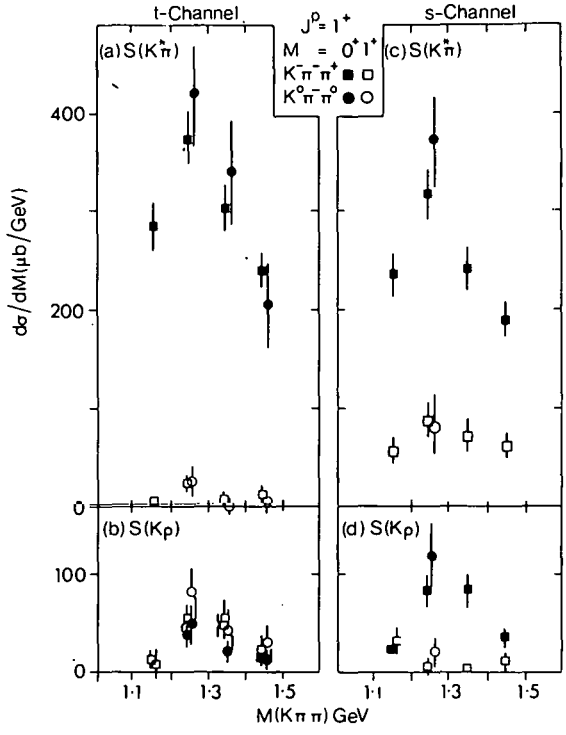

Fig.4 The cross sections for decay of the $J^P = 1^+$ waves. (a) and (b) show the results in the t-channel and (c) and (d) in the s-channel. Cross sections for the $\bar{K}^0\rho^-$ reaction have been reduced by a factor 2 for easier comparison.

Secondly, the 1^+S $K^*(890)\pi$ is produced mainly with M = 0 in the t-channel, and is therefore said to conserve t-channel helicity, TCHC. In contrast both M = 0 and M = 1 polarization is present for the Kρ, thus showing that eqn.(3) is not valid. The existence of at least two Q's is thus proven. Thirdly, the fits were repeated in the s-channel.

In this channel the M = 0 is dominant for the 1^+S Kρ state. One can then conclude that one has s-channel helicity conservation, SCHC, for the 1^+S Kρ system to the same precision as one has TCHC for 1^+S $K^*\pi$.

It has been shown[8] that also 1^+S Kω agrees better with SCHC than TCHC. When studying[6] the density matrix elements of the 1^+S $K^*(890)\pi$ and 1^+S Kρ systems as function of t', it is found both in the t-channel and s-channel that ρ_{11} increases linearly with t' and that ρ_{01} has opposite sign in the two systems.

Finally, fig.5 shows the ratio of the Kρ amplitude

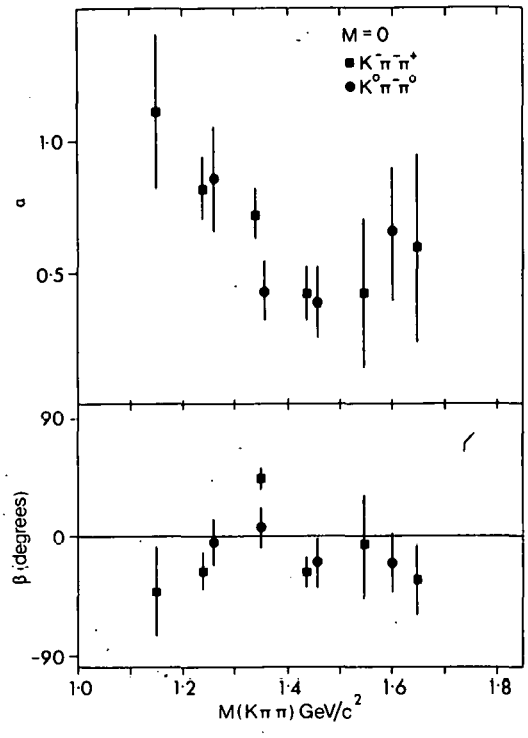

*Fig.5 The magnitude (α) of the ratio of the Kρ/K*π amplitudes in the $J^P M^\eta = 1^+0^+$ state and the phase (β) between them.*

to the $K^*\pi$ amplitude. This ratio is the ratio of the C's from eqn.(4) corrected for phase space defined to be asymptotically equal to 3/4 for reaction (1) and 3/1.9 for reaction (2). The measured value in the two channels agree. The magnitude α is close to 1.0 near threshold and decreases with mass to about 0.5. The value of the phase β is close to zero as expected for pure 8_F-coupling (C = +1), which also requires α to be 1.0.

4. CONCLUSIONS

Evidence has been presented for the existence of at least two Q-systems both with isospin $\frac{1}{2}$. Further the polarizations of the 1^+S $K^*(890)\pi$ and 1^+S Kρ systems are found to be different such that 1^+S $K^*(890)\pi$ approximately obeys TCHC and 1^+S Kρ SCHC.

REFERENCES

1. S.N.Tovey et al, Rutherford Laboratory preprint, RPP/H/135, (1975). To be published.

2. S.N.Tovey et al, Rutherford Laboratory preprint, RPP/H/127, RL-74-073, (1974).

3. J.D.Hansen, Proc. 4th Int. Conf. on Experimental Meson Spectroscopy, Boston, 1974, AIP No.21, 173.

4. M.Deutschmann et al, Phys. Letts. 49B, (1974) 388.

5. Yu.M.Antipov et al, Illinois preprint, COO-1195-29, (1974). Submitted to Nucl. Phys. B.

6. ABCLV Collaboration to be published.

7. J.D.Hansen, G.T.Jones, G.Otter and G.Rudolf, Nucl. Phys. B81, (1974) 403.

8. ABCLV Collaboration CERN/D.Ph.II/HEC 74-8, (1974). Submitted to Nucl. Phys. B.

SESSION 8

Chairman: A. Donnachie

Invited Talk

CONCLUSIONS AND OUTLOOK

C. Michael
University of Liverpool

THIS PAGE

WAS INTENTIONALLY

LEFT BLANK

CONCLUSIONS AND OUTLOOK

by

C. Michael
Department of Applied Mathematics and Theoretical Physics,
University of Liverpool.

A 21

1. INTRODUCTION

We have had several excellent expositions at this meeting of the techniques and assumptions involved in extracting angular momentum information about three body systems. I shall first review such analyses. The main application of these techniques lies in the extraction of resonance contributions and the resulting study of spectra, decay schemes and production mechanisms. These I shall review with a particular emphasis on likely production mechanisms. We have heard special mention at this meeting of the A_1 system and I shall try to draw some conclusions concerning the $J^{PC} = 1^{++}$ $q\bar{q}$ states.

2. TECHNIQUES FOR 3 PARTICLE ANGULAR MOMENTUM ANALYSIS

The basic analysis of the angular momentum content of the three body system a + b + c has been given in terms of the overall angular momentum and of the angular momentum in particular subsystems (i.e. b + c). The assumptions involved in converting such an analysis into a practical extraction of information from data have also been well discussed: the need to truncate the angular momentum sum to a few terms both in the overall system and in the subsystems; the factorization of production and decay and the dependence of the phase and modulus of the amplitude on the sub-energy in channel b + c that results from a factorized form using information from the bc elastic scattering amplitude.

These assumptions were all criticized at the meeting but an overall concensus seems to appear; that whenever the states in the 2-body subchannels are indeed narrow resonances, then the analysis will be valid. Thus the assumptions of factorization in the sequential decay of the three particle state as well as of limited angular momentum are most natural when narrow resonances dominate. More explicitly, the unitarity corrections due to coupling between decays via (a + b) + c and a + (b + c), for instance, were shown to be small when the widths of the states were narrow. When the three particle state itself is not a resonance, then the assumption of factorization between production and decay is less convincing and some evidence was shown[2] that in the Q region $K^*\pi$ and $K\rho$ decays may indeed be produced from different overall angular momentum projections.

Specific discussions of whether the Illinois density matrix parametrization or direct amplitude parametrization was preferable led to the conclusion that they are equivalent if the rank of the density matrix is constrained to be at its theoretical value. In both cases warnings[3,4] were given associated with the extent to which incoherence due to variations of distributions across bins etc. can fake true spin incoherence or phase differences.

To return to the question of unitary corrections; the K-matrix method for corrections leads to tractable expressions but at present no improvement[1] in the description of 3π decays. The more theoretically complete dispersion techniques are much more difficult to put into practice. One simple idea that can have a bearing on this problem is the discussion in terms of collision broadening. This has been applied successfully[5] to the N^*N intermediate state in πd scattering and leads in essence to a broadening of the N^* width due to the possibility of absorption (or de-excitation) on the N. This is analogous to the collision broadening of atomic lines in gases under pressure. The problem of the propagation of resonance states produced in the neighbourhood of other hadronic matter has also been much discussed elsewhere[6] in connection with resonance production on nuclei. This discussion implies that analysis of data for three particle systems coherently produced on nuclei may be at variance with

similar data on a proton target.

In the case of the $\pi\pi$ S-wave state ε which is needed experimentally, the problems mentioned above are certainly fully realized. The ε state is very broad and need not factorize. Thus results directly connected with $\varepsilon\pi$ channels are clearly on a much weaker footing than those involving $\rho\pi$ or $f_0\pi$ channels.

I conclude this section by mention of some formation experiments which involve 3-particle analysis and could lead to advances in meson spectroscopy. The e^+e^- channel is particularly appropriate for vector mesons and $\rho' \to \omega\pi$ or $\eta\pi\pi$ and ω', $\phi' \to \omega\pi\pi$ or $\phi\pi\pi$ are some clear examples - to say nothing of $\psi(J)$ and $\psi'(J)$! The accessibility of $\gamma\gamma$ initial states in $e^+e^- \to e^+e^-$ + ... should also allow formation of positive C meson states. The Primakóff effect or inelastic Coulomb scattering allows radiative couplings to be studied likewise (i.e. formation via $\gamma\gamma$, $\pi\gamma$, $K\gamma$ channels).

3. PRODUCTION MECHANISMS FOR MESON STATES

3.1 Propitious Channels

I shall first list some effective mass channels which should be particularly fruitful for meson states. My notation of states is self-explanatory except for the $J^{PC} = 2^{--}$ states of isospin 0 and 1: Z_0 and Z_1. Besides the well studied channels such as (3π), $(K\pi\pi)$, $(K\pi)$, $(\pi\pi)$ and $(\bar{K}K)$ one should consider channels

$\omega\pi$: $\underline{B}$ ρ' Z_1

$\omega\pi\pi$: A_1 ω' $\underline{A_2}$ $\pi^*(2^-)$ (H, Z_0)

$\eta\pi$: $\underline{\delta}$ $\underline{A_2}$ $A_2^*(4^+)$

$\eta\pi\pi$: $\underline{\eta'}$ $\underline{E}$ ρ' B $\underline{D}$ Z_1 $\eta^*(2^-)$ (f_0)

$\pi K\bar{K}$: as $\eta\pi\pi$ plus 3π

The states underlined are already seen experimentally while those in brackets involve decay to a D-wave $\pi\pi$ state. Of particular value is interference between neighbouring resonances in their decay into a common channel. Thus the electromagnetic decay of $\omega \to \pi\pi$ allows ρ-ω interference effects and subsequent measurements of the relative phase of their production amplitudes. An analogous case exists for f_0 and A_2 production in the $(K\bar{K})^0$ decay channel where interesting questions await answer[7]. The interference between A_1-quantum number production and A_2 in $\rho\pi$ has also been exploited to the full and I shall return to this later.

3.2 Resonance Production Mechanisms

The two basic features of the meson spectrum are the SU(3) or quark model aspect of octets (or nonets) and the Regge or orbital angular momentum excitation aspect of recurrence states. Combining these features with a Regge pole exchange approach allows a discussion of the production mechanisms for those states seen experimentally as well as the missing or confused states.

The SU(3) (or $SU(6)_w$ etc) aspect is closely related to that involved in calculating decay schemes. Thus a knowledge of $A_2 \to \pi\rho$ and $A_1 \to \pi\rho$ allows a comparison of $\pi \to A_1$ and $\pi \to A_2$ production via the ρ-exchange. This gives estimates[8] of 13.5 μb for $\pi^-p \to A_1^0 n$ at 5 GeV and, expressed differently, a ratio[9] of A_1^0 to A_2^0 production by charge exchange of $\Gamma_{A_1}/0.1$ GeV. A check of these ideas[10] comes from comparing them also with $\pi \to B$ via ω-exchange which is related to the decay $B \to \pi\omega$; this gives a $\pi^-p \to A_1^0 n$ production of about 20 μb at 4 GeV/c. Similar estimates have been made for hypercharge exchange production of A_1 etc. and also of production mechanisms for other missing $q\bar{q}$ states. In general SU(3) applied to t channel exchanges is found to give a very reasonable description of different production reactions.

The Regge-recurrence aspect can be approached from specific quark model L-excitation schemes but also via the dual-resonance model. This latter model also has the advantage of incorporating Regge pole exchange so that it gives full details[11] of the helicity structure and dependence on production momentum transfer of the production amplitude for the state. Observed meson Regge recurrences include the ρ - f - g, ω - A_2 - ω^* and K^* - K^{**} - $K^*(3^-)$ sequences, where the 2^+ state is related via exchange degeneracy. For the unnatural parity states we would expect π - H - π^* and η - B - η^* and, with the same slope on the Chew-Frautschi plot as for $\rho \to g$, this gives a $\pi^*(2^-)$ at 1.5 GeV and a $\eta^*(2^-)$ at 1.6 GeV. The latter figure is not so far from the 1.42 GeV mass of the E which is commonly assumed to be 0^- but could as well be 2^-. Any hypothetical trajec-

tory through the $J^{PC} = 1^{++}$ states A_1 and D would have no 0^{--} states but 2^{--} states Z_0 and Z_1.

As an example of the relative production of recurrence states, Table 1 shows a dual model calculation for $\pi \to \rho$ etc. via π exchange. The model also gives the $\pi\pi$ partial widths and the value for the g is in excellent accord with data so lending encouragement to the method. The basic point to note is that the production amplitude decreases very little for the higher spin states. Observation in any given channel x will result in an extra factor Γ_x/Γ_{tot} which will decrease faster for increasing J if Γ_{tot} remains substantially constant. A further point to note is that π-exchange is particularly sensitive to t_{min} effects and the production differential cross section off a nucleon is reduced at peak by 12% for lab. momentum $P_L \sim 10\ m^2$ and by 50% for $P_L \sim 4\ m^2$ where the state produced has mass m.

Table 1

Using a straight line through the ρ and g meson masses on a Chew-Frautschi plot and a parallel line through the f_0 mass yields the mass values shown for the Regge recurrence states. Normalized to the ρ partial width to $\pi\pi$ in GeV, the $\pi^+\pi^- \to \pi^+\pi^-$ dual model estimates (TH) for the higher states are shown and are compared with known experimental values (EXP). The modulus of the production amplitude to produce these resonances by π exchange at $t = m_\pi^2$ and with $\lambda_t = 0$ is compared by the factor $|A|^2$ relative to ρ production. The production amplitude in any given channel must be multiplied by the branching ratio to that channel. The total width Γ_{tot} is not predicted by the theoretical model but is expected to be roughly constant for increasing J. In the limit of large J, $\Gamma_{\pi\pi}$ and $|A|^2$ decrease by 1.47 for each increase of J by one.

	ρ	f	g	f*	g*
J	1	2	3	4	5
Mass	0.77	1.27	1.68	1.96	2.25
$\Gamma_{\pi\pi}$(EXP)	0.15	0.141	0.047	-	-
$\Gamma_{\pi\pi}$(TH)	0.15	0.116	0.051	0.046	0.018
$\lvert A\rvert^2_{\lambda_t=0}$	1.0	1.4	1.6	1.4	1.0

The relative importance of higher or lower lying exchanges can also be estimated. For the production of a state of mass m by an exchange trajectory $\alpha(t)$, duality arguments[11-13] lead to a factor $(s/m^2)^{2\alpha(t)}$ in the production cross sections. Thus lower lying exchanges $\alpha(t)$ dominate for increasing m^2 at fixed s and higher lying exchanges of course dominate for increasing s at fixed m^2.

The relative production of Regge recurrences by other exchanges can thus be estimated using the fact that Table 1 gives approximately a constant m^2 dependence for π exchange and then scaling by the factor $(s/m^2)^{2\alpha(t)}$. Thus natural parity, $\alpha = 0.5$, production of recurrences should decrease as $1/m^2$ with increasing m while the decrease could be more like $1/m^4$ for diffractive production with $\alpha \sim 1$. Some check of the dependence for diffractive production can come from comparing $\gamma N \to gN$ with $\gamma N \to \rho N$ or $NN \to N^*(F_{15})N$ with $NN \to NN$. A suppression of $1/m^4$ gives a factor of 1/25 suppression of g photoproduction together with an extra factor of 1/4 in the $\pi\pi$ channel since $\Gamma_{\pi\pi}/\Gamma_{tot} \sim 1/4$ for the g. Data seem to indicate[14] a suppression that is even stronger (< 0.01 for g to ρ photoproduction in $\pi\pi$) and this may be evidence that diffractive production of high mass resonances is especially suppressed. Similar data on $N \to N^*(1700)$ diffraction dissociation need a J^P analysis of the 1700 bump to separate out the F_{15} component in order to check this assertion.

Other features of the production amplitude, such as t- or helicity- structure and Regge cut contributions have also been discussed as a function of m^2 and very interesting light is shed on the details of the production mechanism. In particular a relative decrease of Regge cut to Regge pole for increasing m^2 has been found in contrast to the expectations of most models for Regge cuts.

3.3 Non-Resonant Production Mechanism

The double exchange diagram of fig.1(a) leads to a π ρN final state and should be considered along with contributions from resonance diagrams such as 1(b). The properties of the diagram of fig.1(a) are well known and are carefully discussed by Berger in these proceedings[15]. The amplitude can be written basically as

$$A \sim \frac{g^2}{t_1 - \mu^2}\, s_2^{\alpha_2}\, e^{at_2}$$

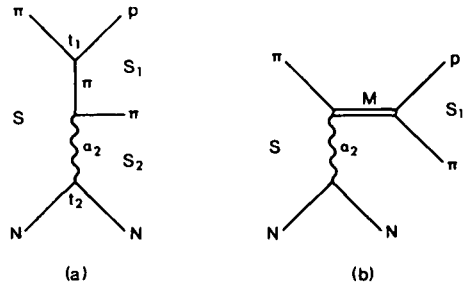

Fig.1 Diagrams for $\pi N \to \rho\pi N$ via (a) one pion exchange and (b) resonance M.

Essentially the kinematics for small t_2 results in the identity $s_1/(t_1 - \mu^2) = s/(s_1 - \mu^2)$ so that the π exchange pole in t_1 tends to be cancelled. This cancellation is exact when t_2 has its minimum value and when the α_2 exchange has intercept 1. The cancellation removes the t_1 dependence from the amplitude and so yields an S-wave $\rho\pi$ production. Modifications from this over-simple case include (i) a Reggeized π exchange propagator (ii) possible phase dependence on the Toller angle of the central vertex (iii) lower lying contributions α_2 (iv) proper consideration of a range of values of t_2. These result in contributions to other waves and, in the case of Reggeized π exchange, the signature factor is sampled over a substantial range of t_1 since there is little peaking in this variable and so yields[16,17] a phase to the S-wave $\rho\pi$ production that is thereby modified and is in agreement with information on A_1 - A_2 interference.

The Reggeized-π exchange modification, if parametrized suitably[16], can indeed give a rough description of the experimentally observed $\rho\pi$ distributions. An intuitive idea of the approximations involved comes from thinking of the sub process in fig.1(a) as Pomeron production $P\pi \to \pi\rho$. This can be compared with photoproduction $\gamma\pi \to \pi\rho$ which has a similar one pion exchange contribution. Data on $\gamma N \to \pi N$ are available and indicate that at low energies a one pion exchange description is inadequate except for the highest partial waves. This and similar experience indicates that one pion exchange in $P\pi \to \pi\rho$ should only be taken seriously at $\pi\rho$ energies rather far above threshold and in the higher partial waves - certainly not in the S-wave in the A_1 mass region!

A further question has been raised - that of combining an eventual A_1 resonance with the one pion exchange contribution discussed above. This does not upset ideas of duality or experience with photoproduction provided a real one pion exchange contribution is retained. However, the unitarity constraints on adding[18] a complex phase π exchange term to an A_1 resonance need to be investigated fully in $P\pi \to \pi\rho$ as well as in the elastic channel $\rho\pi \to \pi\rho$. This unitarity analysis would be on a sounder footing if the 'P' initial state could be avoided, so that experiments such as $\pi^- \to (\rho\pi)^0$ by ρ exchange or $\gamma \to (3\pi)^+$ by π exchange would yield data closer to elastic $\rho\pi$ scattering. One should mention in passing that adding a π exchange contribution to a resonance is indeed the appropriate description in other cases, for instance in 2π photoproduction where the π exchange Drell term is added to the ρ resonance contribution.

4. EXPERIMENTAL EVIDENCE FOR MISSING QUARK MODEL STATES

I shall try to summarize the evidence presented at this meeting on the missing states and give some indications of fruitful future lines of attack.

The A_1 remains the prima donna hiding in the wings. The conventional $\varepsilon\pi$ and $\rho\pi$ analyses[17] of $\pi^\pm \to (3\pi)^\pm$ show no phase variation of the 1^+ S-wave relative to other waves across the A_1 bump. If the A_1 resonance couples to $\pi\rho$, a substantial phase change in $\pi\rho$ elastic scattering will result and this will show in the $\pi\rho$ channel in production unless there is a rather contrived admixture of Reggeized one pion exchange[16]. An alternative let-out is that the $\varepsilon\pi$ garbage channel in the analysis is improperly treated and unitarity corrections etc. are needed so that the extracted phase information may be unreliable. The A_1 question can be clarified in part by comparable analyses of $\pi^\pm N \to (3\pi)^0 N$, $\pi^+ p \to (3\pi)^0 \Delta^{++}$, $\gamma p \to (3\pi)^+ n$, $\bar{K}N \to (3\pi)\Lambda$, etc. Preliminary data on the first two of these were discussed at this meeting[19] and limits were set on the level of $J^P = 1^+$ produced. Disagreements between these two limits mean one cannot conclude strongly, but there still seems to be enough space for the expected $q\bar{q}$ A_1

signal to creep in. Data on photoproduction[20] will help particularly since the π exchange mechanism is particularly well understood and being a low-lying trajectory it favours higher mass resonance production.

Based on the observation that the ρ is copiously produced in photoproduction, one should also seek the A_1 in $\nu N \to \mu(3\pi)N$ where the axial current has 1^+ quantum numbers and should feed the A_1 $q\bar{q}$ resonance with no inhibitions. Reasonably small lepton q^2 and largish lepton energy loss should be optimum for an A_1 search. It is also worth while looking for an signal in other decay modes such as $\omega\pi\pi$ and $K\bar{K}\pi$.

The missing π^* and η^* states are also of considerable interest. Their production by charge or quantum number exchange should be predominantly natural parity exchange so that a suppression of about $m^2(0^-)/m^2(2^-)$ of the corresponding π or η production cross sections is to be expected. In diffraction production the rates are less easy to predict.

5. SUMMARY

This meeting has seen a lot of enthusiasm and interest in analysing 3 meson systems. Many experimental results are available in a preliminary form and more experiments of great interest are underway. The techniques of analysis are well tuned and we can expect answers to many questions soon. Particular emphasis should be placed on the missing $J^{PC} = 1^{++}$, 2^{--} and 2^{-+} quark model states produced in as varied a way as possible.

REFERENCES

1. I.J.R. Aitchison, these proceedings.
2. J.D. Hansen, these proceedings.
3. G.T. Jones, these proceedings.
4. V. Chaloupka, these proceedings.
5. D.V. Bugg, Rutherford Laboratory preprint, RL-74-140, (1974).
6. L. Van Hove, in Particle Interactions at Very High Energies, Proc. 2nd Summer Institute on High Energy Physics, Louvain, 1973, eds. D. Speiser, F. Halzen and J. Weyers, (N.Y., London, Plenum Press 1974), p.A371; K. Gothfried, Acta Phys. Pol. B3, (1972) 769.
7. A. Irving and C. Michael, Nucl. Phys. B82, (1974) 282.
8. G. Fox and A.J.G. Hey, Nucl. Phys. B56, (1973) 386.
9. G. Kane, University of Michigan preprint, presented at Argonne National Laboratory Symposium on Resonance Production 1974.
10. A. Irving and V. Chaloupka, Nucl. Phys. B, (to be published).
11. C. Michael, Nucl. Phys. B63, (1973) 431.
12. P. Hoyer, R.G. Roberts and D.P. Roy, Nucl. Phys. B56, (1973) 173.
13. P. Hoyer and J. Kwiecinski, Nucl. Phys. B60, (1973) 26.
14. Y. Eisenberg et al, Phys. Rev. D5, (1972) 15.
15. E.L. Berger, these proceedings.
16. G. Ascoli et al, (to be published).
17. U. Kruse, these proceedings.
18. M. Bowler, these proceedings.
19. D. Crennell, these proceedings. F. Wagner, these proceedings.
20. Daresbury Laboratory Proposal DL/SCP/97, January, 1974. (Unpublished).

THIS PAGE

WAS INTENTIONALLY

LEFT BLANK

LIST OF DELEGATES

THIS PAGE

WAS INTENTIONALLY

LEFT BLANK

LIST OF DELEGATES

I.J.R. AITCHISON
Department of Theoretical Physics, University of Oxford, 12 Parks Road, Oxford OX1 3PQ.

D. BARBER
Science Research Council, Daresbury Laboratory Daresbury, Warrington WA4 4AD.

R. BARLOW
Cavendish Laboratory, University of Cambridge Madingley Road, Cambridge CB3 OHE.

K.W.J. BARNHAM
Department of Physics, Imperial College of Science & Technology, Prince Consort Road, London SW7 2BZ.

E.L. BERGER
High Energy Physics, Argonne National Laboratory, 9700 South Cass Avenue, Argonne, Illinois 60439, U.S.A.

M.G. BOWLER
Nuclear Physics Laboratory, University of Oxford, Keble Road, Oxford OX1 3RH.

G.R. BROOKES
Department of Physics, University of Sheffield The Hicks Building, Sheffield S3 7RH.

G.H. BURKHARDT
Department of Mathematical Physics, University of Birmingham, P.O. Box 363, Birmingham B15 2TT.

R.J. CASHMORE
Nuclear Physics Laboratory, University of Oxford, Keble Road, Oxford OX1 3RH.

V. CHALOUPKA
T.C. Division, C.E.R.N., CH-1211 Geneva 23, Switzerland.

C.F. CHO
Institut f. Physik, Max-Planck-Institut f. Physik u. Astrophysik, 8 München 40, Föhringer Ring 6, Germany.

A.B. CLEGG
Department of Physics, University of Lancaster, Lancaster LA1 4YB.

G.C. COSTA
Istituto di Fisica, Università di Milano, Via Celoria 16, I-20133 Milano, Italy.

D.J. CRENNELL
Science Research Council, Rutherford Laboratory, Chilton, Didcot, Oxon OX11 0QX.

J.B. DAINTON
Science Research Council, Daresbury Laboratory Daresbury, Warrington WA4 4AD.

A. DONNACHIE
Department of Theoretical Physics, University of Manchester, Manchester M13 9PL.

A. ESKRAYS
Institut f. Physik, Max-Planck-Institut f. Physik u. Astrophysik, 8 München 40, Föhringer Ring 6, Germany.

H. FRANZ
Institut f. Physik, Max-Planck-Institut f. Physik u. Astrophysik, 8 München 40 Föhringer Ring 6, Germany.

E. GABATHULER
Science Research Council, Daresbury Laboratory
Daresbury, Warrington WA4 4AD.

J. GARVEY
Science Research Council, Rutherford
Laboratory, Chilton, Didcot, Oxon OX11 0QX.

M.G. GREEN
Department of Physics, Westfield College,
Kidderpore Avenue, London NW3 7ST.

J.D. HANSEN
Niels Bohr Institute, Blegdamsvej 17,
Copenhagen Ø, DK-2100 Denmark.

A.J.G. HEY
Department of Physics, University of
Southampton, Southampton SO9 5NH.

A.C. IRVING
Department of Applied Mathematics &
Theoretical Physics, University of Liverpool,
P.O. Box 147, Liverpool L69 3BX.

M.F. JAMES
Department of Physics, University of
Birmingham, P.O. Box 363, Birmingham B15 2TT.

G.T. JONES
Department of Physics, University of
Birmingham, P.O. Box 363, Birmingham B15 2TT.

L.M. JONES
Department of Applied Mathematics &
Theoretical Physics, University of Cambridge,
Silver Street, Cambridge CB3 9EW.

I.R. KENYON
Department of Physics, University of
Birmingham, P.O. Box 363, Birmingham B15 2TT.

U.E. KRUSE
Institut f. Physik, Max-Planck-Institut f.
Physik u. Astrophysik, 8 Munchen 40,
Fohringer Ring 6, Germany.

L. LEE CHI KWONG
Science Research Council, Daresbury Laboratory
Daresbury, Warrington WA4 4AD.

P.J. LITCHFIELD
Science Research Council, Rutherford
Laboratory, Chilton, Didcot, Oxon OX11 0QX.

R. MARSHALL
Science Research Council, Daresbury Laboratory
Daresbury, Warrington WA4 4AD.

C. MICHAEL
Department of Applied Mathematics &
Theoretical Physics, University of Liverpool,
P.O. Box 147, Liverpool L69 3BX.

D. MORGAN
Science Research Council, Rutherford
Laboratory, Chilton, Didcot, Oxon OX11 0QX.

S.J. OREBI GANN
Nuclear Physics Laboratory, University of
Oxford, Keble Road, Oxford OX1 3RM.

C.D. PROCTOR
Department of Natural Philosophy, University
of Glasgow, Glasgow G12 8QQ, Scotland.

V.H. RAJARATNAM
Department of Physics, University of Sheffield
The Hicks Building, Sheffield S3 7RH.

S. RATTI
Istituto di Fisica Nucleare dell'Università,
Via Bassi 6, I-27100 Pavia, Italy.

R.L. SEKULIN
Science Research Council, Rutherford Laboratory, Chilton, Didcot, Oxon OX11 0QX.

I.O. SKILLICORN
Department of Natural Philosophy, University of Glasgow, Glasgow G12 8QQ, Scotland.

B.J. STACEY
Department of Physics, Westfield College, Kidderpore Avenue, London NW3 7ST.

K. SUMOROK
Science Research Council, Rutherford Laboratory, Chilton, Didcot, Oxon OX11 0QX.

C. SUTTON
Department of Physics, University of Sheffield The Hicks Building, Sheffield S3 7RH.

J.C. THOMPSON
Science Research Council, Daresbury Laboratory Daresbury, Warrington WA4 4AD.

G. THOMPSON
Nuclear Physics Laboratory, University of Oxford, Keble Road, Oxford OX1 3RH.

P.R. THORNTON
Department of Physics, Imperial College of Science & Technology, Prince Consort Road, London SW7 2BZ.

F. WAGNER
Institut f. Physik, Max-Planck-Institut f. Physik u. Astrophysik, 8 München 40. Föhringer Ring 6, Germany.

R.M. WATERS
Department of Physics, Imperial College of Science & Technology, Prince Consort Road, London SW7 2BZ.

P. WOODWORTH
Department of Physics, University of Birmingham, P.O. Box 363, Birmingham B15 2TT.